ABSTRACT

LIN, CHIEN-YUAN. Regulation of 3-Hydroxylation in Monolignol Biosynthesis and Identification of Lignin Peroxidase in *Populus trichocarpa*. (Under the direction of Prof. Vincent L. Chiang and Ronald R. Sederoff).

Lignin, as heterogeneous phenolic polymer, is one of the major components of the plant secondary cell wall. Lignin is important for plant erect growth, water transport and pathogen resistance. Lignin also provides recalcitrance of the plant biomass during delignification for paper or biofuel production. With a radical coupling mechanism, the polymerization of lignin results from combinatorial events with varied subunits. Ten monolignol biosynthetic enzyme families have been proposed in the monolignol biosynthetic pathway since 1955 and the knowledge of the monolignol biosynthesis still undergoes revision. Recently, the discovery of inhibitory effect by pathway intermediates and protein-protein interactions among monolignol biosynthetic enzymes implicate complex regulation in monolignol biosynthesis.

In order to build a mathematical model that can predict the metabolic flux of the monolignol biosynthesis, we need to acquire knowledge of the individual enzyme, including their isoforms or genetic variations, the single nucleotide polymorphism (SNPs). In this study, SNPs are identified among monolignol biosynthetic enzymes and their activities are evaluated, while the enzyme kinetics of 4-hydroxycinnamoyl-coenzyme A (CoA):shikimic acid hydroxycinnamoyl transferase (HCT) is also characterized. First, SNP variants are identified among the 10 monolignol biosynthetic enzyme families in *P. trichocarpa*. The activities of the SNP variants, such as 4-coumaric acid:CoA ligase (4CL), caffeoyl-CoA *O*-methyltransferase (CCoAOMT) and cinnamoyl-CoA reductase (CCR), are examined and show similar catalytic activities compared to their original identified ones. Second, two HCTs in *P. trichocarpa*, the PtrHCT1 and PtrHCT6, were identified as the most abundant

PtrHCTs in the wood forming tissue; however, their enzyme kinetic properties have not yet been characterized. Basic enzyme kinetic studies are performed on both PtrHCTs for their substrates, the 4-coumaroyl-CoA, caffeoyl-CoA, 4-coumaroyl shikimic acid and caffeoyl shikimic acid, where CoA thioesters are identified as preferred substrates for PtrHCTs than shikimic acid esters. Therefore, a bottleneck from caffeoyl shikimic acid to caffeoyl-CoA is suggested in the monolignol biosynthetic pathway by the enzyme kinetics of PtrHCTs, which led to the investigation of the regulation for 3-hydroxyaltion of monolignol biosynthesis. Both 4-coumaroyl and caffeoyl shikimic acids were identified as inhibitors of *P. trichocarpa* 4CL (Ptr4CL), which is an essential enzyme that controls lignin content. The stronger inhibitory effect on Ptr4CL for 4-coumaroyl-CoA than caffeoyl-CoA production by shikimic acid esters indicates 3-hydroxyation from 4-coumaric acid to caffeic acid may be modulated.

Protein complexes have been proposed in the monolignol biosynthesis of *P. trichocarpa*. Here, a Ptr4CL-PtrHCT complex was studied and several lines of evidences are provided: bimolecular fluorescence complementation (BiFC), immunoprecipitation (IP), recombinant enzyme assays, mechanistic modeling and PtrHCT downregulated transgenics. A previously established mechanistic model for analyzing the protein-protein interaction between monolignol biosynthetic enzymes is incorporated to reveal the stoichiometry of the Ptr4CL-PtrHCT complex.

Moreover, lignin polymerization in *P. trichocarpa* was also studied. PtrPO2 was identified as an abundant and specifically expressed peroxidase in the stem differentiating xylem (SDX). Downregulation of PtrPO2 shows reddish stem internodes, growth reduction, lignin reduction and wood composition alteration. A role for PtrPO2 in lignin polymerization is proposed in *P. trichocarpa*.

Overall, these findings may advance our knowledge on monolignol biosynthesis and help to improve biomass for pulp and paper or biofuel production in the future.

Regulation of 3-Hydroxylation in Monolignol Biosynthesis and Identification of Lignin Peroxidase in *Populus trichocarpa*

by
Chien-Yuan Lin

A dissertation submitted to the Graduate Faculty of
North Carolina State University
in partial fulfillment of the
requirements for the degree of
Doctor of Philosophy

Forestry and Environmental Resources

Raleigh, North Carolina

2015

APPROVED BY:

_____	_____
Vincent L. Chiang Co-Chair of Advisory Committee	Ronald R. Sederoff Co-Chair of Advisory Committee
_____	_____
David C. Muddiman	Robert B. Rose

DEDICATION

To my family, for their unconditional support, that made this come true. My father is a true mentor in my life, and he always taught me to think positively and wisely. Every time I encounter challenges, his theory of “positive thinking” helps me to actively overcome any situations. My mother is a gentle and diligent woman, who raised my older brother and me with her whole heart. Her warmest comfort and helpful advice function as the lighthouse that guided me through all the ups and downs during my life. She is the most lovely and thoughtful mother in the world. My brother is a humorous and trustable man. He is the greatest brother I can imagine in my life and he takes care of the entire family during my time in U.S.A. perusing my doctoral degree. Also, I want to express my gratefulness to my two beloved grandfather and grandfather-in-law, who I lost during my study. It is a great sadness that I cannot share this moment with them anymore, but I want to say thank you for everything you gave me and I will miss you forever. With all your support, I have finally achieved the goal of my life. Thank you all and I dedicate my work to all of you.

BIOGRAPHY

Chien-Yuan, Lin, who was born in June 4th, 1985 in Taipei, Taiwan. When he was a child, he liked to explore the world that he was not familiar with. He was always eager to find the answers to every question, for example: why is grass green and why can birds fly? Since he was in Taipei Municipal Dazhi High School, he developed interest in science and he even saved all his pocket money to buy a child's microscope to experience the feeling of a scientist. He was an outstanding student in junior high school, he won the recommendation and screening entrance examination and entered the Taipei Municipal Jianguo High School, the highest ranked high school in Taiwan. During his life in high school, he determined that being a scientist was his goal and he actively joined the laboratory activities in Taiwan Academia Sinica for his extracurricular time. Due to his interest in biology, he chose Life Science as his major when he entered National Taiwan University (NTU), the highest ranked university in Taiwan. In NTU, he also participated in the oversea summer research program where he first met Prof. Vincent L. Chiang in North Carolina State University (NCSU). After his graduation from NTU, he decided to pursue his master degree in Taiwan Academia Sinica before he went to study abroad. Under Prof. Wu, Jen-Leih's guidance, he learned about the world of molecular biology and developed a greater interest in science. It was through Prof. Wu's and Prof. Chiang's encouragements that he decided to go abroad in 2010 and pursue his doctoral degree in Forestry and Environmental Resources of NCSU under the auspices of Prof. Vincent L. Chiang.

ACKNOWLEDGMENTS

During my life in pursuing doctoral degree, lots of people had helped and guiled me to get through every circumstance. First of all, I want to thank to my advisor Prof. Vincent L. Chiang, who always gives me great advice and is patient with me. Prof. Chiang is a great academic mentor for me. He always points out my weakness and helps me to build up the skill to become a scientist. In my entire Ph.D. study life, he has provided me with his knowledge and years of experience for my research. Without his guidance, I will never have chance to get through this intense academic environment. Second, I want to thank to my co-advisor Prof. Ronald R. Sederoff, who always help me to clear up my mind and to think in different aspects. Every time I come to his office, I will always end up with an informed opinion or conclusive decision. With all your help for the past 4 years, I have become a more independent researcher. And I also want to thank to my two committee members, Prof. David C. Muddiman and Prof. Robert B. Rose, they have taught me a lot, both in classes and in my professional studies. They are really helpful and have been very supportive committee members through my doctoral study. Finally, I want to say thank you to all of my colleagues in the Forestry Biotechnology Group and my collaborators at NCSU, especially Dr. Jack P. Wang, who was always there to help me every time I needed him. He is a true great friend. Without all your help, I would not have had a chance to accomplish all this works. Thank you very much.

TABLE OF CONTENTS

LIST OF TABLES xi
LIST OF FIGURES xii
LIST OF PUBLICATIONS xvi
LIST OF PRESENTATIONS xvii
Chapter 1: Introduction 1
1.1 The Plant Cell Wall 1
1.1.1 The Primary Plant Cell Wall 1
1.1.2 The Secondary Plant Cell Wall 3
1.2 Plant Cell Wall Components 5
1.2.1 Cellulose 5
1.2.2 Hemicellulose 7
1.2.3 Lignin 10
1.3 The Monolignol Biosynthetic Pathway 13
1.4 Lignin Polymerization 16
1.5 Monolignol Biosynthesis in *Populus trichocarpa* 17
1.6 Synopsis of Completed Research 20
1.7 References 23
Chapter 2: Characterization of *Populus trichocarpa* Hydroxycinnamoyl-Coenzyme A:Shikimic Acid Hydroxycinnamoyl Transferase (PtrHCT) and Activity Evaluation of the Single Nucleotide Polymorphism (SNP) Variants in the Monolignol Biosynthetic Enzymes of *Populus trichocarpa* 46
2.1 Introduction 46
2.2 Materials and Methods 51
2.2.1 Synthesis of Monolignol Precursors 51
2.2.2 Plasmid Constructions 52
2.2.3 Expression and Purification of the Recombinant Proteins 52
2.2.4 Western Blotting 53
2.2.5 Enzyme Reactions and High Performance Liquid Chromatography (HPLC)

Analysis 53
2.2.6 Activity Evaluation of the Single Nucleotide Polymorphism (SNP) Variants of the Monolignol Biosynthetic Enzymes in *P. trichocarpa* 54
2.3 Results..... 55
2.3.1 Identification of the Two PtrHCTs, PtrHCT1 and PtrHCT6 55
2.3.2 Expression and Purification of PtrHCT1 and PtrHCT6 56
2.3.3 Specificity of PtrHCT1 and PtrHCT6 Rabbit Antibodies 57
2.3.4 Optimization of the Enzyme Reactions for PtrHCT1 and PtrHCT6 58
2.3.5 Michaelis-Menten Kinetics of PtrHCT1 and PtrHCT6 59
2.3.6 Additive Activity of PtrHCT1 and PtrHCT6 63
2.3.7 Activity Evaluation of the Single Nucleotide Polymorphism (SNP) Variants of the Monolignol Biosynthetic Enzymes in *P. trichocarpa* 65
2.4 Discussion 68
2.4.1 PtrHCT1 and PtrHCT6 are both Functional Monolignol Biosynthetic Enzymes in *P. trichocarpa* 68
2.4.2 PtrHCT1 and PtrHCT6 have Similar Kinetic Properties 69
2.4.3 The Functions of PtrHCT1 and PtrHCT6 Appear Redundant 70
2.4.4 A Bottleneck is Present in the Current Monolignol Biosynthetic Pathway 71
2.4.5 The Single Nucleotide Polymorphism (SNP) Variants of Ptr4CL3, PtrCCoAOMT3 and PtrCCR2 are Identical in Activity 71
2.5 References 72
Chapter 3: 4-Coumaroyl and Caffeoyl Shikimic Acids Inhibit 4-Coumaric Acid:Coenzyme A Ligases and Modulate Metabolic Flux for 3-Hydroxylation in Monolignol Biosynthesis of *Populus trichocarpa* 79
3.1 Introduction 79
3.2 Materials and Methods..... 84
3.2.1 Plant Materials 84
3.2.2 Synthesis of Monolignol Precursors 85
3.2.3 Recombinant Ptr4CL3 and Ptr4CL5 Expression and Purification 85

3.2.4 Quantification of Transcripts, Metabolites and Proteins in Stem Differentiating Xylem (SDX) 86
3.2.5 Total Protein Extraction from SDX 87
3.2.6 Enzyme Assays and HPLC Analysis 88
3.2.7 Inhibition Kinetics of Ptr4CL3 and Ptr4CL5 89
3.3 Results..... 90
3.3.1 4-Coumaroyl and Caffeoyl Shikimic Acids Inhibit Recombinant Ptr4CL3 and Ptr4CL5 Activities 90
3.3.2 Inhibition Kinetics Indicate that 4-Coumaroyl Shikimic Acid Shows Stronger Inhibition on Ptr4CL3 and Ptr4CL5 Activities than Caffeoyl Shikimic Acid 94
3.3.3 4-Coumaroyl and Caffeoyl Shikimic Acids Inhibit Ptr4CL Activities in the SDX Protein Extracts of *P. trichocarpa* and in Mixtures of Ptr4CL3 and Ptr4CL5 ... 99
3.3.4 4-Coumaroyl Shikimic Acid, Caffeoyl Shikimic Acid and 4-Coumaric Acid Accumulate in PtrC3H3 Downregulated Transgenic *P. trichocarpa* 102
3.3.5 Evaluation of the Roles of 4-Coumaroyl and Caffeoyl Shikimic Acids as Inhibitors Using the Estimated Flux Based on Mass Action Kinetics and Inhibition Parameters 105
3.4 Discussion 108
3.5 References..... 112
Chapter 4: Identification of Enzyme Complex of 4-Coumaric Acid:CoA Ligase (4CL)-Hydroxycinnamoyl-CoA:Shikimic Acid Hydroxycinnamoyl Transferase (HCT) in *Populus trichocarpa* 116
4.1 Introduction..... 116
4.2 Materials and Methods..... 121
4.2.1 Plant Materials 121
4.2.2 Expression and Purification of Recombinant Proteins 121
4.2.3 Total Protein Extraction from Stem Differentiating Xylem (SDX) and Enzyme Assays 121

4.2.4 Plasmid Construction for Bimolecular Fluorescence Complementation (BiFC) 123
4.2.5 Plasmid Preparation for BiFC 124
4.2.6 *P. trichocarpa* SDX Protoplast Preparation for BiFC 125
4.2.7 Immunoprecipitation (IP) 127
4.2.8 Mechanistic Modeling and Numerical Analysis 127
4.2.9 PtrHCT1 and PtrHCT6 Downregulated Transgenic and Next Generation Sequencing (RNA-seq) Analysis 128
4.2.10 Chemical Cross-linking 129
4.3 Results 130
4.3.1 Coenzyme A (CoA) Ligation Activity with Mixtures of Ptr4CL3 and PtrHCTs Indicates a Protein-Protein Interaction 130
4.3.2 The Ptr4CL-PtrHCT Complex was also Identified by Bimolecular Fluorescence Complementation (BiFC) and Immunoprecipitation (IP) 131
4.3.3 Mixed Enzyme Effect Analysis for 4-Coumaric Acid 135
4.3.4 Mixed Enzyme Effect Analysis for Caffeic acid 136
4.3.5 Mechanistic Modeling and Stoichiometry Analysis of Ptr4CL-PtrHCT Complex 138
4.3.6 The Ptr4CL-PtrHCT Complex is Found *in vivo* in SDX 140
4.3.7 CoA Ligation Activities are Decreased when both PtrHCT1 and PtrHCT6 are Downregulated in *P. trichocarpa* 141
4.4 Discussion 144
4.4.1 Enzyme Complexes Affects the Metabolic Flux of Monolignol Biosynthesis ... 145
4.4.2 The Ptr4CL-PtrHCT Complex Affects Metabolic Flux 146
4.4.3 More Enzymes may be Involved in Monolignol Biosynthetic Complex Formation 148
4.5 References 152

Chapter 5: PtrPO2, a Lignin Peroxidase in *Populus trichocarpa* 161
5.1 Introduction 161
5.2 Materials and Methods 167
5.2.1 Plant Materials 167
5.2.2 RNA Extractions 168
5.2.3 Transcriptome (RNA-seq) and Differentially Expressed Gene (DEG) Analysis 168
5.2.4 Identification of Class III Peroxidases in *P. trichocarpa* and Phylogenetic Analysis 169
5.2.5 RNA Interference (RNAi) Plasmid Constructions and Plant Transformation 169
5.2.6 Real-time PCR (RT-PCR) 170
5.2.7 Lignin Content and Carbohydrate Determination 171
5.2.8 Nitrobenzene Oxidation for Lignin Composition 172
5.2.9 Mechanical Properties of Wood 173
5.3 Results 173
5.3.1 PtrPO2 is a Xylem-Abundant and Xylem-Specific Class III peroxidase in *Populus trichocarpa* 173
5.3.2 PtrPO2 Shares Conserved Domains with Coniferyl Alcohol-Specific Peroxidase from *Arabidopsis thaliana* and Sinapyl Alcohol-Specific Peroxidase from *Zinnia elegans*..... 178
5.3.3 PtrPO2 is an Unusual Peroxidase in the SDX of *P. trichocarpa* 179
5.3.4 Downregulation of PtrPO2 in *P. trichocarpa* 182
5.3.5 PtrPO2 Downregulated Transgenics in *P. trichocarpa* have Reduced Growth and Reddish Internodes in the Stem Wood 184
5.3.6 Cell Wall Component Analysis of PtrPO2 Downregulated Transgenics 185
5.3.7 Mechanical Properties of the Wood of PtrPO2 Downregulated Transgenics ... 187
5.3.8 Lignin Composition Analysis of PtrPO2 Downregulated Transgenics 187
5.3.9 Differentially Expressed Gene (DEG) Analysis of the PtrPO2 Downregulated

Transgenics 189
5.4 Discussion 192
5.4.1 PtrPO2 is an Unusual Peroxidase Involved in Lignification 194
5.4.2 PtrPO2 Possesses Similar Structural motifs to G- and S-Specific Peroxidases 195
5.4.3 Reddish Internode of Stem in PtrPO2 Downregulated Transgenics 196
5.4.4 The Role of Peroxidases and Laccases in Lignin Polymerization 197
5.4.5 Transcriptome Analysis of PtrPO2 Downregulated Transgenics 198
5.5 References 199

LIST OF TABLES

Table 2.1 Michaelis–Menten kinetic parameters of PtrHCT1 and PtrHCT6 62

Table 2.2 The SNP variants in the monolignol enzymes of *P. trichocarpa* 66

Table 3.1 Estimated Ptr4CL flux based on mass action kinetics and inhibition parameters 107

Table 4.1 Primer list for construction of BiFC plasmids 123

Table 5.1 Summary of the lignin peroxidases transgenics and mutants in plants ... 166

Table 5.2 Primer list for PtrPO2 for RNAi construction 170

Table 5.3 Primer list for RT-PCR 171

Table 5.4 Amino acid sequence identity (%) of PtrPO2 and other lignin peroxidases among plants 179

Table 5.5 Summary of protein properties of PtrPOs and lignin peroxidases among plants 180

Table 5.6 Cell wall composition of PtrPO2 transgenics and wildtype *P. trichocarpa* 186

Table 5.7 Lignin composition of PtrPO2 transgenics and wildtype *P. trichocarpa* ... 188

Table 5.8 Expression of the xylem-abundant *P. trichocarpa* peroxidases in PtrPO2 downregulated transgenics 190

Table 5.9 Expression of the *P. trichocarpa* laccases in PtrPO2 downregulated transgenics 191

Table 5.10 Expression of the *P. trichocarpa* monolignol biosynthetic genes in PtrPO2 downregulated transgenics 192

LIST OF FIGURES

Figure 1.1 The current monolignol biosynthetic pathway ……..…… 15

Figure 2.1 Protein alignment between PtrHCT1 and PtrHCT6 ……..…… 55

Figure 2.2 Visualization of the purified PtrHCT1 and PtrHCT6 in SDS-PAGE …… 56

Figure 2.3 Western blot for PtrHCT1 and PtrHCT6 antibody specificity …… 57

Figure 2.4 Optimization of temperature and pH for PtrHCTs reactions …… 58

Figure 2.5 Velocity plot of the PtrHCT1 and PtrHCT6 enzyme reactions …… 60

Figure 2.6 Double reciprocal plot of the PtrHCT1 and PtrHCT6 enzyme reactions … 61

Figure 2.7 Additive activity between PtrHCT1 and PtrHCT6 …… 64

Figure 2.8 Protein purification for the SNP variants of Ptr4CL3, PtrCCOAOMT3 and PtrCCR2 …… 67

Figure 2.9 Activity comparison for SNP variants of Ptr4CL3, PtrCCOAOMT3 and PtrCCR2 …… 68

Figure 3.1 A section of the *P. trichocarpa* monolignol biosynthetic pathway …… 81

Figure 3.2 1D-SDS-PAGE of His-tag purified recombinant Ptr4CL3 and Ptr4CL5 stained with coomassie blue …… 86

Figure 3.3 4-Coumaroyl and caffeoyl shikimic acids inhibit recombinant Ptr4CL3 and Ptr4CL5 activities …… 92

Figure 3.4 Inhibition tests for the Ptr4CL3 and Ptr4CL5 Reactions A and B, using phenylalanine, cinnamic acid, coniferaldehyde and coniferyl alcohol …… 93

Figure 3.5 Inhibition tests for the Ptr4CL3 and Ptr4CL5 Reactions A and B, when shikimic acid is added …… 94

Figure 3.6 Inhibition kinetics show that 4-coumaroyl and caffeoyl shikimic acids have distinct effects on Ptr4CL3 and Ptr4CL5 reactions …… 96

Figure 3.7 The experimental data from inhibition kinetics was analyzed by nonlinear regression using Equation 1 or Equation 3…… 97

Figure 3.8 The Michaelis-Menten kinetic parameters of Ptr4CL3 and Ptr4CL5 for 4-coumaric acid (Reaction A) and caffeic acid (Reaction B) …… 98

Figure 3.9 4-Coumaroyl and caffeoyl shikimic acids inhibit Ptr4CL reactions in SDX extracts of *P. trichocarpa* …… 100
Figure 3.10 4-Coumaroyl and caffeoyl shikimic acids inhibit Ptr4CL reactions in a mixture of the recombinant proteins in a 3 to 1 ratio of Ptr4CL3 and Ptr4CL5, where shikimic acid has not inhibitory effect …… 101
Figure 3.11 Quantification of transcript and metabolite levels of 4-coumaroyl shikimic acid and 4-coumaric acid in PtrC3H3 downregulated transgenic and wildtype of *P. trichocarpa* …… 104
Figure 3.12 The equations from Chen et al. (2014) have been modified to include the effects of inhibition by 4-coumaroyl and caffeoyl shikimic acids on Ptr4CL reactions …… 106
Figure 4.1 Rule-based modeling and evolutionary computation for multi-enzymatic reaction modeling framework …… 128
Figure 4.2 CoA ligation activity of Ptr4CL3 is affected when PtrHCT1 or PtrHCT6 is present …… 131
Figure 4.3 Protein-protein interactions between Ptr4CLs and PtrHCTs were detected by BiFC approach …… 132
Figure 4.4 Western blot using specific PtrHCT antibody to detect PtrHCT from crude SDX protein extracts …… 133
Figure 4.5 Protein-protein interactions between Ptr4CLs and PtrHCTs were detected by immunoprecipitation …… 134
Figure 4.6 Impact of Ptr4CL-PtrHCT complex formation on the CoA ligation activity toward 4-coumaric acid…… 136
Figure 4.7 Impact of Ptr4CL-PtrHCT complex formation on the CoA ligation activity toward caffeic acid…… 137
Figure 4.8 Numerical analysis of CoA ligation activity toward 4-coumaric acid …… 139
Figure 4.9 Numerical analysis of CoA ligation activity toward caffeic acid …… 139
Figure 4.10 Chemical cross-linking in SDX extracts using DSP cross-linker …… 141

Figure 4.11 Transcriptome analysis for the transcript abundance of both PtrHCT1 and PtrHCT6 transcripts in the PtrHCT downregulated transgenic and wildtype *P. trichocarpa* 142
Figure 4.12 CoA ligation activity for 4-coumaric acid and caffeic acid in the PtrHCT downregulated transgenic and wildtype *P. trichocarpa* 143
Figure 4.13 Transcriptome analysis for the transcript abundance of both Ptr4CL3 and Ptr4CL5 transcripts in the PtrHCT downregulated transgenic and wildtype *P. trichocarpa* 143
Figure 4.14 BiFC assay for the positive protein-protein interaction between PtrHCTs, PtrCAD1, PtrCOMT2 and PtrCCR2 149
Figure 4.15 BiFC assay for the negative signal between PtrHCTs, PtrCCoAOMTs and PtrCAldHs 150
Figure 4.16 The proposed monolignol biosynthetic complex from BiFC assay 151
Figure 5.1 The quantification of transcript abundance of the 42 detectable class III peroxidases in the stem wood of *P. trichocarpa* 175
Figure 5.2 Transcript abundance of the 42 detectable class III peroxidases in different tissues in *P. trichocarpa* 177
Figure 5.3 Amino acid alignment of PtrPO2, classic G peroxidase (ATP-A2) and classic S peroxidase (Zeprx) 178
Figure 5.4 Phylogenetic analysis between the PtrPOs, poplar lignin peroxidases (CWPO-C, prxA3a and PXP3-4), Arabidopsis lignin peroxidase (ATP-A2, AtPrx2, AtPrx 25, AtPrx71 and AtPrx72) and all class III peroxidases in *Arabidopsis* 181
Figure 5.5 The illustration of pBI121-based RNAi construct for downregulation of PtrPO2 in *P. trichocarpa* 182
Figure 5.6 Transcript abundance of PtrPO2 in PtrPO2 downregulated *P. trichocarpa* transgenics 183
Figure 5.7 The RNAi specificity for PtrPO2 downregulated *P. trichocarpa* transgenics 183

Figure 5.8 Reduced growth phenotype in PtrPO2 downregulated *P. trichocarpa* transgenics 184
Figure 5.9 Red internodes of stem wood in the PtrPO2 downregulated *P. trichocarpa* transgenics 185
Figure 5.10 Reddish wood powder of the PtrPO2 downregulated *P. trichocarpa* transgenics 185
Figure 5.11 Modulus of elasticity (MOE) of PtrPO2 downregulated transgenic stem wood 187

LIST OF PUBLICATIONS

4. **Chien-Yuan Lin**, Jack P. Wang, Quanzi Li, Hsi-Chuan Chen, Jie Liu, Philip Loziuk, Jina Song, Cranos Williams, David C. Muddiman, Ronald R. Sederoff, and Vincent L. Chiang (2014). 4-Coumaroyl and Caffeoyl Shikimic Acids Inhibit 4-Coumaric Acid:Coenzyme A Ligases and Modulate Metabolic Flux for 3-Hydroxylation in Monolignol Biosynthesis of *Populus trichocarpa*. Molecular Plant (2014): ssu117 (In Press)
3. Jack P. Wang, Punith P. Naik, Hsi-Chuan Chen, Rui Shi, **Chien-Yuan Lin**, Jie Liu, Christopher M. Shuford, Quanzi Li, Ying-Hsuan Sun, Sermsawat Tunlaya-Anukit, Cranos M. Williams, David C. Muddiman, Joel J. Ducoste, Ronald R. Sederoff and Vincent L. Chiang (2014). Complete Proteomic-Based Enzyme Reaction and Inhibition Kinetics Reveal How Monolignol Biosynthetic Enzyme Families Affect Metabolic Flux and Lignin in *Populus trichocarpa*. Plant Cell. **26**, 894-914.
2. Ying-Chung Lin, Wei Li, Hao Chen, Quanzi Li, Ying-Hsuan Sun, Rui Shi, **Chien-Yuan Lin**, Jack P. Wang, Hsi-Chuan Chen, Ling Chuang, Guanzheng Qu, Ronald R. Sederoff, and Vincent L. Chiang (2014). A simple high throughput xylem protoplast system for studying wood formation. **Nature Protocols**, 9(9): 2194-2205 (2014).
1. Wei Li, Ying-Chung Lin, Quanzi Li, Rui Shi, **Chien-Yuan Lin**, Hao Chen, Ling Chuang, Guanzheng Qu, Ronald R. Sederoff, and Vincent L. Chiang (2014). A robust chromatin immunoprecipitation (ChIP) protocol for studying transcription factor (TF)-DNA interactions and histone modifications in wood forming tissue **Nature Protocols**, 9(9): 2180-2193 (2014)

LIST OF PRESENTATIONS

2. Oral Presentations: FORBIRC (2013). Dynamic Metabolic-Flux (PDMF) Model: Data acquisition
1. Poster Presentations: American Society of Plant Biologist (2013). Proteomic Based Predictive Dynamic Metabolic-Flux Model of Monolignol Biosynthesis in *Populus trichocarpa*. Plant Biology 2013, ASPB. Providence, RI.

Chapter 1

Introduction

1.1 The Plant Cell Wall

One of the distinct features of plant cells from animal cells is that plant cell possesses a cell wall. The Plant cell wall is located outside the plasma membrane of the plant cell and they may contact directly by turgor pressure [1] or indirectly using extracellular molecules, such as arabinogalactan proteins (AGPs) and wall-associated kinases (WAKs) [2]. The functions of plant cell wall are to maintain shape of plant cell and support the plant cell from collapse caused by the osmotic pressure [3, 4]. Plant cell wall is also important for plant growth [5], cell differentiation [6, 7], intercellular communication and pathogen defense [8-10]. Two types of plant cell walls, primary plant cell wall and secondary plant cell wall, can be distinguished by their time of deposition, function and the composition.

1.1.1 The Primary Plant Cell Wall

The primary plant cell wall is relatively thin (often approximately 0.1 μm thick) and basically composed of cellulose microfibrils, crosslinked glycans and proteins. The primary plant cell wall is highly hydrated and approximately about 90% polysaccharides and 10%

protein [11]. The primary cell wall is produced by the growing cell and has the ability to elongate or swell during growth of plant cell [12, 13]. Two types of primary plant cell walls, Type I and Type II, are classified according to their crosslinking glycans, the hemicelluloses [14]. Type I primary plant cell walls are representative cell walls of Dicotyledonae, where xyloglucan (XG) is the major crosslinking glycan [14]. Type I primary plant cell wall is composed of 15-40% cellulose, 20-30% XG and 30-50% pectin [12, 13]. Pectin functions as matrix that embeds cellulose, hemicelluloses and cell wall proteins, which have been proposed as important molecules for controlling cell porosity for cell-cell adhesion [15-18]. The two main components of pectin are polygalacturonic acids (PGAs), which are helical homopolymers of α-1,4-linked D-galacturonic acid, and the rhamnogalacturonan I (RG I), which is a twisted rod-like heteropolymer that has a α-1, 4-linked D-galacturonic acid backbone but is interrupted by α-1, 2-linked L-rhamnose residues [19]. Type II primary plant cell walls can be found in the monocot family Poaceae and closely related grasses. Type II primary plant cell walls have a similar cellulose microfibril structure as the Type I cell wall but glucuronoarabinoxylans (GAXs) are the main hemicellulose interweaving with the cellulose microfibrils in the Type II primary plant wall. The Type II primary plant cell wall can be distinguished from the Type I plant cell wall because it is poor in pectin and lacks structural proteins, such as extensins [14, 20].

1.1.2 The Secondary Plant Cell Wall

The secondary plant cell walls are thicker than primary plant cell wall and are deposited in the primary cell wall when cell expansion ceases. The secondary cell wall, which is typically a lignified plant cell wall, is the main target for studying the lignin biosynthesis. The secondary plant cell walls are present in specialized cells that function for greater mechanical and structural support are mostly sclerenchyma cells, which include xylem vessels, tracheary elements, fibers in the xylem tissue of woody plants and sclereids [5, 21-23]. In addition to sclerenchyma, secondary cell wall can also be found in other cells, such as cotton fibers, guard cells and root endodermal cells [24]. The production of the secondary cell wall among vascular plants began 430 million years ago and is considered as one of the most important evolutionary advances for vascular plants to overcome the dry environment of the land [25]. With the support from secondary cell walls, trees are able to grow over 100 meters in height, such as Hyperion (California redwood), and able to withstand natural decay over a long period of time (~4800 years) [26]. The secondary plant cell walls produced by vascular plants is the major component of the plant biomass in our ecosystem and, also, an abundant carbon reservoir for carbon recycling [26]. Because the large quantity and the renewability of the plant biomass, secondary cell wall is utilized in many different aspects through our daily activities, such as food, clothing, furniture, paper and biofuel fuel production.

The plant secondary cell wall is less hydrated than the primary cell wall and contains only ~30% of water [5]. The three major components of plant secondary cell wall are cellulose (40-80%), hemicelluloses (10-40%) and lignin (5-25%) [27-29]. In plant secondary cell walls, cellulose microfibrils are embedded in lignin, which is a heterogeneous phenolic polymer that gives additional rigidity and physical strength to the plant cell wall [20]. Different from primary wall, xylan and glucomannan are the major hemicelluloses of the secondary cell wall [30]. In woody plants, xylan is predominant in the secondary cell wall of angiosperms, such as poplar, while galactoglucomannan is the major hemicellulose of gymnosperms, such as pine [26].

According to the different orientation of cellulose microfibrils, the secondary cell wall can be further divided into three layers, namely S1, S2 and S3, whereas the cellulose microfibrils in the plant primary cell wall are aligned irregularly [31]. The S1 layer of the plant secondary cell wall is adjacent to the plant primary cell wall and it is the first produced secondary cell wall layer, which has thickness between 0.1 to 0.35 μm. The S3 layer is located next to the cell membrane and has thickness from 0.5 to 1.10 μm. The S1 and S3 layers have flat helix orientated cellulose microfibrils, which are about 60°-90° with regard to the elongation axis of the cell. The S2 layer is between S1 and S3 layers, which has thickness between 1 to 10 μm and is about 75-85% of the thickness of the total plant cell wall. The orientation of the cellulose microfibrils in S2 layer is only 5°-30° to the plant cell axis [32].

The cellulose microfibril angle of the S2 layer has a great influence on the strength of the cell wall [31]; however, how plant cell determines the angle of the cellulose microfibril is still unknown. Because of the thickness and the arrangement of the cellulose microfibrils, the S2 layer is the main layer that gives the mechanical support to the plant tissue. Lignification of the secondary cell wall occurs in the S1 and S2 layers, while rarely occurs in S3 layer [27].

1.2 Plant Cell Wall Components

Plant cell walls, when principally composed of secondary cell walls, are made of three major components, cellulose, hemicelluloses and lignin. For example, poplar wood consists of 48- 50% cellulose, 27-30% hemicelluloses and 20-21% lignin [33], whereas pine wood contains 41% cellulose, 27% hemicelluloses and 29% lignin [30]. In this section, the structure and the biosynthesis of these three components in the plant secondary cell wall are briefly introduced and compared to the plant primary cell wall.

1.2.1 Cellulose

Cellulose, as the most abundant biopolymer in plants, is the fundamental building block of microfibrils of the plant cell wall [34, 35]. Cellulose is composed of linear, unbranched and parallel chains of several hundred over ten thousand β-1, 4-linked D-glucose units. The position C-1 of exposed glucose at end of cellulose chain is the reducing end, which is ring-

open and exposes an aldehyde group. Cellobiose represents two glucoses linked by a β-1, 4-linked bond and is the basic repeat unit of cellulose [34]. The degree of polymerization of cellulose in a primary cell wall is in a range from 5,000 to 7,000, whereas in wood (secondary cell wall) is around 10,000-15,000 [36, 37]. Hydroxyl groups are the functional groups of cellulose chain, which they can interact with each other, as well as to water molecules, to form hydrogen bonds; therefore, cellulose is mostly hydrophilic in their character because the existence of hydrogen bonds. In its natural format, cellulose is highly crystalline due to the strong association of inter- and intra- hydrogen bonds and Van Der Waals force between the different cellulose chains. Those non-covalent bondings provide microfibrils better mechanical support for encountering internal and external force [38].

It was proposed in 1996 by Brown that cellulose biosynthesis occurs on a membrane, through a rosette form of a cellulose synthase (CesA) complex [39-43]. There are 10 *CESA* genes in the genome of *Arabidopsis thaliana*; six of *CESA*s (*CesA*1, *CesA2*, *CesA*3, *CesA*5, *CesA*6 and *CesA*9) and other three *CesA*s (*CesA*4, *CesA*7, and *CesA*8) are the main catalytic subunits for primary and secondary cell wall synthesis, respectively [44-48]; Other proteins (KORRIGAN (KOR), COBRA (COB) and KOBITO1 (KOB1) and cellulose synthase-interactive protein1 (CSI1)) identified from *Arabidopsis* mutants are also important for the cellulose biosynthesis [47, 49]. *KORRIGAN* encodes a membrane bound endo-1,4-β-glucanase [50-53], *COBRA* encodes an anchored protein for oriented cell expansion [54, 55] and *KOBITO1* encodes a membrane protein necessary for cellulose biosynthesis [56].

In *Populus trichocarpa*, 18 gene models of *CesA* catalytic subunits had been identified and categorized into 9 distinct groups according to their sequence similarities [57]. The nomenclature and gene models have been updated [58]. Recently, Two types of cellulose synthase complexes (CSCs) in *Populus* (*P. deltoides* x *P. trichocarpa*) have been studied, which Type I CSC (*CesA4*, *CesA7-A*, *CesA7-B*, *CesA8-A* and *CesA8-B*) and Type II CSC (*CesA1-A*, *CesA1-B*, *CesA3-C*, *CesA3-D*, *CesA6-E* and *CesA6-F*) are the CSCs for secondary and primary cell wall syntheses, respectively [59].

1.2.2 Hemicelluloses

Hemicelluloses, classified as the non-cellulosic polysaccharides, are low-molecular weight polymers that use hydrogen bonds to link to the surface of cellulose microfibrils. Hemicelluloses are defined as polysaccharides in plant cell walls that are, less frequently, solubilized by water but can be solubilized by aqueous alkali [60, 61]. The composition of hemicellulose principally consists of β-1, 4-linked glycans within its backbone with a complex combination of heterogeneous glycosyl substituents or linkages, such as D-xylose, D-mannose, D-galactose, D-glucose, L-arabinose, 4-*O*-methyl-D-glucuronic acid, D-galacturonic acid, and D-glucuronic acid or, rarely, L-rhamnose and L-fucose [30]. Hemicelluloses are present in the cell walls of all terrestrial plants including XGs, xylans, mannans and glucomannans [62]. The degree of polymerization of hemicelluloses is averaged at between 70 and 200 [37].

As mentioned in **Section 1.1.1**, the major hemicellulose in the primary cell walls of dicotyledons is XG, which can make up 20-25% of the wall such as in *Arabidopsis* [14, 62-64]. The backbone of XG is made of *β*-1, 4-linked glucose units, up to 75% in dicotyledons and 40% in grasses, the C-6 locations of the glucose residues are substituted with xylose units [64]. In plants, xylosyl-groups are found to be substituted at the *O*-2 position with galactosyl, galacturonosyl, arabinosyl, or other glycosyl residues [65-68], where the galactosyl residues can be further substituted with fucosyl- and/or *O*-acetyl substituents [65]. In monocots (grasses and related plants), GAX is the main hemicellulose in their Type II primary cell wall, which is a linear chain of *β*-1, 4-linked D-xylose with either arabinose at the *O*-3 or glucosyluronic acid at the *O*-2 of the xylosyl unit [62]. In plant primary cell walls, XG interacts with celluloses and forms the major "load-bearing" network to prevent cells from collapsing under osmotic stress [4]. It had been shown that XG can also covalently link to pectin in primary cell wall [69].

In the secondary cell wall of dicots, xylan is the main hemicellulose [65], constituting about 20-30% of the biomass. In some tissues of monocots, xylan can be up to 50% [64]. Xylan is a linear polymer of *β*-1, 4-linked xylose that has a degree of polymerization of around 100 to 145 [70, 71]. The xylose can be replaced by *α*-1, 2-linked glucuronic acid, *α*-1, 2-linked 4-*O*-methylglucuronic acid or *α*-1, 3-linked arabinose. In dicots, glucuronoxylan (GX) is the dominate hemicellulose present in the secondary cell wall by substituting glucuronic acid with xylan. In gymnosperms, galactoglucomannan is the main hemicellulose.

It has a similar backbone as glucomannan but has α-1, 6-linked galactose added onto the mannose, and the hydroxyl groups in locations C-2 and C-3 of mannose are partially acetylated. The structure of the glucomannan is a linear polymer composed of β-1, 4-linked D-mannose and β-1, 4-linked D-glucose with a ratio around 2:1 [72]. In wood, two major hemicelluloses in the secondary cell wall are *O*-acetyl-4-*O*-methylglucuronoxylan and glucomannan, which is about 85% and 15% of total hemicelluloses, respectively [64, 73-80].

Hemicelluloses were proposed to be synthesized by cellulose synthase-like (Csl) enzymes on the Golgi membrane [28, 44, 62, 81]. In *P. trichocarpa*, 30 gene models have been identified as *Csl* gene families, which are classified into *PtCslA*, *B*, *C*, *D*, *E*, and *G* subfamilies [77]. The tissue expression profile of 21 *PtCsl* genes has also been studied; only four are xylem-specific (*PtCslA1*, *A2*, *A5*, and *D6*), two are shoot specific (*PtCslC1* and *C4*) and other *PtCsls* are inconclusive due to their low-expression level; moreover, *PtCslA1* and *PtCslA3* encode a β-mannan synthase (ManS) activity, whereas *PtCslA5* has essentially no such activity [77]. However, the hypothesis that Csls are the major hemicellulose synthetic enzymes has been challenged because only mannan synthase (CslA) is induced during wood formation and other *Csls* have no xylan synthase activity [76, 82]. Later on, by using microarray analysis, the glycosyltransferase (GT) family was identified as the source of the xylosyltransferases (xylTs) used during wood formation [76]. From complementation analysis, GTs in poplar, such as GT47C, GT8D, GT43B and GT8E/F are functional orthologs of *Arabidopsis* IRX7/FRA8 (GT family 47), IRX8/AtGAUT12 (GT family 8), IRX9 (GT

family 43) and PARVUS, respectively [80, 83-85]. Detailed dissection of the functions of the GT43 and GT8D family in *P. trichocarpa* revealed that PtrGT43A/B/E (Group1) and PtrGT43C/D (Group2) are involved in the biosynthesis of xylan backbones, and GT8D is essential for the biosynthesis of the xylan reducing end sequences [86], which are conserved in *Arabidopsis* [85]. It has been demonstrated that NAC TFs and their downstream effectors, such as MYB46 and MYB83, directly regulate xylan biosynthesis genes, including *PARVUS*, IRX10 and *UDP-Xyl synthase* (*UXS3/6*) [24, 32, 87]. In *P. trichocarpa*, overexpression of wood NAC domain 2B (PtrWND2B) can induce *PtrGT43A* and *PtrGT47C* [88].

1.2.3 Lignin

Lignin, as one of three major components of the secondary cell wall, is a heterogeneous phenolic polymer with average molecular weight about 8,000 to 11,000. Lignin content can range widely from 15-36% in different woody plants species [38, 89, 90]. Lignin is composed of phenylpropanoid subunits linked by ether bonds and interweaves with cellulose microfibrils through ferulic acid by ester and ether bonds [91]. The three principal phenylpropanoid subunits as known as 4-hydroxyphenyl (H), guaiacyl (G) and syringyl (S) subunits, polymerized from 4-coumaryl, coniferyl and sinapyl alcohols, respectively [92]. In angiosperms, such as *P. trichocarpa*, S and G subunits (ratio= 2:1) with traces of H subunits are found in lignin polymer [93], whereas in most of gymnosperms, such as pine, G unit is the main subunit [90]. In grasses, higher amounts of H subunits (<~5%) can be found in

lignin with similar amount of G and S subunits [94, 95]. However, in the same species, the content and composition of lignin can vary among different cell types including xylem vessels, tracheary elements and fibers in the xylem tissue of woody plants [96, 97]. For example, in angiosperm wood, G subunits are enriched in vessels and S subunits are enriched in fibers [98-100]. The deposition of S subunits succeeds after G subunits deposition in the differentiating xylem elements [101-103], where H subunits deposit occur in cell corners and middle lamella [104]. Moreover, phenolic compounds other than H, G and S subunits can also be incorporated into lignin when they accumulate to a high level, such as hydroxycinnamaldehydes are found in the lignin of cinnamyl alcohol dehydrogenase (CAD) deficient mutants of pine and transgenic tobacco [105, 106] and 5-hydroxylated guaiacyl (5-OH-G) subunit is identified in the lignin of caffeic acid *O*-methyltransferase (AldOMT) transgenic plants and deficient maize mutants [107-113].

The difference between H, G and S subunits is the substitution number of methoxyl group (-OH) on the phenyl ring. The lignin polymerization from monolignol subunits is believed to occur by combinatorial events through radical coupling [90, 114-116]. The more methoxyl substitutions are on the phenyl ring of monolignol subunits (S > G > H), the lesser reactive sites are available for the combinatorial events of lignin polymerization [29, 113, 117-119]. The S subunit possesses two methoxyl groups on its phenyl ring and is prone to link using the labile and less condensed ether bonds, the β-aryl ether (β-O-4), at the 4-hydroxyl group [120]. Thus, lignin that has more S subunits will be easier to delignify, which

has a positive impact on cell wall degradability [121-123]. Compared to the S subunit, the G subunit has a free C-5 position that will form more condensed lignin composed of a greater portion of biphenyl (5-O-4) and other carbon-carbon (C-C) linkages ("condense bonds") [120, 124]. The G subunits will produce lignin polymers with more branched structures and a higher degree of polymerization that could hinder the delignification process [125]. The H subunit has no methoxyl substitution on the phenyl ring; therefore, the unpaired electron density is greatest on the carbon, and consequently, the preference is for C-C linkage and will create a highly condensed lignin structure [89, 122, 126, 127].

Lignin provides additional mechanical support to the plant secondary cell wall and makes plant cell wall become more rigid and stable. As a phenolic polymer, lignin is hydrophobic. The complex of cellulose, hemicelluloses and lignin in the secondary cell wall reduces the permeability and porosity of plant cell wall, but facilitates the vertical water transport through xylem [89]. The lignification of the secondary cell wall is considered as the last step in the xylem differentiation before entering into programming cell death [128, 129]. The diverse and versatile lignin structure provides plant cell walls with additional stability and resistance from degradation by biological and chemical attack.

Overall, lignin is an important component in secondary cell wall for plant erect growth, water transport and pathogen resistance [90, 130]. However, lignin is also considered as the hindrance of plant biomass for economic processing, which results in more chemical waste during paper pulping and decreased the conversion efficiency as livestock forage [131, 132].

Both lignin content and composition in plant species determine their recalcitrance during delignification for paper and pulp or biofuel production. Lowering lignin content or increasing S/G ratio in lignin composition have shown positive correlations with the yield of fermentable sugars and the economic value of plant biomass for industrial needs [110, 112, 113, 132-143].

1.3 The Monolignol Biosynthetic Pathway

The phenylpropanoids are defined as a diverse compounds, derived from the phenylalanine, involved in plant defense, structural support, pigmentation, signaling and plant survival, such as benzoates and salicylates, flavonoids, hydroxycinnamic acid conjugates, coumarins, and lignans in addition to lignin [144-146]. Lignin, as a phenolic compound, is polymerized from monolignols synthesized from the phenylpropanoid pathway. After many decades of efforts, ten monolignol biosynthetic enzyme families have been characterized and depicted as successive steps in a metabolic grid since 1955 (**Figure 1.1**) [94, 128, 147-156]. The main path of metabolic flux of the current view of the monolignol biosynthetic pathway starts from phenylalanine (Compound 1 in **Figure 1.1**). First, phenylalanine (1) is deaminated to cinnamic acid (Compound 2) by phenylalanine ammonia-lyase (PAL). Second, Cinnamic acid (2) is hydroxylated at the position C-4 by cinnamic acid 4-hydroxylase (C4H) to form 4-coumaric acid (Compound 3). Third, 4-coumaric

acid:coenzyme A (CoA) ligase (4CL) activates the 4-coumaric acid (3) to the 4-courmaroyl-CoA (Compound 8) by consuming an ATP. Forth, the 3-hydroxylation of 4-courmaroyl-CoA (8) is catalyzed sequentially by the 4-hydroxycinnamoyl-coenzyme A:shikimic acid hydroxycinnamoyl transferase (HCT) to form 4-coumaroyl shikimic acid (compound 9) followed by 4-coumaric acid 3-hydroxylase (C3H) to form caffeoyl shikimic acid (compound 10) and subsequently, the conversion of caffeoyl shikimic acid (10) by HCT to form caffeoyl-CoA (compound 11). The 3-hydroxylation can also occur directly from 4-coumaric acid (3) to caffeic acid (Compound 4) by a C3H/C4H protein complex. Fifth, the caffeoyl-CoA (11) is methylated at the 3-OH position by caffeoyl-CoA *O*-methyltransferase (CCoAOMT) to feruloyl-CoA (compound 12) and then reduced to coniferaldehyde (compound 17) by cinnamoyl-CoA reductase (CCR). Finally, coniferaldehyde (17) is reduced by cinnamyl alcohol dehydrogenase (CAD) to form coniferyl alcohol (compound 22), the G subunit precursor. Alternatively, coniferaldehyde (17) can also proceed by additional 5-hydroxylation at the position C-5 by coniferaldehyde 5-hydroxylase (CAld5H) to 5-hydroxylconiferaldehyde (compound 18). 5-hydroxylconiferaldehyde (18) is then methylated at the position of 5-OH by caffeic acid *O*-methyltransferase (AldOMT) to form sinapaldehyde (compound 19) and then reduced by CAD to sinapyl alcohol (compound 24), the S subunit precursor.

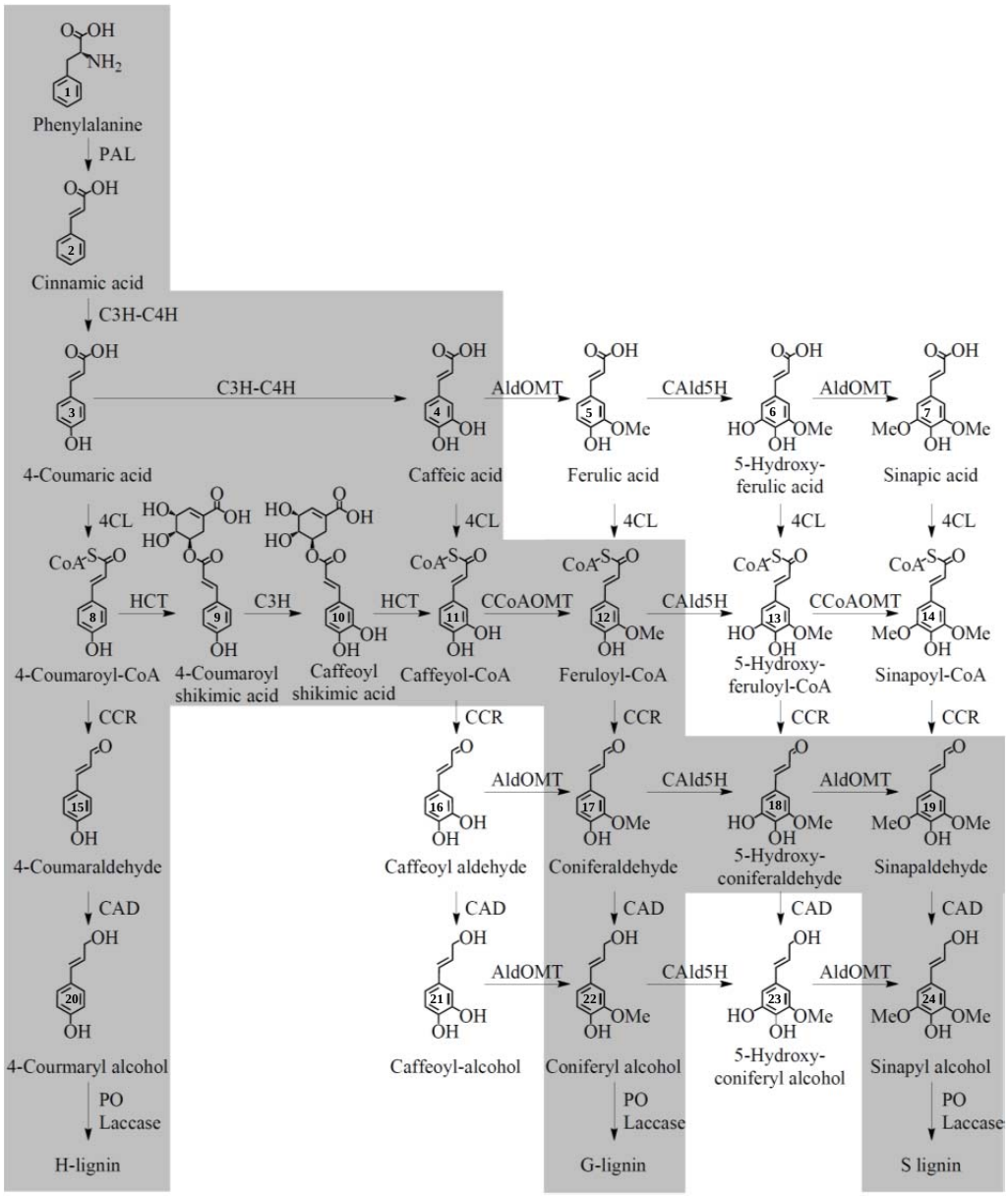

Figure 1.1 – The current monolignol biosynthetic pathway. The main metabolic flux for the biosynthesis of three types of monolignols (4-coumaryl, coniferyl and sinapyl alcohols) is highlighted in grey. There are 10 monolignol biosynthetic enzyme families involved in the monolignol biosynthetic pathway, which are phenylalanine ammonia-lyase (PAL), cinnamic acid 4-hydroxylase (C4H), 4-coumaric acid 3-hydroxylase (C3H), 4-coumaric acid:coenzyme A ligase (4CL), 4-hydroxycinnamoyl-CoA:shikimic Acid hydroxycinnamoyl Transferase (HCT), caffeoyl-CoA *O*-methyltransferase (CCoAOMT), coniferaldehyde 5-hydroxylase (CAld5H), 5-hydroxyconiferaldehyde *O*-methyltransferase (AldOMT), cinnamoyl-CoA reductase (CCR) and cinnamyl alcohol dehydrogenase (CAD). 24 metabolites are numbered.

1.4 Lignin Polymerization

After more than a century of debate, lignin polymerization, as the final step of lignin biosynthesis, is supported by two contradictory hypotheses: protein (dirigent) controlling polymerization [157-164] and random radical coupling [29, 92, 115, 158, 160, 165-169]. However, the combinatorial coupling model by radicals is widely recognized because it gives the better explanation for the versatile structure of lignin [89, 114-116]. The successive steps of lignin polymerization are as follow: First, the hydroxyl groups of monolignol precursors are oxidized by peroxidase to form resonance-stabilized phenoxy radical [170]. Second, the monolignol free radicals generated by an oxidase or by an oxidase-generated monolignol radical undergo radical coupling reaction to form dilignols. Then, the combination of these processes will lead to longer lignin polymer. The β-O-4 and β-5 coupling lead to a linear lignin polymer, whereas branching of the polymer will occur when different types of coupling are taking place [61, 171].

So far, both peroxidases [172-197] and laccases [198-206] are the oxidases proposed to be involved in lignin polymerization in plants. The role of laccase is suggested to involve in the early stages of lignification before peroxidase. Recently, in *P. trichocarpa*, overexpression of Ptr-mirRNA397 can downregulate 17 PtrLACs and showed reduction in Klason lignin content from 12% to 22% [207]. However, the discovery of lignin peroxidase in *P. trichocarpa* is still ongoing.

1.5 Monolignol Biosynthesis in *Populus trichocarpa*

The studies of monolignol biosynthesis have been conducted extensively in woody plant, such as poplar, to attempt to decrease the recalcitrance of biomass for the increasing demand of forest products [110, 113, 133, 134, 136]. The genus *Populus* includes various species commonly called “poplar”, “aspen” or “cottonwood” and *Populus trichocarpa* is one of the best known species [33]. The species in *Populus* are fast-growing and have other advantageous characters, such as moisture-loving and shade-intolerant [33, 208]. In 2006, the full genome of *P. trichocarpa* had been sequenced, which was the first tree species that had been sequenced at that time [209]. The genome of *P. trichocarpa* has a total 485 million base-pairs (Mb) divided into 19 chromosomes and 45,555 putative genes were estimated to be encoded in its diploid (2n=38) genome [209]. Understanding monolignol biosynthesis in *P. trichocarpa* could lead us to design better strategies to improve biomass.

A systematic approach had been performed toward the whole monlignol biosynthetic pathway in *P. trichocarpa* [155]. Overall, 95 gene models were identified as putative phenylpropanoid biosynthesis genes, systematically and manually. Within 95 gene models, the most xylem abundant monolignol biosynthetic genes were identified by comparing the expression level among 4 different tissues including, stem differentiating xylem (SDX), stem differentiating phloem (SDP), shoot tip (S) and fully expanded leaf (L). Of 95 genes, 18 genes were determined as abundant and specific to the SDX tissue and the result showed

most of the monolignol biosynthesis genes exist in gene families. In summary, the xylem-specific monolignol biosynthetic enzymes in *P. trichocarpa* are five in the phenylalanine ammonia-lyase (PAL) family (PtrPAL1, 2, 3, 4 and 5), two in the cinnamic acid 4-hydroxylase (C4H) family (PtrC4H1 and PtrC4H2), one in the 4-coumaric acid 3-hydroxylase family (PtrC3H3), three in the 4-coumaric acid:coenzyme A (CoA) ligase (4CL) family (Ptr4CL3 and Ptr4CL5), two in the 4-hydroxycinnamoyl-coA:shikimic acid hydroxycinnamoyl transferase (HCT) family (PtrHCT1 and PtrHCT6), three in the caffeoyl-CoA *O*-methyltransferase (CCoAOMT) family (PtrCCoAOMT1, PtrCCoAOMT2, and PtrCCoAOMT3), one in the cinnamoyl-CoA reductase (CCR) family (PtrCCR2), one in the cinnamyl alcohol dehydrogenase (CAD) family (PtrCAD1), two in the coniferaldehyde 5-hydroxylase (CAld5H) family (PtrCAld5H1 and PtrCAld5H2) and one in the caffeic acid *O*-methyltransferase (AldOMT) family (PtrCOMT2) [155]. All those putative monolignol biosynthetic enzymes were identified by quantitative real-time PCR.

Recently, enzyme kinetic studies have been performed on these identified monolignol biosynthetic enzymes in *P. trichocarpa*, which extends our knowledge of those newly identified enzymes and the regulation mechanisms in the monolignol biosynthetic pathway in *P. trichocarpa*. Regulation between all five PtrPAL family (PtrPAL1 to 5) had been revealed [210]. The five *PtrPAL* genes can be classified into two subgroups while the subgroup A (*PtrPAL2*, *4* and *5*) is about five times more abundant than subgroup B (*PtrPAL1* and *3*) in stem wood forming tissue, which indicates a greater functional significance of subgroup A

PtrPALs for stem wood formation [210]. The 3- and 4-hydroxylations of the monolignol precursors had also been studied in *P. trichocarpa* and a novel 3-hydroxylation activity of 4-coumaric acid (3) to caffeic acid (4) catalyzed by the newly identified PtrC3H3/PtrC4H1/PtrC4H2 membrane protein complex was discovered [148]. This alternative 3-hydroxylation route has been incorporated into the current proposed monolignol biosynthetic pathway (**Figure 1.1**). For the CoA ligation step in *P. trichocarpa*, two studies had been successively published; first, of three xylem-specific Ptr4CLs (Ptr4CL3, 5 and 17), Ptr4CL3 and Ptr4CL5 are abundant in wood forming tissue and have CoA ligation activity, where Ptr4CL5 is identified as a regulatory enzyme [149]. Second, a systematic approach was conducted to understand the regulatory mechanism between Ptr4CL3 and Ptr4CL5. This study revealed that Ptr4CL3 and Ptr4CL5 form a heterotetrameric protein complex with a Ptr4CL3 to Ptr4CL5 ratio of 3 to 1 and, further, to regulate the metabolic flux of the CoA ligation steps [211]. The study on the two xylem-specific and functional 5-hydroxylases (PtrCAld5H1 and PtrCald5H2) has shown that they have essentially the same biochemical functions, suggesting functional redundancy and independence of these two enzymes [212].

In order to have a comprehensive understanding the metabolic flux of the whole monolignol biosynthetic pathway in *P. trichocarpa,* we need to have, at least, the basic enzyme kinetic information of all identified *P. trichocarpa* monolignol biosynthetic enzymes [155]. A comprehensive metabolic flux model of the whole monolignol biosynthesis in *P. trichocarpa* can be built when the model includes the information of pathway enzymes, such

as absolute quantity of the each enzymes, enzyme kinetics, inhibitory effect of pathway intermediates and enzyme-enzyme interaction among monolignol biosynthetic enzymes.

1.6 Synopsis of Completed Research

Our ultimate goal is to establish a bioinformatic model to predict how monolignol biosynthetic enzymes can affect the lignin formation in *P. trichocarpa*. Several studies had attempted to describe monolignol biosynthesis in plants by mathematical modeling. In quaking aspen (*Populus tremuloides*), a mathematical model incorporates the published results using flux balance analysis (FBA) and nonlinear dynamic modeling to describe the monolignol biosynthesis network in *Populus* xylem was produced [213], but lack of the experimental data of reaction rates for several enzymes limit the power to describe the dynamic range of flux *in vivo*. A similar study using static flux-based analysis model combined with a Monte Carlo simulation model was conducted to explore the unforeseen consequences from genetic manipulations of monolignol biosynthetic enzymes in alfalfa (*Medicago sativa* L.) [153]. This model evaluates randomly chosen sets of kinetic parameters against kinetic models of lignin biosynthesis in different stem internodes of wildtype and lignin-modified alfalfa plants and reveals a feedforward regulatory mechanism for monolignol biosynthesis in *Medicago* [153]. Subsequently, a computational approach was used to assess the possible metabolic channeling in lignin biosynthesis of *Medicago* that

could arise *in vivo* and the method helped to distinguish crosstalk between the G subunit-specific channel and S subunit-specific channeling [214]; however, the experimental validations are still needed to support their hypothesis of metabolic channeling [215]. To build a comprehensive model, the predictive kinetic metabolic-flux (PKMF) model, for the whole monolignol biosynthetic pathway in *P. trichocarpa,* we considered the dynamic and regulatory behavior of all the enzymes in the metabolic network and described them by differential equations with mass action kinetics [215].

Before building the PKMF model for monolignol biosynthesis in *P. trichocarpa*, several parameters in the pathway need to be obtained, including the abundance of the all the monolignol biosynthetic enzymes and their isoforms, the concentration of the 24 pathway metabolites and, most importantly, the characteristics of their reactions and inhibition kinetic parameters. In **Chapter 2**, the Michaelis-Menten enzyme kinetics of PtrHCT is reported. The two xylem-specific PtrHCTs, the PtrHCT1 and PtrHCT6, were cloned from *P. trichocarpa* cDNA library. Both PtrHCTs were expressed in *Escherichia coli* and purified by glutathione-S-transferase (GST) affinity chromatography. The optimal reaction temperature and pH values for these two PtrHCT enzymes are first evaluated by a range of different conditions before conducting the Michaelis-Menten kinetic analysis. Kinetic parameters, such as K_m and k_{cat}, of all the PtrHCT substrates were obtained, which allowed us to incorporate these data into the PKMF model for complete metabolic flux prediction. Also, the enzyme activities of the single nucleotide polymorphism (SNP) variants of Ptr4CL3, PtrCCR2 and

PtrCCoAOMT3 are also evaluated. In **Chapter 3,** the regulation on the Ptr4CL CoA ligation activity by shikimic acid esters, the 4-coumaroyl and caffeoyl shikimic acids, is described based on the enzyme kinetic properties of PtrHCTs. Both 4-coumaroyl and caffeoyl shikimic acids are identified as inhibitors of Ptr4CL3 and Ptr4CL5. 4-Coumaroyl shikimic acid strongly inhibits formation of 4-coumaroyl-CoA and caffeoyl-CoA. Caffeoyl shikimic acid inhibits only formation of 4-coumaroyl-CoA. Using equations that combine the mass action kinetics and inhibition kinetics, the regulatory role of the two shikimic acid esters on the metabolic flux of 3-hydroxylation is proposed. In **Chapter 4**, a protein-protein interaction between monolignol biosynthetic enzymes of Ptr4CL and PtrHCT is identified. Based on several lines of evidence, such as bimolecular fluorescence complementation (BiFC), immunoprecipitation, chemical crosslinking, mechanistic modeling and PtrHCT downregulated transgenics, a Ptr4CL-PtrHCT protein complex is proposed. In **Chapter 5**, a study on the lignin polymerization in *P. trichocarpa* is performed. Using a systemic approach, a unique anionic *P. trichocarpa* peroxidase (PtrPO2) is identified as the most xylem-abundant and xylem-specific peroxidase. Downregulation of PtrPO2 shows reduction in growth and lignin content, reddish internodes of stem and wood composition. A possible role of PtrPO2 in lignin polymerization is discussed.

1.7 References

1. Roberts, K., *Structures at the plant cell surface.* Current opinion in cell biology, 1990. **2**(5): p. 920-8.

2. Kohorn, B.D., *Plasma membrane-cell wall contacts.* Plant physiology, 2000. **124**(1): p. 31-8.

3. Zhu, J.K., et al., *Enrichment of vitronectin- and fibronectin-like proteins in NaCI-adapted plant cells and evidence for their involvement in plasma membrane-cell wall adhesion.* The Plant journal : for cell and molecular biology, 1993. **3**(5): p. 637-46.

4. Albersheim, P., et al., *Plant cell walls: from chemistry to biology*2010: Garland Science, Taylor and Francis Group, LLC.

5. Cosgrove, D.J., *Growth of the plant cell wall.* Nature reviews. Molecular cell biology, 2005. **6**(11): p. 850-61.

6. Fukuda, H. and A. Komamine, *Establishment of an Experimental System for the Study of Tracheary Element Differentiation from Single Cells Isolated from the Mesophyll of Zinnia elegans.* Plant physiology, 1980. **65**(1): p. 57-60.

7. Fukuda, H. and A. Komamine, *Lignin synthesis and its related enzymes as markers of tracheary-element differentiation in single cells isolated from the mesophyll of Zinnia elegans.* Planta, 1982. **155**(5): p. 423-30.

8. Esquerre-Tugaye, M.T., et al., *Cell Surfaces in Plant-Microorganism Interactions: II. Evidence for the Accumulation of Hydroxyproline-rich Glycoproteins in the Cell Wall of Diseased Plants as a Defense Mechanism.* Plant physiology, 1979. **64**(2): p. 320-6.

9. Ryan, C.A., *Protease Inhibitors in Plants: Genes for Improving Defenses Against Insects and Pathogens.* Annual Review of Phytopathology, 1990. **28**(1): p. 425-449.

10. Keegstra, K., *Plant cell walls.* Plant physiology, 2010. **154**(2): p. 483-6.

11. Albersheim, P., *The walls of growing plant cells.* Scientific American, 1975. **232**(4): p. 80-95.

12. Hayashi, T., *Xyloglucans in the Primary Cell Wall.* Annual Review of Plant Physiology and Plant Molecular Biology, 1989. **40**(1): p. 139-168.

13. Cosgrove, D. and m. Jarvis, *Comparative structure and biomechanics of plant primary and secondary cell walls.* Frontiers in Plant Science, 2012. **3**.

14. Carpita, N.C. and D.M. Gibeaut, *Structural models of primary cell walls in flowering plants: consistency of molecular structure with the physical properties of the walls during growth.* The Plant journal : for cell and molecular biology, 1993. **3**(1): p. 1-30.

15. Jarvis, M.C., S.P.H. Briggs, and J.P. Knox, *Intercellular adhesion and cell separation in plants.* Plant, Cell & Environment, 2003. **26**(7): p. 977-989.

16. McNeil, M., et al., *Structure and function of the primary cell walls of plants.* Annual review of biochemistry, 1984. **53**: p. 625-63.

17. Baron-Epel, O., P.K. Gharyal, and M. Schindler, *Pectins as mediators of wall porosity in soybean cells.* Planta, 1988. **175**(3): p. 389-95.

18. Mccann, M.C., B. Wells, and K. Roberts, *Direct visualization of cross-links in the primary plant cell wall.* Journal of Cell Science, 1990. **96**(2): p. 323-334.

19. Lau, J.M., et al., *Structure of the backbone of rhamnogalacturonan I, a pectic polysaccharide in the primary cell walls of plants.* Carbohydrate Research, 1985. **137**(0): p. 111-125.

20. Sticklen, M.B., *Plant genetic engineering for biofuel production: towards affordable cellulosic ethanol.* Nature reviews. Genetics, 2008. **9**(6): p. 433-43.

21. Mauseth, J.D., *Plant anatomy*1988, Menlo Park, Calif.: Benjamin/Cummings Pub. Co.

22. Ivakov, A. and S. Persson, *Plant Cell Walls*, in *eLS*2001, John Wiley & Sons, Ltd.

23. Somerville, C., et al., *Toward a systems approach to understanding plant cell walls.* Science, 2004. **306**(5705): p. 2206-11.

24. Zhong, R., C. Lee, and Z.H. Ye, *Global analysis of direct targets of secondary wall NAC master switches in Arabidopsis.* Mol Plant, 2010. **3**(6): p. 1087-103.

25. Raven, P.H., R.F. Evert, and S.E. Eichhorn, *Biology of plants.*1999, New York: W.H. Freeman : Worth Publishers.

26. Zhong, R. and Z.-H. Ye, *Secondary Cell Walls*, in *eLS*2001, John Wiley & Sons, Ltd.

27. Bidlack, J., M. Malone, and R. Benson, *Molecular structure and component integration of secondary cell walls in plants.* Proc. Okla. Acad. Sci., 1992. **72**: p. 51-56.

28. Zhang, G.F. and L.A. Staehelin, *Functional compartmentation of the Golgi apparatus of plant cells : immunocytochemical analysis of high-pressure frozen- and freeze-substituted sycamore maple suspension culture cells.* Plant Physiol, 1992. **99**(3): p. 1070-83.

29. Adler, E., *Lignin chemistry—past, present and future.* Wood Science and Technology, 1977. **11**(3): p. 169-218.

30. Timell, T.E., *Recent progress in the chemistry of wood hemicelluloses.* Wood Science and Technology, 1967. **1**(1): p. 45-70.

31. Plomion, C., G. Leprovost, and A. Stokes, *Wood formation in trees.* Plant physiology, 2001. **127**(4): p. 1513-23.

32. McCarthy, R.L., R. Zhong, and Z.H. Ye, *MYB83 is a direct target of SND1 and acts redundantly with MYB46 in the regulation of secondary cell wall biosynthesis in Arabidopsis.* Plant Cell Physiol, 2009. **50**(11): p. 1950-64.

33. Balatinecz, J.J., D.E. Kretschmann, and A. Leclercq, *Achievements in the utilization of poplar wood-guideposts for the future.* The Forestry Chronicle, 2001. **77**(2): p. 265-269.

34. Cocinero, E.J., et al., *The building blocks of cellulose: the intrinsic conformational structures of cellobiose, its epimer, lactose, and their singly hydrated complexes.* Journal of the American Chemical Society, 2009. **131**(31): p. 11117-23.

35. Payen, A., *Mémoire sur la composition du tissu propre des plantes et du ligneux.* Comptes Rendus, 1838. **7**: p. 1052-1056.

36. O'Sullivan, A., *Cellulose: the structure slowly unravels.* Cellulose, 1997. **4**(3): p. 173-207.

37. Feldman, D., *Wood—chemistry, ultrastructure, reactions, by D. Fengel and G. Wegener, Walter de Gruyter, Berlin and New York, 1984, 613 pp. Price: 245 DM*, 1985, Wiley Online Library.

38. Novaes, E., et al., *Lignin and biomass: a negative correlation for wood formation and lignin content in trees.* Plant Physiol, 2010. **154**(2): p. 555-61.

39. Brown, R.M., *The Biosynthesis of Cellulose.* Journal of Macromolecular Science, Part A, 1996. **33**(10): p. 1345-1373.

40. Kimura, S., et al., *Immunogold labeling of rosette terminal cellulose-synthesizing complexes in the vascular plant vigna angularis.* Plant Cell, 1999. **11**(11): p. 2075-86.

41. Ding, S.Y. and M.E. Himmel, *The maize primary cell wall microfibril: a new model derived from direct visualization.* J Agric Food Chem, 2006. **54**(3): p. 597-606.

42. Brown, R.M., Jr. and D. Montezinos, *Cellulose microfibrils: visualization of biosynthetic and orienting complexes in association with the plasma membrane.* Proc Natl Acad Sci U S A, 1976. **73**(1): p. 143-7.

43. Kimura, S., et al., *Immunogold labeling of rosette terminal cellulose-synthesizing complexes in the vascular plant vigna angularis.* The Plant cell, 1999. **11**(11): p. 2075-86.

44. Richmond, T.A. and C.R. Somerville, *The cellulose synthase superfamily.* Plant Physiol, 2000. **124**(2): p. 495-8.

45. Taylor, N.G., et al., *Interactions among three distinct CesA proteins essential for cellulose synthesis.* Proc Natl Acad Sci U S A, 2003. **100**(3): p. 1450-5.

46. Desprez, T., et al., *Organization of cellulose synthase complexes involved in primary cell wall synthesis in Arabidopsis thaliana.* Proc Natl Acad Sci U S A, 2007. **104**(39): p. 15572-7.

47. Endler, A. and S. Persson, *Cellulose Synthases and Synthesis in Arabidopsis.* Molecular Plant, 2011. **4**(2): p. 199-211.

48. Li, S., L. Lei, and Y. Gu, *Functional analysis of complexes with mixed primary and secondary cellulose synthases.* Plant signaling & behavior, 2013. **8**(3): p. e23179.

49. Gu, Y., et al., *Identification of a cellulose synthase-associated protein required for cellulose biosynthesis.* Proc Natl Acad Sci U S A, 2010. **107**(29): p. 12866-71.

50. Nicol, F., et al., *A plasma membrane-bound putative endo-1,4-beta-D-glucanase is required for normal wall assembly and cell elongation in Arabidopsis.* The EMBO journal, 1998. **17**(19): p. 5563-76.

51. His, I., et al., *Altered pectin composition in primary cell walls of korrigan, a dwarf mutant of Arabidopsis deficient in a membrane-bound endo-1,4-beta-glucanase.* Planta, 2001. **212**(3): p. 348-58.

52. Sato, S., et al., *Role of the putative membrane-bound endo-1,4-beta-glucanase KORRIGAN in cell elongation and cellulose synthesis in Arabidopsis thaliana.* Plant & cell physiology, 2001. **42**(3): p. 251-63.

53. Zuo, J., et al., *KORRIGAN, an Arabidopsis endo-1,4-beta-glucanase, localizes to the cell plate by polarized targeting and is essential for cytokinesis.* The Plant cell, 2000. **12**(7): p. 1137-52.

54. Schindelman, G., et al., *COBRA encodes a putative GPI-anchored protein, which is polarly localized and necessary for oriented cell expansion in Arabidopsis.* Genes & development, 2001. **15**(9): p. 1115-27.

55. Roudier, F., et al., *COBRA, an Arabidopsis Extracellular Glycosyl-Phosphatidyl Inositol-Anchored Protein, Specifically Controls Highly Anisotropic Expansion through Its Involvement in Cellulose Microfibril Orientation.* The Plant Cell Online, 2005. **17**(6): p. 1749-1763.

56. Pagant, S., et al., *KOBITO1 encodes a novel plasma membrane protein necessary for normal synthesis of cellulose during cell expansion in Arabidopsis.* The Plant cell, 2002. **14**(9): p. 2001-13.

57. Djerbi, S., et al., *The genome sequence of black cottonwood (Populus trichocarpa) reveals 18 conserved cellulose synthase (CesA) genes.* Planta, 2005. **221**(5): p. 739-46.

58. Kumar, M., et al., *An update on the nomenclature for the cellulose synthase genes in Populus.* Trends Plant Sci, 2009. **14**(5): p. 248-54.

59. Song, D., J. Shen, and L. Li, *Characterization of cellulose synthase complexes in Populus xylem differentiation.* New Phytol, 2010. **187**(3): p. 777-90.

60. Selvendran, R.R. and M.A. O'Neill, *Isolation and Analysis of Cell Walls from Plant Material*, in *Methods of Biochemical Analysis*2006, John Wiley & Sons, Inc. p. 25-153.

61. Sjöström, E., *Wood chemistry: fundamentals and applications*1993: Gulf Professional Publishing.

62. Scheller, H.V. and P. Ulvskov, *Hemicelluloses.* Annu Rev Plant Biol, 2010. **61**: p. 263-89.

63. Fry, S.C. and J.G. Miller, *Toward a working model of the growing plant cell wall.* Plant cell wall polymers. American Chemical Society, Washington, DC, 1989: p. 33-46.

64. Ebringerová, A., Z. Hromádková, and T. Heinze, *Hemicellulose*, in *Polysaccharides I*, T. Heinze, Editor 2005, Springer Berlin Heidelberg. p. 1-67.

65. Pauly, M., et al., *Hemicellulose biosynthesis.* Planta, 2013. **238**(4): p. 627-642.

66. Hantus, S., et al., *Structural characterization of novel L-galactose-containing oligosaccharide subunits of jojoba seed xyloglucans.* Carbohydrate Research, 1997. **304**(1): p. 11-20.

67. Hoffman, M., et al., *Structural analysis of xyloglucans in the primary cell walls of plants in the subclass Asteridae.* Carbohydrate Research, 2005. **340**(11): p. 1826-40.

68. Ray, B., et al., *Structural investigation of hemicellulosic polysaccharides from Argania spinosa: characterisation of a novel xyloglucan motif.* Carbohydrate Research, 2004. **339**(2): p. 201-8.

69. Popper, Z.A. and S.C. Fry, *Xyloglucan-pectin linkages are formed intra-protoplasmically, contribute to wall-assembly, and remain stable in the cell wall.* Planta, 2008. **227**(4): p. 781-94.

70. Jacobs, A. and O. Dahlman, *Characterization of the molar masses of hemicelluloses from wood and pulps employing size exclusion chromatography and matrix-assisted laser desorption ionization time-of-flight mass spectrometry.* Biomacromolecules, 2001. **2**(3): p. 894-905.

71. Jacobs, A., et al., *Characterization of water-soluble hemicelluloses from spruce and aspen employing SEC/MALDI mass spectroscopy.* Carbohydrate Research, 2002. **337**(8): p. 711-7.

72. Katsuraya, K., et al., *Constitution of konjac glucomannan: chemical analysis and 13C NMR spectroscopy.* Carbohydrate polymers, 2003. **53**(2): p. 183-189.

73. Awano, T., et al., *Deposition of glucuronoxylans on the secondary cell wall of Japanese beech as observed by immuno-scanning electron microscopy.* Protoplasma, 2000. **212**(1-2): p. 72-79.

74. Gustavsson, M., et al., *Isolation, characterisation and material properties of 4-O-methylglucuronoxylan from aspen*, in *Biorelated Polymers*2001, Springer. p. 41-52.

75. Teleman, A., et al., *Isolation and characterization of O-acetylated glucomannans from aspen and birch wood.* Carbohydrate Research, 2003. **338**(6): p. 525-34.

76. Aspeborg, H., et al., *Carbohydrate-active enzymes involved in the secondary cell wall biogenesis in hybrid aspen.* Plant Physiol, 2005. **137**(3): p. 983-97.

77. Suzuki, S., et al., *The cellulose synthase gene superfamily and biochemical functions of xylem-specific cellulose synthase-like genes in Populus trichocarpa.* Plant Physiol, 2006. **142**(3): p. 1233-45.

78. Ye, Z.-H., W.S. York, and A.G. Darvill, *Important new players in secondary wall synthesis.* Trends in Plant Science, 2006. **11**(4): p. 162-164.

79. Pena, M.J., et al., *Arabidopsis irregular xylem8 and irregular xylem9: implications for the complexity of glucuronoxylan biosynthesis.* The Plant cell, 2007. **19**(2): p. 549-63.

80. Lee, C., et al., *The poplar GT8E and GT8F glycosyltransferases are functional orthologs of Arabidopsis PARVUS involved in glucuronoxylan biosynthesis.* Plant Cell Physiol, 2009. **50**(11): p. 1982-7.

81. Richmond, T.A. and C.R. Somerville, *Integrative approaches to determining Csl function.* Plant Mol Biol, 2001. **47**(1-2): p. 131-43.

82. Pauly, M., et al., *Hemicellulose biosynthesis.* Planta, 2013. **238**(4): p. 627-42.

83. Zhou, G.K., et al., *The poplar glycosyltransferase GT47C is functionally conserved with Arabidopsis Fragile fiber8.* Plant Cell Physiol, 2006. **47**(9): p. 1229-40.

84. Zhou, G.K., et al., *Molecular characterization of PoGT8D and PoGT43B, two secondary wall-associated glycosyltransferases in poplar.* Plant Cell Physiol, 2007. **48**(5): p. 689-99.

85. Kong, Y., et al., *Two Poplar Glycosyltransferase Genes, PdGATL1.1 and PdGATL1.2, Are Functional Orthologs to PARVUS/AtGATL1 in Arabidopsis.* Molecular Plant, 2009. **2**(5): p. 1040-1050.

86. Lee, C., et al., *Molecular Dissection of Xylan Biosynthesis during Wood Formation in Poplar.* Molecular Plant, 2011. **4**(4): p. 730-747.

87. Kim, W.-C., et al., *Transcription factor MYB46 is an obligate component of the transcriptional regulatory complex for functional expression of secondary wall-associated cellulose synthases in Arabidopsis thaliana.* Journal of Plant Physiology, 2013. **170**(15): p. 1374-1378.

88. Zhong, R., et al., *Dissection of the transcriptional program regulating secondary wall biosynthesis during wood formation in poplar.* Plant Physiol, 2011. **157**(3): p. 1452-68.

89. Campbell, M.M. and R.R. Sederoff, *Variation in Lignin Content and Composition (Mechanisms of Control and Implications for the Genetic Improvement of Plants).* Plant physiology, 1996. **110**(1): p. 3-13.

90. Sarkanen, K.V. and C.H. Ludwig, *Lignins: occurrence, formation, structure and reactions*1971, New York: Wiley-Interscience.

91. Mathew, S. and T.E. Abraham, *Ferulic acid: an antioxidant found naturally in plant cell walls and feruloyl esterases involved in its release and their applications.* Critical reviews in biotechnology, 2004. **24**(2-3): p. 59-83.

92. Higuchi, T., *Biochemistry and molecular biology of wood*1997, Berlin; New York: Springer.

93. Christiernin, M., et al., *Lignin isolated from primary walls of hybrid aspen cell cultures indicates significant differences in lignin structure between primary and secondary cell wall.* Plant physiology and biochemistry : PPB / Societe francaise de physiologie vegetale, 2005. **43**(8): p. 777-85.

94. Barrière, Y., et al., *Genetics and genomics of lignification in grass cell walls based on maize as a model system.* Genes Genomes Genomics, 2007. **1**: p. 133-156.

95. Vanholme, R., et al., *Lignin biosynthesis and structure.* Plant physiology, 2010. **153**(3): p. 895-905.

96. Whiting, P. and D. Goring, *Chemical characterization of tissue fractions from the middle lamella and secondary wall of black spruce tracheids.* Wood Science and Technology, 1982. **16**(4): p. 261-267.

97. Agarwal, U.P. and R.H. Atalla, *In-situ Raman microprobe studies of plant cell walls: Macromolecular organization and compositional variability in the secondary wall of Picea mariana (Mill.) B.S.P.* Planta, 1986. **169**(3): p. 325-32.

98. Fergus, B. and D. Goring, *The distribution of lignin in birch wood as determined by ultraviolet microscopy.* Holzforschung-International Journal of the Biology, Chemistry, Physics and Technology of Wood, 1970. **24**(4): p. 118-124.

99. Fergus, B. and D. Goring, *The location of guaiacyl and syringyl lignins in birch xylem tissue.* Holzforschung-International Journal of the Biology, Chemistry, Physics and Technology of Wood, 1970. **24**(4): p. 113-117.

100. Musha, Y. and D. Goring, *Distribution of syringyl and guaiacyl moieties in hardwoods as indicated by ultraviolet microscopy.* Wood Science and Technology, 1975. **9**(1): p. 45-58.

101. Terashima, N. and K. Fukushima, *Heterogeneity in formation of lignin—XI: An autoradiographic study of the heterogeneous formation and structure of pine lignin.* Wood Science and Technology, 1988. **22**(3): p. 259-270.

102. Saka, S. and D.A. Goring, *The distribution of lignin in white birch wood as determined by bromination with TEM-EDXA.* Holzforschung-International Journal of the Biology, Chemistry, Physics and Technology of Wood, 1988. **42**(3): p. 149-153.

103. Li, L., et al., *The last step of syringyl monolignol biosynthesis in angiosperms is regulated by a novel gene encoding sinapyl alcohol dehydrogenase.* The Plant cell, 2001. **13**(7): p. 1567-86.

104. Grünwald, C., K. Ruel, and U. Schmitt, *Differentiation of xylem cells in rolC transgenic aspen trees-a study of secondary cell wall development.* Annals of Forest Science, 2002. **59**(5-6): p. 679-685.

105. Chabannes, M., et al., *In situ analysis of lignins in transgenic tobacco reveals a differential impact of individual transformations on the spatial patterns of lignin*

deposition at the cellular and subcellular levels. The Plant Journal, 2001. **28**(3): p. 271-282.

106. Lapierre, C., et al., *Lignin structure in a mutant pine deficient in cinnamyl alcohol dehydrogenase.* Journal of agricultural and food chemistry, 2000. **48**(6): p. 2326-31.

107. Dwivedi, U.N., et al., *Modification of lignin biosynthesis in transgenic Nicotiana through expression of an antisense O-methyltransferase gene from Populus.* Plant molecular biology, 1994. **26**(1): p. 61-71.

108. Ni, W., N. Paiva, and R. Dixon, *Reduced lignin in transgenic plants containing a caffeic acidO-methyltransferase antisense gene.* Transgenic Research, 1994. **3**(2): p. 120-126.

109. Atanassova, R., et al., *Altered lignin composition in transgenic tobacco expressing O-methyltransferase sequences in sense and antisense orientation.* The Plant Journal, 1995. **8**(4): p. 465-477.

110. Van Doorsselaere, J., et al., *A novel lignin in poplar trees with a reduced caffeic acid/5-hydroxyferulic acid O-methyltransferase activity.* The Plant Journal, 1995. **8**(6): p. 855-864.

111. Meyermans, H., et al., *Modifications in lignin and accumulation of phenolic glucosides in poplar xylem upon down-regulation of caffeoyl-coenzyme A O-methyltransferase, an enzyme involved in lignin biosynthesis.* The Journal of biological chemistry, 2000. **275**(47): p. 36899-909.

112. Guo, D., et al., *Downregulation of caffeic acid 3-O-methyltransferase and caffeoyl CoA 3-O-methyltransferase in transgenic alfalfa. impacts on lignin structure and implications for the biosynthesis of G and S lignin.* The Plant cell, 2001. **13**(1): p. 73-88.

113. Lapierre, C., et al., *Structural alterations of lignins in transgenic poplars with depressed cinnamyl alcohol dehydrogenase or caffeic acid O-methyltransferase activity*

have an opposite impact on the efficiency of industrial kraft pulping. Plant physiology, 1999. **119**(1): p. 153-64.

114. Sederoff, R.R., et al., *Unexpected variation in lignin.* Curr Opin Plant Biol, 1999. **2**(2): p. 145-52.

115. Ralph, J., et al., *Lignins: Natural polymers from oxidative coupling of 4-hydroxyphenyl-propanoids.* Phytochemistry Reviews, 2004. **3**(1-2): p. 29-60.

116. McDougall, G., D. Stewart, and I. Morrison, *Cell-wall-bound oxidases from tobacco (Nicotiana tabacum) xylem participate in lignin formation.* Planta, 1994. **194**(1): p. 9-14.

117. Higuchi, T., *Lignin biochemistry: biosynthesis and biodegradation.* Wood Science and Technology, 1990. **24**(1): p. 23-63.

118. Ziebell, A., et al., *Increase in 4-Coumaryl Alcohol Units during Lignification in Alfalfa (Medicago sativa) Alters the Extractability and Molecular Weight of Lignin.* Journal of Biological Chemistry, 2010. **285**(50): p. 38961-38968.

119. Li, M., et al., *Structural characterization of alkaline hydrogen peroxide pretreated grasses exhibiting diverse lignin phenotypes.* Biotechnology for biofuels, 2012. **5**(1): p. 38.

120. Ferrer, J.L., et al., *Structure and function of enzymes involved in the biosynthesis of phenylpropanoids.* Plant Physiology and Biochemistry, 2008. **46**(3): p. 356-370.

121. Chiang, V.L. and M. Funaoka, *The difference between guaiacyl and guaiacyl-syringyl lignins in their responses to kraft delignification.* Holzforschung-International Journal of the Biology, Chemistry, Physics and Technology of Wood, 1990. **44**(4): p. 309-313.

122. Ziebell, A., et al., *Increase in 4-coumaryl alcohol units during lignification in alfalfa (Medicago sativa) alters the extractability and molecular weight of lignin.* The Journal of biological chemistry, 2010. **285**(50): p. 38961-8.

123. Li, X., et al., *Lignin monomer composition affects Arabidopsis cell-wall degradability after liquid hot water pretreatment.* Biotechnol Biofuels, 2010. **3**(1): p. 27.

124. Chiang, V., et al., *Comparison of softwood and hardwood kraft pulping.* Tappi journal, 1988. **71**(9): p. 173-176.

125. Santos, R.B., et al., *Wood Based Lignin Reactions Important to the Biorefinery and Pulp and Paper Industries*. 2013. Vol. 8. 2013.

126. Pu, Y., et al., *NMR Characterization of C3H and HCT Down-Regulated Alfalfa Lignin.* BioEnergy Research, 2009. **2**(4): p. 198-208.

127. Lourenco, A., et al., *Reactivity of syringyl and guaiacyl lignin units and delignification kinetics in the kraft pulping of Eucalyptus globulus wood using Py-GC-MS/FID.* Bioresource technology, 2012. **123**: p. 296-302.

128. Dixon, R.A., et al., *The biosynthesis of monolignols: a "metabolic grid", or independent pathways to guaiacyl and syringyl units?* Phytochemistry, 2001. **57**(7): p. 1069-84.

129. Rogers, L.A. and M.M. Campbell, *The Genetic Control of Lignin Deposition during Plant Growth and Development.* New Phytologist, 2004. **164**(1): p. 17-30.

130. Vance, C.P., T.K. Kirk, and R.T. Sherwood, *Lignification as a Mechanism of Disease Resistance.* Annual Review of Phytopathology, 1980. **18**(1): p. 259-288.

131. Vogel, K.P. and H.J.G. Jung, *Genetic modification of herbaceous plants for feed and fuel.* Critical Reviews in Plant Sciences, 2001. **20**(1): p. 15-49.

132. Ragauskas, A.J., et al., *The path forward for biofuels and biomaterials.* Science, 2006. **311**(5760): p. 484-9.

133. Baucher, M., et al., *Red Xylem and Higher Lignin Extractability by Down-Regulating a Cinnamyl Alcohol Dehydrogenase in Poplar.* Plant physiology, 1996. **112**(4): p. 1479-1490.

134. Hu, W.J., et al., *Repression of lignin biosynthesis promotes cellulose accumulation and growth in transgenic trees.* Nat Biotechnol, 1999. **17**(8): p. 808-12.

135. Chang, V.S. and M.T. Holtzapple, *Fundamental factors affecting biomass enzymatic reactivity.* Applied biochemistry and biotechnology, 2000. **84-86**: p. 5-37.

136. Jouanin, L., et al., *Lignification in transgenic poplars with extremely reduced caffeic acid O-methyltransferase activity.* Plant physiology, 2000. **123**(4): p. 1363-74.

137. Chiang, V.L., *From rags to riches.* Nat Biotechnol, 2002. **20**(6): p. 557-8.

138. Eckardt, N.A., *Probing the Mysteries of Lignin Biosynthesis: The Crystal Structure of Caffeic Acid/5-Hydroxyferulic Acid 3/5-O-Methyltransferase Provides New Insights.* The Plant Cell Online, 2002. **14**(6): p. 1185-1189.

139. Chen, F. and R.A. Dixon, *Lignin modification improves fermentable sugar yields for biofuel production.* Nature biotechnology, 2007. **25**(7): p. 759-61.

140. Rubin, E.M., *Genomics of cellulosic biofuels.* Nature, 2008. **454**(7206): p. 841-5.

141. Hinchee, M., et al., *Short-rotation woody crops for bioenergy and biofuels applications.* In Vitro Cell Dev Biol Plant, 2009. **45**(6): p. 619-629.

142. Hisano, H., R. Nandakumar, and Z.-Y. Wang, *Genetic modification of lignin biosynthesis for improved biofuel production.* In Vitro Cellular & Developmental Biology - Plant, 2009. **45**(3): p. 306-313.

143. Studer, M.H., et al., *Lignin content in natural Populus variants affects sugar release.* Proc Natl Acad Sci U S A, 2011. **108**(15): p. 6300-5.

144. Vogt, T., *Phenylpropanoid biosynthesis.* Molecular Plant, 2010. **3**(1): p. 2-20.

145. Fraser, C.M. and C. Chapple, *The phenylpropanoid pathway in Arabidopsis.* The Arabidopsis book / American Society of Plant Biologists, 2011. **9**: p. e0152.

146. D'Auria, J.C. and J. Gershenzon, *The secondary metabolism of Arabidopsis thaliana: growing like a weed.* Current opinion in plant biology, 2005. **8**(3): p. 308-16.

147. Brown, S.A. and A.C. Neish, *Shikimic acid as a precursor in lignin biosynthesis.* Nature, 1955. **175**(4459): p. 688-9.

148. Chen, H.C., et al., *Membrane protein complexes catalyze both 4- and 3-hydroxylation of cinnamic acid derivatives in monolignol biosynthesis.* Proc Natl Acad Sci U S A, 2011. **108**(52): p. 21253-8.

149. Chen, H.-C., et al., *Monolignol Pathway 4-Coumaric Acid:CoA Ligases in Populus trichocarpa: Novel Specificity, Metabolic Regulation, and Simulation of CoA Ligation Fluxes.* Plant Physiology, 2013. **161**: p. 1501-1516.

150. Hamberger, B., et al., *Genome-wide analyses of phenylpropanoid-related genes in Populus trichocarpa, Arabidopsis thaliana, and Oryza sativa: the Populus lignin toolbox and conservation and diversification of angiosperm gene familiesThis article is one of a selection of papers published in the Special Issue on Poplar Research in Canada.* Canadian Journal of Botany, 2007. **85**(12): p. 1182-1201.

151. Higuchi, T., *Pathways for monolignol biosynthesis via metabolic grids: coniferyl aldehyde 5-hydroxylase, a possible key enzyme in angiosperm syringyl lignin biosynthesis.* Proceedings of the Japan Academy. Series B: physical and biological sciences., 2003. **79**: p. 227-236.

152. Higuchi, T. and S.A. Brown, *Studies of lignin biosynthesis using isotopic carbon. XIII. The phenylpropanoid system in lignification.* Can J Biochem Physiol, 1963. **41**: p. 621-8.

153. Lee, Y., et al., *Integrative analysis of transgenic alfalfa (Medicago sativa L.) suggests new metabolic control mechanisms for monolignol biosynthesis.* PLoS Comput Biol, 2011. **7**(5): p. e1002047.

154. Raes, J., et al., *Genome-wide characterization of the lignification toolbox in Arabidopsis.* Plant Physiol, 2003. **133**(3): p. 1051-71.

155. Shi, R., et al., *Towards a systems approach for lignin biosynthesis in Populus trichocarpa: transcript abundance and specificity of the monolignol biosynthetic genes.* Plant Cell Physiol, 2010. **51**(1): p. 144-63.

156. Vanholme, R., et al., *Lignin biosynthesis and structure.* Plant Physiol, 2010. **153**(3): p. 895-905.

157. Erdtman, H., *Outstanding Problems in Lignin Chemistry.* Industrial & Engineering Chemistry, 1957. **49**(9): p. 1385-1386.

158. Lewis, N.G. and L.B. Davin, *The Biochemical Control of Monolignol Coupling and Structure During Lignan and Lignin Biosynthesis*, in *Lignin and Lignan Biosynthesis*1998, American Chemical Society. p. 334-361.

159. Gang, D.R., et al., *Regiochemical control of monolignol radical coupling: a new paradigm for lignin and lignan biosynthesis.* Chem Biol, 1999. **6**(3): p. 143-51.

160. Davin, L.B. and N.G. Lewis, *Dirigent proteins and dirigent sites explain the mystery of specificity of radical precursor coupling in lignan and lignin biosynthesis.* Plant Physiol, 2000. **123**(2): p. 453-62.

161. Burlat, V., et al., *Dirigent proteins and dirigent sites in lignifying tissues.* Phytochemistry, 2001. **57**(6): p. 883-97.

162. Chen, Y.-r. and S. Sarkanen, *Macromolecular lignin replication: A mechanistic working hypothesis.* Phytochemistry Reviews, 2003. **2**(3): p. 235-255.

163. Davin, L.B. and N.G. Lewis, *Lignin primary structures and dirigent sites.* Curr Opin Biotechnol, 2005. **16**(4): p. 407-15.

164. Freudenberg, K., *Lignin: Its Constitution and Formation from p-Hydroxycinnamyl Alcohols: Lignin is duplicated by dehydrogenation of these alcohols; intermediates explain formation and structure.* Science, 1965. **148**(3670): p. 595-600.

165. Freudenberg, K., *Biosynthesis and constitution of lignin.* Nature, 1959. **183**(4669): p. 1152-5.

166. Hatfield, R. and W. Vermerris, *Lignin formation in plants. The dilemma of linkage specificity.* Plant Physiol, 2001. **126**(4): p. 1351-7.

167. Harkin, J.M., *Lignin - a natural polymeric product of phenol oxidation*, in *Oxidative Coupling of Phenols*, W.I. Taylor and A.R. Battersby, Editors. 1967, Marcel Dekker: New York. p. 243-321.

168. Freudenberg, K. and A.C. Neish, *Constitution and biosynthesis of lignin*1968: Springer.

169. Morreel, K., et al., *Profiling of oligolignols reveals monolignol coupling conditions in lignifying poplar xylem.* Plant Physiol, 2004. **136**(3): p. 3537-49.

170. Freudenberg, K., *Biosynthesis and Constitution of Lignin.* Nature, 1959. **183**(4669): p. 1152-1155.

171. Karhunen, P., et al., *Dibenzodioxocins; a novel type of linkage in softwood lignins.* Tetrahedron Letters, 1995. **36**(1): p. 169-170.

172. Botella, M.A., et al., *Induction of a tomato peroxidase gene in vascular tissue.* FEBS Lett, 1994. **347**(2-3): p. 195-8.

173. Quiroga, M., et al., *A tomato peroxidase involved in the synthesis of lignin and suberin.* Plant Physiol, 2000. **122**(4): p. 1119-27.

174. Smith, C.G., et al., *Tissue and subcellular immunolocalisation of enzymes of lignin synthesis in differentiating and wounded hypocotyl tissue of French bean (Phaseolus vulgaris L.).* Planta, 1994. **192**(2): p. 155-164.

175. Zimmerlin, A., P. Wojtaszek, and G.P. Bolwell, *Synthesis of dehydrogenation polymers of ferulic acid with high specificity by a purified cell-wall peroxidase from French bean (Phaseolus vulgaris L.).* Biochem J, 1994. **299 (Pt 3)**: p. 747-53.

176. Lagrimini, L.M., et al., *Molecular cloning of complementary DNA encoding the lignin-forming peroxidase from tobacco: Molecular analysis and tissue-specific expression.* Proc Natl Acad Sci U S A, 1987. **84**(21): p. 7542-6.

177. Blee, K.A., et al., *A lignin-specific peroxidase in tobacco whose antisense suppression leads to vascular tissue modification.* Phytochemistry, 2003. **64**(1): p. 163-176.

178. Ostergaard, L., et al., *Arabidopsis ATP A2 peroxidase. Expression and high-resolution structure of a plant peroxidase with implications for lignification.* Plant Molecular Biology, 2000. **44**(2): p. 231-43.

179. Nielsen, K.L., et al., *Differential activity and structure of highly similar peroxidases. Spectroscopic, crystallographic, and enzymatic analyses of lignifying Arabidopsis*

thaliana peroxidase A2 and horseradish peroxidase A2. Biochemistry, 2001. **40**(37): p. 11013-21.

180. Shigeto, J., et al., *Putative Cationic Cell-Wall-Bound Peroxidase Homologues in Arabidopsis, AtPrx2, AtPrx25, and AtPrx71, Are Involved in Lignification.* Journal of Agricultural and Food Chemistry, 2013. **61**(16): p. 3781-3788.

181. Herrero, J., et al., *Bioinformatic and functional characterization of the basic peroxidase 72 from Arabidopsis thaliana involved in lignin biosynthesis.* Planta, 2013. **237**(6): p. 1599-612.

182. Masuda, H., H. Fukuda, and A. Komamine, *Changes in Peroxidase Isoenzyme Patterns during Tracheary Element Differentiation in a Culture of Single Cells Isolated from the Mesophyll of Zinnia elegans.* Zeitschrift für Pflanzenphysiologie, 1983. **112**(5): p. 417-426.

183. Sato, Y., et al., *Isolation and characterization of a novel peroxidase gene ZPO-C whose expression and function are closely associated with lignification during tracheary element differentiation.* Plant Cell Physiol, 2006. **47**(4): p. 493-503.

184. Sato, Y., et al., *Separation and characterization of the isoenzymes of wall-bound peroxidase from cultured Zinnia cells during tracheary element differentiation.* Planta, 1995. **196**(1): p. 141-147.

185. Gabaldon, C., et al., *Cloning and molecular characterization of the basic peroxidase isoenzyme from Zinnia elegans, an enzyme involved in lignin biosynthesis.* Plant Physiol, 2005. **139**(3): p. 1138-54.

186. Gabaldón, C., et al., *Characterization of the last step of lignin biosynthesis in Zinnia elegans suspension cell cultures.* FEBS Letters, 2006. **580**(18): p. 4311-4316.

187. Osakabe, K., et al., *Molecular cloning of two tandemly arranged peroxidase genes from Populus kitakamiensis and their differential regulation in the stem.* Plant Molecular Biology, 1995. **28**(4): p. 677-89.

188. Christensen, J.H., et al., *Purification and characterization of peroxidases correlated with lignification in poplar xylem.* Plant Physiol, 1998. **118**(1): p. 125-35.

189. Christensen, J.H., et al., *The syringaldazine-oxidizing peroxidase PXP 3-4 from poplar xylem: cDNA isolation, characterization and expression.* Plant Molecular Biology, 2001. **47**(5): p. 581-93.

190. Polle, A., T. Otter, and F. Seifert, *Apoplastic Peroxidases and Lignification in Needles of Norway Spruce (Picea abies L.).* Plant Physiol, 1994. **106**(1): p. 53-60.

191. Fagerstedt, K., P. Saranpää, and R. Piispanen, *Peroxidase activity, isoenzymes and histological localisation in sapwood and heartwood of Scots pine (Pinus sylvestris L.).* Journal of Forest Research, 1998. **3**(1): p. 43-47.

192. Karkonen, A., et al., *Lignification related enzymes in Picea abies suspension cultures.* Physiol Plant, 2002. **114**(3): p. 343-353.

193. Marjamaa K, K.E.L.T.K.P.S.P.F.K.V., *Monolignol oxidation by xylem peroxidase isoforms of Norway spruce (Picea abies) and silver birch (Betula pendula).* Tree physiology, 2006. **26**(5): p. 605-11.

194. Koutaniemi, S., et al., *Characterization of basic p-coumaryl and coniferyl alcohol oxidizing peroxidases from a lignin-forming Picea abies suspension culture.* Plant Molecular Biology, 2005. **58**(2): p. 141-57.

195. Fagerstedt, K.V., et al., *Cell wall lignin is polymerised by class III secretable plant peroxidases in Norway spruce.* Journal of Integrative Plant Biology, 2010. **52**(2): p. 186-194.

196. Koutaniemi, S., et al., *Expression profiling of the lignin biosynthetic pathway in Norway spruce using EST sequencing and real-time RT-PCR.* Plant Molecular Biology, 2007. **65**(3): p. 311-28.

197. McDougall, G.J., *Cell-wall-associated peroxidases from the lignifying xylem of angiosperms and gymnosperms: monolignol oxidation.* Holzforschung, 2001. **55**(3): p. 246-249.

198. Driouich, A., et al., *Characterization and localization of laccase forms in stem and cell cultures of sycamore.* The Plant Journal, 1992. **2**(1): p. 13-24.

199. Bao, W., et al., *A laccase associated with lignification in loblolly pine xylem.* Science, 1993. **260**(5108): p. 672-4.

200. O'Malley, D.M., et al., *The role of of laccase in lignification.* The Plant Journal, 1993. **4**(5): p. 751-757.

201. Dean Jeffrey, F.D. and L. Eriksson Karl-Erik, *Laccase and the Deposition of Lignin in Vascular Plants*, in *Holzforschung - International Journal of the Biology, Chemistry, Physics and Technology of Wood*1994. p. 21.

202. Sato, Y., et al., *Molecular Cloning and Expression of Eight Laccase cDNAs in Loblolly Pine (Pinus taeda)*.* Journal of Plant Research, 2001. **114**(2): p. 147-155.

203. Liu, L., et al., *A laccase-like phenoloxidase is correlated with lignin biosynthesis in Zinnia elegans stem tissues.* The Plant Journal, 1994. **6**(2): p. 213-224.

204. Richardson, A. and G.J. McDougall, *A laccase-type polyphenol oxidase from lignifying xylem of tobacco.* Phytochemistry, 1997. **44**(2): p. 229-235.

205. Richardson, A., J. Duncan, and G.J. McDougall, *Oxidase activity in lignifying xylem of a taxonomically diverse range of trees: identification of a conifer laccase.* Tree physiology, 2000. **20**(15): p. 1039-1047.

206. Zhao, Q., et al., *LACCASE Is Necessary and Nonredundant with PEROXIDASE for Lignin Polymerization during Vascular Development in Arabidopsis.* The Plant Cell Online, 2013. **25**(10): p. 3976-3987.

207. Lu, S., et al., *Ptr-miR397a is a negative regulator of laccase genes affecting lignin content in Populus trichocarpa.* Proceedings of the National Academy of Sciences, 2013. **110**(26): p. 10848-10853.

208. Jansson, S. and C.J. Douglas, *Populus: A Model System for Plant Biology.* Annual Review of Plant Biology, 2007. **58**(1): p. 435-458.

209. Tuskan, G.A., et al., *The genome of black cottonwood, Populus trichocarpa (Torr. & Gray)*, 2006.

210. Shi, R., et al., *Regulation of phenylalanine ammonia-lyase (PAL) gene family in wood forming tissue of Populus trichocarpa.* Planta, 2013. **238**(3): p. 487-97.

211. Chen, H.C., et al., *Systems Biology of Lignin Biosynthesis in Populus trichocarpa: Heteromeric 4-Coumaric Acid:Coenzyme A Ligase Protein Complex Formation, Regulation, and Numerical Modeling.* The Plant cell, 2014. **26**(3): p. 876-93.

212. Wang, J.P., et al., *Functional redundancy of the two 5-hydroxylases in monolignol biosynthesis of Populus trichocarpa: LC-MS/MS based protein quantification and metabolic flux analysis.* Planta, 2012. **236**(3): p. 795-808.

213. Lee, Y. and E.O. Voit, *Mathematical modeling of monolignol biosynthesis in Populus xylem.* Mathematical biosciences, 2010. **228**(1): p. 78-89.

214. Lee, Y., et al., *Functional analysis of metabolic channeling and regulation in lignin biosynthesis: a computational approach.* PLoS computational biology, 2012. **8**(11): p. e1002769.

215. Schallau, K. and B.H. Junker, *Simulating plant metabolic pathways with enzyme-kinetic models.* Plant physiology, 2010. **152**(4): p. 1763-71.

Chapter 2

Characterization of *Populus trichocarpa* Hydroxycinnamoyl-Coenzyme A:Shikimic Acid Hydroxycinnamoyl Transferase (PtrHCT) and Activity Evaluation of the Single Nucleotide Polymorphism (SNP) Variants in the Monolignol Biosynthetic Enzymes of *Populus trichocarpa*

2.1 Introduction

Lignin, as one of the three major components in the plant secondary cell wall, has important functions for supporting plant development. First, lignin embeds both cellulose and hemicelluloses to strengthen the cell wall and to sustain the erect growth of woody plant. Second, lignin, with its hydrophobic characteristics and amorphous structure, facilitates the water transport through the whole plant and inhibits natural degradation [1-4]. However, for economic utilization of biomass, lignin is considered as the major hindrance of the plant biomass, which may result in wasting more energy and increasing environment pollution during delignification [5, 6].

Lignin is principally composed of three major types phenylpropanoid subunits known as 4-hydroxyphenyl (H), guaiacyl (G) and syringyl (S) subunits, polymerized from 4-coumaryl,

coniferyl, and sinapyl alcohols, respectively [7]. As a major barrier for biomass utilization, both lignin content and composition are important factors that determine the recalcitrance of the biomass; therefore, scientists have focused on modifying either lignin content or composition. Results have shown lowering lignin content or increasing S/G ratio of the lignin composition has positive correlation with the yield of fermentable sugar and the economic value of wood for pulping [6, 8-19].

The monolignol biosynthetic pathway undergoes different types of reactions, such as deamination, hydroxylation, coenzyme A (CoA)-mediated ligation, esterification/de-esterification, *O*-methylation, NADPH-mediated reduction and NADPH-mediated dehydrogenation [20, 21]. In the monolignol biosynthesis, 10 enzyme families are proposed for those complex reactions, including phenylalanine ammonia-lyase (PAL), cinnamic acid 4-hydroxylase (C4H), 4-coumaric acid:coenzyme A ligase (4CL), 4-hydroxycinnamoyl-coenzyme A:shikimic acid hydroxycinnamoyl transferase (HCT), 4-coumaric acid 3-hydroxylase (C3H), caffeoyl-CoA *O*-methyltransferase (CCoAOMT), cinnamoyl coenzyme A (CoA) reductase (CCR), cinnamyl alcohol dehydrogenase (CAD), coniferaldehyde 5-hydroxylase (CAld5H) and caffeic acid *O*-methyltransferase (AldOMT) [22-32]. By the successive reactions of these enzyme families, phenylalanine is converted into 4-coumaryl, coniferyl, or sinapyl alcohol, the major types of monolignols for lignin polymerization.

Because of the large number of the reactions and components, including enzymes, metabolites and cofactors, are involved in the monolignol biosynthetic pathway, it will be

helpful to unveil the complexity of the monolignol biosynthetic pathway by a systematic approach [30, 33-35]. Building a mathematical model by mass action kinetics using differential equations can create a more comprehensive simulation for plant metabolic flux, which has elastic and dynamic properties that need to be considered as well [34]. However, in order to construct such a metabolic flux predictive model for the monolignol biosynthesis in *Populus trichocarpa*, basic kinetic properties of every enzyme involved in the pathway need to be characterized. Moreover, enzyme variants, including isoforms of the enzyme and mutant enzymes that can result from single nucleotide polymorphisms (SNPs), are also needed to be considered before constructing the model because enzyme variants may affect the metabolic flux significantly if they possess relative different kinetic behaviors or relative abundance.

Analysis of the whole genome of *P. trichocarpa* had shown a whole-genome duplication event [36] and SNPs are considered as a major source of genetic variation and potential plasticity in *P. trichocarpa* [37, 38]. Duplication of 8000 pairs of genes within the whole genome in *P. trichocarpa* [36] resulted in about 561,302 putative SNPs distributed over 26,595 expressed genes in the developing secondary xylem of *P. trichocarpa* [39]. In 2010, all putative xylem-specific monolignol biosynthetic enzymes in *P. trichocarpa* were identified which may be due to the genome duplication [28]. In *P. trichocarpa*, there are five members in the phenylalanine ammonia-lyase (PtrPAL) family, two in cinnamic acid 4-hydroxylase (PtrC4H) family, one in 4-coumaric acid 3-hydroxylase family, three in 4-

coumaric acid:coenzyme A (CoA) ligase (Ptr4CL) family, two in the 4-hydroxycinnamoyl-CoA:shikimic acid hydroxycinnamoyl transferase (PtrHCT) family, three in the caffeoyl-CoA *O*-methyltransferase (PtrCCoAOMT) family, one in cinnamoyl CoA reductase (PtrCCR) family, one in the cinnamyl alcohol dehydrogenase (PtrCAD) family, two in the coniferaldehyde 5-hydroxylase (PtrCAld5H) family and one in the caffeic acid *O*-methyltransferase (PtrAldOMT) family [28]. The enzyme characterization had been performed on several monolignol biosynthetic enzyme families, such as the PtrPAL family [40], the PtrC3H and the PtrC4H families [31], the Ptr4CL family [32, 41] and the PtrCAld5H family [42]. However, the kinetic information of the PtrHCT family has not been characterized in *P. trichocarpa* yet, which is a critical step to explore the 3-hydroxylation of the monolignol precursors to produce the two dominant forms of monolignol subunits in *P. trichocarpa*, the G and S subunits [43, 44].

HCT (EC 2.3.1.133) catalyzes the transfer of shikimic acid and CoA between shikimic acid esters and CoA thioesters. HCT has been first characterized to have high specificity with 4-coumaroyl-CoA and shikimic acid [45] and has been further identified as an essential monolignol enzyme specifically expressed in xylem tissue [44]. The role of HCT in the phenylpropanoid pathway is to divert monolignol biosynthesis from H units to G and S units [43, 46]; all the transgenics with downregulation of HCT showed dwarfism and significant H unit incorporation into lignin. In contrast to *Arabidopsis thaliana* and tobacco (*Nicotiana tabacum* and *Nicotiana benthamiana*), which possess only one copy of HCT in their genome

for monolignol biosynthesis, there are seven HCT gene models in the genome of *P. trichocarpa* that have been identified [43, 47]. Two HCT genes, PtrHCT1 and PtrHCT6, were identified with highest and specific expression in stem differentiating xylem (SDX) [28]. The absolute protein quantification shows the amount of PtrHCT1 is about 2-fold to PtrHCT6 [48].

In this study, enzyme kinetic characterization was performed on the two members in the PtrHCT family, PtrHCT1 and PtrHCT6, to obtain Michaelis-Menten kinetic parameters [49, 50]. PtrHCT has four substrates in the monolignol biosynthetic pathway, which are the 4-coumaroyl-CoA, caffeoyl-CoA, 4-coumaroyl shikimic acid and caffeoyl shikimic acid. All substrates were enzymatically synthesized and used to perform the enzyme kinetic study for PtrHCT's transesterification and de-esterification reactions. The result shows PtrHCTs have stronger catalytic activities for the CoA thioesters, the 4-coumaroyl-CoA and caffeoyl-CoA, than shikimic acid esters, the 4-coumaroyl and caffeoyl shikimic acids. In addition, protein-protein interaction between the PtrHCT1 and PtrHCT6 are also examined and the result shows additive activity for all four substrates, which implies the redundant functions of PtrHCT1 and PtrHCT6.

Moreover, SNPs in the monolignol biosynthetic enzymes of *P. trichocarpa* (Nisqually-1) had also been screened by our transcriptome analysis from SDX tissue. 8 of 10 monolignol biosynthetic enzyme families had identified with SNPs, which in total are 32 SNP variants and 6 of 32 SNP variants are non-synonymous SNPs that lead to the single amino acid

alterations of the enzymes. Three of the non-synonymous SNPs in PtrCAld5H family were studied and they are identical in activity [42]. In this study, the activities of the other 3 non-synonymous SNP variants of Ptr4CL3, PtrCCoAOMT3 and PtrCCR2 are evaluated. They possess similar activity compared to the original enzymes.

2.2 Materials and Methods

2.2.1 Synthesis of Monolignol Precursors

4-Coumaric acid, caffeic acid and shikimic acid were purchased from Sigma-Aldrich (St. Louis, MO). 4-Coumaroyl-CoA and caffeoyl-CoA were enzymatically synthesized from their corresponding hydroxycinnamic acids following Chen et al. (2013). 4-Coumaroyl and caffeoyl shikimic acids were synthesized enzymatically using recombinant PtrHCT6 expressed in *Escherichia coli* and purified by glutathione S-transferase (GST) protein tag affinity chromatography. 15 mg of either 4-coumaroyl-CoA or caffeoyl-CoA was added with 5 mg of shikimic acid to 20 mL of 50 mM $NaHPO_4$ (pH 7). Purified PtrHCT6 (0.2 mg) was added to the mixture to start the reaction. After 60 min at 30 °C, 800 µL of glacial acetic acid was added to stop the reaction. The shikimic acid esters were purified by ethyl acetate extraction (3 times, 20 mL). The total 60mL ethyl acetate extract was dried in a Rotavapor® R II (BUCHI, Flawil, Switzerland) and frozen at -80 °C. The purity and identity of all

synthesized products were confirmed by mass spectrometry (Liu et al., 2012).

2.2.2 Plasmid Constructions

For PtrHCTs, full length of PtrHCT1 or PtrHCT6 cDNA (*PtrHCT1*, GenBank accession number EU603313; *PtrHCT6*, EU603314) was previously identified in Shi et al. (2010) and amplified by specific primers [48] and cloned into the pGEX-KG-1 vector using *Sal*I and *Hind*III restriction enzymes, respectively. For SNP variants of Ptr4CL3, PtrCCoAOMT3 and PtrCCR2, specific primers were used [48]. The SNPs were identified by randomly sequencing 10 colonies for each gene. The SNP of Ptr4CL3 or PtrCCoAOMT3 were cloned into the pET101 protein expression vector according to the manufacturers protocol (Invitrogen, Grand Island, NY), whereas PtrCCR2 was cloned into the pGEX-KG-1 vector using the primer set in Shuford et al. (2012) and *Nco*I and *Sal*I restriction enzymes. All vectors were transformed into *E. coli* (BL21) and stored at -80 °C.

2.2.3 Expression and Purification of the Recombinant Proteins

For recombinant protein expression, bacteria containing the specific vector was first inoculated into 3 mL LB medium and incubated at 37 °C for 12 hours. 1 mL of the fresh 3 mL bacteria culture was transferred into 1 L of the LB medium and incubated at 37 °C until O.D.600 reached around 0.6. 1 mL of 1 M of Isopropyl β-D-1-thiogalactopyranoside (IPTG) was added into 1 L of the bacteria culture and incubated at 25 or 28°C for 12 ~ 16 hours.

Collected bacteria were disrupted by a Branson Sonifier® ultrasonic cell disruptor (Emerson, Danbury, CT) at frequency of 15 seconds on and 45 seconds off for a total of 20 mins at 4 °C. Lysed bacteria were centrifuged at 12,000 x g for 15 min at 4 °C before the supernatant was fractionated by affinity chromatography. The enzymes purified by GST tag affinity chromatography, particularly PtrHCT1, PtrHCT6 and SNPs of PtrCCR2. The SNPs of Ptr4CL3 and PtrCCoAOMT3 were cloned into pET-101 which was fused with a 6X histidine (6X His) tag. All purification procedures followed Shuford et al. (2012).

2.2.4 Western Blotting

Proteins were denatured in Laemmli SDS-PAGE buffer, resolved on 12% SDS-PAGE and transferred to an Immun-Blot PVDF Membrane (Bio-Rad, Hercules, CA) using a Trans-Blot® SD Semi-Dry Transfer Cell (Bio-Rad, Hercules, CA) under the constant current (0.2 Amp) for 1 hour. The PVDF membrane was then blocked by 1% bovine serum albumin for 1 hour at room temperature. The PtrHCT1 and PtrHCT6 were detected by specific PtrHCT1 or PtrHCT6 rabbit antibodies (Antagene, Santa Clara, CA).

2.2.5 Enzyme Reactions and High Performance Liquid Chromatography (HPLC) Analysis

First, recombinant proteins of PtrHCT1 and PtrHCT6 were used to determine the optimal conditions for their enzyme activity. 4-coumaroyl-CoA was used as substrate. A range of temperatures (20-55 °C) and pH (6.0-8.5) were tested. The enzyme activities of the

recombinant PtrHCTs were measured in a mixture of 100 μL containing 100 mM phosphate buffer with an optimal pH (pH 6.6 for PtrHCT1 and pH 7.2 for PtrHCT6), 1 mM dithiothreitol (DTT) and 1 mM of shikimic acid as described in Hoffmann et al. (2004). 10-250 μg of the purified recombinant PtrHCT1 or PtrHCT6 and 10-400 μM of substrates were used for the enzyme kinetic studies to determine the K_m and V_{max} values. The reactions were initiated by adding enzyme to the mixture, incubated at the optimal temperature (PtrHCT1 is 43 °C and PtrHCT6 is 39 °C) for 8 min and then quenched by 40 μL of 4% trichloroacetic acid (TCA) dissolved in 1:1 of H_2O and acetonitrile. Then, the mixtures were centrifuged at 20,000 x g for 20 min and analyzed by HPLC following Liu et al. (2012).

2.2.6 Activity Evaluation of the Single Nucleotide Polymorphism (SNP) Variants of the Monolignol Biosynthetic Enzymes in *P. trichocarpa*

The *E. coli* (BL21) containing the vector and either one of the SNP variants were, in parallel, inoculated into LB medium, incubated at 37 °C and induced at 25 °C by 1 mM IPTG as previously described. The bacteria containing recombinant proteins were disrupted and enzymes were purified by affinity chromatography depending on the fusion tag. The evaluation of the enzyme activity followed the method of Wang et al. (2012) and Liu et al. (2012). The concentration of the substrate is 50 μM and the most preferred substrate of the individual enzyme was used.

2.3 Results

2.3.1 Identification of the Two PtrHCTs, PtrHCT1 and PtrHCT6

In the genome of *Populus trichocarpa*, seven *PtrHCT* gene models had been identified [28]. Only two of the seven PtrHCT gene models were xylem-specific and were considered as the monolignol biosynthetic enzymes, which are the *PtrHCT1* (POPTR_0003s18210) and *PtrHCT6* (POPTR_0001s03440) [28]. Both *PtrHCT1* and *PtrHCT6* were successfully amplified from *P. trichocarpa* SDX cDNA and cloned for sequence verification. The gene length of PtrHCT1 is 1,302 bp and PtrHCT6 is 1,296 bp. In amino acid sequence, PtrHCT1 and PtrHCT6 show fairly high similarity (92.8% identity) (**Figure 2.1**) and they are located on linkage groups 3 and 1, respectively, in the genome of *P. trichocarpa*.

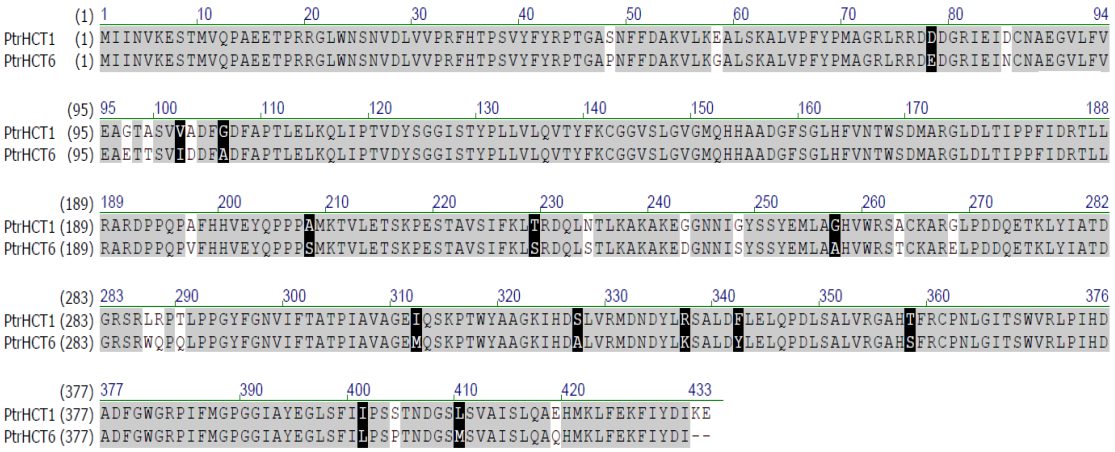

Figure 2.1 – Protein alignment between PtrHCT1 and PtrHCT6. Grey box indicates the identical amino acids; black box indicates the amino acids with similar chemical relationships; white indicates different amino acids.

2.3.2 Expression and Purification of PtrHCT1 and PtrHCT6

The full length coding sequence of PtrHCT1 or PtrHCT6 was further cloned into the pGEX-KG-1 expression vector using *Sal*I and *Hind*III restriction enzymes and transformed into *Escherichia coli* (BL21) for protein expression. Recombinant PtrHCT1 or PtrHCT6 was purified by glutathione S-transferase (GST) affinity chromatography because the fusion of GST in the pGEX-KG-1 vector. The recombinant PtrHCT1 or PtrHCT6 was released from glutathione (GSH) agarose beads by thrombin to cleave the linkage between GST-tag and recombinant protein. The purified proteins were resolved in SDS-PAGE to measure the protein size. We detected a band around 50 kDa, which is the size of the predicted PtrHCT1 and PtrHCT6.

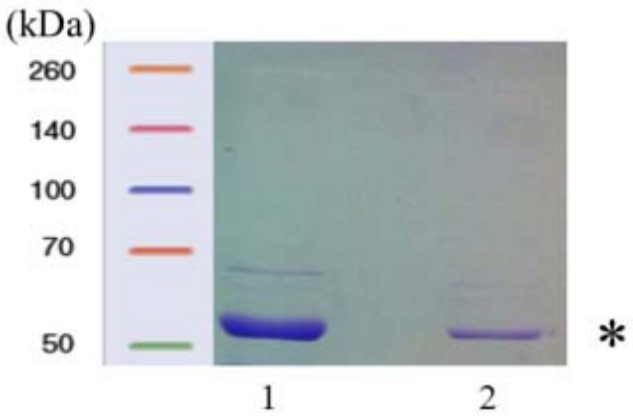

Figure 2.2 – Purified PtrHCT1 and PtrHCT6 protein. Lane 1: purified recombinant PtrHCT1. lane 2: purified recombinant PtrHCT6. The asterisk (*) are the PtrHCT proteins, which are around 50 kDa.

2.3.3 Specificity of PtrHCT1 and PtrHCT6 Rabbit Antibodies

The specific antibodies were raised from rabbits for the detection of the PtrHCT1 and PtrHCT6, respectively. Using a short peptide near the N-terminus of the PtrHCT polypeptides, specific antibodies for PtrHCT1 and PtrHCT6 were raised, where the short peptide sequence for PtrHCT1 is "EAGTASVVADFGDFA" and PtrHCT6 is "EAETTSVIDDFADFA". Prior to applications of these antibodies, the specificity of the antibodies was examined using the purified recombinant PtrHCT1 and PtrHCT6 proteins. The recombinant PtrHCT1 and PtrHCT6 were run in adjacent lanes in SDS-PAGE and specific antibodies were used to detect the PtrHCTs. PtrHCT1 antibody only detected PtrHCT1 recombinant protein (**Figure 2.3A**), while PtrHCT6 antibody only detected the PtrHCT6 recombinant protein (**Figure 2.3B**). Therefore, the PtrHCT antibodies are specific.

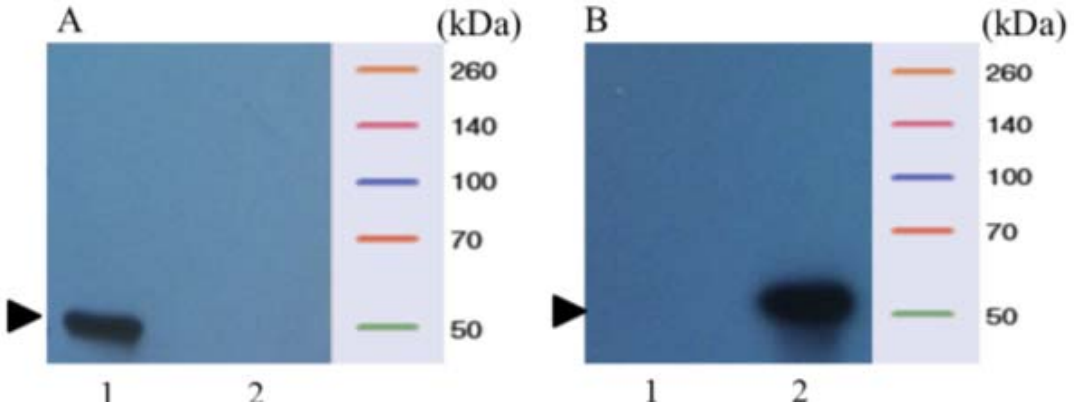

Figure 2.3 – Western blot for PtrHCT1 and PtrHCT6 antibody specificity. (**A**) Specific PtrHCT1 antibody is used. (**B**) Specific PtrHCT6 antibody is used. Lane 1: purified recombinant PtrHCT1. Lane 2: purified recombinant PtrHCT6. The arrowhead showed the size of PtrHCT.

2.3.4 Optimization of the Enzyme Reactions for PtrHCT1 and PtrHCT6

Both pH and temperature are important factors that can affect the catalytic activity of the enzymes. Therefore, prior to performing the enzyme kinetic study of the PtrHCTs, the optimal pH and temperature for both PtrHCTs were examined. Using 4-coumaroyl-CoA as the substrate, the optimal conditions for PtrHCT1 and PtrHCT6 enzymes were tested and the activities were based on the formation of the product, the 4-coumaroyl shikimic acid.

A range of temperatures, from 20 °C to 55 °C, was used, and the results showed that the highest reaction rate of both PtrHCTs is around 40 °C, where the best temperature for PtrHCT1 is 43 °C and for PtrHCT6 is 39 °C (**Figure 2.4A**). For the optimal pH, a range of pH, from pH 6.0 to pH 8.5, was used. The highest activities for both PtrHCTs are around pH 7, where the preferred pH value for PtrHCT1 is pH 6.6 and for PtrHCT6 is pH 7.2 (**Figure 2.4B**).

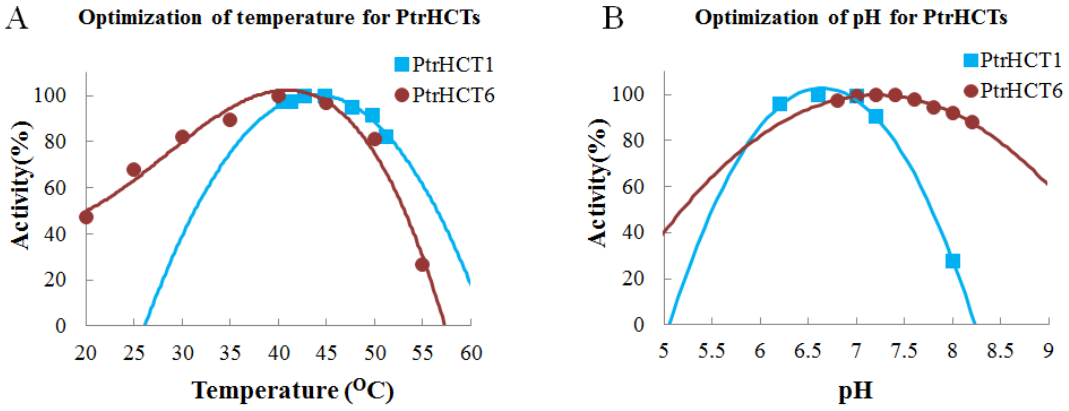

Figure 2.4 – Optimization of temperature and pH for PtrHCTs reactions. (**A**) Temperature optimization. (**B**) pH optimization. 4-Coumaroyl-CoA is used as substrate.

2.3.5 Michaelis-Menten Kinetics of PtrHCT1 and PtrHCT6

All the transesterification and de-esterification reactions of PtrHCT1 and PtrHCT6 were performed and monitored by high-performance liquid chromatography (HPLC). The products of the reaction were used to calculate the enzyme activity and the authentic compounds of the corresponding products were used to verify and quantity the enzyme reaction. The enzyme kinetic studies of the PtrHCTs for all substrates followed Michaelis-Menten kinetics [49, 50]. Four substrates, 4-coumaroyl-CoA, caffeoyl-CoA, 4-coumaroyl shikimic acid and caffeoyl shikimic acid, were serial diluted to perform an enzyme kinetic study at a constant enzyme concentration. The result of the initial velocity [V_i] of PtrHCT1 or PtrHCT6 was graphed versus substrate concentration [S] (**Figure 2.5**). The determinations of the K_m and k_{cat} values were performed using Lineweaver-Burke plots (**Figure 2.6**), which is the double reciprocal plot of the [V_i] versus [S] (**Figure 2.5**).

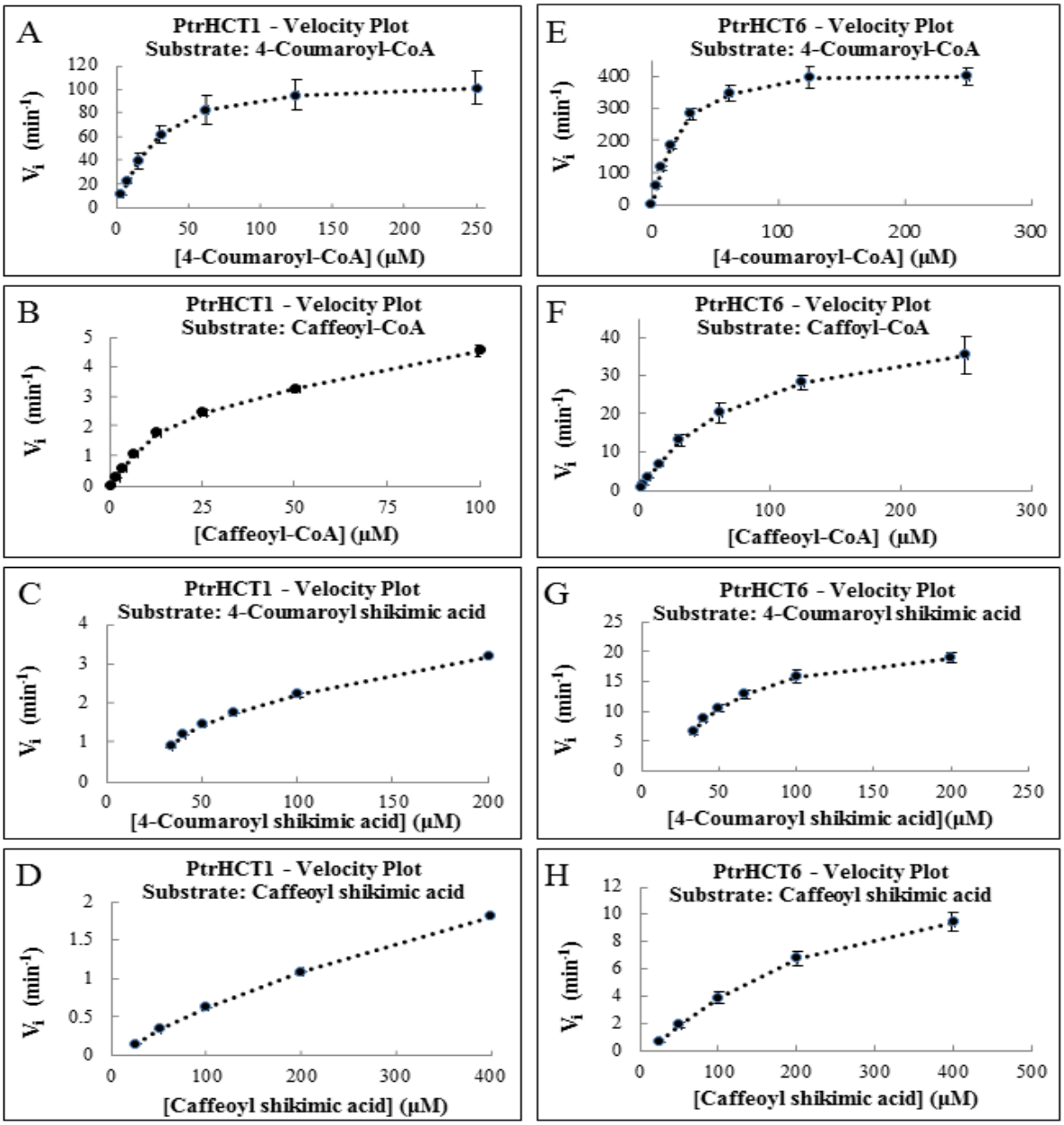

Figure 2.5 – Velocity plot of the PtrHCT1 and PtrHCT6 enzyme reactions. (**A**) PtrHCT1 with 4-coumaroyl-CoA as substrate. (**B**) PtrHCT1 with caffeoyl-CoA as substrate. (**C**) PtrHCT1 with 4-coumaroyl shikimic as substrate. (**D**) PtrHCT1 with caffeoyl shikimic acid as substrate. (**E**) PtrHCT6 with 4-coumaroyl-CoA as substrate (**F**) PtrHCT6 with caffeoyl-CoA as substrate. (**G**) PtrHCT6 with 4-coumaroyl shikimic acid. (**H**) PtrHCT6 with caffeoyl shikimic acid as substrate. The error bars represent one standard error of three technical replicates.

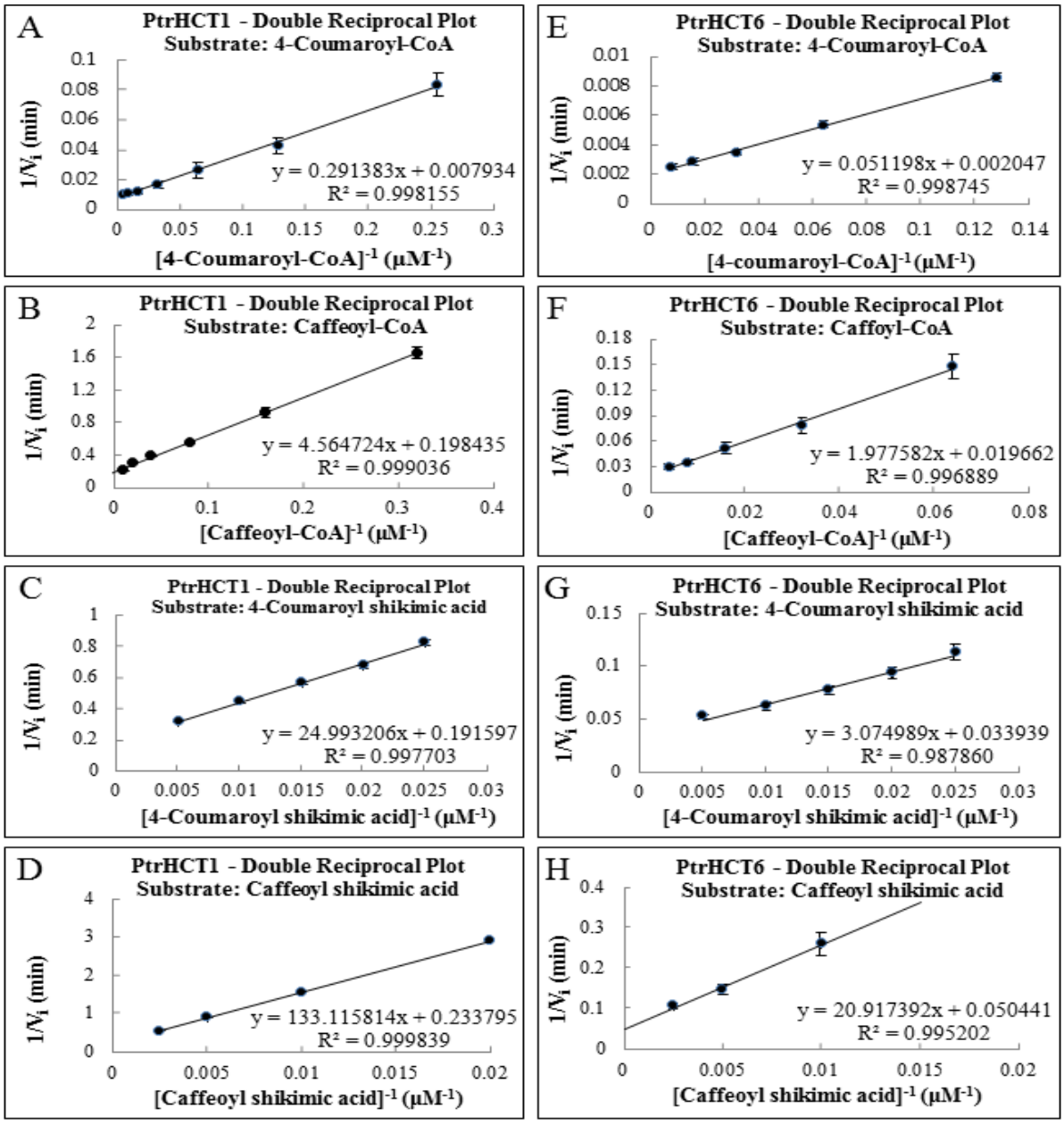

Figure 2.6 – Double reciprocal plot of the PtrHCT1 and PtrHCT6 enzyme reactions. (**A**) PtrHCT1 with 4-coumaroyl-CoA as substrate. (**B**) PtrHCT1 with caffeoyl-CoA as substrate. (**C**) PtrHCT1 with 4-coumaroyl shikimic as substrate. (**D**) PtrHCT1 with caffeoyl shikimic acid as substrate. (**E**) PtrHCT6 with 4-coumaroyl-CoA as substrate (**F**) PtrHCT6 with caffeoyl-CoA as substrate. (**G**) PtrHCT6 with 4-coumaroyl shikimic acid. (**H**) PtrHCT6 with caffeoyl shikimic acid as substrate. The error bars represent one standard error of three technical replicates.

To obtain sufficient signal for reaction rate determinations, the initial velocity measurements were performed under the optimal PtrHCT concentration to have 10-30% substrate conversion within 5 min. The concentration of PtrHCT is 20 nM for 4-coumaroyl-CoA, 100 nM for caffeoyl-CoA, 25 nM for 4-coumaroyl shikimic acid and 300 nM for caffeoyl shikimic acid. Compared to the Michaelis constants (K_m), 4-coumaroyl-CoA and caffeoyl-CoA are the better substrates for both PtrHCT1 and PtrHCT6 (**Table 2.1**). However, PtrHCT6 has a higher turnover rate (k_{cat}) than PtrHCT1. Moreover, both PtrHCT1 and PtrHCT6 have high specificity constant (k_{cat}/K_m) toward the CoA thioesters, the 4-coumaroyl-CoA and caffeoyl-CoA and have less preference (high K_m and low k_{cat}) toward the shikimic acid esters, the 4-coumaroyl and caffeoyl shikimic acids in the monolignol biosynthetic pathway (**Table 2.1**).

Table 2.1 – Michaelis–Menten kinetic parameters of PtrHCT1 and PtrHCT6

Enzmye	Substrates	K_m (μM)	k_{cat} (min^{-1})	k_{cat}/K_m ($\mu M^{-1} \cdot min^{-1}$)
PtrHCT1	4-Coumaroyl-CoA	39 ± 5	138.3 ± 27.2	3.55 ± 0.83
	Caffeoyl-CoA	23.1 ± 0.8	5 ± 0.1	0.22 ± 0.01
	Feruoyl-CoA	153 ± 10.1	4.1 ± 0.3	0.03 ± 0.003
	4-Coumaroyl shikimic acid	131.1 ± 9.2	5.2 ± 0.2	0.04 ± 0.003
	Caffeoyl shikimic acid	572.1 ± 31.6	4.3 ± 0.2	0.008± 0.001
	Feruloyl shikimic acid	ND	ND	ND
PtrHCT6	4-Coumaroyl-CoA	24.9 ± 0.7	488.1 ± 36.8	19.60 ± 1.58
	Caffeoyl-CoA	103.1 ± 8.0	48.8 ± 3.5	0.47 ± 0.05
	Feruoyl-CoA	251.1 ± 19.3	44.3 ± 2.5	0.18 ± 0.02
	4-Coumaroyl shikimic acid	91.4 ± 6.2	29.5 ± 1.3	0.32 ± 0.03
	Caffeoyl shikimic acid	415.6 ± 57.7	19.8 ± 3.3	0.05± 0.01
	Feruloyl shikimic acid	751.7± 104.8	1.6 ± 0.2	0.002± 0.19

*ND, non-detectable

2.3.6 Additive Activity of PtrHCT1 and PtrHCT6

The Michaelis-Menten kinetics of PtrHCT1 and PtrHCT6 indicates that both PtrHCTs are active enzymes for monolignol biosynthesis in xylem of *P. trichocarpa*. Both PtrHCTs have similar substrate preferences but are distinct in their enzyme activity. PtrHCT6 shows a significantly higher turnover rate (k_{cat}) than PtrHCT1 does for all substrates (**Table 2.1**). However, we wonder why there are two functional PtrHCTs with different kinetic behavior present in the xylem of *P. trichocarpa*? Protein-protein interactions of the monolignol biosynthetic enzymes in *P. trichocarpa* may alter their activities, such as we observed for PtrC3H3/PtrC4H1/PtrC4H2 and PtrAld5H1/PtrAld5H2 membrane protein complexes [31, 42]. Therefore, we hypothesized that protein-protein interaction may exist between the PtrHCT1 and PtrHCT and change the activities of PtrHCT reaction. To reveal the interaction between the two PtrHCTs in the monolignol biosynthesis, we examined whether mixture of the two enzymes modulate their transesterification and de-esterification reactions. If PtrHCTs interact, a change in catalytic activity should be expected and a regulatory role would be disclosed.

To detect an interaction between PtrHCT1 and PtrHCT6, enzyme activities were monitored under different molar ratios of the two PtrHCTs. Using a fixed amount of one enzyme concentration with different molar ratios of PtrHCT1 to PtrHCT6, all PtrHCT substrates, 4-coumaroyl-CoA, caffeoyl-CoA, 4-coumaroyl shikimic acid and caffeoyl shikimic acid, were examined. The simulation of additive activity was derived from the

PtrHCTs concentration and calculated based on their individual enzyme activity. For CoA thioesters, PtrHCT activities from the experiment fit with the simulation of the additive activity and as well as, for shikimic acid esters (**Figure 2.7**). The results show that activities of PtrHCT1 and PtrHCT6 are additive, which indicates that their function in SDX of *P. trichocarpa* may be redundant.

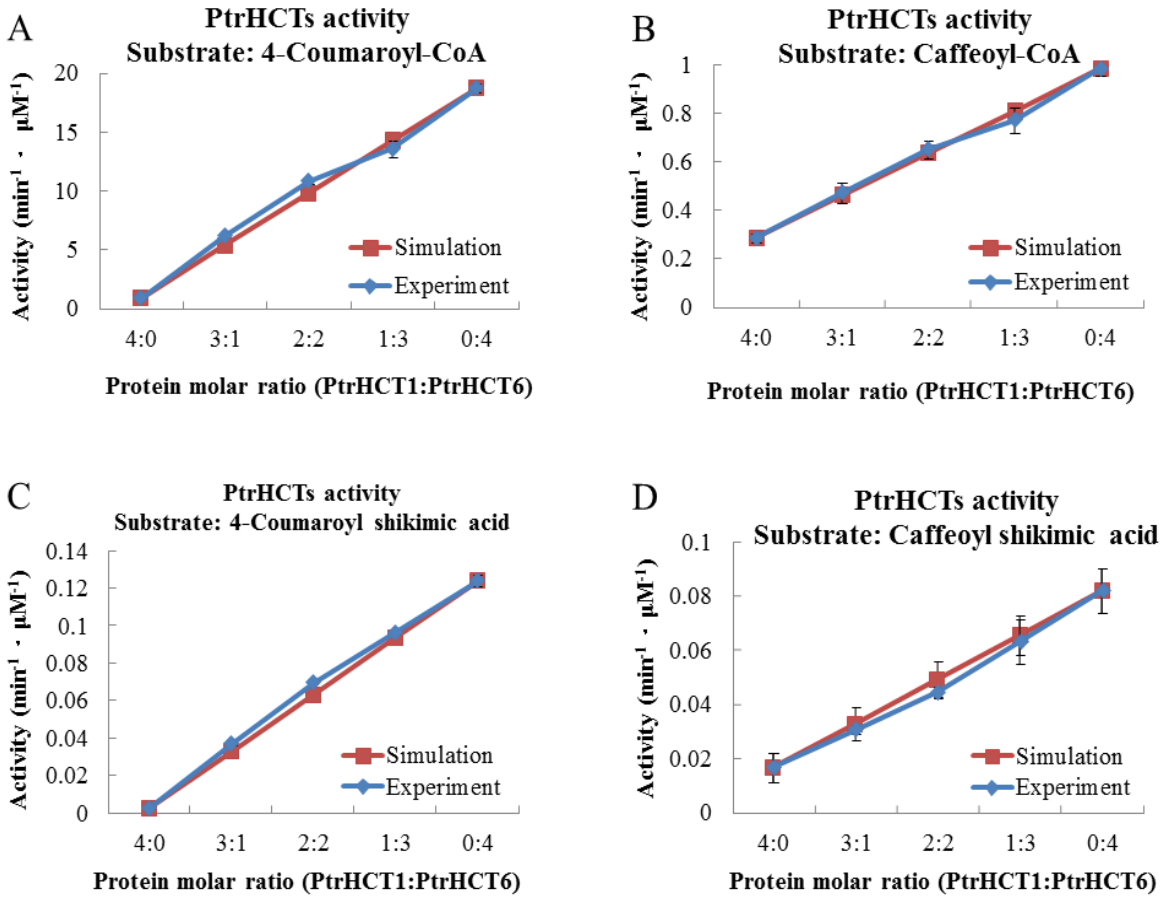

Figure 2.7 – Additive activity between PtrHCT1 and PtrHCT6. (**A**) 4-Coumaroyl-CoA is used as substrate. (**B**) Caffeoyl-CoA is used as substrate. (**C**) 4-Coumaroyl shikimic acid is used as substrate. (**D**) Caffeoyl shikimic acid is used as substrate. The error bars represent one standard error of three technical replicates.

2.3.7 Activity Evaluation of the Single Nucleotide Polymorphism (SNP) Variants of the Monolignol Biosynthetic Enzymes in *P. trichocarpa*

Prior to constructing a predictive metabolic flux model for monolignol biosynthesis in *P. trichocarpa*, the natural variants among monolignol biosynthetic enzymes, the single nucleotide polymorphisms (SNPs), need to be considered. From our previous transcriptome analysis using SDX of the *P. trichocarpa*, 32 SNP variants were identified in 8 of the 10 monolignol biosynthetic enzyme families (**Table 2.2**). Within the 32 SNP variants, 26 of the SNPs are synonymous SNPs and 6 are non-synonymous SNPs, where the non-synonymous SNPs lead to a single amino acid substitution in the whole enzyme. Because SNPs may produce enzyme variants with significantly different activity, the activities of the SNPs need to be evaluated.

The six identified non-synonymous SNP variants were distributed into Ptr4CL3, PtrCCoAOMT3, PtrCCR2 and PtrCAld5H families. Previously, the three non-synonymous SNPs in the PtrCAld5H family had been evaluated and showed essentially identical enzyme activities [42]. In this study, the activity of the three SNP variants of Ptr4CL3, PtrCCoAOMT3 and PtrCCR2 were studied. In Ptr4CL3 family, a single C/G SNP was identified that results in an amino acid change from glutamic acid to asparagine. In PtrCCoAOMT3, a single G/T SNP was identified that results in an amino acid change from alanine to glutamic acid. In PtrCCR2, a single G/A SNP was identified that results in an amino acid change from glycine to glutamic acid (**Table 2.2**).

Table 2.2 –The SNP variants in the monolignol enzymes of *P. trichocarpa*

No.	Gene	Amino Acids	Scaffold	Base	Genome Sequence	RNA-Seq Sequences
1	PAL1	Lys/Lys	scaffold_6	10034330	T	Y
2	PAL2	Leu/Leu	scaffold_8	2053326	T	Y
		Thr/Thr	scaffold_10	19775321	T	Y
		Ala/Ala	scaffold_10	19775807	C	Y
		Lys/Lys	scaffold_10	19775861	A	R
		Tyr/Tyr	scaffold_10	19775906	C	Y
3	PAL5	Thr/Thr	scaffold_10	19781996	A	C
		Asn/Asn	scaffold_10	19782824	C	T
		Gln/Gln	scaffold_10	19783271	A	G
4	C4H1	Leu/Leu	scaffold_13	15378110	G	R
		Phe/Phe	scaffold_13	15381180	G	Y
5	C4H2	Gly/Gly	scaffold_19	15705883	T	W
		Phe/Leu	scaffold_19	15707492	A	Y
6	4CL3	Tyr/Tyr	scaffold_1	5572191	C	Y
		Lys/Lys	scaffold_1	5572238	C	Y
		Glu/Asp	scaffold_1	5571941	C	*S
7	4CL5	Gly/Gly	scaffold_3	17691787	A	R
8	CCR2	Gly/Glu	scaffold_3	17211828	G	*R
9	C3H3	Pro/Pro	scaffold_6	2004783	A	R
		Ser/Ser	scaffold_6	2004789	T	Y
10	CCoAOMT1	Tyr/Tyr	scaffold_9	8859033	A	R
		Lys/Lys	scaffold_9	8859249	T	Y
11	CCoAOMT3	Ala/Glu	scaffold_8	8961572	G	*K
12	CAld5H1	Leu/Phe	scaffold_5	8721692	G	*R
		Thr/Pro	scaffold_5	8722148	T	*K
13	CAld5H2	Ala/Ala	scaffold_7	13783347	A	M
		Leu/Met	scaffold_7	13784320	T	*W
		Leu/Leu	scaffold_7	13784182	C	Y
		Ser/Ser	scaffold_7	13784196	T	Y
		Glu/Glu	scaffold_7	13784361	G	R
14	COMT2	Val/Val	scaffold_12	371215	G	S
		Ser/Ser	scaffold_12	372954	T	Y

SNP variants are identified by Prof. Ying-Hsuan Sun and Sermsawat Tunlaya-Anuki
This table is from Dr. Jack P. Wang

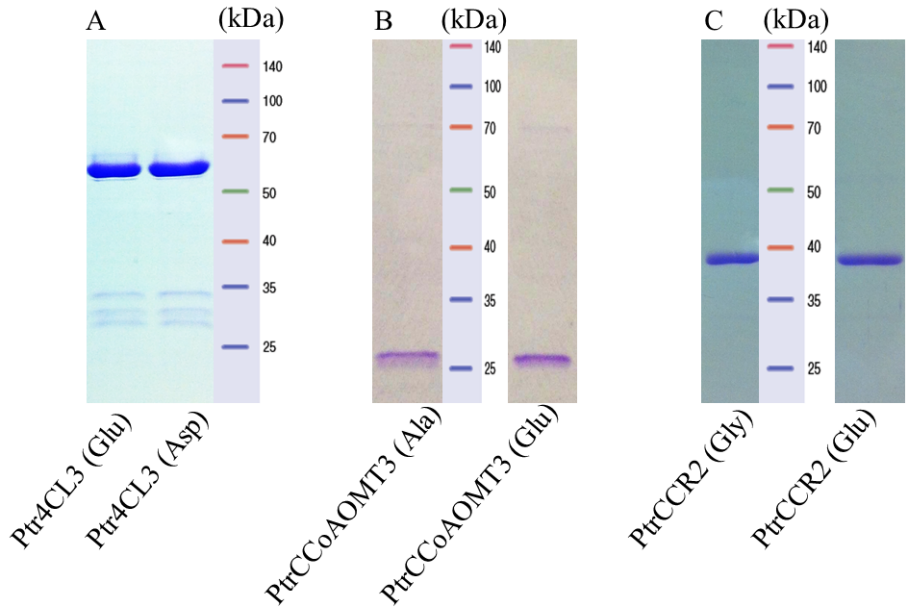

Figure 2.8 – Protein purification for the SNP variants of Ptr4CL3, PtrCCOAOMT3 and PtrCCR2. (**A**) SNP variants of Ptr4CL3. (**B**) SNP variants of PtrCCOAOMT3. (**C**) SNP variants of PtrCCR2.

For activity evaluation of the SNP variants, all the recombinant proteins (SNP variants of the Ptr4CL3, PtrCCoAOMT3 and PtrCCR2) were cloned, expressed and purified simultaneously. The purified recombinant proteins were resolved in SDS-PAGE to verify the size and the purity (**Figure 2.8**). The evaluation of the enzyme activities and conditions follow established methods [51]. The substrate used for activity evaluation for Ptr4CL3 was 4-coumaric acid; for PtrCCoAOMT3, it was caffeoyl-CoA and for PtrCCR2, it was feruloyl-CoA. The activities for all the SNP variants are without significant different.

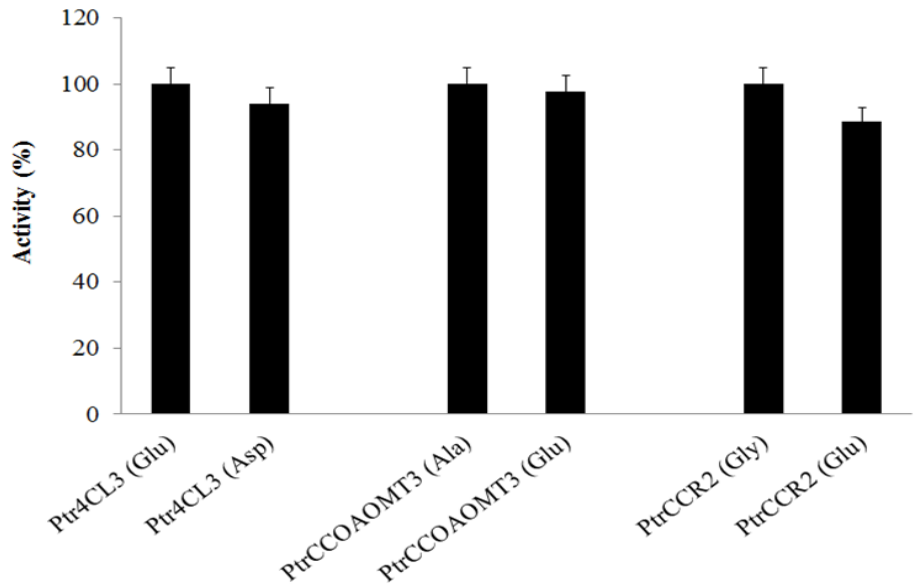

Figure 2.9 – Activity comparison for SNP variants of Ptr4CL3, PtrCCOAOMT3and PtrCCR2. The error bars represent one standard error of three technical replicates.

2.4 Discussion

2.4.1 PtrHCT1 and PtrHCT6 are both Functional Monolignol Biosynthetic Enzymes in *P. trichocarpa*

There are seven HCT gene models in the genome of *P. trichocarpa*, and, through a systematic approach, PtrHCT1 and PtrHCT6 were identified the xylem-specific HCTs. In this study, both PtrHCT1 and PtrHCT6 are studied and characterized. By comparing the amino acid sequence, PtrHCT1 and PtrHCT6 showed 92.8% similarity (**Figure 2.1**). The

enzyme activity of PtrHCT1 and PtrHCT6 shows that they are able to react with all the proposed substrates, 4-coumaroyl-CoA, caffeoyl-CoA, 4-coumaroyl shikimic acid and caffeoyl shikimic acid, which indicates they are functional monolignol biosynthetic enzymes.

2.4.2 PtrHCT1 and PtrHCT6 have Similar Kinetic Properties

HCT is known as an essential monolignol biosynthetic enzyme that mediates the 3-hydroxylation of monolignol precursors by its transesterification and de-esterification reaction [44]. Although HCT is proposed to use CoA thioesters or shikimic acid esters as its substrate, its enzyme kinetics for CoA thioesters in monolignol biosynthesis was mainly studied [30, 52]. Michaelis-Menten kinetic parameters of HCT for 4-coumaroyl-CoA, caffeoyl-CoA and feruloyl-CoA has been determined in different plant species; according to the specificity constant (k_{cat}/K_m), caffeoyl-CoA and feruloyl-CoA are the most efficient donors in tobacco and rice (*Oryza sativa* L.), respectively [44, 53]. In dates (*Phoenix dactylifera* L.), 4-coumaroyl-CoA was the preferred substrate among all CoA thioesters [54].

Unlike *Arabidopsis* and tobacco, *P. trichocarpa* possesses two active PtrHCTs in the xylem [43, 47]. PtrHCT1 and PtrHCT6 required similar temperature and pH conditions for optimum activities (**Figure 2.4**). In order to characterize the two PtrHCTs, enzyme kinetic studies are performed on all the proposed substrates for the HCT reactions in the monolignol biosynthetic pathway. Although PtrHCT1 and PtrHCT6 have high amino acid similarity, PtrHCT6 has a higher catalytic rate (k_{cat}) than PtrHCT1 (**Table 2.1**). Compared to the k_{cat}/K_m

values with all substrates for PtrHCT1 or PtrHCT6, 4-coumaroyl-CoA is the best substrate. All the shikimic acid esters have lower specificity constants (k_{cat}/K_m), which indicate that the de-esterification of the PtrHCT reactions are slow and less preferred than the transesterification of the CoA thioesters (**Table 2.1**). This result is similar to the HCT reaction in switchgrass [55].

2.4.3 The Functions of PtrHCT1 and PtrHCT6 Appear Redundant

HCT is known as an essential monolignol biosynthetic enzyme that mediates the 3-hydroxylation of monolignol precursors by its transesterification and de-esterification reactions. From the enzyme kinetic study of PtrHCTs, the de-esterification of the caffeoyl-shikimic acid to caffeoyl-CoA is the slowest reaction (**Table 2.1**), which may restrain the current proposed 3-hydroxlyation route. Previous studies had shown that protein-protein interaction between monolignol biosynthetic enzyme families in *P. trichocarpa*, such as PtrC3H3/PtrC4H1/PtrC4H2 and PtrAld5H1/PtrAld5H2 membrane protein complexes, may regulate the metabolic flux of the monolignol biosynthetic pathway [31, 42]. Therefore, the interaction between the two PtrHCTs is worthwhile to be examined.

The PtrHCT1 and PtrHCT6 are the two isoforms of PtrHCT with biochemical function in *P. trichocarpa*. Using different ratios of PtrHCT1 and PtrHCT6 for all the HCT substrates (4-coumaroyl-CoA, caffeoyl-CoA, 4-coumaroyl shikimic acid and caffeoyl shikimic acid), their activities are additive (**Figure 2.7**). The additive reaction indicates that their functions are

redundant and their activities are independent.

2.4.4 A Bottleneck is Present in the Current Monolignol Biosynthetic Pathway

From the Michaelis-Menten kinetics and the protein-protein interaction study of PtrHCT, the de-esterification reaction from caffeoyl-shikimic acid to caffeoyl-CoA by PtrHCTs is slow in the current proposed 3-hydroxylation route. This slow catalytic activity suggests a bottleneck for the 3-hydroxylation of the monolignol precursors in *P. trichocarpa*. Similarly, this slow activity is also observed in the kinetic analysis of HCT in switchgrass [55]. In *P. trichocarpa*, a newly identified activity from 4-coumaric acid to caffeic acid catalyzed by a PtrC3H3/PtrC4H1/PtrC4H2 membrane protein complex may be an alternative 3-hydroxylation route to bypass this bottleneck [31]. However, we are also wondering whether other possible routes could overcome the bottleneck of the HCT reaction.

2.4.5 The Single Nucleotide Polymorphism (SNP) Variants of Ptr4CL3, PtrCCoAOMT3 and PtrCCR2 are Identical in Activity

Single nucleotide polymorphisms (SNPs) are known as the major source of genetic variations and phenotypic plasticity [37], which is an important strategy to adapt to natural selection in *P. trichocarpa* [38]. Due to advances in sequencing technology, SNPs are now identified as frequent events in genomes of plant species. In some species of *Eucalyptus*, the frequency of SNPs can be one SNP per 16 base pairs of DNA [53, 56, 57], while, in *Populus,*

transcriptome analysis using developing secondary xylem of *P. trichocarpa* showed about 561,302 putative SNPs distributed over 26,595 expressed genes [39], which represents one SNP per 750 base pairs of genomic DNA. Because SNPs may produce enzymes that have distinct behavior and therefore affect metabolic flux, we also considered the SNP variants among the monolignol biosynthetic enzymes before constructing a mathematical model to predict the metabolic flux for monolignol biosynthetic pathway. The result showed similar catalytic activity among the SNP variants, which means the effect of those variants on the metabolic flux may be negligible.

2.5 References

1. Houtman, C.J. and R.H. Atalla, *Cellulose-Lignin Interactions (A Computational Study).* Plant physiology, 1995. **107**(3): p. 977-984.

2. Campbell, M.M. and R.R. Sederoff, *Variation in Lignin Content and Composition (Mechanisms of Control and Implications for the Genetic Improvement of Plants).* Plant physiology, 1996. **110**(1): p. 3-13.

3. Sarkanen, K.V. and C.H. Ludwig, *Lignins: occurrence, formation, structure and reactions*1971, New York: Wiley-Interscience.

4. Vance, C.P., T.K. Kirk, and R.T. Sherwood, *Lignification as a Mechanism of Disease Resistance.* Annual Review of Phytopathology, 1980. **18**(1): p. 259-288.

5. Vogel, K.P. and H.J.G. Jung, *Genetic modification of herbaceous plants for feed and fuel.* Critical Reviews in Plant Sciences, 2001. **20**(1): p. 15-49.

6. Ragauskas, A.J., et al., *The path forward for biofuels and biomaterials.* Science, 2006. **311**(5760): p. 484-9.

7. Higuchi, T., *Biochemistry and molecular biology of wood*1997: Springer series in wood science. Berlin, etc.:]. Springer-Verlag.

8. Doorsselaere, J., et al., *A novel lignin in poplar trees with a reduced caffeic acid/5-hydroxyferulic acid O-methyltransferase activity.* The Plant Journal, 1995. **8**(6): p. 855-864.

9. Baucher, M., et al., *Red Xylem and Higher Lignin Extractability by Down-Regulating a Cinnamyl Alcohol Dehydrogenase in Poplar.* Plant physiology, 1996. **112**(4): p. 1479-1490.

10. Hu, W.J., et al., *Repression of lignin biosynthesis promotes cellulose accumulation and growth in transgenic trees.* Nat Biotechnol, 1999. **17**(8): p. 808-12.

11. Lapierre, C., et al., *Structural alterations of lignins in transgenic poplars with depressed cinnamyl alcohol dehydrogenase or caffeic acid O-methyltransferase activity have an opposite impact on the efficiency of industrial kraft pulping.* Plant physiology, 1999. **119**(1): p. 153-64.

12. Chang, V.S. and M.T. Holtzapple, *Fundamental factors affecting biomass enzymatic reactivity.* Applied biochemistry and biotechnology, 2000. **84-86**: p. 5-37.

13. Jouanin, L., et al., *Lignification in transgenic poplars with extremely reduced caffeic acid O-methyltransferase activity.* Plant physiology, 2000. **123**(4): p. 1363-74.

14. Guo, D., et al., *Downregulation of caffeic acid 3-O-methyltransferase and caffeoyl CoA 3-O-methyltransferase in transgenic alfalfa. impacts on lignin structure and implications for the biosynthesis of G and S lignin.* The Plant cell, 2001. **13**(1): p. 73-88.

15. Chiang, V.L., *From rags to riches.* Nat Biotechnol, 2002. **20**(6): p. 557-8.

16. Chen, F. and R.A. Dixon, *Lignin modification improves fermentable sugar yields for biofuel production.* Nature biotechnology, 2007. **25**(7): p. 759-61.

17. Rubin, E.M., *Genomics of cellulosic biofuels.* Nature, 2008. **454**(7206): p. 841-5.

18. Hisano, H., R. Nandakumar, and Z.-Y. Wang, *Genetic modification of lignin biosynthesis for improved biofuel production.* In Vitro Cellular & Developmental Biology - Plant, 2009. **45**(3): p. 306-313.

19. Studer, M.H., et al., *Lignin content in natural Populus variants affects sugar release.* Proc Natl Acad Sci U S A, 2011. **108**(15): p. 6300-5.

20. Del Signore, G. and O.M. Berner, *Recent developments in the asymmetric synthesis of lignans.* Studies in Natural Products Chemistry, 2006. **33**: p. 541-600.

21. Joet, T., et al., *Use of the growing environment as a source of variation to identify the quantitative trait transcripts and modules of co-expressed genes that determine chlorogenic acid accumulation.* Plant, cell & environment, 2010. **33**(7): p. 1220-33.

22. Higuchi, T. and S.A. Brown, *Studies of lignin biosynthesis using isotopic carbon. XIII. The phenylpropanoid system in lignification.* Can J Biochem Physiol, 1963. **41**: p. 621-8.

23. Dixon, R.A., et al., *The biosynthesis of monolignols: a "metabolic grid", or independent pathways to guaiacyl and syringyl units?* Phytochemistry, 2001. **57**(7): p. 1069-84.

24. Higuchi, T., *Pathways for monolignol biosynthesis via metabolic grids: coniferyl aldehyde 5-hydroxylase, a possible key enzyme in angiosperm syringyl lignin biosynthesis.* Proceedings of the Japan Academy. Series B: physical and biological sciences., 2003. **79**: p. 227-236.

25. Raes, J., et al., *Genome-wide characterization of the lignification toolbox in Arabidopsis.* Plant physiology, 2003. **133**(3): p. 1051-71.

26. Barrière, Y., et al., *Genetics and genomics of lignification in grass cell walls based on maize as a model system.* Genes Genomes Genomics, 2007. **1**: p. 133-156.

27. Hamberger, B., et al., *Genome-wide analyses of phenylpropanoid-related genes in Populus trichocarpa, Arabidopsis thaliana, and Oryza sativa: the Populus lignin toolbox and conservation and diversification of angiosperm gene familiesThis article is one of a selection of papers published in the Special Issue on Poplar Research in Canada.* Canadian Journal of Botany, 2007. **85**(12): p. 1182-1201.

28. Shi, R., et al., *Towards a systems approach for lignin biosynthesis in Populus trichocarpa: transcript abundance and specificity of the monolignol biosynthetic genes.* Plant Cell Physiol, 2010. **51**(1): p. 144-63.

29. Vanholme, R., et al., *Lignin biosynthesis and structure.* Plant Physiol, 2010. **153**(3): p. 895-905.

30. Lee, Y., et al., *Integrative analysis of transgenic alfalfa (Medicago sativa L.) suggests new metabolic control mechanisms for monolignol biosynthesis.* PLoS Comput Biol, 2011. **7**(5): p. e1002047.

31. Chen, H.C., et al., *Membrane protein complexes catalyze both 4- and 3-hydroxylation of cinnamic acid derivatives in monolignol biosynthesis.* Proc Natl Acad Sci U S A, 2011. **108**(52): p. 21253-8.

32. Chen, H.-C., et al., *Monolignol Pathway 4-Coumaric Acid:CoA Ligases in Populus trichocarpa: Novel Specificity, Metabolic Regulation, and Simulation of CoA Ligation Fluxes.* Plant physiology, 2013. **161**: p. 1501-1516.

33. Kacser, H. and J.A. Burns, *The control of flux.* Symposia of the Society for Experimental Biology, 1973. **27**: p. 65-104.

34. Schallau, K. and B.H. Junker, *Simulating plant metabolic pathways with enzyme-kinetic models.* Plant physiology, 2010. **152**(4): p. 1763-71.

35. Lee, Y., et al., *Functional analysis of metabolic channeling and regulation in lignin biosynthesis: a computational approach.* PLoS computational biology, 2012. **8**(11): p. e1002769.

36. Tuskan, G.A., et al., *The genome of black cottonwood, Populus trichocarpa (Torr. & Gray).* Science, 2006. **313**(5793): p. 1596-604.

37. Wullschleger, S.D., et al., *Revisiting the sequencing of the first tree genome: Populus trichocarpa.* Tree Physiology, 2012.

38. Slavov, G.T., et al., *Genome resequencing reveals multiscale geographic structure and extensive linkage disequilibrium in the forest tree Populus trichocarpa.* New Phytologist, 2012. **196**(3): p. 713-725.

39. Geraldes, A., et al., *SNP discovery in black cottonwood (Populus trichocarpa) by population transcriptome resequencing.* Molecular ecology resources, 2011. **11 Suppl 1**: p. 81-92.

40. Shi, R., et al., *Regulation of phenylalanine ammonia-lyase (PAL) gene family in wood forming tissue of Populus trichocarpa.* Planta, 2013. **238**(3): p. 487-97.

41. Chen, H.C., et al., *Systems Biology of Lignin Biosynthesis in Populus trichocarpa: Heteromeric 4-Coumaric Acid:Coenzyme A Ligase Protein Complex Formation, Regulation, and Numerical Modeling.* The Plant cell, 2014. **26**(3): p. 876-93.

42. Wang, J.P., et al., *Functional redundancy of the two 5-hydroxylases in monolignol biosynthesis of Populus trichocarpa: LC-MS/MS based protein quantification and metabolic flux analysis.* Planta, 2012. **236**(3): p. 795-808.

43. Hoffmann, L., et al., *Silencing of hydroxycinnamoyl-coenzyme A shikimate/quinate hydroxycinnamoyltransferase affects phenylpropanoid biosynthesis.* Plant Cell, 2004. **16**(6): p. 1446-65.

44. Hoffmann, L., et al., *Purification, cloning, and properties of an acyltransferase controlling shikimate and quinate ester intermediates in phenylpropanoid metabolism.* J Biol Chem, 2003. **278**(1): p. 95-103.

45. Ulbrich, B. and M.H. Zenk, *Partial purification and properties of p-hydroxycinnamoyl-CoA: Shikimate-p-hydroxycinnamoyl transferase from higher plants.* Phytochemistry, 1980. **19**(8): p. 1625-1629.

46. Shadle, G., et al., *Down-regulation of hydroxycinnamoyl CoA: Shikimate hydroxycinnamoyl transferase in transgenic alfalfa affects lignification, development and forage quality.* Phytochemistry, 2007. **68**(11): p. 1521-1529.

47. Besseau, S., et al., *Flavonoid accumulation in Arabidopsis repressed in lignin synthesis affects auxin transport and plant growth.* Plant Cell, 2007. **19**(1): p. 148-62.

48. Shuford, C.M., et al., *Comprehensive Quantification of Monolignol-Pathway Enzymes in Populus trichocarpa by Protein Cleavage Isotope Dilution Mass Spectrometry.* Journal of Proteome Research, 2012. **11**(6): p. 3390-3404.

49. Michaelis, L. and M.L. Menten, *Die kinetik der invertinwirkung.* Biochem. z, 1913. **49**(333-369): p. 352.

50. Michaelis, L., et al., *The original Michaelis constant: translation of the 1913 Michaelis-Menten paper.* Biochemistry, 2011. **50**(39): p. 8264-9.

51. Liu, J., et al., *A standard reaction condition and a single HPLC separation system are sufficient for estimation of monolignol biosynthetic pathway enzyme activities.* Planta, 2012. **236**(3): p. 879-85.

52. Sullivan, M., *A novel red clover hydroxycinnamoyl transferase has enzymatic activities consistent with a role in phaselic acid biosynthesis.* Plant Physiol, 2009. **150**(4): p. 1866-79.

53. Kim, I.A., et al., *Characterization of hydroxycinnamoyltransferase from rice and its application for biological synthesis of hydroxycinnamoyl glycerols.* Phytochemistry, 2012. **76**: p. 25-31.

54. Lotfy, S., A. Fleuriet, and J.-J. Macheix, *Partial purification and characterization of hydroxycinnamoyl CoA: Transferases from apple and date fruits.* Phytochemistry, 1992. **31**(3): p. 767-772.

55. Escamilla-Trevino, L.L., et al., *Early lignin pathway enzymes and routes to chlorogenic acid in switchgrass (Panicum virgatum L.).* Plant molecular biology, 2014. **84**(4-5): p. 565-76.

56. Grattapaglia, D., et al., *High-throughput SNP genotyping in the highly heterozygous genome of Eucalyptus: assay success, polymorphism and transferability across species.* BMC plant biology, 2011. **11**: p. 65.

57. Külheim, C., et al., *Comparative SNP diversity among four Eucalyptus species for genes from secondary metabolite biosynthetic pathways.* Bmc Genomics, 2009. **10**(1): p. 452.

Chapter 3

4-Coumaroyl and Caffeoyl Shikimic Acids Inhibit 4-Coumaric Acid:Coenzyme A Ligases and Modulate Metabolic Flux for 3-Hydroxylation in Monolignol Biosynthesis of *Populus trichocarpa*

3.1 Introduction

Lignin is one of the most abundant biological polymers on the earth's land, second only to cellulose. Lignin is a heterogeneous phenolic polymer deposited in and between the secondary cell walls of land plants. It is a major determinant of the ability of woody plants to grow to great heights and withstand the force of gravity. Lignin provides a hydrophobic surface in cells specialized for water transport, and augments defense against biotic and abiotic stresses [1]. Lignin itself is highly resistant to microbial enzymatic degradation and persists in soils or as coal, as a reservoir in the carbon cycle. Lignin is considered a hindrance for some economic uses of plants, because of its resistance to degradation.

Lignin inhibits the enzymatic and chemical digestion of cellulose and hemicelluloses of plant secondary cell walls. Lignin must be removed from the cell walls for chemical digestion processes in the production of pulp and paper. High lignin content may create more chemical waste during pulping, decrease the conversion efficiency of livestock forage, or

limit the efficiency of biomass-energy conversion in the production of biofuels [2, 3]. Studies of lignin biosynthesis have led to greater understanding of monolignol precursor formation and the mechanisms of lignin polymerization [4]. The development of technology to modify lignin content or composition has led to new strategies to produce improved plants to meet the needs of our society for forage, paper and bioenergy.

Lignin itself is a high molecular weight polymer with crosslinks across lignin chains and crosslinks to the cellulosic polymers within secondary cell walls [5]. . The lignin polymer consists mainly of three major phenylpropanoid monomeric subunits known as 4-hydroxyphenyl (H), guaiacyl (G) and syringyl (S) subunits. These subunits are derived from the oxidative polymerization of three corresponding monolignol precursors known as 4-coumaryl, coniferyl, and sinapyl alcohols, respectively [6].

In woody flowering plants (dicotyledons), such as *Populus trichocarpa*, S and G are the most abundant subunits. In most gymnosperms such as conifers, G is the major lignin subunit [1]. In grasses, higher amounts of H subunits (<~5%) can be found in lignin with equal amounts of abundant G and S subunits [7]. Both lignin content and composition, that is, the proportion of different subunits, are important factors for hydrolysis and biomass utilization. Lowering lignin content or increasing the S/G ratio improves the economic value of wood by reducing the recalcitrance to lignin removal during pulp and paper or biofuel production [8-11].

In flowering plants, monolignols are synthesized from the aromatic amino acid phenylalanine by 10 enzyme families [7, 12-20]. The biosynthesis of all monolignols involves the deamination of phenylalanine, followed by hydroxylation at the 4 position and the reduction of the acid at the end of the propane side-chain to an alcohol (**Figure 3.1**). Monolignols differ in the degree of hydroxylation and methylation at the 3 and 5 positions of the phenyl ring. 3-Hydroxylation of the phenyl ring is essential for the formation of the coniferyl and sinapyl alcohols (**Figure 3.1**).

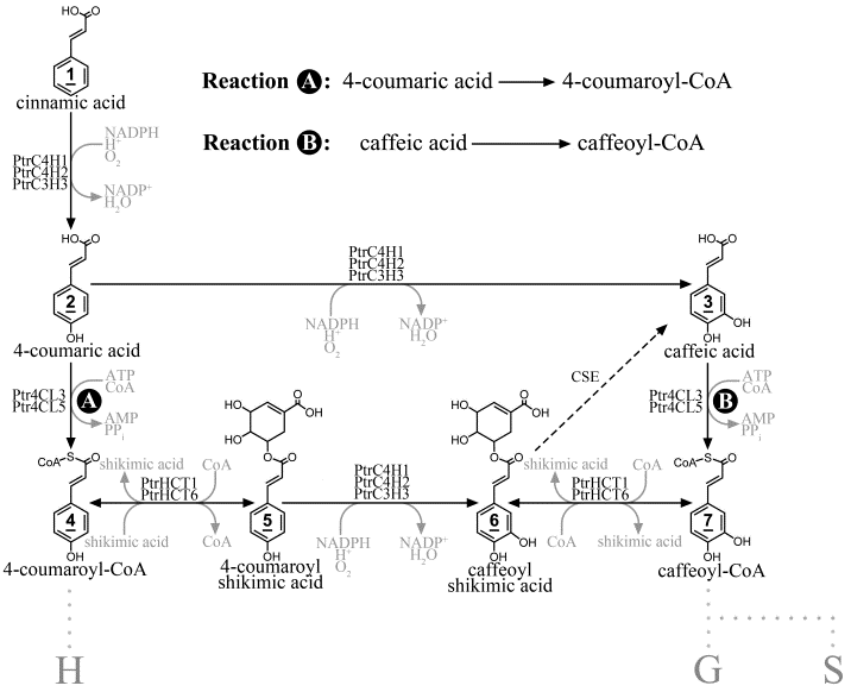

Figure 3.1 – A section of the *P. trichocarpa* monolignol biosynthetic pathway. Starting from cinnamic acid, all metabolites in this section of the monolignol biosynthetic pathway are numbered and underlined. The cofactors are also depicted in each reaction in gray. Reaction A is the formation of 4-coumaroyl-CoA from 4-coumaric acid and reaction B is the formation of caffeoyl-CoA from caffeic acid. H, G and S refer to the type of subunits in lignin, 4-hydroxyphenyl, guaiacyl and syringyl, respectively.

3-Hydroxylation was proposed to be catalyzed by 4-hydroxycinnamoyl-CoA:shikimic acid hydroxycinnamoyl transferase (HCT; EC 2.3.1.133) to form 4-coumaroyl shikimic acid followed by 4-coumaric acid 3-hydroxylase (C3H; EC 1.14.13.36) and subsequently, the conversion by HCT to form caffeoyl-CoA (**Figure 3.1**) [21, 22]. However, the reaction rate of HCT for the conversion of caffeoyl shikimic acid to caffeoyl-CoA is slow in *P. trichocarpa* (and switchgrass), which may create a bottleneck for 3-hydroxylation leading to G and S monolignol biosynthesis [23, 24]. The slow catalytic efficiency of the conversion of caffeoyl shikimic acid to caffeoyl-CoA by PtrHCT (kcat/Km less than 0.05 $\mu M^{-1} \cdot min^{-1}$) restrains the formation of caffeoyl-CoA [24] (**Chapter 2**).

Recently, a new enzyme has been described in *Arabidopsis thaliana* that hydrolyzes caffeoyl shikimic acid to caffeic acid called caffeoyl shikimate esterase (CSE) (**Figure 3.1**) [25]. . Caffeic acid in turn can be converted to caffeoyl-CoA by 4-coumaric acid:coenzyme A ligase (4CL; EC 6.2.1.12). 4CL catalyzes the conversion of the hydroxycinnamic acids to their CoA thioester derivatives (**Figure 3.1**). Alternatively, in *P. trichocarpa*, the slow reaction rate of PtrHCT may be bypassed through the more direct conversion of 4-coumaric acid to caffeic acid by a PtrC4H1/C4H2/C3H3 membrane protein complex (**Figure 3.1**) [22]. These two alternative routes highlight the importance of the reactions of Ptr4CL in the formation of caffeoyl-CoA either from caffeic acid or through caffeoyl shikimic acid for coniferyl and sinapyl monolignol biosynthesis (**Figure 3.1**).

The *P. trichocarpa* genome sequence contains 17 gene models encoding 4CL candidate proteins [19]. Of these 17 gene models, only Ptr4CL3 and Ptr4CL5 have transcripts that are abundant in stem differentiating xylem (SDX) and encode proteins that have CoA ligation activity [19, 26]. Ptr4CL3 and Ptr4CL5 recombinant proteins exhibit distinct substrate affinity and kinetic properties. In single substrate reactions, Ptr4CL3 prefers 4-coumaric acid while Ptr4CL5 has broader substrate affinity. Ptr4CL3 shows competitive inhibition (at the active site) while Ptr4CL5 shows both allosteric regulation and substrate self-inhibition [26]. In SDX, Ptr4CL3 and Ptr4CL5 are found in a heterotetrameric protein complex. The heterotetramer contains 3 subunits of Ptr4CL3 and 1 subunit of Ptr4CL5 [27]. There are two steps in monolignol biosynthesis catalyzed by Ptr4CL, shown as Reactions A and B (**Figure 3.1**). The protein-protein interactions of the Ptr4CL tetramer affect the direction and metabolic flux of CoA ligation for Reaction A and Reaction B (**Figure 3.1**) [27]. The protein complex can affect the relative efficiency of CoA ligation of caffeic acid compared to 4-coumaric acid [24, 26, 27].

In vitro and *in vivo* experiments demonstrated that many pathway intermediates can substantially affect the metabolic flux through enzyme inhibition to fine-tune the monolignol biosynthetic pathway [28-31]. It is not yet clear why there are alternative pathways for the formation of caffeoyl-CoA (**Figure 3.1**). 4-Coumaroyl and caffeoyl shikimic acids were selected as potential inhibitors of the Ptr4CLs because these shikimic acid esters may have a role in regulating the flux through the alternative A and B pathways. Ptr4CL3 and Ptr4CL5

show competitive and uncompetitive inhibition by substrates 4-coumaric acid and caffeic acid. Ferulic acid, 5-hydroxyferulic acid and sinapic acid are either very weak or inactive as substrates or inhibitors [26, 27]. Here, we report novel inhibitory effects on Ptr4CL activities caused by 4-coumaroyl and caffeoyl shikimic acids. These shikimic acid esters inhibit the metabolic flux from 4-coumaric acid to 4-coumaroyl-CoA. These inhibitory effects may modulate the 3-hydroxylation from 4-coumaric acid to caffeic acid. In addition, the Ptr4CL directed conversion of caffeic acid to caffeoyl-CoA is inhibited by 4-coumaroyl shikimic acid. 4-Coumaroyl shikimic acid can inhibit both 4-coumaroyl-CoA and caffeoyl-CoA production. Caffeoyl shikimic acid can only inhibit the production of 4-coumaroyl-CoA. Therefore, the inhibition of Reaction A by 4-coumaroyl and caffeoyl shikimic acids increase flux through the direct 3-hydroxylation of 4-coumaric acid to caffeic acid and subsequently to the formation of caffeoyl-CoA.

3.2 Materials and Methods

3.2.1 Plant Materials

Clonal propagules of *Populus trichocarpa* (Nisqually-1) wildtype and transgenic PtrC3H3 in this wildtype background, were grown in a greenhouse in soil containing a 1:1 ratio of peat moss to potting-mix, using 16 h light and 8 h dark photoperiods for six months.

Stem differentiating xylem (SDX) tissues were harvested following procedures described by Shi et al. (2010).

3.2.2 Synthesis of Monolignol Precursors

4-Coumaric acid, caffeic acid and shikimic acid were purchased from Sigma-Aldrich (St. Louis, MO). 4-Coumaroyl-CoA and caffeoyl-CoA were enzymatically synthesized from their corresponding hydroxycinnamic acids following Chen et al. (2013). 4-Coumaroyl and caffeoyl shikimic acids were synthesized enzymatically using recombinant PtrHCT6 expressed in *E. coli* and purified by GST-tag affinity chromatography[22, 32]. 15 mg of either 4-coumaroyl-CoA or caffeoyl-CoA were added with 5 mg of shikimic acid to 20 mL of 50 mM NaHPO4 (pH 7). Purified PtrHCT6 (0.2 mg) was added to the mixture to start the reaction. After 60 min at 30 °C, 800 μL of glacial acetic acid was added to stop the reaction. The shikimic acid esters were purified by ethyl acetate extraction (3 times, 20 mL). The total 60 mL ethyl acetate extracts was dried in a Rotavapor® R II (BUCHI, Flawil, Switzerland) and frozen at -80 OC. The purity and identity of all synthesized products were confirmed by mass spectrometry [26, 31, 32].

3.2.3 Recombinant Ptr4CL3 and Ptr4CL5 Expression and Purification

Functional recombinant proteins of Ptr4CL3 and Ptr4CL5 were expressed with C-terminal His-tag fusions in *E. coli* and purified using nickel-immobilized metal ion affinity

chromatography (Ni-IMAC; Shuford et al., 2012; Chen et al., 2013, 2014). The recombinant proteins of Ptr4CL3 and Ptr4CL5 were resolved in SDS-PAGE (**Figure 3.2**).

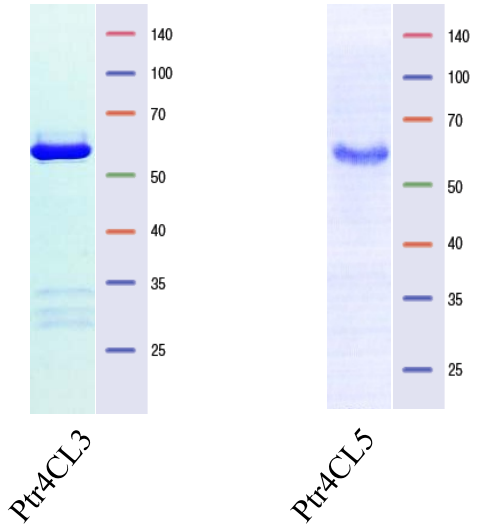

Figure 3.2 – 1D-SDS-PAGE of His-tag purified recombinant Ptr4CL3 and Ptr4CL5 stained with coomassie blue.

3.2.4 Quantification of Transcripts, Metabolites and Proteins in Stem Differentiating Xylem (SDX)

The RNAi-silencing construct with an inverted repeat that downregulated PtrC3H3 was used for these experiments (Li et al. unpublished). One PtrC3H3 transgenic line was selected based on qRT-PCR [19]. The SDX tissues of wildtype and PtrC3H3 downregulated transgenic trees were used to extract metabolites and proteins for absolute quantification by

LC-MS/MS. 4-Coumaric acid, caffeic acid, 4-coumaroyl shikimic acid and caffeoyl shikimic acid were quantified by replicate injection LC-MS/MS analysis using selected reaction monitoring and [^{13}C]-labeled internal standards following Chen et al. (2013). Absolute abundances of PtrC3H3, Ptr4CL3 and Ptr4CL5 were obtained by PC-IDMS using isotopically labeled surrogate peptides following procedures described by Shuford et al. (2012).

3.2.5 Total Protein Extraction from SDX

3 g of freshly isolated SDX tissue was ground under liquid nitrogen to a fine powder, and suspended in extraction buffer (50 mM Tris-HCl, pH 7.5, 20 mM sodium ascorbate, 0.4 M sucrose, 100 mM sodium chloride, 5 mM DTT, 20% glycerol, 10% PVPP, 2 mM PMSF, 2 μg/mL pepstatin A and 2 μg/mL leupeptin), homogenized on ice using an Ultra-Turrax T-18 basic disperser (IKA, Wilmington, NC), and spun at 4000 x g to remove debris. The supernatant was filtered through an Amicon Ultra 10 kDa centrifugal filter (Millipore, Billerica, MA) using a 5X sample volume of extraction buffer, and stored at -80 °C before enzyme assays. Total protein concentration of the SDX extracts was determined according to Bradford (1976).

3.2.6 Enzyme Assays and HPLC Analysis

For enzyme reaction of recombinant Ptr4CLs, a 100 μL reaction containing 50 μM of substrate (4-coumaric acid or caffeic acid), 50 μM of shikimic acid esters (4-coumaroyl shikimic acid or caffeoyl shikimic acid), 200 μM CoA, 5 mM ATP and 2.5 mM MgCl2 in 50 mM Tris-HCl buffer (pH 8.0 for Ptr4CL3 and pH 7.0 for Ptr4CL5) starts with a final enzyme concentration of 10 nM for a reaction time of 10 min. Enzyme assay for SDX and Ptr4CLs mixture were conducted under the same condition as recombinant Ptr4CL enzyme reactions; however, 50 mM Tris-HCl buffer (pH 7.5) was used and, for SDX enzyme assay, experiment was carried out by using 20 μg of crude SDX protein at 40 °C for 30 min. All enzyme reactions were stopped by adding 5 μL of 3 M trichloroacetic acid (TCA). The mixture was centrifuged at 20,000 x g for 10 min and analyzed by HPLC following Liu et al. (2012). The substrates and products of the enzyme assays were separated on a Zorbax SB-C18 5 μm, 4.6 x 150-mm column (Agilent, Santa Clara, CA). Analyses of reactions involving hydroxycinnamyl CoAs were carried out using a HPLC gradient method (solvent A, 5 mM ammonium acetate, pH 5.6; solvent B, water: acetonitrile: acetic acid, 2: 97.8: 0.2; 8% to 10% B for 3 min, 10 to 30% B for 5 min, 30 to 100% for 5 min; flow rate: 1 mL/min). The metabolites were quantified in a Diode-Array Detector SL (Agilent, Santa Clara, CA) based on authentic compounds [24, 32].

3.2.7 Inhibition Kinetics of Ptr4CL3 and Ptr4CL5

Kinetic analysis was carried out following procedures described by Wang et al. (2012, 2014) and Chen et al. (2013). 4 to 5 concentrations of shikimic acid ester inhibitors (10 μM to 50 μM) were tested with varying concentrations of substrates to determine the extent and mode of inhibition, competitive (K_m increased), uncompetitive (both K_m decreased and V_{max} decreased), noncompetitive (V_{max} decreased), or mixed mode inhibition (both K_m and V_{max} altered). Inhibition plots of K_m'/V_{max}' against inhibitor concentration [I], and 1/ V_{max}' against [I] were used to obtain the K_{ic} and K_{iu} values, respectively.

Equation 1 is derived from the basic Michaelis-Menten equation, which describes a reaction mechanism for a mixture of competitive and uncompetitive inhibition. K_{ic}, the competitive inhibition constant, is the dissociation constant of the enzyme-inhibitor complex. K_{iu}, the uncompetitive inhibition constant, is the dissociation constant of the inhibitor from the enzyme-substrate complex. Equation 3 describes the mixed inhibition mechanism of competitive and non-competitive inhibition. K_{in} is the non-competitive inhibition constant. Equation 2 and 4 are the inverted forms of Equation 1 and 3 respectively, which are used for the Lineweaver-Burk plots to determine the K_m' and V_{max}' values. Increased K_m' and decreased V_{max}' can result from either mixed competitive with uncompetitive or mixed competitive with noncompetitive inhibition. K_m' and V_{max}' were analyzed as a function of [I] according to both Equation 1 and Equation 3 to determine the mode of inhibition.

$$V = \frac{V_{max} \cdot [\mathrm{S}]}{K_m \cdot \left(1 + \frac{[\mathrm{I}]}{K_{\mathrm{ic}}}\right) + [S] \cdot \left(1 + \frac{[\mathrm{I}]}{K_{\mathrm{iu}}}\right)} \qquad \text{(Equation 1)}$$

$$\frac{1}{V} = \frac{1}{[S]} \cdot \frac{K_m \cdot \left(1 + \frac{[\mathrm{I}]}{K_{\mathrm{ic}}}\right)}{V_{max}} + \frac{\left(1 + \frac{[\mathrm{I}]}{K_{\mathrm{iu}}}\right)}{V_{max}} \qquad \text{(Equation 2)}$$

$$V = \frac{\frac{V_{max}}{\left(1 + \frac{[\mathrm{I}]}{K_{\mathrm{in}}}\right)} \cdot [\mathrm{S}]}{K_m \cdot \left(1 + \frac{[\mathrm{I}]}{K_{\mathrm{ic}}}\right) + [S]} \qquad \text{(Equation 3)}$$

$$\frac{1}{V} = \frac{1}{[S]} \cdot \frac{K_m \cdot \left(1 + \frac{[\mathrm{I}]}{K_{\mathrm{ic}}}\right) \cdot \left(1 + \frac{[\mathrm{I}]}{K_{\mathrm{in}}}\right)}{V_{max}} + \frac{\left(1 + \frac{[\mathrm{I}]}{K_{\mathrm{in}}}\right)}{V_{max}} \qquad \text{(Equation 4)}$$

3.3 Results

3.3.1 4-Coumaroyl and Caffeoyl Shikimic Acids Inhibit Recombinant Ptr4CL3 and Ptr4CL5 Activities

We investigated the potential inhibition of Ptr4CL activity by other intermediates in the monolignol biosynthetic pathway. To do this we purified recombinant Ptr4CL3 and Ptr4CL5 proteins with C-terminal 6x His-tag expressed in *Escherichia coli* for enzyme assays *in vitro*. C-terminal 6x His-tag does not affect the substrate specificity and reaction rates of Ptr4CL3 and Ptr4CL5 [26]. Phenylalanine, cinnamic acid, coniferaldehyde and coniferyl alcohol were obtained commercially. 4-Coumaroyl and caffeoyl shikimic acids were enzymatically synthesized and verified by mass spectrometry. 4-Coumaric acid or caffeic acid was used as the substrate. The synthesis of the corresponding CoA thioesters was monitored by HPLC.

The activity of Ptr4CL3 or Ptr4CL5 on 4-coumaroyl-CoA and caffeoyl-CoA production was significantly inhibited when either 4-coumaroyl or caffeoyl shikimic acid was added into the reactions (**Figure 3.3**). Phenylalanine, cinnamic acid, coniferaldehyde and coniferyl alcohol showed no inhibitory effects (**Figure 3.4**). Ptr4CL3 and Ptr4CL5 have distinct responses to inhibition by 4-coumaroyl or caffeoyl shikimic acid. For Ptr4CL3, 4-coumaroyl shikimic acid produced stronger inhibition than caffeoyl shikimic acid. When 4-coumaroyl shikimic acid was added, Ptr4CL3 activity was reduced to 26.4% of control for 4-coumaroyl-CoA production and to 18.9% for caffeoyl-CoA production. When caffeoyl shikimic acid was added, Ptr4CL3 activity was only reduced to 67.7% of control for 4-coumaroyl-CoA production and to 80.8% for caffeoyl-CoA production (**Figures 3.3A** and **3.3B**). For Ptr4CL5, the production of 4-coumaroyl-CoA was reduced to 65.2% of control when 4-coumaroyl shikimic acid was added and to 67.2% when caffeoyl shikimic acid was added (**Figure 3.3C**). However, Ptr4CL5 activity for production of caffeoyl-CoA was reduced only to 86.0% by 4-coumaroyl shikimic acid. Caffeoyl shikimic acid had no inhibitory effect on Ptr4CL5 for caffeoyl-CoA formation (**Figure 3.3D**). Ptr4CL3 and Ptr4CL5 activities were usually unaffected by shikimic acid for both 4-coumaroyl-CoA and caffeoyl-CoA formation (**Figure 3.5**). The exception was Ptr4CL5. When 4-coumaric acid was the substrate, product was reduced to 76.3% of control (**Figure 3.5D**). To better understand how 4-coumaroyl and caffeoyl shikimic acids inhibit Ptr4CL reactions with 4-coumaric acid and caffeic acid *in vivo*, we studied Ptr4CL enzyme inhibition kinetics.

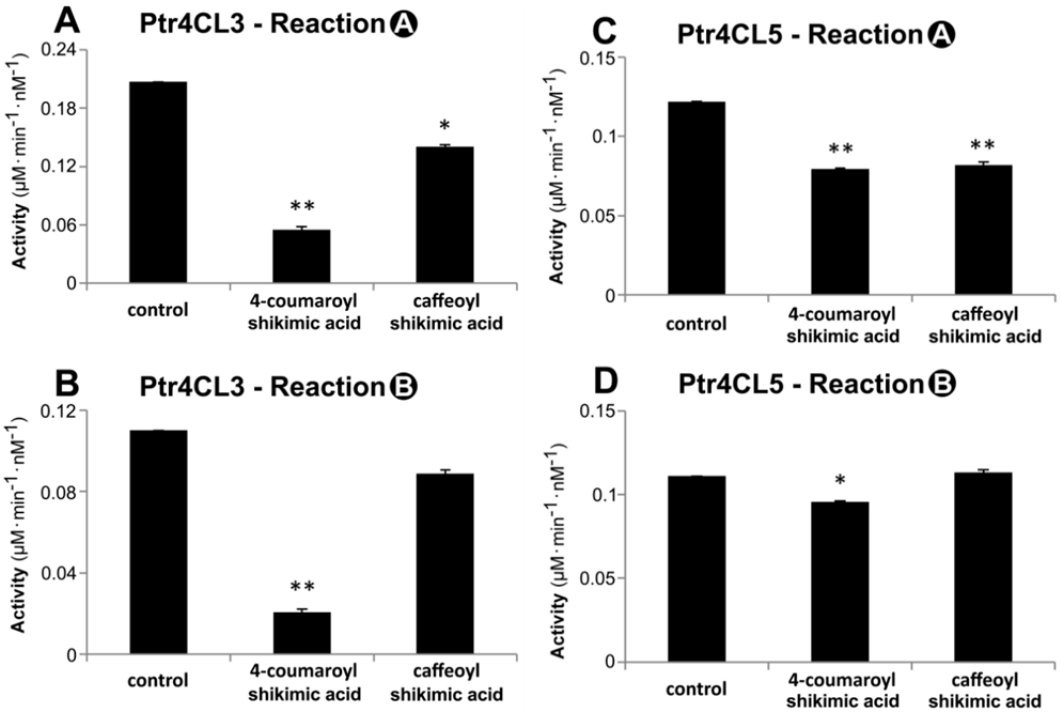

Figure 3.3 – 4-Coumaroyl and caffeoyl shikimic acids inhibit recombinant Ptr4CL3 and Ptr4CL5 activities. (**A**) Inhibition by shikimic acid esters of Ptr4CL3 activity for 4-coumaroyl-CoA production. (**B**) Inhibition by shikimic acid esters of Ptr4CL3 activity for caffeoyl-CoA production. (**C**) Inhibition by shikimic acid esters of Ptr4CL5 activity for 4-coumaroyl-CoA production. (**D**) Inhibition by shikimic acid esters of Ptr4CL5 activity for caffeoyl-CoA production. Concentration of all substrates and inhibitors were 50 μM. The error bars represent one standard error of three technical replicates. Statistical testing was performed using Student's t-test (*, $p < 0.05$; **, $p < 0.01$).

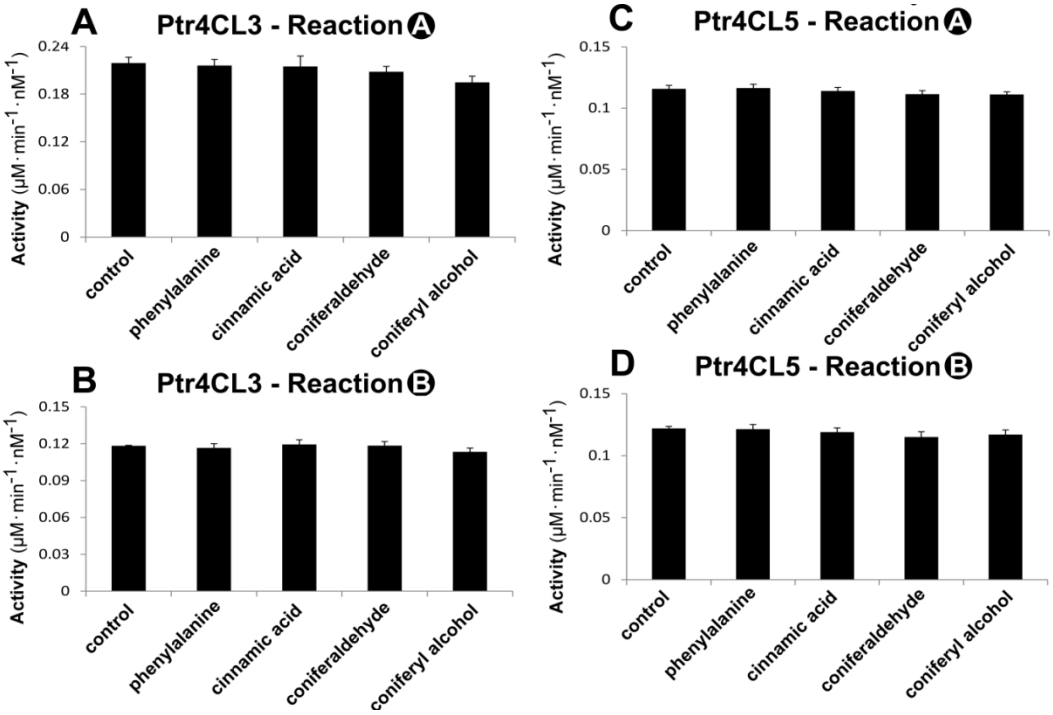

Figure 3.4 – Inhibition tests for the Ptr4CL3 and Ptr4CL5 Reactions A and B, using phenylalanine, cinnamic acid, coniferaldehyde and coniferyl alcohol. (**A**) Ptr4CL3 Reaction A. (**B**) Ptr4CL3 Reaction B. (**C**) Ptr4CL5 Reaction A. (**D**) Ptr4CL5 Reaction B. Concentration of all substrates and inhibitors were 50 μM. The error bars represent one standard error of three technical replicates.

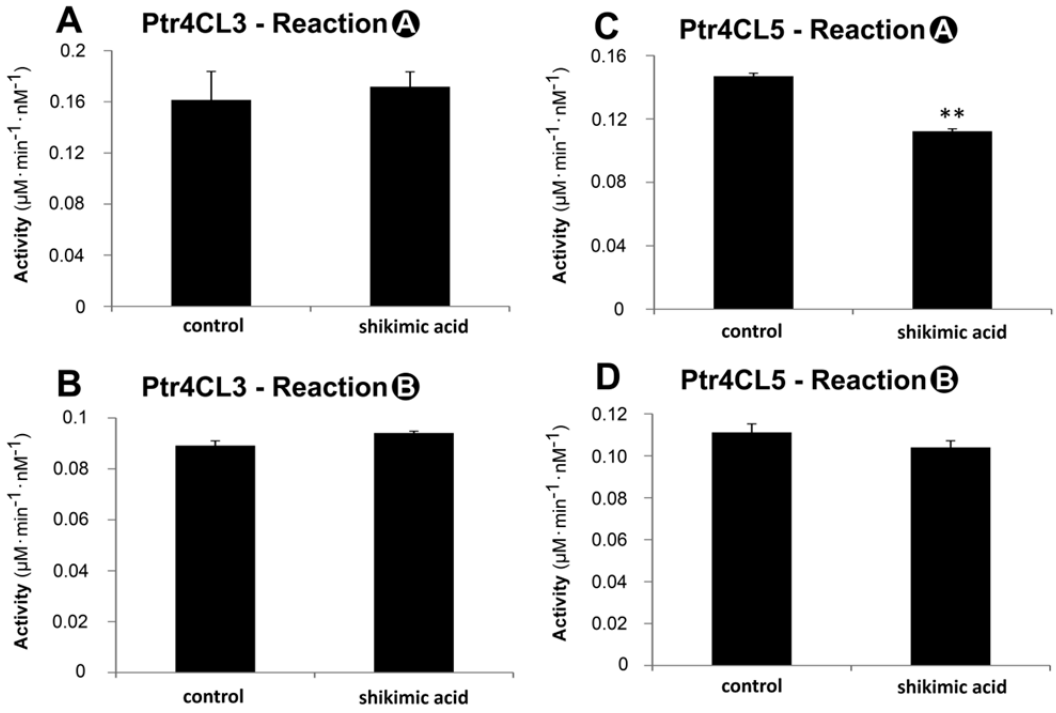

Figure 3.5 – Inhibition tests for the Ptr4CL3 and Ptr4CL5 Reactions A and B, when shikimic acid is added. (**A**) Ptr4CL3 activity for 4-coumaroyl-CoA production with and without shikimic acid. (**B**) Ptr4CL3 activity for caffeoyl-CoA production with and without shikimic acid. (**C**) Ptr4CL5 activity for 4-coumaroyl-CoA production is slightly inhibited by shikimic acid. (**D**) Ptr4CL5 activity for caffeoyl-CoA production with and without shikimic acid. Concentration of all substrates and inhibitors were 50 μM. The error bars represent one standard error of three technical replicates. Statistical testing was performed using Student's t-test (**, $p < 0.05$).

3.3.2 Inhibition Kinetics Indicate that 4-Coumaroyl Shikimic Acid Shows Stronger Inhibition on Ptr4CL3 and Ptr4CL5 Activities than Caffeoyl Shikimic Acid

Our long term goal has been to develop predictive metabolic models of the monolignol pathway [24, 27]. To do this we need reliable estimates of inhibition kinetic parameters. We estimated inhibition kinetic parameters for Ptr4CL3 and Ptr4CL5 using 4-coumaroyl or

caffeoyl shikimic acid as the inhibitor and 4-coumaric or caffeic acid as the substrate. The inhibition kinetic assays for either 4-coumaroyl or caffeoyl shikimic acid on Ptr4CL3 and Ptr4CL5 activities were carried out (**Figure 3.3**). Inhibition kinetics for caffeoyl shikimic acid inhibiting Ptr4CL3 and Ptr4CL5 Reaction B were precluded because of the weak and insignificant inhibition ($p > 0.05$) (**Figures 3.3B** and **3.3D**).

The double reciprocal Lineweaver-Burk plots show that inhibition of Ptr4CL reactions by 4-coumaroyl or caffeoyl shikimic acid follows a mixed inhibition mode, for mixtures of competitive and either uncompetitive or non-competitive inhibition (**Figure 3.6**). The increased K_m' indicates that the substrate and inhibitor compete for the enzyme active site (competition inhibition, K_{ic}). The decreased V_{max}' indicates that the inhibitor can also bind to an allosteric site to cause uncompetitive (K_{iu}) or non-competitive (K_{in}) inhibition. To distinguish uncompetitive from non-competitive inhibition, nonlinear regression was used to fit the 6 inhibition datasets (**Figure 3.6**) into two Ptr4CL inhibition equations (Materials and Methods), either Equation 1 (competitive with uncompetitive) or Equation 3 (competitive with noncompetitive) from Chen et al. (2013). The data best fit a mode of competitive with uncompetitive inhibition giving high R^2 values (greater than or equal to 0.9756) using nonlinear regression (**Figure 3.7**).

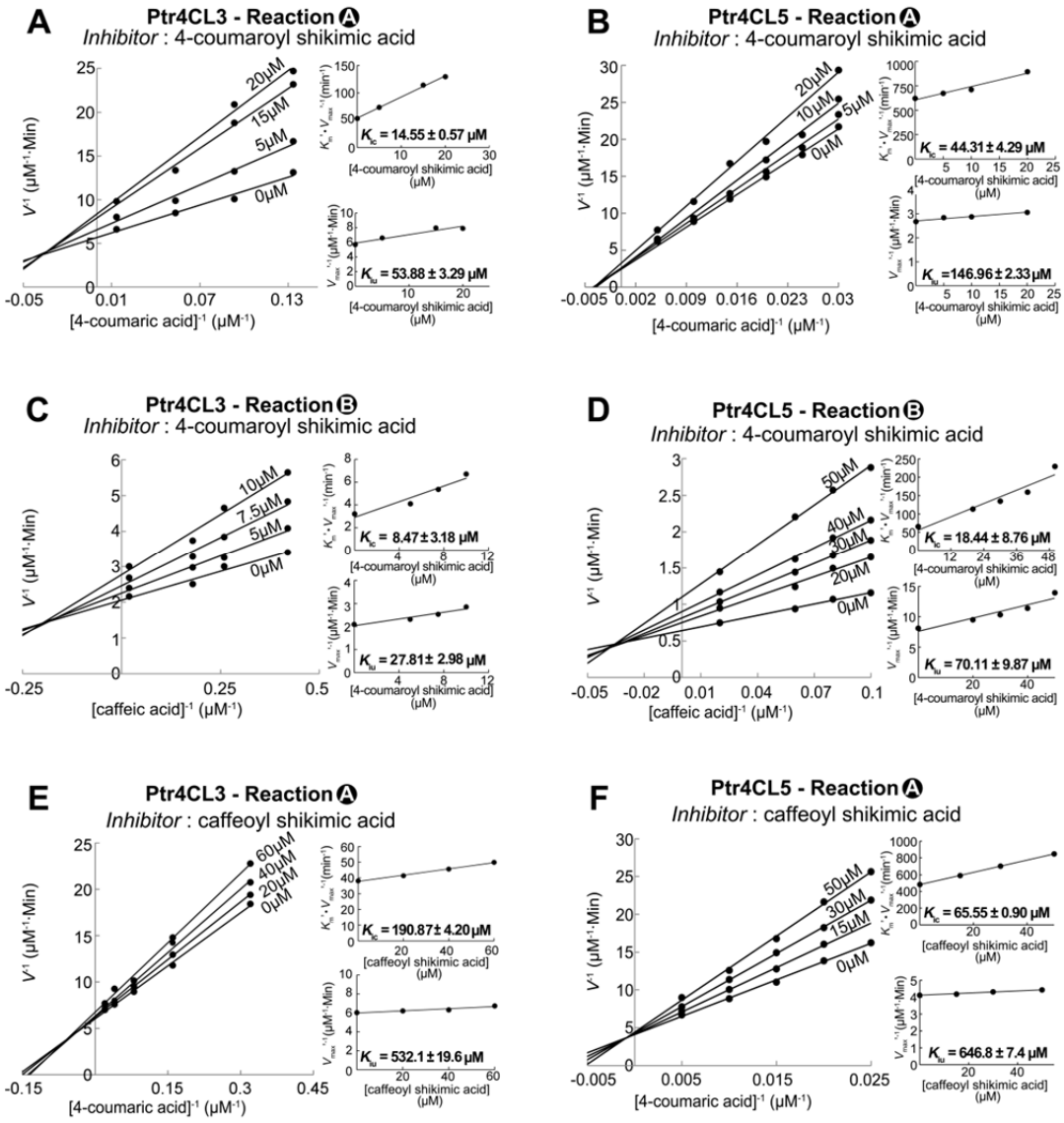

Figure 3.6 – Inhibition kinetics show that 4-coumaroyl and caffeoyl shikimic acids have distinct effects on Ptr4CL3 and Ptr4CL5 reactions. (**A**) Inhibition kinetics of Ptr4CL3 activity with 4-coumaric acid as the substrate and 4-coumaroyl shikimic acid as the inhibitor. (**B**) Inhibition kinetics of Ptr4CL5 activity with 4-coumaric acid as the substrate and 4-coumaroyl shikimic acid as the inhibitor. (**C**) Inhibition kinetics of Ptr4CL3 with caffeic acid as the substrate and 4-coumaroyl shikimic acid as the inhibitor. (**D**) Inhibition kinetics of Ptr4CL5 activity with caffeic acid as the substrate and 4-coumaroyl shikimic acid as the inhibitor. (**E**) Inhibition kinetics of Ptr4CL3 activity with 4-coumaric acid as the substrate and caffeoyl shikimic acid as the inhibitor. (**F**) Inhibition kinetics of Ptr4CL5 activity with 4-coumaric acid as the substrate and caffeoyl shikimic acid as the inhibitor. The plots of K_m'/V_{max}' are used to determine the K_{ic} values and K_{iu} values are derived from 1/V_{max}' plots.

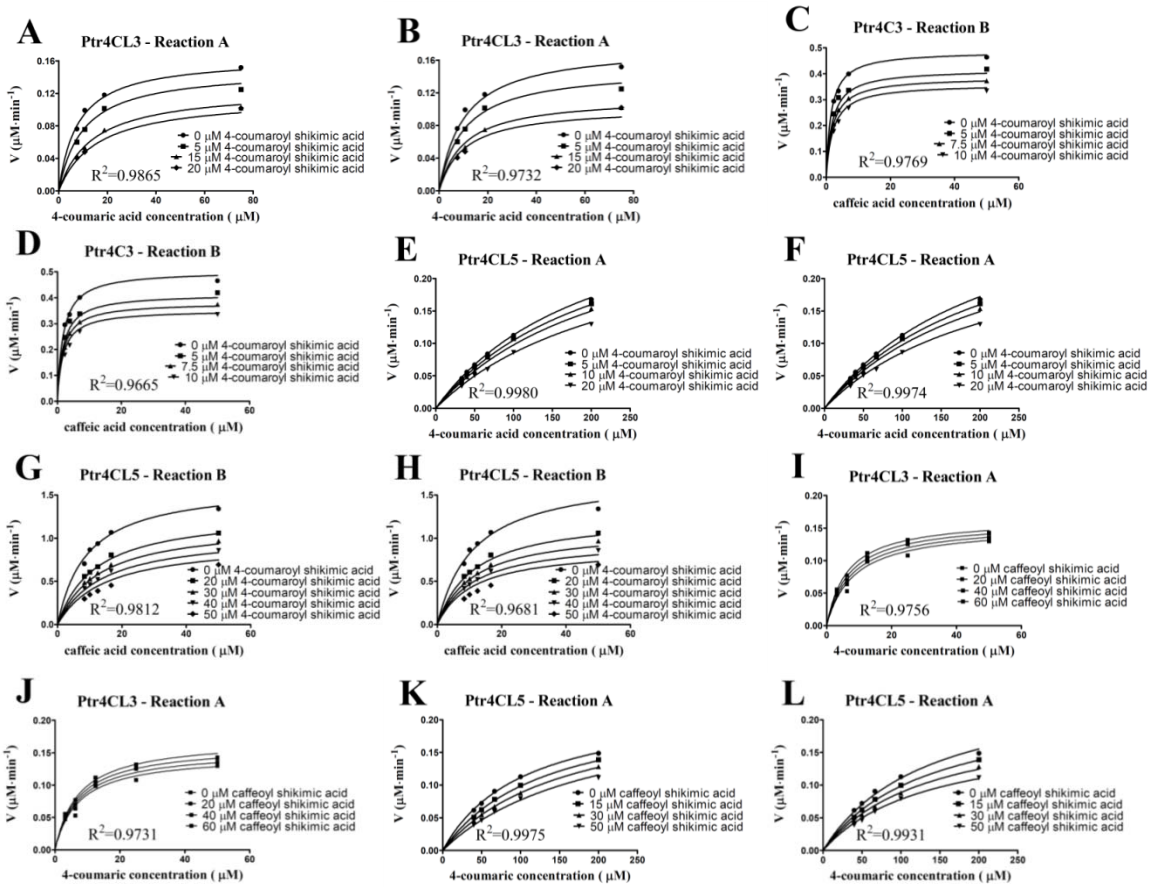

Figure 3.7 – The experimental data from inhibition kinetics was analyzed by nonlinear regression using Equation 1 or Equation 3. (**A**) 4-Coumaryol shikimic acid inhibits Reaction A of Ptr4CL3 using Equation 1. (**B**) 4-Coumaryol shikimic acid inhibits Reaction A of Ptr4CL3 using Equation 3. (**C**) 4-Coumaryol shikimic acid inhibits Reaction B of Ptr4CL3 using Equation 1. (**D**) 4-Coumaryol shikimic acid inhibits Reaction B of Ptr4CL3 using Equation 3. (**E**) 4-Coumaryol shikimic acid inhibits Reaction A of Ptr4CL5 using Equation 1. (**F**) 4-Coumaryol shikimic acid inhibits Reaction A of Ptr4CL5 using Equation 3. (**G**) 4-Coumaryol shikimic acid inhibits Reaction B of Ptr4CL5 using Equation 1. (**H**) 4-Coumaryol shikimic acid inhibits Reaction B of Ptr4CL5 using Equation 3. (**I**) Caffeoyl shikimic acid inhibits Reaction A of Ptr4CL3 using Equation 1. (**J**) Caffeoyl shikimic acid inhibits Reaction A of Ptr4CL3 using Equation 3. (**K**) Caffeoyl shikimic acid inhibits Reaction A of Ptr4CL5 using Equation 1. (**L**) Caffeoyl shikimic acid inhibits Reaction A of Ptr4CL5 using Equation 3. R^2 indicates the goodness of fit of the nonlinear regression analysis.

The inhibition kinetic parameters (K_{ic} and K_{iu}) were determined by plotting K_m'/V_{max}' over inhibitor [I] and 1/V_{max}' over [I] (**Figure 3.6**). All K_{ic} values are smaller than the K_{iu} values. Therefore competitive inhibition is the dominant effect. Then, we compared the K_{ic} values to K_m values of the Ptr4CL3 and Ptr4CL5 (**Figure 3.8**). For Ptr4CL3, 4-coumaroyl shikimic acid was an effective inhibitor of 4-coumaric acid CoA ligation because 4-coumaroyl shikimic acid had a similar enzyme affinity to the substrate (K_m = 10.51 μM and K_{ic} = 14.55 μM). 4-Coumaroyl shikimic acid is also a strong inhibitor of Ptr4CL3 caffeic acid CoA ligation, as the K_{ic} (8.47 μM) is lower than the K_m (10.56 μM).

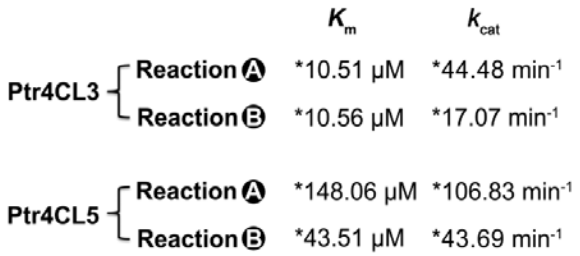

Figure 3.8 – The Michaelis-Menten kinetic parameters of Ptr4CL3 and Ptr4CL5 for 4-coumaric acid (Reaction A) and caffeic acid (Reaction B). Michaelis-Menten kinetic parameters (*) for Ptr4CL3 and Ptr4CL5 are from Wang et al. (2014).

The inhibitory effect of 4-coumaroyl shikimic acid is stronger for Ptr4CL5 than for Ptr4CL3 when either 4-coumaric acid or caffeic acid was the substrate. The K_{ic} value for 4-coumaric acid as substrate is 44.31 μM and for caffeic acid as substrate is 18.44 μM. These K_{ic} values are less than their corresponding K_m values (148.06 μM for 4-coumaric acid and

43.51 μM for caffeic acid). In contrast, caffeoyl shikimic acid is a weak inhibitor of the Ptr4CL3 and Ptr4CL5 reactions (**Figures 3.3B and 3.3D**). Caffeoyl shikimic acid showed inhibition for Ptr4CL3 and Ptr4CL5 conversion of 4-coumaric acid to 4-coumaroyl-CoA. For Ptr4CL3, K_{ic} = 190.87 μM and K_m = 10.51 μM and for Ptr4CL5, K_{ic} = 65.55 μM and K_m = 148.06 μM. Taken together, the inhibition kinetic data show that 4-coumaroyl and caffeoyl shikimic acids are mixed mode inhibitors for Ptr4CL3 and Ptr4CL5. 4-Coumaroyl shikimic acid shows a stronger inhibitory effect than caffeoyl shikimic acid.

3.3.3 4-Coumaroyl and Caffeoyl Shikimic Acids Inhibit Ptr4CL Activities in the SDX Protein Extracts of *P. trichocarpa* and in Mixtures of Ptr4CL3 and Ptr4CL5

It was important to test if 4-coumaroyl and caffeoyl shikimic acids could have inhibitory effects *in vivo* on Ptr4CL activity during monolignol biosynthesis in *P. trichocarpa*. Therefore, we collected SDX tissues from rapidly growing wildtype *P. trichocarpa* and prepared protein extracts for enzyme assays. 4-Coumaroyl or caffeoyl shikimic acid was added into the SDX extracts of *P. trichocarpa* using 4-coumaric acid or caffeic acid as substrate. Both 4-coumaroyl and caffeoyl shikimic acids inhibited the Ptr4CL reactions for both 4-coumaroyl-CoA and caffeoyl-CoA production in the extracts (**Figure 3.9**). 4-Coumaric and caffeic acids are the main substrates for the Ptr4CL reactions in monolignol biosynthesis [26, 27]. Therefore, the inhibitory effects of 4-coumaroyl and caffeoyl shikimic acids on Ptr4CL activity indicate that these two shikimic acid esters could regulate metabolic

flux to caffeoyl-CoA *in vivo* (**Figure 3.1**). The activity measured in SDX extracts or in mixtures of Ptr4CL3 and Ptr4CL5 results from the sum of the activities of individual enzymes and the activity of the Ptr4CL3/Ptr4CL5 complex [27] In a previous paper, we showed by chemical crosslinking and immunoprecipitation that most of the Ptr4CL proteins in the tissue and in the extracts are found in a heterotetrameric complex rather than as individual enzymes [27].

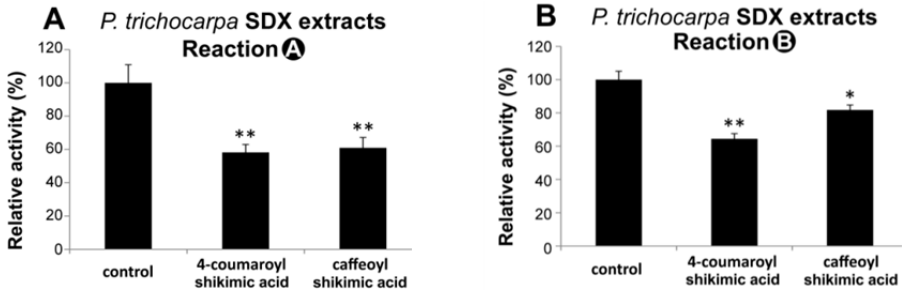

Figure 3.9 – 4-Coumaroyl and caffeoyl shikimic acids inhibit Ptr4CL reactions in SDX extracts of *P. trichocarpa*. (A) Inhibition by 4-coumaroyl and caffeoyl shikimic acids on the formation of 4-coumaroyl-CoA in SDX extracts of *P. trichocarpa*. (B) Inhibition by 4-coumaroyl and caffeoyl shikimic acids on the formation of caffeoyl-CoA in SDX extracts of *P. trichocarpa*. Concentration of all substrates and inhibitors were 50 µM. The error bars represent one standard error of three technical replicates. Statistical testing was performed using Student's t-test (*, $p < 0.05$; **, $p < 0.01$).

The similarity of the inhibition in SDX extracts and the inhibition with the individual enzymes suggests that the inhibitory effect on the complex *in vivo* is consistent with effects on purified individual enzymes. To test this inference further, we carried out inhibition assays on a mixture of the recombinant proteins in a 3 to 1 ratio of Ptr4CL3 and Ptr4CL5.

We found that the inhibition on the mixture is very similar to the inhibitory effects on individual Ptr4CLs (**Figures 3.3 and 3.10**) indicating that there is no apparent difference between the inhibition on the individual enzymes and the protein complex. In a mixture containing both Ptr4CL3 and Ptr4CL5, shikimic acid does not inhibit Reaction A or B (**Figure 3.10**). Hence, we have excluded shikimic acid as a significant inhibitor of Ptr4CL3 and Ptr4CL5 reactions. This result is consistent with our finding that the inhibitory effects of the individual enzymes are conserved in the protein complex [27].

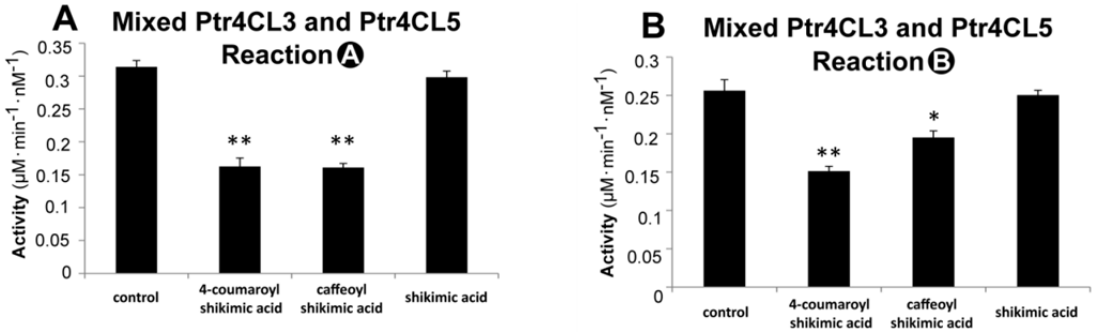

Figure 3.10 – 4-Coumaroyl and caffeoyl shikimic acids inhibit Ptr4CL reactions in a mixture of the recombinant proteins in a 3 to 1 ratio of Ptr4CL3 and Ptr4CL5, where shikimic acid has not inhibitory effect. (**A**) Inhibition by 4-coumaroyl and caffeoyl shikimic acids on the formation of 4-coumaroyl-CoA, but not by shikimic acid. (**B**) Inhibition by 4-coumaroyl and caffeoyl shikimic acids on the formation of caffeoyl-CoA, but not by shikimic acid. Concentration of all substrates and inhibitors were 50 μM. The error bars represent one standard error of three technical replicates. Statistical testing was performed using Student's t-test (*, $p < 0.05$; **, $p < 0.01$).

3.3.4 4-Coumaroyl Shikimic Acid, Caffeoyl Shikimic Acid and 4-Coumaric Acid Accumulate in PtrC3H3 Downregulated Transgenic *P. trichocarpa*

On the basis of these results, the major question becomes to what extent does flux during monolignol biosynthesis go to caffeoyl-CoA (compound 7 in **Figure 3.1**) through 4-coumaroyl-CoA (compound 4) following Reaction A in Figure 1, or through 4-coumaric acid (compound 2) to caffeic acid (compound 3) and then to caffeoyl-CoA (Reaction B in **Figure 3.1**). Therefore, we have developed methods to quantitate the metabolites 4-coumaric acid, caffeic acid, 4-coumaroyl shikimic acid and caffeoyl shikimic acid (compounds 2, 3, 5 and 6 in **Figure 3.1**) in *P. trichocarpa* SDX [26] (Materials and Methods). The CoA thioester derivatives, 4-coumaroyl-CoA and caffeoyl-CoA (compounds 4 and 7 in **Figure 3.1**), are sufficiently unstable during extraction to preclude quantitation.

We determined the levels of metabolites 2, 3, 5 and 6 in wildtype *P. trichocarpa* and in *P. trichocarpa* transgenic plants downregulated by RNA interference (RNAi) [24] for PtrC3H3. PtrC3H3 is the functional 3-hydroxylase in monolignol biosynthesis in *P. trichocarpa* [19, 22]. In addition, an *Arabidopsis thaliana* mutant carrying a defect in the *C3H* gene, (*ref8*), accumulated 4-coumaric acid esters including 4-coumaroyl shikimic acid [33, 34]. PtrC3H3 transgenics showed a reduction of PtrC3H3 transcript abundance to 8.7% of wildtype, as shown by qRT-PCR (**Figure 3.11A**). PtrC3H3 protein abundance was reduced to 7% of wildtype, as shown by protein cleavage-isotope dilution mass spectrometry (PC-IDMS; **Figure 3.11B**; Shuford et al., 2012).

The SDX extracts of wildtype and PtrC3H3 transgenics were prepared for metabolite quantitation by mass spectrometry (Materials and Methods) [31, 32]. 4-Coumaric acid, 4-coumaroyl shikimic acid and caffeoyl shikimic acid accumulated in the PtrC3H3 downregulated transgenic *P. trichocarpa*. 4-Coumaroyl shikimic acid accumulated from 0.23 to 426 pmol/mg SDX while 4-coumaric acid accumulated from 1.5 to 12 pmol/mg SDX (**Figures 3.11C and 3.11D**), suggesting a substantial inhibition of Ptr4CL activity in the downregulated transgenics. Caffeoyl shikimic acid accumulated from 0.45 to 16 pmol/mg SDX (**Figure 3.11E**).

The accumulation of caffeoyl shikimic acid could be due to the extremely high concentration of 4-coumaroyl shikimic acid and the residual activity of PtrC3H3. The accumulated level of caffeoyl shikimic acid is only 4% of the level of accumulated 4-coumaroyl shikimic acid. However, the protein abundance of PtrC3H3 is only 7% of wildtype. Our current PKMF metabolic model [24] can explain only part of the excess of caffeoyl shikimic acid. Simulation using this updated PKMF model shows that when 4-coumaroyl shikimic acid is 426 pmol/mg, and protein abundance of PtrC3H3 is 7% of wildtype, the caffeoyl shikimic acid level is elevated compared to wildtype by 2.5 fold. The extent of increase in the PtrC3H3 transgenic however is 35.6 fold. This result suggests that there is another component of the pathway not yet defined, contributing to the higher level of caffeoyl shikimic acid.

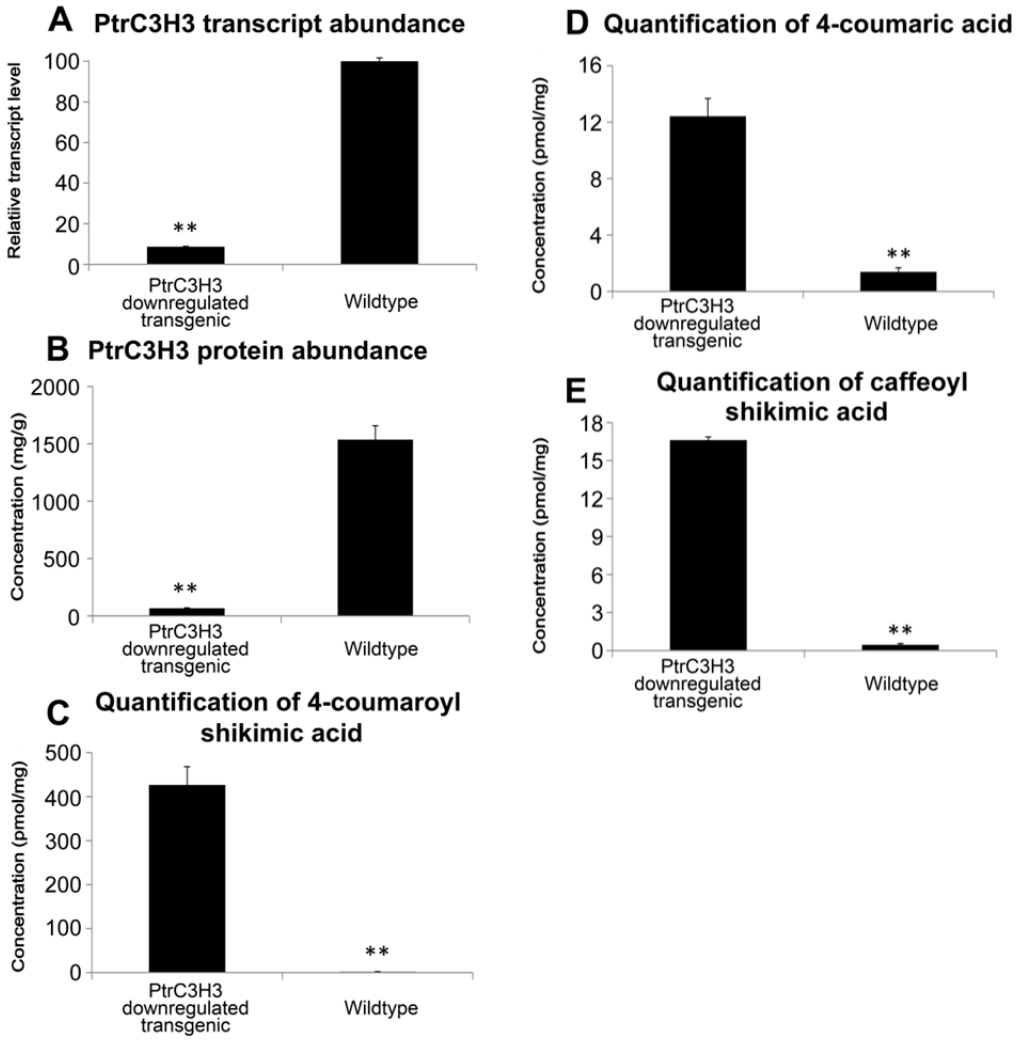

Figure 3.11 – Quantification of transcript and metabolite levels of 4-coumaroyl shikimic acid and 4-coumaric acid in PtrC3H3 downregulated transgenic and wildtype of *P. trichocarpa*. (**A**) qRT-PCR result shows the reduced level of PtrC3H3 transcript in transgenic compared to wildtype. (*B*) Absolute protein quantification of PtrC3H3 in wildtype and transgenic plants. (**C**) Absolute quantification of 4-coumaroyl shikimic acid. (**D**) Absolute quantification of 4-coumaric acid. (E) Absolute quantification of caffeoyl shikimic acid. The error bars represent one standard error of three technical replicates. Statistical testing was performed using Student's t-test (**, $p < 0.01$).

3.3.5 Evaluation of the Roles of 4-Coumaroyl and Caffeoyl Shikimic Acids as Inhibitors Using Estimated Flux Based on Mass Action Kinetics and Inhibition Parameters

We have estimates of the absolute protein quantities of Ptr4CL3 and Ptr4CL5 in SDX [31] (Supplemental Methods). We have also obtained absolute quantitation of the metabolites 4-coumaric acid, caffeic acid, 4-coumaroyl shikimic acid and caffeoyl shikimic acid (compounds 2, 3, 5 and 6 in **Figure 3.1**). These values can now be used in equations that describe the mass action kinetics and inhibition parameters of the Ptr4CL reactions. These equations mathematically describe, in a metabolic model, how inhibition by 4-coumaroyl and caffeoyl shikimic acids may affect the metabolic flux *in vivo* (**Figure 3.12**). In **Table 3.1**, we show the estimated values of metabolic flux for wildtype and PtrC3H3 transgenics based on these equations with and without the shikimic acid ester inhibitors.

In wildtype, at the observed levels of the substrates and inhibitors, there is little inhibition by the shikimic acid esters on flux through the Ptr4CL reactions for either 4-coumaric acid or caffeic acid as the substrate. However, in the PtrC3H3 transgenics, 4-coumaric acid, 4-coumaroyl shikimic acid and caffeoyl shikimic acid accumulate and flux for conversion of 4-coumaric acid to 4-coumaroyl-CoA is increased by 9.4-fold in the absence of inhibition (**Figures 3.11C and 3.11D**; **Table 3.1**). Inhibition by the shikimic acid esters can reduce flux to a normal level (**Table 3.1A**). Similarly, for caffeic acid as substrate (**Table 3.1B**), there is little inhibition of flux in wildtype but an estimated inhibition to 65% of flux by the shikimic acid esters in the PtrC3H3 transgenics. Therefore, the estimated fluxes show that inhibition

by 4-coumaroyl and caffeoyl shikimic acids could play a significant biological role when these metabolic intermediates accumulate.

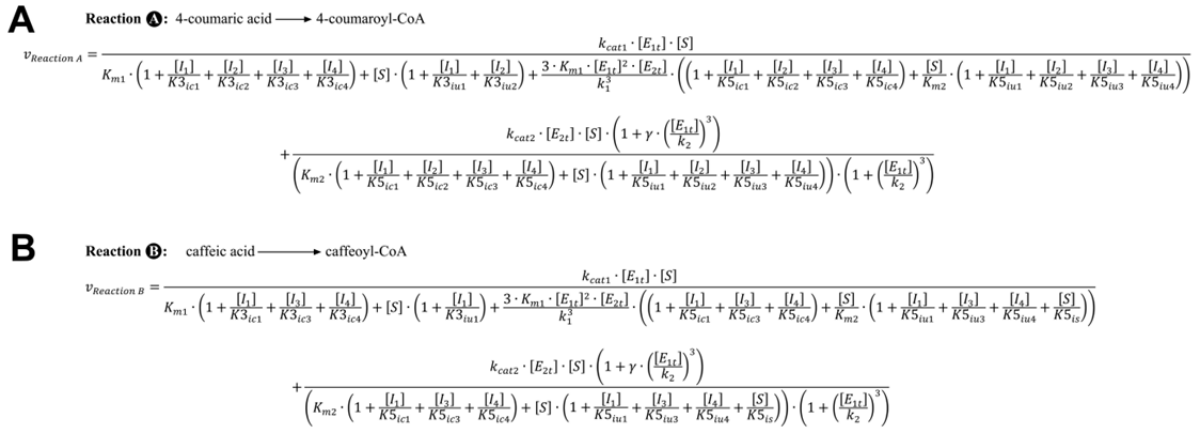

Figure 3.12 – The equations from Chen et al. (2014) have been modified to include the effects of inhibition by 4-coumaroyl and caffeoyl shikimic acids on Ptr4CL reactions using 4-coumaric acid as the substrate (**A**) and caffeic acid as the substrate (**B**). These equations allow us to calculate reaction rates at different concentrations of substrates and inhibitors. Abbreviations: K_{m1} and K_{m2}, the Michaelis-Menten constants for Ptr4CL3 and Ptr4CL5 respectively; k_{cat1} and k_{cat2}, the turnover constants for Ptr4CL3 and Ptr4CL5 respectively; $[E_{1t}]$ and $[E_{2t}]$, the concentrations of Ptr4CL3 and Ptr4CL5 respectively [24, 31]; $[I_1]$ and $[I_2]$, the concentrations of 4-coumaroyl shikimic acid and caffeoyl shikimic acid respectively; $[I_3]$, $[I_4]$, the concentration of caffeic and ferulic acids for Reaction A, and 4-coumaric and ferulic acids for Reaction B, respectively; $K3_{ic1}$, $K3_{iu1}$, $K5_{ic1}$ and $K5_{iu1}$, the competitive and uncompetitive inhibition constants for Ptr4CL3 and Ptr4CL5 when 4-coumaroyl shikimic acid is the inhibitor; $K3_{ic2}$, $K3_{iu2}$, $K5_{ic2}$ and $K5_{iu2}$, the competitive and uncompetitive inhibition constants for Ptr4CL3 and Ptr4CL5 when caffeoyl shikimic acid is the inhibitor; $K3_{ic3}$, $K3_{iu3}$, $K5_{ic3}$, and $K5_{iu3}$, the competitive and uncompetitive inhibition constants for Ptr4CL3 and Ptr4CL5 when caffeic acid is the inhibitor (Reaction A) and 4-coumaric acid is the inhibitor (Reaction B); $K3_{ic4}$, $K3_{iu4}$, $K5_{ic4}$, and $K5_{iu4}$, the competitive and uncompetitive inhibition constants for Ptr4CL3 and Ptr4CL5 when ferulic acid is the inhibitor; $K5_{is}$, the substrate self-inhibition constant for Ptr4CL5 when caffeic acid is the substrate [26]; k_1, k_2 and γ, the optimized parameters for Ptr4CL protein complex formation and regulation [27].

Table 3.1 – Estimated Ptr4CL flux based on mass action kinetics and inhibition parameters for 4-coumaric acid as substrate (**A**) and caffeic acid as substrate (**B**).

A	Ptr4CL Reaction Flux (μM/min)	
	Substrate: 4-Coumaric acid	
	Wildtype	PtrC3H3 transgenics
Without shikimic acid esters	0.0115	0.291
With shikimic acid esters	0.0114 (99.6%)	0.0382(13.1%)

B	Ptr4CL Reaction Flux (μM/min)	
	Substrate: Caffeic acid	
	Wildtype	PtrC3H3 transgenics
Without shikimic acid esters	1.69	0.350
With shikimic acid esters	1.66 (98.4%)	0.0168 (4.79%)

The numbers in parentheses denote percentage of flux after inhibition.

3.4 Discussion

A recent comprehensive Predictive Kinetic Metabolic Flux (PKMF) model of monolignol biosynthesis reveals extensive control of metabolic flux by metabolite inhibitions at many steps in the pathway [24]. For example: cinnamic acid and caffeic acid are competitive inhibitors of phenylalanine ammonia-lyase (PAL), which regulates the entry point of monolignol biosynthesis [28, 35]. Inhibitory effects of coniferaldehyde on coniferaldehyde 5-hydroxylase (CAld5H) for ferulic acid 5-hydroxylation and 5-hydroxyconiferaldehyde on caffeic acid *O*-methyltransferase (AldOMT) for caffeic acid and 5-hydroxyferulic acid methylation, direct the metabolic flux for S monolignol biosynthesis [24, 29, 30, 36]. Also, inhibitory effects of the hydroxycinnamic acid substrates for Ptr4CL3 and Ptr4CL5 modulate the CoA ligation flux [26, 27]. A potential role for 4-coumaroyl and caffeoyl shikimic acids as inhibitors regulating early steps of monolignol biosynthesis, for example, to facilitate the 3-hydroxylation of 4-coumaric acid and 4-coumaroyl shikimic acid, had not been explored. Our results demonstrate that 4-coumaroyl and caffeoyl shikimic acids work as mixed mode inhibitors of the Ptr4CLs. The mixed mode inhibition for these enzymes is a combination of competitive and uncompetitive inhibition. Therefore, the flux through Ptr4CL may be regulated either by competition with substrates and or by interaction of inhibitors with the enzyme-substrate complex at a regulatory site. Plants, such as *P. trichocarpa*, may have a more complex regulation for the metabolic flux associated with 3-hydroxylation than has

been previously considered.

The Ptr4CL enzyme reaction itself in monolignol biosynthesis is complex [26, 27]. Both Ptr4CL3 and Ptr4CL5 can function as monomeric enzymes and in a heterotetrameric enzyme complex [27]. In this complex, Ptr4CL5 has a regulatory role with respect to substrate and inhibitor specificity. 4-Coumaric acid, caffeic acid and ferulic acid are all effective substrates. In reactions containing both enzymes and mixtures of substrates, inhibition of enzyme activity by alternative substrates plays an important role [26, 27]. The shikimic acid ester inhibitors affect the two Ptr4CL reactions shown in Figure 1 (Reaction A and Reaction B) differently. Inhibition by shikimic acid esters is stronger for conversion of 4-coumaric acid than for conversion of caffeic acid. 4-Coumaroyl shikimic acid is a stronger inhibitor than caffeoyl shikimic acid. These results now add additional complexity to this important step of the monolignol biosynthetic pathway.

PtrC3H3 has a role in the direct conversion of 4-coumaric acid to caffeic acid, and an alternative role in the conversion of 4-coumaroyl shikimic acid to caffeoyl shikimic acid [22]. PtrC3H3 is one component of a three-protein complex of PtrC3H3/PtrC4H1/PtrC4H2 [22]. When PtrC3H3 is a member of the complex, the rates of conversion of 4-coumaric acid to caffeic acid and 4-coumaroyl shikimic acid to caffeoyl shikimic acid are increased for both reactions. The extent of the increase is far higher for the conversion of 4-coumaric acid to caffeic acid compared to the alternative reaction from 4-coumaroyl shikimic acid to caffeoyl shikimic acid or compared to the activity of PtrC3H3 as a purified protein [22].

The PtrC3H3 downregulated transgenic used in this experiment (called i20-5) showed a proportional reduction of transcript and protein when transcript abundance is reduced to 8.7% (Figure 6A). This reduction suggests that the abundance of transcript is sufficient to determine the observed abundance of protein. The i20-5 transgenic was one of three constructs used to downregulate PtrC3H3 to different levels of transcript abundance. i20-5 had the strongest reduction of transcript and the highest accumulation of 4-coumaroyl shikimic acid and 4-coumaric acid. The properties of the transgenic i20-5 are consistent with the PKMF mathematical metabolic model of Wang et al. (2014) based on the kinetic properties of the wildtype enzyme and the relative abundance of the protein and metabolites.

Caffeoyl shikimate esterase (CSE) is a recently discovered monolignol enzyme that hydrolyzes caffeoyl shikimic acid to caffeic acid and shikimic acid [25] and can modify lignin content and composition in Arabidopsis thaliana. An Arabidopsis mutant of CSE results in lignin highly enriched in 4-hydroxyphenyl units (H subunits). The conversion of caffeoyl shikimic acid to caffeic acid catalyzed by CSE provides a novel path to bypass the slow HCT reaction from caffeoyl shikimic acid to caffeoyl-CoA. The 3-hydroxylation from 4-coumaroyl-CoA to caffeic acid and then to caffeoyl-CoA through CSE requires a second CoA ligation step to synthesize caffeoyl-CoA, which consumes an additional ATP for downstream G and S monolignol biosynthesis. Nevertheless, CSE is important in Arabidopsis for the formation of caffeoyl-CoA.

The state of CSE activity and its function in *P. trichocarpa* are still unclear. In a previous study [24], we were unable to detect CSE activity in SDX of *P. trichocarpa*, although transcripts of CSE homologs were present at low levels. There are two CSE homologs in the *P. trichocarpa* genome, but we have no direct evidence yet showing that these genes encode and express active CSE enzymes. LC-MS/MS based global proteomics of *P. trichocarpa* SDX detected only one of the *P. trichocarpa* CSE homologs, with low spectral counts. CSE maybe expressed in *P. trichocarpa* but at a very low level. Much more work is needed to learn the role of CSE in this pathway in *P. trichocarpa*. Further experiments using transgenic plants modified in several monolignol enzymes to different levels of expression may resolve these questions.

Our recent PKMF model of monolignol biosynthesis described the kinetic behavior of metabolic flux for the 21 enzymes and 24 metabolites of the pathway [24]. The model explains how pathway enzymes synthesize monolignol precursors and how the ratios of lignin subunits are regulated. We can now include the effects of inhibition of Ptr4CL reactions by 4-coumaroyl and caffeoyl shikimic acids to the overall metabolic flux model to improve its predictive power under an extended range of conditions.

3.5 References

1. Sarkanen, K.V. and C.H. Ludwig, Lignins: occurrence, formation, structure and reactions1971, New York: Wiley-Interscience.

2. Vogel, K.P. and H.-J.G. Jung, Genetic Modification of Herbaceous Plants for Feed and Fuel. Critical Reviews in Plant Sciences, 2001. **20**(1): p. 15-49.

3. Chen, F. and R.A. Dixon, Lignin modification improves fermentable sugar yields for biofuel production. Nature biotechnology, 2007. **25**(7): p. 759-61.

4. Ralph, J., et al., Lignins: Natural polymers from oxidative coupling of 4-hydroxyphenyl- propanoids. Phytochemistry Reviews, 2004. **3**(1-2): p. 29-60.

5. Yuan, T.Q., et al., Characterization of lignin structures and lignin-carbohydrate complex (LCC) linkages by quantitative 13C and 2D HSQC NMR spectroscopy. Journal of agricultural and food chemistry, 2011. **59**(19): p. 10604-14.

6. Higuchi, T., Biochemistry and molecular biology of wood1997, Berlin; New York: Springer.

7. Barrière, Y., et al., Genetics and genomics of lignification in grass cell walls based on maize as a model system. Genes Genomes Genomics, 2007. **1**: p. 133-156.

8. Eckardt, N.A., Probing the Mysteries of Lignin Biosynthesis: The Crystal Structure of Caffeic Acid/5-Hydroxyferulic Acid 3/5-O-Methyltransferase Provides New Insights. The Plant Cell Online, 2002. **14**(6): p. 1185-1189.

9. Hu, W.J., et al., Repression of lignin biosynthesis promotes cellulose accumulation and growth in transgenic trees. Nat Biotechnol, 1999. **17**(8): p. 808-12.

10. Chiang, V.L., From rags to riches. Nat Biotechnol, 2002. **20**(6): p. 557-8.

11. Hinchee, M., et al., Short-rotation woody crops for bioenergy and biofuels applications. In Vitro Cell Dev Biol Plant, 2009. **45**(6): p. 619-629.

12. Brown, S.A. and A.C. Neish, Shikimic acid as a precursor in lignin biosynthesis. Nature, 1955. **175**(4459): p. 688-9.

13. Dixon, R.A., et al., The biosynthesis of monolignols: a "metabolic grid", or independent pathways to guaiacyl and syringyl units? Phytochemistry, 2001. **57**(7): p. 1069-84.

14. Hamberger, B., et al., Genome-wide analyses of phenylpropanoid-related genes in *Populus trichocarpa*, *Arabidopsis thaliana*, and *Oryza sativa*: the *Populus* lignin toolbox and conservation and diversification of angiosperm gene familiesThis article is one of a selection of papers published in the Special Issue on Poplar Research in Canada. Canadian Journal of Botany, 2007. **85**(12): p. 1182-1201.

15. Higuchi, T., Pathways for monolignol biosynthesis via metabolic grids: coniferyl aldehyde 5-hydroxylase, a possible key enzyme in angiosperm syringyl lignin biosynthesis. Proceedings of the Japan Academy. Series B: physical and biological sciences., 2003. **79**: p. 227-236.

16. Higuchi, T. and S.A. Brown, Studies of lignin biosynthesis using isotopic carbon. XIII. The phenylpropanoid system in lignification. Can J Biochem Physiol, 1963. **41**: p. 621-8.

17. Lee, Y., et al., Integrative analysis of transgenic alfalfa (*Medicago sativa* L.) suggests new metabolic control mechanisms for monolignol biosynthesis. PLoS Comput Biol, 2011. **7**(5): p. e1002047.

18. Raes, J., et al., Genome-wide characterization of the lignification toolbox in *Arabidopsis*. Plant Physiol, 2003. **133**(3): p. 1051-71.

19. Shi, R., et al., Towards a systems approach for lignin biosynthesis in *Populus trichocarpa*: transcript abundance and specificity of the monolignol biosynthetic genes. Plant Cell Physiol, 2010. **51**(1): p. 144-63.

20. Vanholme, R., et al., Lignin biosynthesis and structure. Plant Physiol, 2010. **153**(3): p. 895-905.

21. Hoffmann, L., et al., Silencing of hydroxycinnamoyl-coenzyme A shikimate/quinate hydroxycinnamoyltransferase affects phenylpropanoid biosynthesis. Plant Cell, 2004. **16**(6): p. 1446-65.

22. Chen, H.C., et al., Membrane protein complexes catalyze both 4- and 3-hydroxylation of cinnamic acid derivatives in monolignol biosynthesis. Proc Natl Acad Sci U S A, 2011. **108**(52): p. 21253-8.

23. Escamilla-Treviño, L., et al., Early lignin pathway enzymes and routes to chlorogenic acid in switchgrass (*Panicum virgatum* L.). Plant Molecular Biology, 2014. **84**(4-5): p. 565-576.

24. Wang, J.P., et al., Complete proteomic-based enzyme reaction and inhibition kinetics reveal how monolignol biosynthetic enzyme families affect metabolic flux and lignin in *Populus trichocarpa*. The Plant cell, 2014. **26**(3): p. 894-914.

25. Vanholme, R., et al., Caffeoyl Shikimate Esterase (CSE) Is an Enzyme in the Lignin Biosynthetic Pathway in *Arabidopsis*. Science, 2013. **341**(6150): p. 1103-1106.

26. Chen, H.-C., et al., Monolignol Pathway 4-Coumaric Acid:CoA Ligases in *Populus trichocarpa*: Novel Specificity, Metabolic Regulation, and Simulation of CoA Ligation Fluxes. Plant Physiology, 2013. **161**: p. 1501-1516.

27. Chen, H.-C., et al., Systems Biology of Lignin Biosynthesis in *Populus trichocarpa*: Heteromeric 4-Coumaric Acid:Coenzyme A Ligase Protein Complex Formation, Regulation, and Numerical Modeling. The Plant cell, 2014. **26**(3): p. 876-93.

28. Sato, T.K.F.S.U., Inhibition of phenylalanine ammonia-lyase by cinnamic acid derivatives and related compounds. Phytochemistry Phytochemistry, 1982. **21**(4): p. 845-850.

29. Li, L., et al., 5-hydroxyconiferyl aldehyde modulates enzymatic methylation for syringyl monolignol formation, a new view of monolignol biosynthesis in angiosperms. J Biol Chem, 2000. **275**(9): p. 6537-45.

30. Osakabe, K., et al., Coniferyl aldehyde 5-hydroxylation and methylation direct syringyl lignin biosynthesis in angiosperms. Proc Natl Acad Sci U S A, 1999. **96**(16): p. 8955-60.

31. Shuford, C.M., et al., Comprehensive quantification of monolignol-pathway enzymes in *Populus trichocarpa* by protein cleavage isotope dilution mass spectrometry. Journal of proteome research, 2012. **11**(6): p. 3390-404.

32. Liu, J., et al., A standard reaction condition and a single HPLC separation system are sufficient for estimation of monolignol biosynthetic pathway enzyme activities. Planta, 2012. **236**(3): p. 879-85.

33. Franke, R., et al., Changes in secondary metabolism and deposition of an unusual lignin in the *ref8* mutant of *Arabidopsis*. Plant J, 2002. **30**(1): p. 47-59.

34. Franke, R., et al., The *Arabidopsis REF8* gene encodes the 3-hydroxylase of phenylpropanoid metabolism. Plant J, 2002. **30**(1): p. 33-45.

35. Blount, J.W., et al., Altering expression of cinnamic acid 4-hydroxylase in transgenic plants provides evidence for a feedback loop at the entry point into the phenylpropanoid pathway. Plant Physiology, 2000. **122**(1): p. 107-16.

36. Wang, J.P., et al., Functional redundancy of the two 5-hydroxylases in monolignol biosynthesis of *Populus trichocarpa*: LC-MS/MS based protein quantification and metabolic flux analysis. Planta, 2012. **236**(3): p. 795-808.

Chapter 4

Identification of Enzyme Complex of 4-Coumaric Acid:CoA Ligase (4CL)-Hydroxycinnamoyl-CoA:Shikimic Acid Hydroxycinnamoyl Transferase (HCT) in *Populus trichocarpa*

4.1 Introduction

Cellulose, hemicellulose and lignin are the three major components of the plant secondary cell wall. Compared to cellulose and hemicellulose, lignin is an important phenolic polymer that principally is deposited around the polysaccharides to provide the mechanical support for the plant tissue. Besides the mechanical support, lignin comes with additional benefits for the plant cell walls. First, the hydrophobicity of the lignin polymer facilitates the water transport from plant roots. Second, the heterogeneous structure of the lignin can prevent plant tissue from the natural degradation [1].

Lignin is predominately composed of three major types of phenylpropanoid subunits known as 4-hydroxyphenyl (H), guaiacyl (G) and syringyl (S) subunits, polymerized from 4-coumaryl, coniferyl, and sinapyl alcohols, respectively [2]. Although lignin has important functions for the development and physiology of plants, lignin contributes to the recalcitrance to degradation and processing of the plant biomass for commercial utilization,

such as forage, chemical feedstocks, paper pulping and biofuel production. Both lignin content and composition are important factors that affect biomass utilization. Several studies have reduced the recalcitrance of the cell walls by lowering lignin content or increasing the S/G ratio for improving the efficiency of delignification during pulp and paper or biofuel production [3-7].

Monolignols synthesized from the monolignol biosynthetic pathway are derived from the phenylpropanoid biosynthesis [8]. Over decades of studies, several enzymes have been proposed for monolignol biosynthesis and have been depicted as a metabolic grid (see **Chapter 1**, **Figure 1.1**), which are phenylalanine ammonia-lyase (PAL), cinnamic acid 4-hydroxylase (C4H), 4-coumaric acid:coenzyme A (CoA) ligase (4CL), 4-hydroxycinnamoyl-CoA:shikimic acid hydroxycinnamoyl transferase (HCT), 4-coumaric acid 3-hydroxylase (C3H), caffeoyl-CoA *O*-methyltransferase (CCoAOMT), cinnamoyl CoA reductase (CCR), cinnamyl alcohol dehydrogenase (CAD), coniferaldehyde 5-hydroxylase (CAld5H) and caffeic acid *O*-methyltransferase (AldOMT) [9-20]. By the successive reactions of the 10 enzyme families, phenylalanine is converted into 4-coumaryl, coniferyl, or sinapyl alcohols, the three major monolignols for lignin polymerization.

In addition to the complexity of enzymes involved in the metabolic pathway, protein-protein interactions play important roles during the biosynthesis of the pathway metabolites [21-31]. The advantage of protein-protein interaction may be to increase local enzyme concentrations, to channel the pathway intermediates between enzymes and to sequester

unstable or toxic intermediates without dispersion into the cytoplasm [27, 28, 30, 32-37]. In order to understand monolignol biosynthesis, the investigation of possible protein-protein interactions among the biosynthetic enzymes is an important task.

Since 1974, a potential multienzyme complex for C_3-C_6 phenolic compounds had been proposed for phenylpropanoid biosynthesis, such as lignin and flavonoids [30, 37, 38]. These "supramolecular complexes of sequential metabolic enzymes and cellular structural elements" had been defined by Paul Srere as metabolons [28]. Later on, both flavonoid and monolignol metabolism had been co-localized on the endoplasmic reticulum (ER) [39-41]. A membrane associated multienzyme complex, at least, had been proposed and shown, at least in part, to facilitate the biosynthesis from phenylalanine to flavonoids [42]. For flavonoid biosynthesis, a study using buckwheat (*Fagopyrum esculentum*) showed that PAL, chalcone synthase (CHS), uridine diphosphate glucose (UDPG) and flavonoid glucosyl transferase (UFGT) were loosely associated with ER [29]. This membrane-associated complex (PAL/CHS/UFGT) is organized through weak interactions with membrane proteins including C4H and flavonoid 3' hydroxylase (F3'H), a hypothesized membrane anchor for localization of some flavonoid enzymes to the ER. [29, 34, 41, 42]. In *Arabidopsis thaliana*, a direct association between CHS, chalcone isomerase (CHI), flavanone 3-hydroxylase (F3H) and dihydroflavonol 4-reductase (DFR) had also been identified by yeast two-hybrid, affinity chromatography and immunoprecipitation assays [43, 44]. The association of those enzymes was further proved by the co-localization of CHS and CHI in cortex cells of *Arabidopsis* roots but not in a *tt7*

mutant, which a mutation eliminates 400 residues of the 492 amino acid-long cytoplasmic domain of the F3'H [44].

In monolignol biosynthesis, protein-protein interactions between monolignol biosynthetic enzymes have also been studied. The membrane-bound enzyme complex of PAL and C4H was first indirectly identified from potato (*Solanum tuberosum* L.) and cucumber *(Cucumis sativus* L.) [32, 33]. This PAL-C4H interaction uses cinnamic acid formed by the PAL reaction as a more effective substrate than cinnamic acid added exogenously [32, 33], while disruption of the PAL-C4H interaction led to the increased conversion of exogenously cinnamic acid [42]. Direct but loose interactions for PAL-C4H were demonstrated in *Nicotiana tabacum* using biochemical and microscopic techniques to strengthen the existence of the metabolic channeling for the entry point of monolignol biosynthesis [45, 46]. Recently, in *Populus trichocarpa*, protein-protein interactions among monolignol biosynthetic enzymes had also been studied. A membrane-bound protein complex of PtrC3H3/PtrC4H1/PtrC4H2 has been identified [20], while a novel 3-hydroxylation activity for 4-coumaric acid was revealed. Moreover, Ptr4CL3 and Ptr4CL5 were also found as a heterotetrameric protein complex with 3 subunits of Ptr4CL3 and 1 subunit of Ptr4CL5 [47]. The protein-protein interaction between Ptr4CL3 and Ptr4CL5 affects the direction and metabolic flux of CoA ligation in monolignol biosynthesis [47]. So far, in plants, multiple enzyme complexes in monolignol biosynthesis, such as the membrane complex of PAL/C4H, C3H/C4H and the soluble 4CL complex had been identified [32, 33, 45, 46]; however, the current knowledge

for the assembled complex structure of other soluble monolignol biosynthetic enzymes, such as HCT, COMT, CCOMT, CCR and CAD, are still rudimentary. Recently, in *Arabidopsis*, a study showed that membrane-bound C3H can bring a soluble enzyme, 4CL and HCT, to the ER and wound repairing can enhance the re-localization of these enzymes [35].

In this study, a protein complex of Ptr4CL-PtrHCT is identified and this protein-protein interaction is confirmed using bimolecular fluorescence complementation (BiFC) and immunoprecipitation (IP). Regulation of the CoA ligation step for both 4-coumaric and caffeic acids by the Ptr4CL-PtrHCT enzyme complex is reported by using recombinant enzymes of PtrHCTs and Ptr4CLs. A simplified mechanistic model developed by Jina Song is incorporated to reveal the stoichiometry of the Ptr4CL-PtrHCT complex [48]. This model is a rule-based model and uses evolutionary computation based on experimental data of enzyme activity. Rule-based modeling can represent the complex biochemical networks by building the model with the interaction topology between enzymes and substrates. Subsequently, the stoichiometry of the Ptr4CL-PtrHCT complex is optimized by evolutionary computation, which is analogous to the biological mechanisms of evolution and adaptation. After the mechanistic modeling, the stoichiometry of the Ptr4CL-PtrHCT complex is revealed as a heterotetrameric protein complex with 1 subunit of Ptr4CL with 2 subunits of PtrHCTs. The Ptr4CL-PtrHCT enzyme complex is further validated by downregulated PtrHCT transgenics, where Ptr4CL activities toward 4-coumaric or caffeic acid are significantly downregulated due to a reduction in enzyme abundance of PtrHCT.

4.2 Materials and Methods

4.2.1 Plant Materials

Clonal propagules of *Populus trichocarpa* (Nisqually-1) wildtype and transgenic PtrHCT were grown in a greenhouse in soil containing a 1:1 ratio of peat moss to potting-mix, using 16 h light and 8 h dark photoperiods for six months. Stem differentiating xylem (SDX) tissues were harvested following procedures described by Shi et al. (2010).

4.2.2 Expression and Purification of Recombinant Proteins

The expression of the recombinant proteins from *Escherichia coli* (BL21) followed the method described in **Chapter 2**. Recombinant proteins of PtrHCT1 and PtrHCT6 were purified as described in **Chapter 2**, where the recombinant proteins of Ptr4CL3 and Ptr4CL5 were purified as described in **Chapter 3.**

4.2.3 Total Protein Extraction from Stem Differentiating Xylem (SDX) and Enzyme Assays

3 g of freshly isolated SDX tissue was ground in liquid nitrogen to a fine powder, and suspended in extraction buffer (50 mM Tris-HCl, pH 7.5, 20 mM sodium ascorbate, 0.4 M sucrose, 100 mM sodium chloride, 5 mM DTT, 20% glycerol, 10% PVPP, 2 mM PMSF, 2 μg/mL pepstatin A and 2 μg/mL leupeptin), homogenized on ice using an Ultra-Turrax T-18 basic disperser (IKA, Wilmington, NC), and centrifuged at 4,000 x g to remove debris. The

supernatant was filtered through an Amicon Ultra 10 kDa Centrifugal Filter (Millipore, Billerica, MA) using a 5X sample volume of extraction buffer, and stored at -80 °C before enzyme assays. Total protein concentration of the SDX extracts was determined according to Bradford (1976).

For reactions of recombinant Ptr4CLs and Ptr4CL activity in SDX extracts of wildtype and PtrHCT transgenics, a 100 µL reaction containing 50 µM of substrate (4-coumaric acid or caffeic acid), 200 µM CoA, 5 mM ATP and 2.5 mM $MgCl_2$ in 50 mM Tris-HCl buffer (pH 8.0 for Ptr4CL3 and pH 7.0 for Ptr4CL5) starts with a final enzyme concentration of 10 nM recombinant Ptr4CLs for a reaction time of 10 min or 25 µg of SDX extracts for 30 min. All enzyme reactions were stopped by adding 5 µL of 3 M trichloroacetic acid (TCA). The mixture was centrifuged at 20,000 x g for 10 min and the supernatant was analyzed by HPLC following Liu et al. (2012). The substrates and products of the enzyme assays were separated on a Zorbax SB-C18 5 µm, 4.6 x 150-mm column (Agilent, Santa Clara, CA). Analysis of reactions involving hydroxycinnamyl CoAs were carried out using a HPLC gradient method (solvent A, 5 mM ammonium acetate, pH 5.6; solvent B, water: acetonitrile: acetic acid, 2: 97.8: 0.2; 8% to 10% B for 3 min, 10 to 30% B for 5 min, 30 to 100% B for 5 min; flow rate: 1 mL/min). The metabolites were quantified in a Diode-Array Detector SL (Agilent, Santa Clara, CA) based on authentic compounds [49].

4.2.4 Plasmid Construction for Bimolecular Fluorescence Complementation (BiFC)

The coding sequences of 8 monolignol enzymes (PtrHCT1, PtrHCT6, PtrCCoAOMT1, PtrCCoAOMT2, PtrCCoAOMT3, PtrCOMT2, PtrCAld5H1 and PtrCAld5H2) were amplified by the specific primer sets (**Table 4.1**) from our previous cloning plasmid pGEM-T easy (Promega, Madison, WI) and cloned into the BiFC vector, pSPYCE-35S or pSPYNE-35S. While in pSPYCE-35S, the enzyme was fused with the C-terminal 86 amino acids of YFP (YFP^N) and, in pSPYNE-35S, the enzyme will be fused with the N-terminal 155 amino acids of YFP (YFP^C) [50, 51]. For cloning of PtrHCT1 and PtrHCT6, restriction enzymes *BamH*I and *Xho*I were used. For cloning of PtrCCoAOMT1, PtrCCoAOMT2, PtrCCoAOMT3, PtrCOMT2, PtrCAld5H1 and PtrCAld5H2, restriction enzymes *Xba*I and *Sma*I were used. The fusions of the YFP fragment are at the C terminus of all the enzymes.

Table 4.1 – Primer list for construction of BiFC plasmids.

Primer name	Oligomer Sequences	Primer name	Oligomer Sequences
PtrHCT1-F	5'- actgggatccatgataatcaatgtgaagga -3'	PtrCCoAOMT1-F	5'- actgtctagaatggccaccaacggagagga -3'
PtrHCT1-R	5'- actgctcgagttctttaatgtcatatataa -3'	PtrCCoAOMT1-R	5'- actgcccgggttggatccgacggcagagag -3'
PtrHCT6-F	5'- actgggatccatgataatcaacgtgaagga -3'	PtrCCoAOMT2-F	5'- actgtctagaatggccgccaacggagagga -3'
PtrHCT6-R	5'- actgctcgagaatgtcatatatgaacttct -3'	PtrCCoAOMT2-R	5'- actgcccgggcttgatccgacggcagagag -3'
PtrCAld5H1-F	5'- actgtctagaatggattctcttctccaatc -3'	PtrCCoAOMT3-F	5'- actgtctagaatggctttcgttttacctgc -3'
PtrCAld5H1-R	5'- actgcccgggaaatggacagaccacgcgct -3'	PtrCCoAOMT3-R	5'- actgcccggggcaaaggcgcctgcatagtg -3'
PtrCAld5H2-R	5'- actgtctagaatggattctcttgtccaatc -3'	PtrCOMT2-F	5'- actgcatatgggttcgacaggtgaaac -3'
PtrCAld5H2-R	5'- actgcccggggagagggcatagcacacgct -3'	PtrCOMT2-R	5'- actgcccgggttagttcttgcggaattcaa -3'

4.2.5 Plasmid Preparation for BiFC

All plasmids for bimolecular fluorescence complementation (BiFC) were prepared by CsCl gradient ultracentrifugation [52-54]. Plasmids were transferred into *E. coli* (TOP10, Invitrogen, Grand Island, NY), respectively. The transformed bacteria was first cultured in 3 mL LB at 37 °C until O.D.600 reached 0.6 and was transferred into 1000 mL Terrific Broth (TB, 23.6 g yeast extract, 11.8 g tryptone, 9.4 g dipotassium phosphate (K_2HPO_4), 2.2 g monopotassium phosphate (KH_2PO_4) and 8 mL glycerol) [55] for 12 hours at 37 °C before being harvested by centrifugation at 6000 x g.

The plasmid DNA was isolated from the collected cell pellet by an alkaline-lysis method [56]. The cell pellet was resuspended in 20 mL of solution I (50 mM glucose, 25 mM Tris-Cl, 10 mM EDTA) and the bacteria were lysed by adding 40 mL solution II (0.2 M NaOH, 1% SDS) and incubated at room temperature for 10 min. Then, 20 mL ice-cold solution III (3 M Potassium acetate, 2 M acetic acid) was added into the solution, with gentle mixing, then incubated on ice for another 10 min and centrifuged at 10,000 x g for 30 min at 4 °C to collect the supernatant into a new tube. The plasmid DNA was precipitated by adding 0.6 volume of 100% isopropanol to the supernatant, gently mixed, and held at room temperature for 10 min. The precipitated plasmid DNA was collected by centrifugation at 12,000 x g for 10 min. The DNA pellet was de-salted by rinsing with 95% ethanol and air-dried.

For CsCl gradient ultracentrifugation, the air-dried plasmid DNA was dissolved in 6.6 mL of 10 mM EDTA. Then, 7.7 g CsCl and 0.41 mL of Ethidium Bromide (EtBr, 10 mg/mL) was added into the DNA solution. The DNA-CsCl-EtBr solution was sealed into a Quick-Seal Polypropylene Tube (Beckman Coulter, Brea, CA) and put in an ultracentrifugation at 80,000 x g for 48 hours using a fixed angle rotor (MLA-80, Beckman Coulter, Brea, CA). The plasmid DNA was recovered by collected the DNA band from the ultracentrifugation tube using a syringe. After DNA recovery, H_2O was added into DNA-CsCl-EtBr solution to 3 mL and EtBr was removed from the plasmid DNA repeatedly using same volume of NaCl-saturated-butanol until the solution became transparent. Then, the DNA-CsCl solution (the aqueous phase) was further de-salted by Amicon Ultra 10 kDa centrifugal filter (Millipore, Billerica, MA) using deionized water for 6-10 times and adjusting the plasmid DNA concentration to 2 μg/μL.

4.2.6 *P. trichocarpa* SDX Protoplast Preparation for BiFC

P. trichocarpa protoplasts were prepared from *P. trichocarpa* stems. The procedure follows an established protocol with modifications in mannitol concentration and the ingredients of the W5 solution [20, 47, 57-60]. The stems of 6-month-old *P. trichocarpa* were cut into 10 cm segments. The segments are debarked and immersed in 40 mL of an enzyme solution (20 mM MES (pH5.7), 500 mM mannitol, 20 mM KCl, 1.5 % (w/v) cellulase R-10 (Yakult), 0.4% Macerozyme R-10 (Yakult), 10 mM CaCl2, and 0.1% (v/v)

BSA) in the 50 mL Falcon tube. After 2 hours of enzyme digestion, segments were transferred into W5 solution (2 mM MES (pH5.7), 154 mM NaCl, 125 mM $CaCl_2$, 50 mM glucose and 5 mM KCl) in a new 50 mL Falcon tube with gentle shaking for at least 2 min to release xylem protoplasts. After protoplasts are released, solution were filtered through 75 μm laboratory sifting mesh (Carolina Biological Supply Company**,** Burlington, NC) to remove large cellular debris and centrifuged at 200 x g for 2 min. After centrifugation, the supernatant was carefully poured off and 10 mL of fresh W5 solution was added. The protoplasts were resuspended in W5 by gentle stirring and put on ice for 30 min. The protoplasts were then centrifuged for 200 x g for 2 min, the supernatant was carefully poured off, then added 10 mL of fresh MMG solution (4 mM MES (pH 5.7), 500 mM mannitol and 15 mM $MgCl_2$) and the cell density was adjusted to an average of $2*10^5$ cell/mL using a haemocytometer (Hausse Scientific, Horsham, PA).

For plasmid transfection, 10 μg of total plasmid DNA (for BiFC, each plasmid is 5 μg) was added into 100 μL of protoplast solution ($2*10^4$ cells) and was added 110 μL PEG solution (20% PEG-4000, 200 mM mannitol, and 100 mM $CaCl_2$) in a 2 mL eppendorf tube. The transfection was initiated by tapping the tube to distribute the mixture and put in room temperature for 15 min and 440 μL of W5 solution was added to stop the transfection. The protoplasts were collected by centrifugation at 200 x g for 2 min and transferred into the WI solution for 12 hour and the YFP signals for BiFC were detected with a confocal laser scanning microscope LSM 510 PASCAL (Carl Zeiss, Oberkochen, Germany).

4.2.7 Immunoprecipitation (IP)

Ptr4CL3 and Ptr4CL5 immunoprecipitation was adapted from our previous work [20]. Anti-PtrHCT1 and PtrHCT6 rabbit antibodies were raised as described in **Chapter 2** and their specificities were also verified (**Chapter 2**). Those antibodies were used to pull-down Ptr4CL3 and Ptr4CL5 from *P. trichocarpa* SDX extracts. 1 mL of SDX protein extract was mixed on a shaker with 40 μL anti-PtrHCT antibody and 40 μL Dynabeads Protein G (Invitrogen, Grand Island, NY) for 2 hours at 4°C. Next, the beads were washed 3 times with 1 mL of protein extraction buffer. Bound Ptr4CL3 and Ptr4CL5 was eluted by boiling the beads for 10 min in 50 μL of 1X SDS sample buffer [61]. The eluted proteins were separated by SDS-PAGE and transferred to a nitrocellulose membrane for Western blot analysis as described in **Chapter 2.** Anti-Ptr4CL3 or anti-Ptr4CL5 antibody was used to detect the signal of Ptr4CLs.

4.2.8 Mechanistic Modeling and Numerical Analysis

Mechanistic modeling is carried out by a rule-based algorithm and evolutionary computation algorithm from Jina Song (2014, Ph.D. Dissertation, Unpublished work). The algorithmic evolutionary processes automatically searches and optimizes the best solution for complex nonlinear problems (**Figure 4.1**).

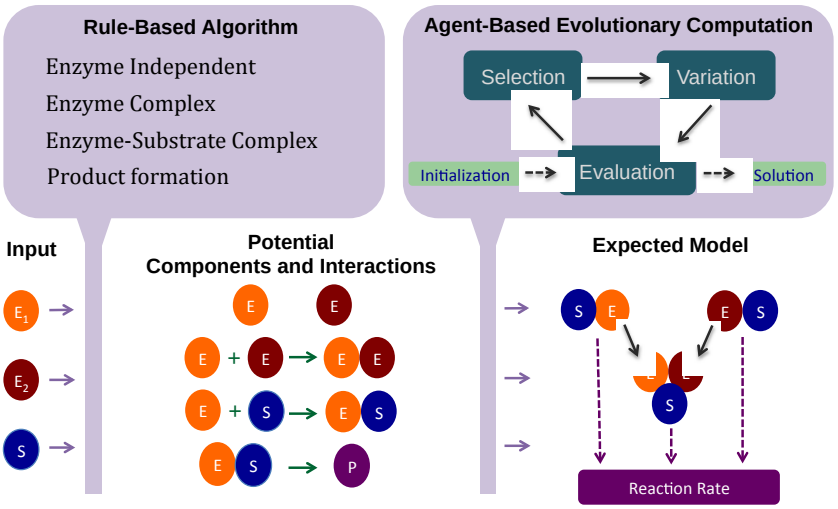

Figure 4.1 – Rule-based modeling and evolutionary computation for multi-enzymatic reaction modeling framework from Jina Song (2014, Ph.D. Dissertation, Unpublished work).

The model is based on the experimental results of Ptr4CL CoA ligation reactions in mixtures of Ptr4CL and PtrHCT and evaluated by the numerical analysis of evolutionary computation. Two different numerical methods were used, the Root Mean Squared Error (RMSE) and Bayesian Information Criterion (BIC). The difference between the predicted values and experimental values are measured by RMSE. RMSE is not only a selection strategy for model optimization, but also provides the fitness comparison indexes during the optimization steps of different rules.

4.2.9 PtrHCT1 and PtrHCT6 Downregulated Transgenic and Next Generation Sequencing (RNA-seq) Analysis

An RNAi-silencing construct with an inverted repeat for downregulation of both PtrHCT1 and PtrHCT6 was prepared as in a previous study [62]. The construct was

introduced into *Agrobacterium tumefaciens* (strain C58) by the freeze thaw method [63] and transferred into *P. trichocarpa* following an established method [64]. Next generation (RNA-seq) sequencing of the PtrHCT1 and PTrHCT6 transgenic *P. trichocarpa* was performed as previously described [65].

4.2.10 Chemical Cross-linking

Dithiobis [succinimidyl propionate] (DSP) (Thermo Scientific, Rockford, IL) was used as a cross-linker. SDX extracts were prepared following the Total Protein Extraction (**Section 4.2.3**) but, instead of using 50 mM of Tris-HCl buffer, 25 mM sodium phosphate buffer (pH 7.4) was used. 1 mL of a SDX extract was used for chemical cross-linking and a 20-fold molar excess of the crosslinker (to protein) was added into the SDX extracts. The cross-linking took place on ice for 2 hours and was quenched by adding Tris-HCl buffer (pH 7.5) to a final concentration of 50 mM. The DSP-treated and the untreated SDX protein extract was first incubated with 2× loading buffer [5% SDS, 50 mM Tris-HCl (pH 6.8), 20% glycerol, and 0.02% bromophenol blue] at 37 °C for 30 min, then separated by SDS/PAGE, and analyzed on Western blots using anti-PtrHCT1 and anti-PtrHCT6 antibodies.

4.3 Results

4.3.1 Coenzyme A (CoA) Ligation Activity with Mixtures of Ptr4CL3 and PtrHCTs Indicates a Protein-Protein Interaction

Because the shikimic acid esters can regulate the activities of *Populus trichocarpa* 4CLs (Ptr4CL3 and Ptr4CL5) (**Chapter 2**); we hypothesized that hydroxycinnamoyl-coenzyme A:shikimic acid hydroxycinnamoyl transferase (PtrHCT), as a downstream enzyme of Ptr4CL that produces the shikimic acid esters, may also play a regulatory role to modulate the activity of Ptr4CL. To investigate the role of PtrHCT, we mixed the PtrHCT1 or PtrHCT6 with Ptr4CL3, an ortholog of the monolignol Ptr4CL reported for many other species, to exam the CoA ligation activity of Ptr4CL3 using 4-coumaric or caffeic acid as the substrate. The measurement of the CoA ligation rate was performed when the Ptr4CL3 molar concentration was held constant at 10 nM, while the PtrHCT molar concentration was held at a constant excess of 40 nM. Here, Ptr4CL3 without adding of PtrHCT1 or PtrHCT6 was as activity control. Ptr4CL3 activity for 4-coumaric acid was increased by 42.8% when PtrHCT1 was present and by 41.1% when PtrHCT6 was present (**Figures 4.2A**). For caffeic acid as substrate, Ptr4CL3 activity was increased by 39.7% when PtrHCT1 was present and by 36.6% when PtrHCT6 was present (**Figures 4.2B**). Moreover, the Ptr4CL3 activities were not changed for 4-coumaric and caffeic acids when bovine serum albumin (BSA) was added as an experimental control (**Figures 4.2A and 4.2B**). The result indicated that specific

interactions may exist between Ptr4CLs and PtrHCTs, which regulates the activity of Ptr4CL.

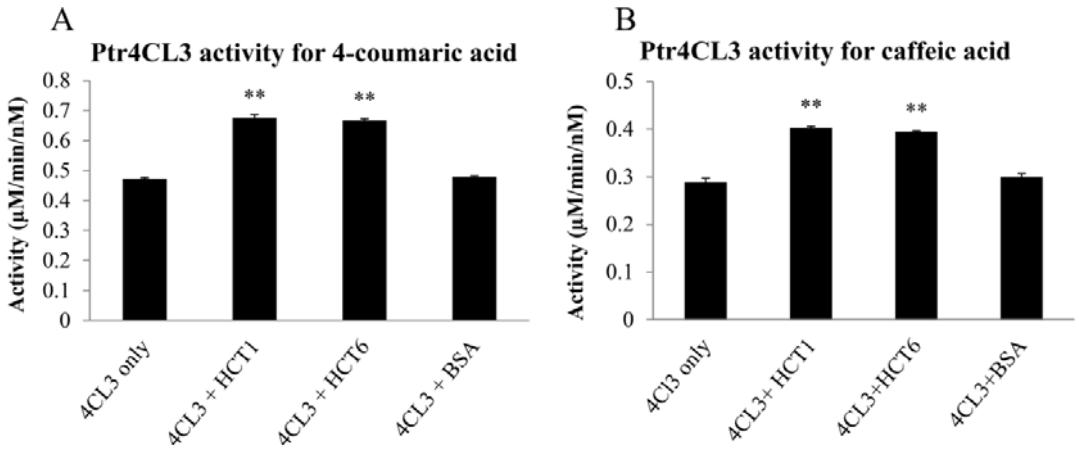

Figure 4.2 – CoA ligation activity of Ptr4CL3 is affected when PtrHCT1 or PtrHCT6 is present. (**A**) 4-Coumaric acid (50 μM) was used as substrate. (B) Caffeic acid was used as substrate. 4CL3 was fixed at 10 nM and HCT concentration was fixed at 40 nM. Error bars represent SE of three replicates. Statistical testing was performed using Student's t-test (**, $p < 0.01$).

4.3.2 The Ptr4CL-PtrHCT Complex was also Identified by Bimolecular Fluorescence Complementation (BiFC) and Immunoprecipitation (IP)

To examine whether protein-protein interactions exist between Ptr4CLs and PtrHCTs, we used bimolecular fluorescence complementation (BiFC) [50]. Different combination of the two pairs of BiFC vectors were co-transformed into *P. trichocarpa* stem differentiating xylem (SDX) protoplasts and the signal of yellow fluorescent protein (YFP) will be used to investigate the interaction between Ptr4CLs and PtrHCTs [59]. Each BiFC vector contains the protein of interest fused with the complementing segments of YFP, YFP^N (N-terminal

155 amino acids) and YFP^{C} (C-terminal 86 amino acids). The Ptr4CL3 or Ptr4CL5 was fused with N-terminal YFP complementing segments to get Ptr4CL3-YFP^{N} or Ptr4CL5-YFP^{N} and PtrHCT1 or PtrHCT6 was fused with C-terminal YFP complementing segments to get PtrHCT1-YFP^{C} or PtrHCT6-YFP^{C}. The positive YFP signals were detected in *P. trichocarpa* SDX protoplasts when Ptr4CL3-YFP^{N} was co-transfected with either PtrHCT1-YFP^{C} or PtrHCT6-YFP^{C} (**Figures 4.3A and 4.3B**). The positive YFP signals were also detected when Ptr4CL5-YFP^{N} was co-transfected with either PtrHCT1-YFP^{C} or PtrHCT6-YFP^{C} (**Figures 4.3C and 4.3D**). These BiFC results showed that in *P. trichocarpa* Ptr4CLs (Ptr4CL3 and Ptr4CL5) have protein-protein interactions with PtrHCTs (PtrHCT1 and PtrHCT6).

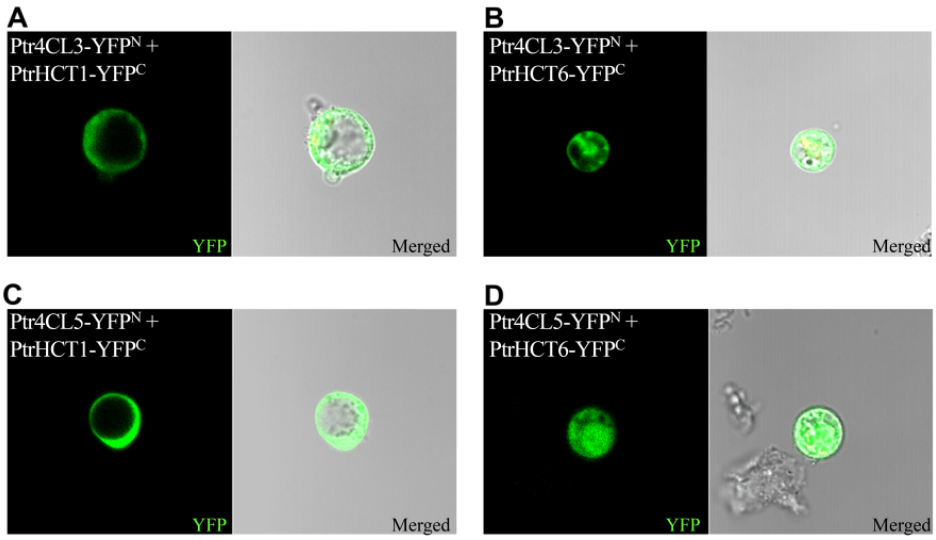

Figure 4.3 – Protein-protein interactions between Ptr4CLs and PtrHCTs were detected by BiFC approach. (**A**) Ptr4CL3-YFP^{N} and PtrHCT1-YFP^{C}. (**B**) Ptr4CL3-YFP^{N} and PtrHCT6-YFP^{C}. (**C**) Ptr4CL5-YFP^{N} and PtrHCT1-YFP^{C}. (**D**) Ptr4CL5-YFP^{N} and PtrHCT1-YFP^{C}.

Next, to further verify the existence of a protein complex of Ptr4CL-PtrHCT in SDX, we used specific anti-PtrHCT1 or anti-PtrHCT6 antibody to carry out immunoprecipitation (IP). The specificities of the anti-PtrHCT1 and anti-PtrHCT6 antibodies have been previously described (**Chapter 2, Figure 2.3**). In addition, before performing the IP, these antibodies were tested to determine whether they can detect PtrHCT from SDX extracts in a Western blot. Both anti-PtrHCT1 and anti-PtrHCT6 antibodies can detect PtrHCT (~50kDa) from the SDX extracts in Western blots (**Figure 4.4**), which indicates that they both are suitable for IP. However, anti-PtrHCT6 antibody is more specific than anti-PtrHCT1 antibody (**Lane 1, Figure 4.4**), where only one clear band was detected from SDX extracts when anti-PtrHCT6 antibody was used (**Lane 2, Figure 4.4**).

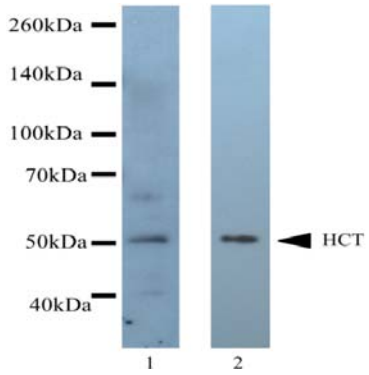

Figure 4.4 – Western blot using specific PtrHCT antibody to detect PtrHCT from crude SDX protein extracts. Lane 1: crude SDX protein extracts detected by anti-PtrHCT1 antibody. Lane 2: crude SDX protein extracts detected by anti-PtrHCT6 antibody. Arrow indicates the sizes of PtrHCT1 or PtrHCT6 (~50kDa).

The immunoprecipitation was performed in crude SDX extracts using anti-PtrHCT1 or anti-PtrHCT6 antibody. If Ptr4CL can form a complex with PtrHCT *in vivo* as shown by BiFC (**Figure 4.3**), the PtrHCT antibodies should be able to precipitate the Ptr4CLs from crude SDX extracts. For detection of the Ptr4CL3 and Ptr4CL5 from the IP in the Western blot, specific anti-Ptr4CL3 and anti-Ptr4CL5 antibodies are required. Their specificity was verified in a previous publication [19]. Either anti-PtrHCT1 or anti-PtrHCT6 antibodies can pull-down Ptr4CL3 or Ptr4CL5 (**Lane 3, Figure 4.5**). For a control, pre-immune serum was used in parallel to perform the immunoprecipitation. In this case, Ptr4CL proteins cannot be detected (**Lane 2, Figure 4.5**).

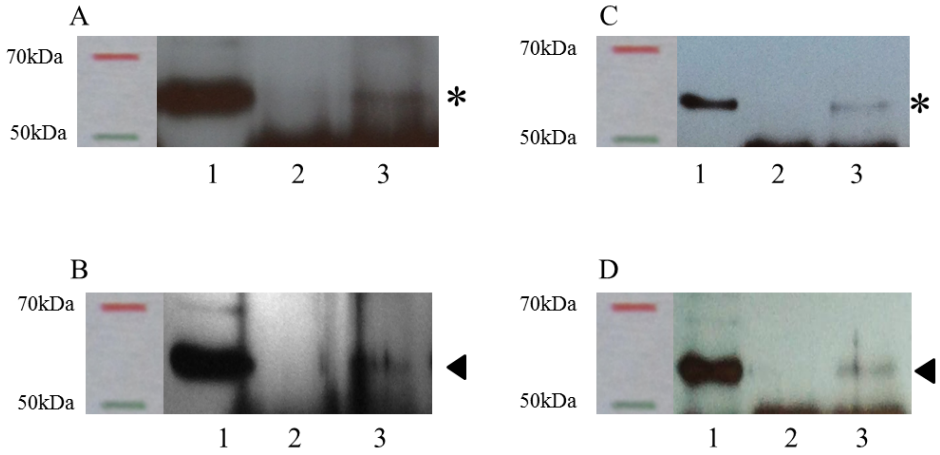

Figure 4.5 – Protein-protein interactions between Ptr4CLs and PtrHCTs were detected by immunoprecipitation. For immunoprecipitation, (**A**) and (**B**) Anti-PtrHCT1 specific antibody was used to pull down PtrHCT1. (**C**) and (**D**) Anti-PtrHCT6 specific antibody was used to pull down PtrHCT6. For Western blots, (**A**) and (**C**) Ptr4CL3-specific antibody was used to detect Ptr4CL3. (**B**) and (**D**) Ptr4CL5-specific antibody was used to detect Ptr4CL5. Lane 1: crude SDX protein before pull-down. Lane 2: crude SDX protein pulled down by pre-immune antibody. Lane 3: crude SDX protein pulled down by specific anti-PtrHCT antibody. Asterisk (*) indicates the Ptr4CL4 and arrow head (◀) indicates the Ptr4CL5.

From the three lines of evidences of recombinant enzyme activity, BiFC and IP, we showed that Ptr4CL and PtrHCT have protein-protein interaction and can from a protein complex *in vivo*. Furthermore, we wondered what the composition of the Ptr4CL-PtrHCT complex was *in vivo*. To answer these questions, we explored the stoichiometry of the Ptr4CL-PtrHCT *in vivo* complex.

4.3.3 Mixed Enzyme Effect Analysis for 4-Coumaric Acid

To have a more comprehensive understanding how a Ptr4CL-PtrHCT complex can affect CoA ligation activities, we examined the mixed enzyme effect on Ptr4CL activity for 4-coumaric acid (**Figure 4.6**). The experiment was designed as in **Section 4.3.1** with a fixed recombinant Ptr4CL concentration but with varying concentrations of recombinant PtrHCT to investigate the effect on the CoA ligation activity by the protein complex. The result using 4-coumaric acid is shown in **Figure 4.6**. The CoA ligation activity when only Ptr4CL3 or Ptr4CL5 is present was the baseline rate. Both the activities of Ptr4CL3 and Ptr4CL5 were increased when the concentration of PtrHCTs became higher and the increasing activity reached a plateau when the Ptr4CL to PtrHCT ratio is 1:2, except Ptr4CL5 with PtrHCT1 (**Figure 4.6C).** A nonlinear deviation from the Ptr4CL baseline was confirmed, where a decrease in Ptr4CL3 and Ptr4CL5 activity was observed when the PtrHCT concentration was lower than 5 nM (**Figures 4.6A and 4.6D**).

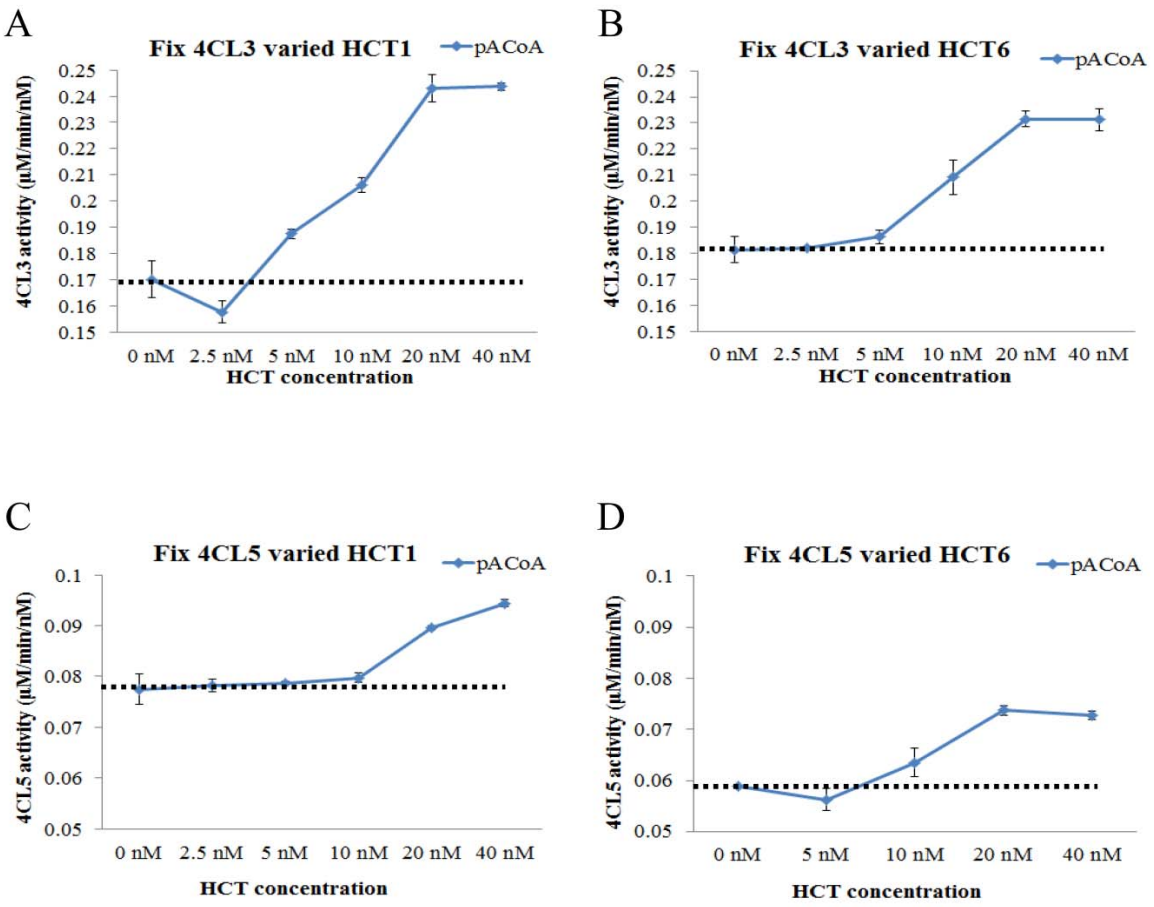

Figure 4.6 – Impact of Ptr4CL-PtrHCT complex formation on the CoA ligation activity toward 4-coumaric acid. (**A**) Ptr4CL3 was fixed at 10 nM and PtrHCT6 concentration was varied. (**B**) Ptr4CL3 was fixed at 10 nM and PtrHCT6 concentration was varied. (**C**) Ptr4CL5 was fixed at 10 nM and PtrHCT1 concentration was varied. (**D**) Ptr4CL5 was fixed at 10 nM and PtrHCT6 concentration was varied. Dashed line indicates the baseline Ptr4CL activity. Error bars represent SE of three replicates.

4.3.4 Mixed Enzyme Effect Analysis for Caffeic acid

A similar experiment was also performed using caffeic acid as substrate (**Figure 4.7**). The concentration of Ptr4CL was also fixed at 10 nM and the concentration of PtrHCT was varied to perform the mixed enzyme assays. The result is similar to that when 4-coumaric

acid was used as substrate; the activities of Ptr4CL increased when the concentration of PtrHCT became higher (**Figure 4.6**). A higher CoA ligation activity was also observed when the ratio of Ptr4CL and PtrHCT is around 1:2. However, the plateau effect for caffeic acid is less obvious than 4-coumaric acid case.

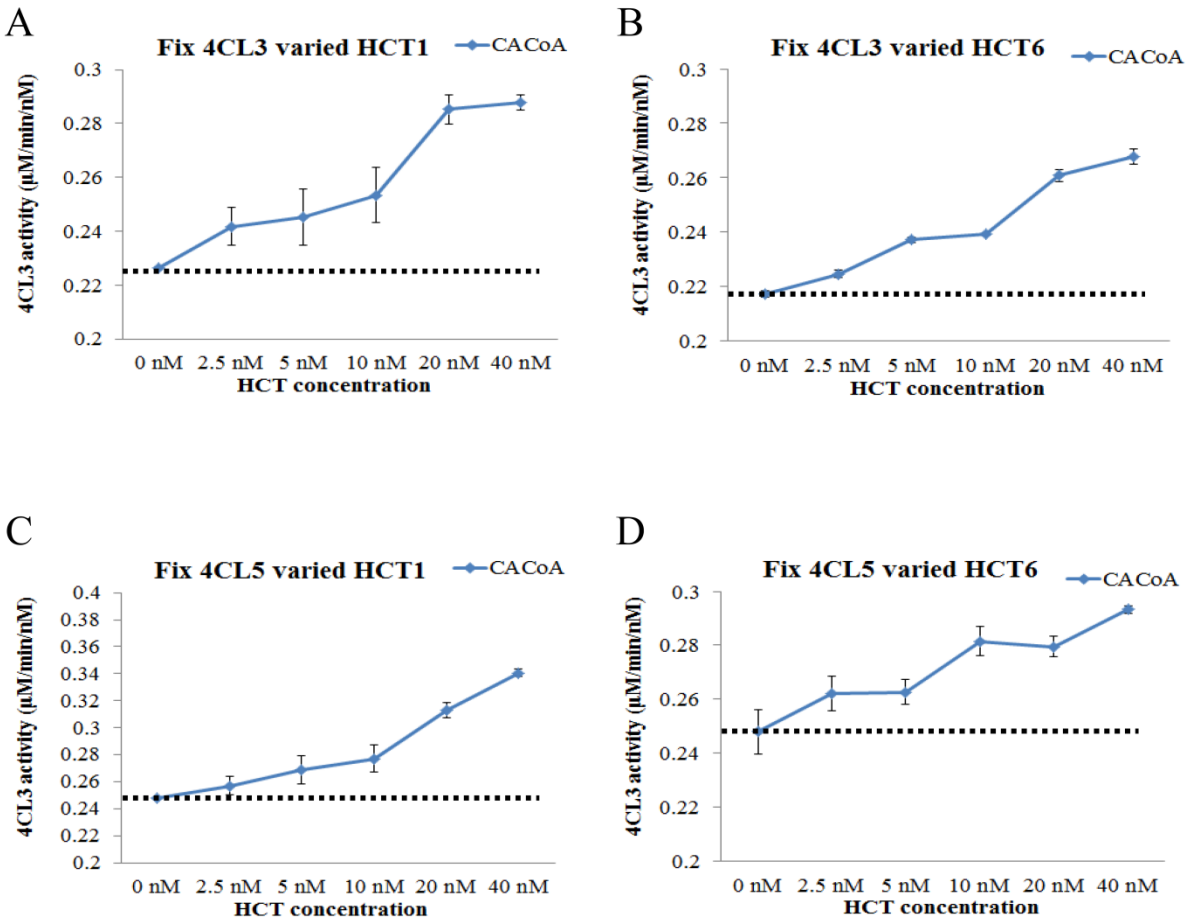

Figure 4.7 – Impact of Ptr4CL-PtrHCT complex formation on the CoA ligation activity toward caffeic acid. (**A**) Ptr4CL3 was fixed at 10 nM and PtrHCT6 concentration was varied. (**B**) Ptr4CL3 was fixed at 10 nM and PtrHCT6 concentration was varied. (**C**) Ptr4CL5 was fixed at 10 nM and PtrHCT1 concentration was varied. (**D**) Ptr4CL5 was fixed at 10 nM and PtrHCT6 concentration was varied. Dashed line indicates the baseline Ptr4CL activity. Error bars represent SE of three replicates.

4.3.5 Mechanistic Modeling and Stoichiometry Analysis of Ptr4CL-PtrHCT Complex

Next, we explored the stoichiometry of the Ptr4CL-PtrHCT complex using mechanistic modeling (**Figure 4.1**). This computational methodology has already been applied to reveal the functional redundancy of PtrCAld5Hs and the heterotetrameric interaction of the Ptr4CL complex [47, 48, 58]. The model is based on experimental data and the mixed enzyme activity of Ptr4CLs in the Ptr4CL-PtrHCT complex (**Figures 4.6 and 4.7**). The CoA ligation activities given a fixed concentration of Ptr4CL and different ratios of PtrHCT for 4-coumaric acid (**Figure 4.8**) or caffeic acid as substrate (**Figure 4.9**) were evaluated by numerically analysis according to the parameters for enzyme activity and enzyme ratios.

The numerical analyses were used to measures of the overall accuracy for stoichiometry predictions of the Ptr4CL-PtrHCT complex, which can evaluate the goodness-of-fit of models to the experimental data. The model incorporated the enzyme activity under different ratios of Ptr4CL and PtrHCT and can indicate the stoichiometry of the complex based on the root mean square error (RMSE) and the Bayesian Information Criterium (BIC) [66]. Both RMSE and BIC had the lowest values when the Ptr4CL to PtrHCT ratio is 1 to 2 (**Figures 4.8A, 4.8B, 4.8D, 4.9A and 4.9B**), except that the ratio for Ptr4CL5 to PtrHCT1 has a 1 to 3 ratio preference (**Figure 4.8C and 4.9C**). The numerical analysis showed that the most likely complex is a heterotrimer of Ptr4CL-PtrHCT with 1 subunit of Ptr4CL with 2 subunits of PtrHCTs. However, **Figures 4.8C** and **4.9C** indicate a 1:3 ratio, for Ptr4CL5 and PtrHCT1, where **Figure 4.9D** indicates a 1:1 ratio for Ptr4CL5 and PtrHCT6.

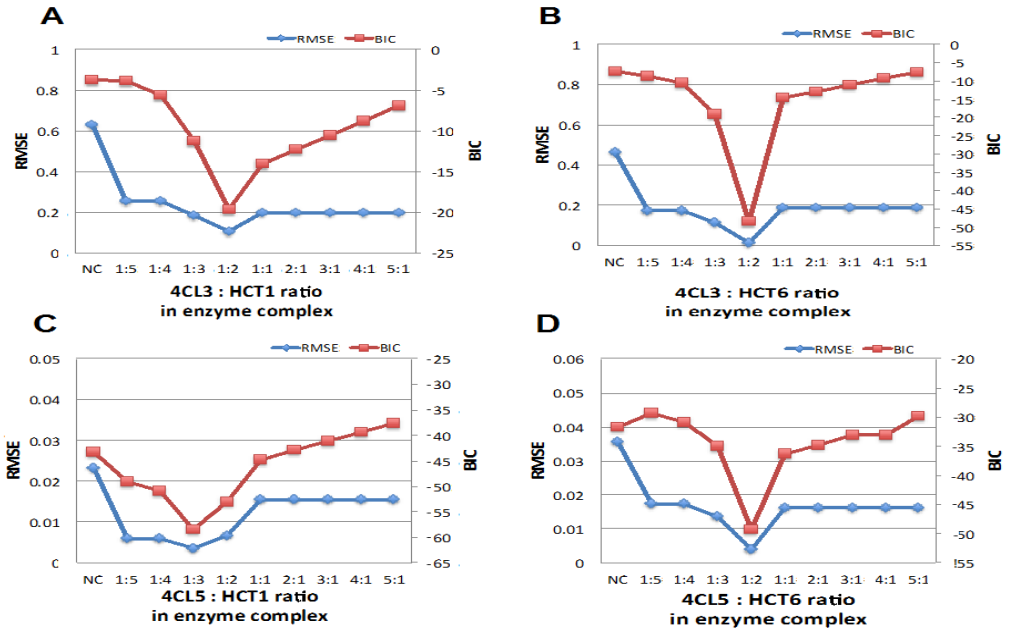

Figure 4.8 – Numerical analysis of CoA ligation activity toward 4-coumaric acid. (**A**) Ptr4CL3 to PtrHCT1 ratio analysis. (**B**) Ptr4CL3 to PtrHCT6 ratio analysis. (**C**) Ptr4CL5 to PtrHCT1 ratio analysis. (**D**) Ptr4CL5 to PtrHCT6 ratio analysis.

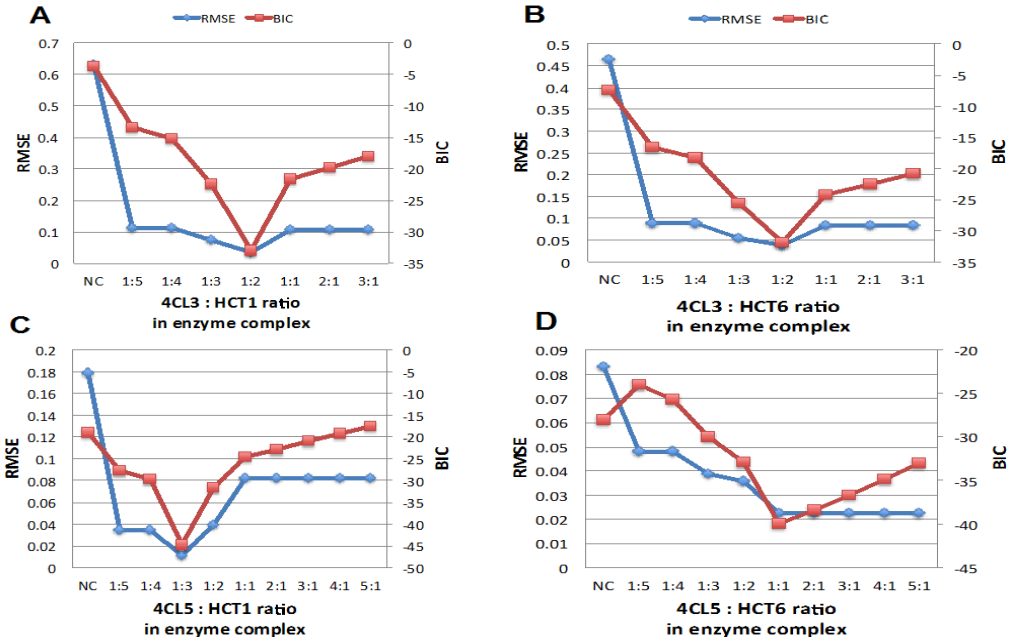

Figure 4.9 – Numerical analysis of CoA ligation activity toward caffeic acid. (**A**) Ptr4CL3 to PtrHCT1 ratio analysis. (**B**) Ptr4CL3 to PtrHCT6 ratio analysis. (**C**) Ptr4CL5 to PtrHCT1 ratio analysis. (**D**) Ptr4CL5 to PtrHCT6 ratio analysis.

4.3.6 The Ptr4CL-PtrHCT Complex is Found *in vivo* in SDX

Further, to obtain physical evidence for the stoichiometry of the Ptr4CL-PtrHCT complex (1 to 2 ratio), a chemical cross-linking experiment was performed to investigate the nature of the Ptr4CL-PtrHCT complex in crude SDX extracts. The SDX extracts was prepared, cross-linked using dithiobis [succinimidyl propionate] (DSP), resolved by SDS-PAGE and using anti-PtrHCT antibodies to perform Western blot to detect the Ptr4CL-PtrHCT complex in crude SDX extracts. Compared to the SDX extracts without chemical cross-linking, the PtrHCT1 or PtrHCT6 in the cross-linked SDX can be detected between 140 to 200 kDa (**Figure 4.10**). The estimated size of the bands were about the expected size of the heterotrimer Ptr4CL-PtrHCT complex for one unit of Ptr4CL (60kDa) and two units of PtrHCT (2 * 50kDa). A similar size band had been observed when SDX extracts were cross-linked and blotted using Ptr4CL3 or Ptr4CL5 antibody [47]. These results indicated the presence of a Ptr4CL-PtrHCT complex in the crude SDX protein extracts and that the ratio of Ptr4CL to PtrHCT is likely to be 1 to 2.

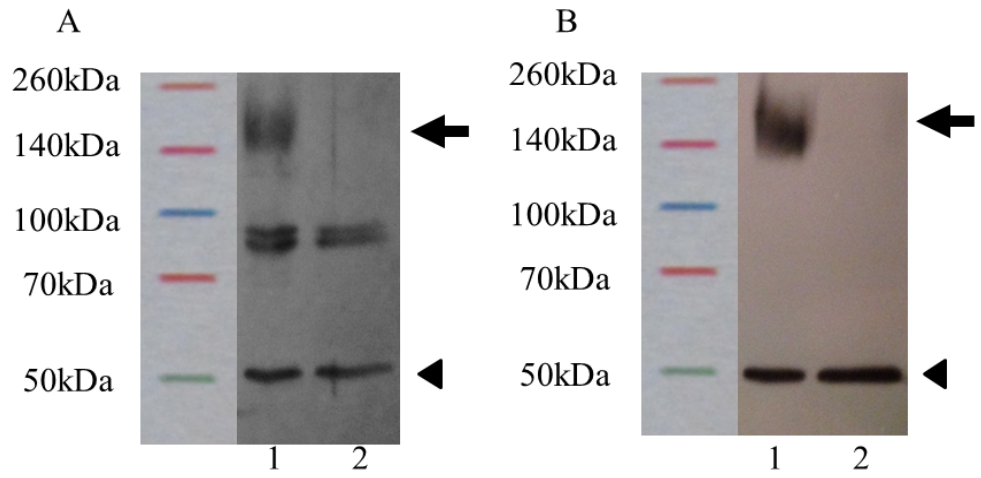

Figure 4.10 – Chemical cross-linking in SDX extracts using DSP cross-linker. (**A**) PtrHCT1 antibody was used. (**B**) PtrHCT6 antibody was used. Lane 1: cross-linked SDX. Lane 2: Non-cross-linked SDX. Arrow indicates the heterotrimer. Arrow head indicates the monomer.

4.3.7 CoA Ligation Activities are Decreased when both PtrHCT1 and PtrHCT6 are Downregulated in *P. trichocarpa*

We had demonstrated that Ptr4CLs interact with PtrHCTs to form a complex and the composition is 1 subunit of Ptr4CL with 2 subunits of PtrHCT. To further validate that Ptr4CL-PtrHCT complex has important biological function for the CoA ligation in *P. trichocarpa*, downregulation of PtrHCT transgenics were generated by RNA interference (RNAi). Because of the potential redundancy of the PtrHCT1 and PtrHCT6 (**Chapter 2, Figure 2.7**), the RNAi for downregulation of PtrHCT was designed to knockdown both PtrHCTs. From the transcriptome analysis, the transcript reads of both PtrHCT1 and PtrHCT6 were downregulated in three independent PtrHCT transgenic trees (1, 2 and 3) (**Figure 4.11**).

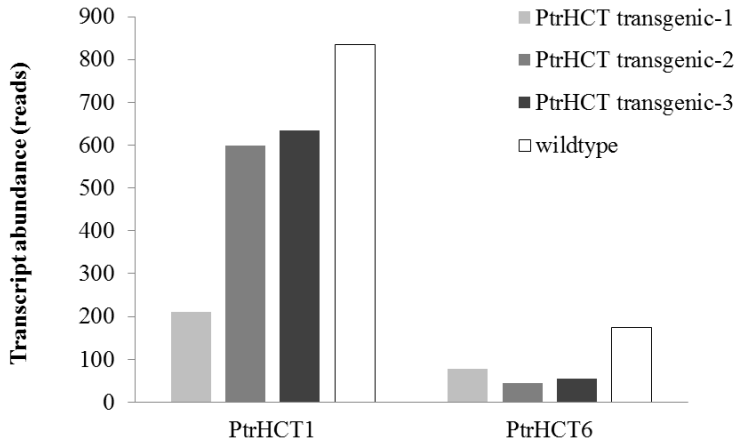

Figure 4.11 – Transcriptome analysis for the transcript abundance of both PtrHCT1 and PtrHCT6 transcripts in the PtrHCT downregulated transgenic and wildtype *P. trichocarpa*.

Next, we examined the CoA ligation activity of these PtrHCT downregulated transgenics and wildtype *P. trichocarpa*. CoA ligation activities of the Ptr4CL reactions for 4-coumaric or caffeic acid were decreased when PtrHCTs were downregulated (**Figure 4.12**), which is consistent with the enzyme activity that the presence of PtrHCT can facilitate the CoA ligation activities of Ptr4CL (**Figures 4.6 and 4.7**).

The CoA ligation activities for 4-coumaric or caffeic acid can be downregulated by 60% when PtrHCT1 and PtrHCT6 were downregulated to 25% and 44%, respectively (**PtrHCT transgenic-1, Figure 4.12**). Moreover, the transcript abundances of the Ptr4CL3 and Ptr4CL5 in PtrHCT downregulated transgenics are similar to the wildtype tree, which indicates that the downregulated of the CoA ligation activity is result from the interruption of the Ptr4CL-PtrHCT complex, not because of a non-specific effect of RNAi on the transcript abundance of Ptr4CL3 and Ptr4CL5 (**Figures 4.13**).

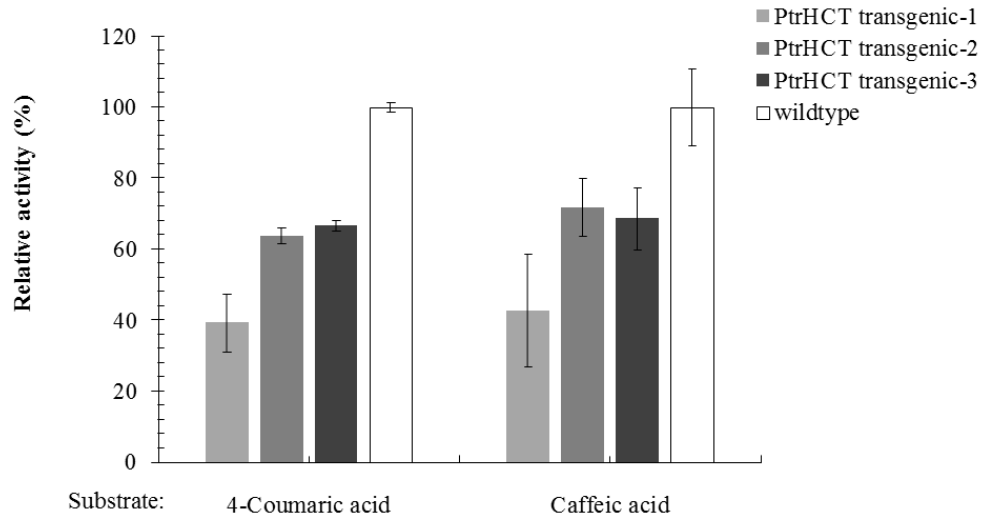

Figure 4.12 – CoA ligation activity for 4-coumaric acid and caffeic acid in the PtrHCT downregulated transgenic and wildtype *P. trichocarpa*. Each bar is present a pool of the three transgenic or wildtype trees.

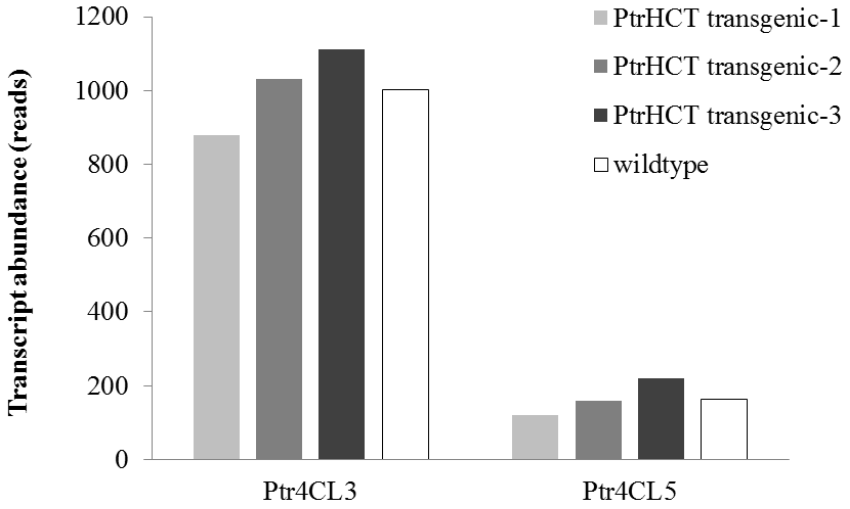

Figure 4.13 – Transcriptome analysis for the transcript abundance of both Ptr4CL3 and Ptr4CL5 transcripts in the PtrHCT downregulated transgenic and wildtype *P. trichocarpa*.

4.4 Discussion

In this study, a protein-protein interaction between Ptr4CLs and PtrHCTs has been identified. Based on five lines of evidences: (1) bimolecular fluorescence complementation (BiFC), (2) immunoprecipitation (IP), (3) chemical cross-linking, (4) mechanistic modeling, and (5) PtrHCT downregulated transgenic trees. Moreover, using a rule-based modeling and evolutionary computation, the most likely composition of the Ptr4CL and PtrHCT complex is predicted to have 1 subunit of Ptr4CL and 2 subunit of PtrHCTs (**Figures 4.8 and 4.9**), while from the chemical cross-linking in SDX, a protein complex size around 160kDa is detected by anti-PtrHCT antibody, which confirmed that the existence of Ptr4CL-PtrHCT complex (**Figures 4.10**). The Ptr4CL-PtrHCT complex appears to modulate the CoA ligation activities based on recombinant enzyme assays and the PtrHCT downregulated transgenics. The present of PtrHCT in the mixture of the Ptr4CL enzymes can facilitate the CoA ligation activity of Ptr4CL for both 4-coumaric acid and caffeic acid (**Figures 4.6 and 4.7**). Moreover, when PtrHCT is downregulated, the CoA ligation activities of the Ptr4CLs are also downregulated (**Figure 4.12**). Overall, the results provide a Ptr4CL-PtrHCT complex for the monolignol biosynthesis and this complex may play a role in regulating the metabolic flux of the CoA ligation.

4.4.1 Enzyme Complexes Affects the Metabolic Flux of Monolignol Biosynthesis

Protein-protein interactions have been identified in many metabolic pathways [21-31]. The benefits of forming the enzyme complexes may be to modulate the metabolic flux of the pathway, provide higher efficiency of the enzyme reactions, or respond quickly to a cell signal for changing the synthesis of the product [25, 32-34]. For example, in *Neurospora crassa,* an aggregate of five enzymes involved in the shikimic acid pathway was identified [21, 23], which preferentially utilizes precursors formed in the biosynthetic sequence than intermediates supplied exogenously [24]. A genetic and physical association between aromatic amino acid biosynthetic enzymes in *Bacillus subtilis* indicates a physiologically significant regulatory function [22].

Protein-protein interactions have been studied in the monolignol biosynthetic pathway as well [11, 20, 32, 33, 35, 45-47, 58]. The monolignol biosynthetic complex studies were mainly focused on the entry point of the pathway. For example, the PAL-C4H complex, identified in in potato, cucumber and tobacco, has a channeling effect to convert phenylalanine to 4-coumaric acid effectively [32, 33, 42, 45, 46]. In 2001, a possible metabolic complex for G and S lignin biosynthesis were been proposed; while COMT and CCoAOMT/CCR belong to independent metabolic routes [11]. However, physical evidence for these complexes is still lacking.

Recently, *Populus trichocarpa,* the protein-protein interactions among monolignol biosynthetic enzymes have been actively studied. A membrane protein complex of the PtrC3H3/PtrC4H1/PtrC4H2 has been identified and this hydroxylase complex shows novel 3-hydroxylation activity for 4-coumaric acid to caffeic acid [20]. A protein complex of the Ptr4CL isoforms has also been identified, which is a Ptr4CL3-Ptr4CL5 complex [47]. This Ptr4CL3-Ptr4CL5 complex showed a regulatory mechanism that affects the direction and rate of CoA ligation flux for monolignol biosynthesis in *P. trichocarpa* [47]. In contrast, some isoforms of the monolignol biosynthetic enzymes do not show interaction and their activities are additive. For example, the two *Populus trichocarpa* xylem specific 5-hydroxylase isoforms, PtrCAld5H1 and PtrCAld5H2, showed functional redundancy and independent activity [58]. In addition, in **Chapter 2**, the two xylem-specific isoforms of PtrHCTs (PtrHCT1 and PtrHCT6) also demonstrate the functional redundancy and independent activity.

4.4.2 The Ptr4CL-PtrHCT Complex Affects Metabolic Flux

In this study, we provide the physical and biochemical evidences for a protein complex of Ptr4CL-PtrHCT. This complex can facilitate the CoA ligation of the Pt4CL *in vitro* (**Figures 4.6 and 4.7**) and *in vivo* (**Figures 4.12**). In the enzyme complex, intermediates can be protected from the degradation, transfer rapidly to adjacent enzyme (channeling) and be prevented from release into the cytosolic environment [27]. For example, a study using

buckwheat seedlings showed that phenylalanine has an apparently low turnover rate and only approximately 20 to 25% of the metabolic end products are released into the cytoplasm [67].

Because PtrHCT is a down-stream enzyme of Ptr4CL in the proposed monolignol biosynthetic model (**Chapter 1, Figure 1.1**), the interaction between Ptr4CL and PtrHCT may facilitate the conversion of 4-coumaric acid to 4-coumaroyl shikimic acid without releasing 4-coumaroyl-CoA into the cytosolic pool. As we know, the CoA thioesters, such as 4-coumaroyl-CoA, are relative unstable and are easily hydrolyzed in protein extracts [68, 69]. The formation of a Ptr4CL-PtrHCT complex can transfer the 4-coumaroyl-CoA directly for downstream biosynthesis. Moreover, a structural analysis of the HCT from Sorghum (*Sorghum bicolor*) shows a significant affinity of SbHCT for 4-coumaroyl-CoA (1.6 μM), and a negligible affinity for shikimic acid, which indicates that 4-coumaroyl-CoA preconditions the binding of shikimic acid to HCT [70]. Therefore, the formation of Ptr4CL-PtrHCT complex may facilitate the binding of the 4-coumaroyl-CoA to PtrHCT as soon as Ptr4CL produce the CoA thioesters. Recently, a protein-protein and protein-membrane associations at the entry point of the lignin pathway in *Arabidopsis* were demonstrated [35], which showed a loose association of 4CL and HCT with ER and C3H (CYP98A3) able to locate both HCT and 4-CL1 nearer to the ER [35], which supports our result for the interaction between Ptr4CL and PtrHCT to form a Ptr4CL-PtrHCT complex.

4.4.3 More Enzymes may be Involved in Monolignol Biosynthetic Complex Formation

A larger monolignol biosynthetic complex has been suggested because of the evidence for a PAL-C4H enzyme complex at the entry point. In 2001, two independent metabolic complexes for G and S lignin biosynthesis were proposed [11]. In 2004, because of the discovery of the two essential monolignol enzymes, the C3H and HCT [71-74], a possible linear complex has been proposed [30]. However, no physical evidence of these hypotheses for the monolignol biosynthetic complex was presented. Recently, a possible complex in *Arabidopsis* showed that C3H is able to bring the HCT and 4CL to the ER, which could extend the monolignol biosynthetic complex for the monolignol biosynthetic pathway [35].

We have investigated the possible monolignol biosynthetic complex in the *P. trichocarpa*. Because all the xylem specific monolignol biosynthetic enzymes had been identified in *P. trichocarpa* [16], we adapted the BiFC assay to identify putative interactions among these monolignol biosynthetic enzymes [75]. A membrane complex of PtrPAL/PtrC3H/PtrC4H/Ptr4CL/PtrHCT had been shown in Hsi-Chuan Chen's dissertation [76]. Here, we identified a soluble protein complex between PtrHCTs, PtrCAD1, PtrCOMT2 and PtrCCR2 from positive BiFC signals (**Figure 4.14**).

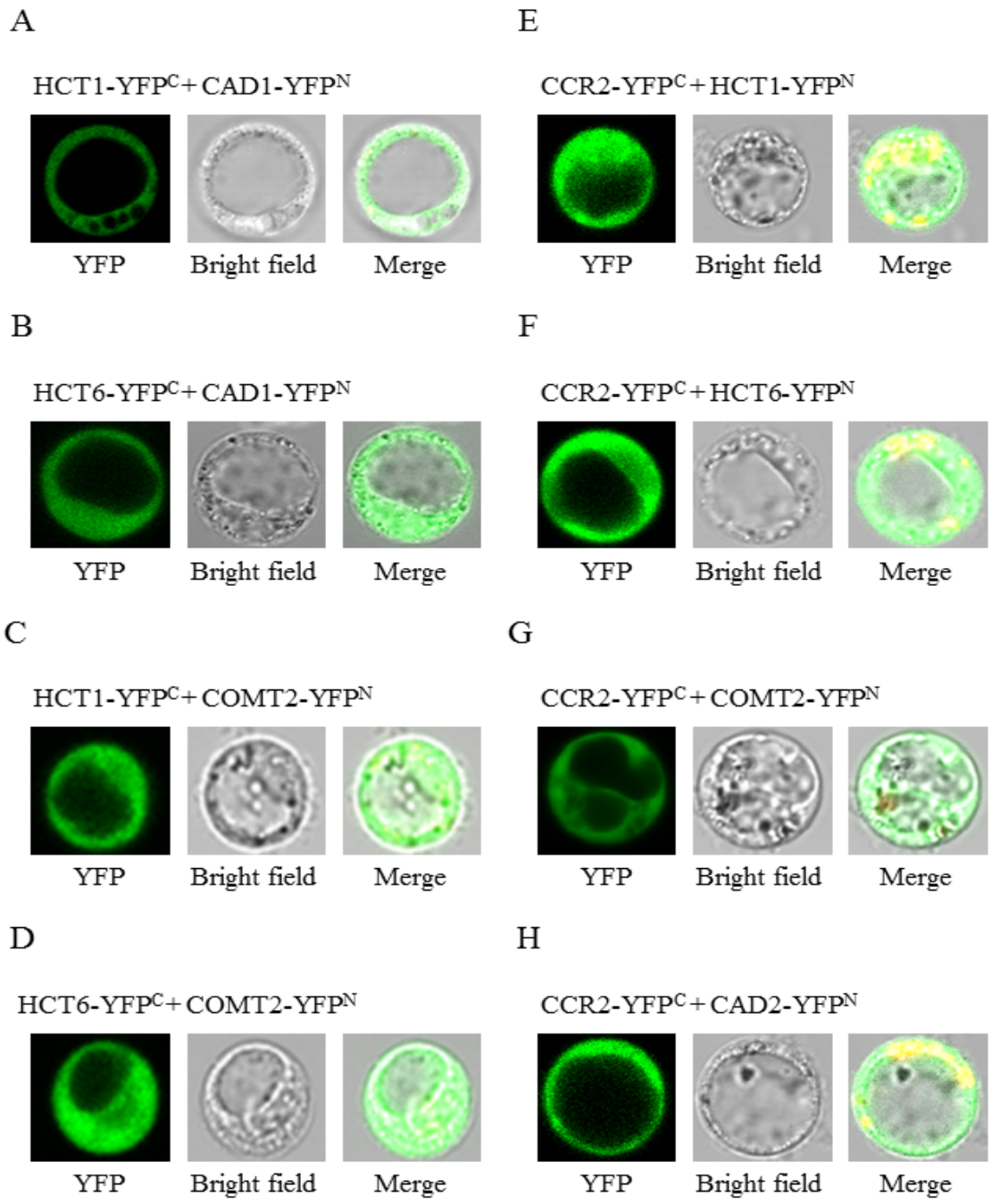

Figure 4.14 – BiFC assay for the positive protein-protein interaction between PtrHCTs, PtrCAD1, PtrCOMT2 and PtrCCR2.

Also, several negative BiFC results indicate that PtrHCT has no interactions with PtrCCoAOMTs and PtrCAld5Hs (**Figure 4.15**).

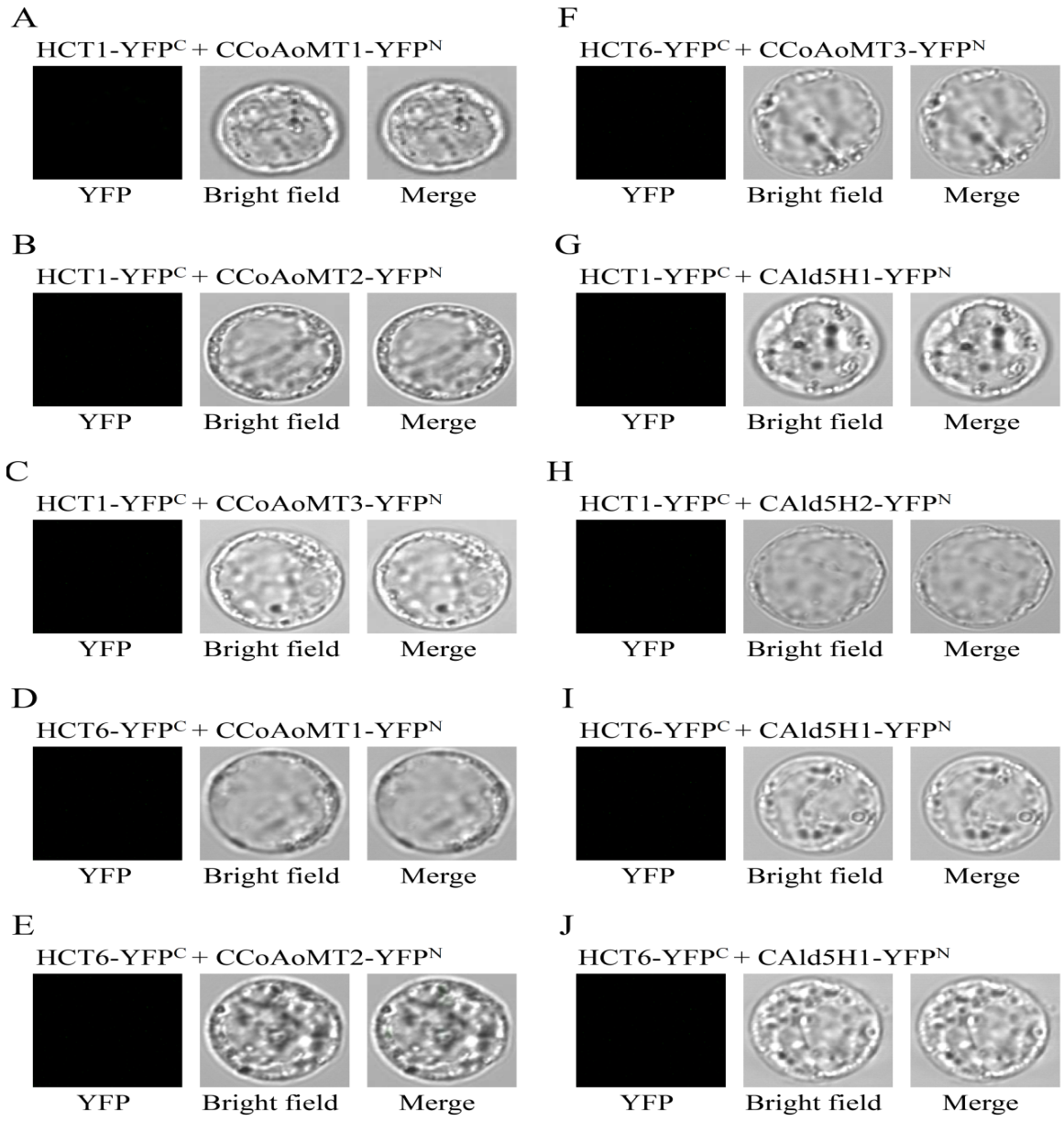

Figure 4.15 – BiFC assay for the negative signal between PtrHCTs, PtrCCoAOMTs and PtrCAldHs.

Based on our present results and unpublished data, a possible monolignol biosynthetic complex in *P. trichocarpa* has been proposed in **Figure 4.16**. In this proposed model, PtrHCT, so far, is considered as the scaffold protein that can bring the membrane complex (PAL/C3H/C4H/4CL) and the soluble protein complex (COMT/CAD/CCR/CCoAOMT) together. However, there is still no evidence suggests whether CAld5H can interact with other monolignol biosynthetic enzymes to synthesize the S subunit monolignol.

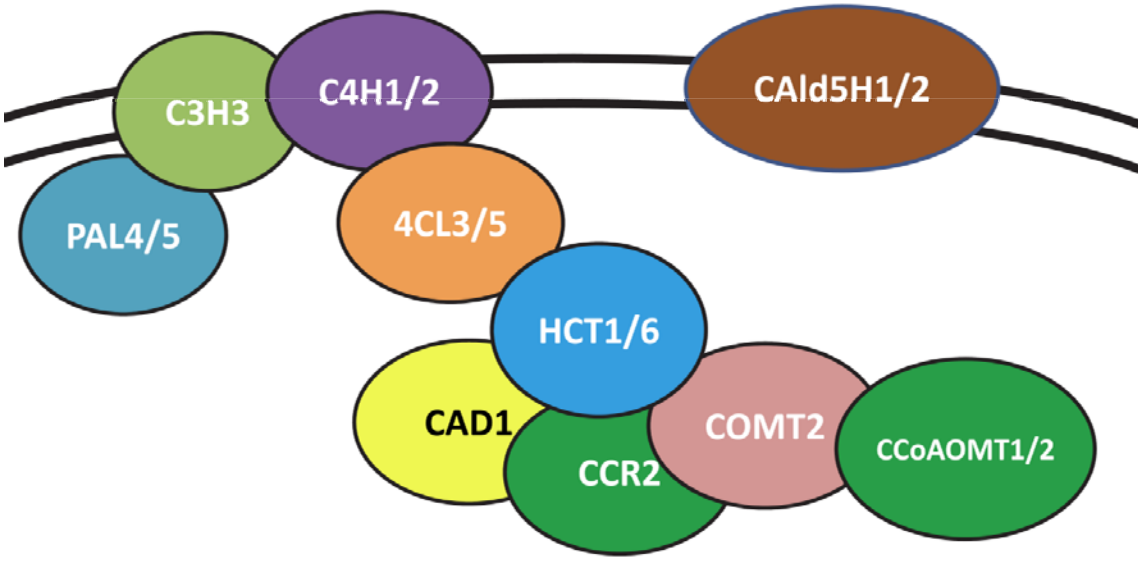

Figure 4.16 – The proposed monolignol biosynthetic complex from BiFC assay.

4.5 References

1. Sarkanen, K.V. and C.H. Ludwig, *Lignins: occurrence, formation, structure and reactions*1971, New York: Wiley-Interscience.

2. Higuchi, T., *Biochemistry and molecular biology of wood*1997, Berlin; New York: Springer.

3. Eckardt, N.A., *Probing the Mysteries of Lignin Biosynthesis: The Crystal Structure of Caffeic Acid/5-Hydroxyferulic Acid 3/5-O-Methyltransferase Provides New Insights.* The Plant Cell Online, 2002. **14**(6): p. 1185-1189.

4. Studer, M.H., et al., *Lignin content in natural Populus variants affects sugar release.* Proc Natl Acad Sci U S A, 2011. **108**(15): p. 6300-5.

5. Hu, W.J., et al., *Repression of lignin biosynthesis promotes cellulose accumulation and growth in transgenic trees.* Nat Biotechnol, 1999. **17**(8): p. 808-12.

6. Chiang, V.L., *From rags to riches.* Nat Biotechnol, 2002. **20**(6): p. 557-8.

7. Hinchee, M., et al., *Short-rotation woody crops for bioenergy and biofuels applications.* In Vitro Cell Dev Biol Plant, 2009. **45**(6): p. 619-629.

8. Vogt, T., *Phenylpropanoid Biosynthesis: Invited Review.* Molecular Plant, 2009.

9. Barrière, Y., et al., *Genetics and genomics of lignification in grass cell walls based on maize as a model system.* Genes Genomes Genomics, 2007. **1**: p. 133-156.

10. Brown, S.A. and A.C. Neish, *Shikimic acid as a precursor in lignin biosynthesis.* Nature, 1955. **175**(4459): p. 688-9.

11. Dixon, R.A., et al., *The biosynthesis of monolignols: a "metabolic grid", or independent pathways to guaiacyl and syringyl units?* Phytochemistry, 2001. **57**(7): p. 1069-84.

12. Hamberger, B., et al., *Genome-wide analyses of phenylpropanoid-related genes in Populus trichocarpa, Arabidopsis thaliana, and Oryza sativa: the Populus lignin toolbox and conservation and diversification of angiosperm gene familiesThis article is one of a selection of papers published in the Special Issue on Poplar Research in Canada.* Canadian Journal of Botany, 2007. **85**(12): p. 1182-1201.

13. Higuchi, T., *Pathways for monolignol biosynthesis via metabolic grids: coniferyl aldehyde 5-hydroxylase, a possible key enzyme in angiosperm syringyl lignin biosynthesis.* Proceedings of the Japan Academy. Series B: physical and biological sciences., 2003. **79**: p. 227-236.

14. Higuchi, T. and S.A. Brown, *Studies of lignin biosynthesis using isotopic carbon. XIII. The phenylpropanoid system in lignification.* Can J Biochem Physiol, 1963. **41**: p. 621-8.

15. Lee, Y., et al., *Integrative analysis of transgenic alfalfa (Medicago sativa L.) suggests new metabolic control mechanisms for monolignol biosynthesis.* PLoS Comput Biol, 2011. **7**(5): p. e1002047.

16. Shi, R., et al., *Towards a systems approach for lignin biosynthesis in Populus trichocarpa: transcript abundance and specificity of the monolignol biosynthetic genes.* Plant Cell Physiol, 2010. **51**(1): p. 144-63.

17. Raes, J., et al., *Genome-wide characterization of the lignification toolbox in Arabidopsis.* Plant Physiol, 2003. **133**(3): p. 1051-71.

18. Vanholme, R., et al., *Lignin biosynthesis and structure.* Plant Physiol, 2010. **153**(3): p. 895-905.

19. Chen, H.-C., et al., *Monolignol Pathway 4-Coumaric Acid:CoA Ligases in Populus trichocarpa: Novel Specificity, Metabolic Regulation, and Simulation of CoA Ligation Fluxes.* Plant physiology, 2013. **161**: p. 1501-1516.

20. Chen, H.C., et al., *Membrane protein complexes catalyze both 4- and 3-hydroxylation of cinnamic acid derivatives in monolignol biosynthesis.* Proceedings of the National Academy of Sciences of the United States of America, 2011. **108**(52): p. 21253-8.

21. Giles, N.H., et al., *A gene cluster in Nuerospora crassa coding for an aggregate of five aromatic synthetic enzymes.* Proceedings of the National Academy of Sciences of the United States of America, 1967. **58**(4): p. 1453-60.

22. Nester, E.W., J.H. Lorence, and D.S. Nasser, *An enzyme aggregate involved in the biosynthesis of aromatic amino acids in Bacillus subtilis. Its possible function in feedback regulation.* Biochemistry, 1967. **6**(5): p. 1553-63.

23. Case, M.E. and N.H. Giles, *Evidence for nonsense mutations in the arom gene cluster of Neurospora crassa.* Genetics, 1968. **60**(1): p. 49-58.

24. Gaertner, F.H., M.C. Ericson, and J.A. DeMoss, *Catalytic facilitation in vitro by two multienyzme complexes from Neurospora crassa.* The Journal of biological chemistry, 1970. **245**(3): p. 595-600.

25. Ginsburg, A. and E.R. Stadtman, *Multienzyme systems.* Annual review of biochemistry, 1970. **39**: p. 429-72.

26. Stafford, H.A., *Compartmentation in natural product biosynthesis by multienzyme complexes.* The biochemistry of plants, 1981. **7**: p. 117-137.

27. Hrazdina, G. and G.J. Wagner, *Compartmentation of plant phenolic compounds; sites of synthesis and accumulation.* Biochemistry of plant phenolics, 1985.

28. Srere, P.A., *Complexes of Sequential Metabolic Enzymes.* Annual review of biochemistry, 1987. **56**(1): p. 89-124.

29. Hrazdina, G., *Compartmentation in Aromatic Metabolism*, in *Phenolic Metabolism in Plants*, H. Stafford and R. Ibrahim, Editors. 1992, Springer US. p. 1-23.

30. Winkel, B.S., *Metabolic channeling in plants.* Annual review of plant biology, 2004. **55**: p. 85-107.

31. Hrazdina, G. and R.A. Jensen, *Spatial Organization of Enzymes in Plant Metabolic Pathways.* Annual Review of Plant Physiology and Plant Molecular Biology, 1992. **43**(1): p. 241-267.

32. Czichi, U. and H. Kindl, *Formation of p-coumaric acid and o-coumaric acid from L-phenylalanine by microsomal membrane fractions from potato: Evidence of membrane-bound enzyme complexes.* Planta, 1975. **125**(2): p. 115-25.

33. Czichi, U. and H. Kindl, *Phenylalanine ammonia lyase and cinnamic acid hydroxylases as assembled consecutive enzymes on microsomal membranes of cucumber cotyledons: Cooperation and subcellular distribution.* Planta, 1977. **134**(2): p. 133-43.

34. Winkel-Shirley, B., *Flavonoid Biosynthesis. A Colorful Model for Genetics, Biochemistry, Cell Biology, and Biotechnology.* Plant physiology, 2001. **126**(2): p. 485-493.

35. Bassard, J.-E., et al., *Protein–Protein and Protein–Membrane Associations in the Lignin Pathway.* The Plant Cell Online, 2012. **24**(11): p. 4465-4482.

36. Jorgensen, K., et al., *Metabolon formation and metabolic channeling in the biosynthesis of plant natural products.* Current opinion in plant biology, 2005. **8**(3): p. 280-91.

37. Ralston, L. and O. Yu, *Metabolons involving plant cytochrome P450s.* Phytochemistry Reviews, 2006. **5**(2-3): p. 459-472.

38. Stafford, H.A., *Possible Multienzyme Complexes Regulating the Formation of C6-C3 Phenolic Compounds and Lignins in Higher Plants*, in *Recent Advances in Phytochemistry*, R. V.C and C. E.E, Editors. 1974, Elsevier. p. 53-79.

39. Hrazdina, G., G.J. Wagner, and H.W. Siegelman, *Subcellular localization of enzymes of anthocyanin biosynthesis in protoplasts.* Phytochemistry, 1978. **17**(1): p. 53-56.

40. Wagner, G.J. and G. Hrazdina, *Endoplasmic reticulum as a site of phenylpropanoid and flavonoid metabolism in hippeastrum.* Plant physiology, 1984. **74**(4): p. 901-6.

41. Hrazdina, G., A.M. Zobel, and H.C. Hoch, *Biochemical, immunological, and immunocytochemical evidence for the association of chalcone synthase with endoplasmic reticulum membranes.* Proceedings of the National Academy of Sciences of the United States of America, 1987. **84**(24): p. 8966-70.

42. Hrazdina, G. and G.J. Wagner, *Metabolic pathways as enzyme complexes: evidence for the synthesis of phenylpropanoids and flavonoids on membrane associated enzyme complexes.* Archives of biochemistry and biophysics, 1985. **237**(1): p. 88-100.

43. Burbulis, I.E. and B. Winkel-Shirley, *Interactions among enzymes of the Arabidopsis flavonoid biosynthetic pathway.* Proceedings of the National Academy of Sciences of the United States of America, 1999. **96**(22): p. 12929-34.

44. Saslowsky, D. and B. Winkel-Shirley, *Localization of flavonoid enzymes in Arabidopsis roots.* The Plant journal : for cell and molecular biology, 2001. **27**(1): p. 37-48.

45. Rasmussen, S. and R.A. Dixon, *Transgene-mediated and elicitor-induced perturbation of metabolic channeling at the entry point into the phenylpropanoid pathway.* The Plant cell, 1999. **11**(8): p. 1537-52.

46. Achnine, L., et al., *Colocalization of L-phenylalanine ammonia-lyase and cinnamate 4-hydroxylase for metabolic channeling in phenylpropanoid biosynthesis.* The Plant cell, 2004. **16**(11): p. 3098-109.

47. Chen, H.-C., et al., *Systems Biology of Lignin Biosynthesis in Populus trichocarpa: Heteromeric 4-Coumaric Acid:Coenzyme A Ligase Protein Complex Formation, Regulation, and Numerical Modeling.* The Plant cell, 2014. **26**(3): p. 876-93.

48. Song, J., *Mechanistic Model Development for Multi-Enzymatic Reactions in Lignin Biosynthesis (Unpublished Doctoral thesis). North Carolina State University, Raleigh, NC, U.S.A.* 2014.

49. Liu, J., et al., *A standard reaction condition and a single HPLC separation system are sufficient for estimation of monolignol biosynthetic pathway enzyme activities.* Planta, 2012. **236**(3): p. 879-85.

50. Hu, C.D., Y. Chinenov, and T.K. Kerppola, *Visualization of interactions among bZIP and Rel family proteins in living cells using bimolecular fluorescence complementation.* Molecular cell, 2002. **9**(4): p. 789-98.

51. Walter, M., et al., *Visualization of protein interactions in living plant cells using bimolecular fluorescence complementation.* The Plant Journal, 2004. **40**(3): p. 428-438.

52. Radloff, R., W. Bauer, and J. Vinograd, *A dye-buoyant-density method for the detection and isolation of closed circular duplex DNA: the closed circular DNA in HeLa cells.* Proceedings of the National Academy of Sciences of the United States of America, 1967. **57**(5): p. 1514-21.

53. Meselson, M., F.W. Stahl, and J. Vinograd, *Equilibrium Sedimentation of Macromolecules in Density Gradients.* Proceedings of the National Academy of Sciences of the United States of America, 1957. **43**(7): p. 581-8.

54. Maniatis, T., *fritsch E, Sambrook J (1982) Molecular Cloning: a Laboratory Manual.* New York: Cold Spring Harb Lab.

55. Tartof, K. and C. Hobbs, *Improved media for growing plasmid and cosmid clones.* Focus, 1987. **9**(2): p. 12.

56. Sambrook, J. and D.W. Russell, *Preparation of Plasmid DNA by Alkaline Lysis with SDS: Maxipreparation.* Cold Spring Harbor Protocols, 2006. **2006**(1): p. pdb.prot4090.

57. Yoo, S.-D., Y.-H. Cho, and J. Sheen, *Arabidopsis mesophyll protoplasts: a versatile cell system for transient gene expression analysis.* Nat. Protocols, 2007. **2**(7): p. 1565-1572.

58. Wang, J.P., et al., *Functional redundancy of the two 5-hydroxylases in monolignol biosynthesis of Populus trichocarpa: LC-MS/MS based protein quantification and metabolic flux analysis.* Planta, 2012. **236**(3): p. 795-808.

59. Lin, Y.C., et al., *SND1 transcription factor-directed quantitative functional hierarchical genetic regulatory network in wood formation in Populus trichocarpa.* The Plant cell, 2013. **25**(11): p. 4324-41.

60. Lin, Y.-C., et al., *A simple improved-throughput xylem protoplast system for studying wood formation.* Nat. Protocols, 2014. **9**(9): p. 2194-2205.

61. Sambrook, J., E.F. Fritsch, and T. Maniatis, *Molecular cloning*. Vol. 2. 1989: Cold spring harbor laboratory press New York.

62. Miki, D., R. Itoh, and K. Shimamoto, *RNA silencing of single and multiple members in a gene family of rice.* Plant Physiol, 2005. **138**(4): p. 1903-13.

63. Holsters, M., et al., *Transfection and transformation of Agrobacterium tumefaciens.* Mol Gen Genet, 1978. **163**(2): p. 181-7.

64. Song, J., et al., *Genetic transformation of Populus trichocarpa genotype Nisqually-1: a functional genomic tool for woody plants.* Plant Cell Physiol, 2006. **47**(11): p. 1582-9.

65. Li, Q., et al., *Splice variant of the SND1 transcription factor is a dominant negative of SND1 members and their regulation in Populus trichocarpa.* Proceedings of the National Academy of Sciences, 2012. **109**(36): p. 14699-14704.

66. Schwarz, G., *Estimating the dimension of a model.* The annals of statistics, 1978. **6**(2): p. 461-464.

67. Margna, U. and T. Vainjärv, *Buckwheat Seedling Flavonoids Do not Undergo Rapid Turnover.* Biochemie und Physiologie der Pflanzen, 1981. **176**(1): p. 44-53.

68. Li, L., et al., *Quantitative Evaluation of 4-Coumarate: CoA Ligase (4CL) Activity and Correlated Chemical Constituents in Four Plant Materials by Chromatographic Analysis.* Chinese Journal of Natural Medicines, 2010. **8**(4): p. 274-279.

69. Loscher, R. and L. Heide, *Biosynthesis of p-hydroxybenzoate from p-coumarate and p-coumaroyl-coenzyme A in cell-free extracts of Lithospermum erythrorhizon cell cultures.* Plant physiology, 1994. **106**(1): p. 271-279.

70. Walker, A.M., et al., *Elucidation of the structure and reaction mechanism of sorghum hydroxycinnamoyltransferase and its structural relationship to other coenzyme a-dependent transferases and synthases.* Plant physiology, 2013. **162**(2): p. 640-51.

71. Franke, R., et al., *The ArabidopsisREF8 gene encodes the 3 - hydroxylase of phenylpropanoid metabolism.* The Plant Journal, 2002. **30**(1): p. 33-45.

72. Franke, R., et al., *Changes in secondary metabolism and deposition of an unusual lignin in the ref8 mutant of Arabidopsis.* The Plant Journal, 2002. **30**(1): p. 47-59.

73. Hoffmann, L., et al., *Silencing of hydroxycinnamoyl-coenzyme A shikimate/quinate hydroxycinnamoyltransferase affects phenylpropanoid biosynthesis.* The Plant Cell Online, 2004. **16**(6): p. 1446-1465.

74. Hoffmann, L., et al., *Purification, Cloning, and Properties of an Acyltransferase Controlling Shikimate and Quinate Ester Intermediates in Phenylpropanoid Metabolism.* Journal of Biological Chemistry, 2003. **278**(1): p. 95-103.

75. Walter, M., et al., *Visualization of protein interactions in living plant cells using bimolecular fluorescence complementation.* The Plant journal : for cell and molecular biology, 2004. **40**(3): p. 428-38.

76. Chen, H.-C., *Protein Complex Formation in Monolignol Biosynthesis. (Unpublished Doctoral thesis). North Carolina State University, Raleigh, NC, U.S.A.* 2012.

Chapter 5

PtrPO2, a Lignin Peroxidase in *Populus trichocarpa*

5.1 Introduction

Lignin, an abundant plant polymer evolved to enable vascular plants to dominate terrestrial ecosystems [1]. Lignin provides the mechanical strength for stems to grow upright. It facilitates water transport from the roots, enhances the pathogen resistance of the plant cell wall and limits plant tissue from natural decay [2-6]. However, lignin hinders the processing of plant materials for paper pulping and biofuel production, and is a limiting factor for biomass utilization [7]. During industrial delignification, physical or chemical pretreatment is required to reduce the recalcitrance of biomass, which often results in energy-consumption and creates environmentally toxic byproducts. Ongoing research to reduce lignin content or to modify lignin structure promises to reduce biomass recalcitrance and increase the yield of extractable cellulose and fermentable sugars for paper pulping and biofuel [8-13].

Lignin is principally composed of three major types of phenylpropanoid subunits known as 4-hydroxyphenyl (H), guaiacyl (G) and syringyl (S) subunits, polymerized from 4-coumaryl, coniferyl and sinapyl monolignols, respectively [14]. In angiosperms, such as

Populus trichocarpa, the lignin is composed mainly of S and G subunits with trace amounts of H subunits. After more than a half century of debate on the mechanism of lignin polymerization, the combinatorial radical coupling model by oxidases (peroxidases and laccases) is widely accepted because it provides the best explanation of the complex and versatile structure of lignin [15-31].

Plant peroxidases are heme-containing oxidases [32] . Higher plants contain class I (*EC 1.11.1.11*) and class III (*EC 1.11.1.7*) peroxidases. Class I peroxidases are intracellular peroxidases, such as ascorbate peroxidase (AP), which removes hydrogen peroxides in the chloroplasts and the cytosol [33]. Class III peroxidases are plant-specific peroxidases, which can be secreted into the cell wall. They are not found in unicellular green algae, which do not produce lignin [34].

Plant peroxidases are also characterized by their isoelectric points (pI), as the cationic (basic, pI > 7) and anionic (acidic, pI < 7) peroxidases [35]. Anionic peroxidases were first considered to contribute to the cell wall peroxidase activity and to lignin polymerization and because of their high affinity to lignin precursors, while cationic peroxidases were implicated in auxin catabolism [36]. In addition, plant peroxidases can be divided into cell wall or vacuolar types based on the presence or absence of a C-terminal extension peptide [37]. The cell wall type peroxidases are considered to act in cell wall metabolism, such as lignin polymerization, whereas the vacuolar peroxidases function in defense against abiotic and biotic stresses [38-41].

Class III peroxidases participate in many cellular processes, such as removal of hydrogen peroxides, oxidation of toxic compounds, suberization, plant hormone metabolism, salt tolerance, senescence, pathogen resistance, wound healing, as well as cell wall biosynthesis [36, 42-53]. Class III peroxidases in plants are a large gene family, suggesting functional redundancy among peroxidase genes [34, 54, 55]. Because of the availability of complete genome sequence, the class III peroxidase gene families have been identified in several plant species, such as *Arabidopsis thaliana* (73 genes) [56-58] and *Oryza sativa* (138 genes) [34].

Since 1967, peroxidases have been suggested to participate in lignification [18, 47, 59]. Lignin associated peroxidases have been identified in several plant species, such as TPX1 in tomato (*Lycopersicon esculentum*) [60, 61], FBP1 in French bean (*Phaseolus vulgaris* L.) [62, 63], TP02 and TP60 in tobacco (*Nicotiana tabacum*) [64, 65], ATP-A2 (AtPrx53), AtPrx2, AtPrx25, AtPrx71 and AtPrx72 in *Arabidopsis* [39, 66-68], ZePrx and ZPO-C in *Zinnia elegans* [40, 69-72], prxA3a and PXP3-4 and cationic cell-wall-peroxidase (CWPO-C) in poplar [73-80] and other tree species, such as Norway spruce and pine [81-88].

In vitro activity assays provided the biochemical evidences of these lignin peroxidases and their substrates preferences. For example, a fast-migrating isoperoxidase group (A_{II}) identified in *Populus x euramericana* has the activity toward syringaldazine (sinapyl alcohol analog) and is indicated in lignification [89]. PXP3-4 in *P. trichocarpa* also shows the syringaldazine-oxidizing activity [74, 75] and, as well as, TPX1 in the tomato [61]. ZePrx, isolated from suspension cell culture of *Z. elegans*, shows greatest activity (the highest k_{cat}

value) toward sinapyl alcohol [40]. Recombinant ZPO-C shows stronger activity toward coniferyl alcohol (11.40 ± 0.22 μmol min^{-1} U^{-1}) and sinapyl alcohol (2.31 ± 0.01 μmol min^{-1} U^{-1}) comparing to guaiacol (1.00 ± 0.04 μmol min^{-1} U^{-1}) as substrate [70]. In contrast, ATP-A2 in *Arabidopsis* has demonstrated with greater activity toward coniferyl alcohol biochemically and structurally [39, 66] and a peroxidase from Norway spruce also prefers coniferyl alcohol [90]. In addition, CWPO-C, isolated from poplar cell culture (*Populus alba L.*), does not only show the activity toward sinapyl alcohol and syringaldazine, but also capable to oxidize the larger polymers, such as synthetic lignin polymers and ferrocytochrome c, which indicates an important role of CWPO-C in lignification [76-80].

Direct functional evidence for lignin peroxidases has come from mutants and transgenic plants (**Supplemental Table S1**). Overexpression of TPX1 in tomato leads to a 40-220% increase in lignin content [91]. Tobacco with downregulation of peroxidase TP60 can have a 50% reduction of lignin affecting both S and G subunits [65]. Another TP60 downregulated tobacco with lignin content reduction of 23% shows changes in vascular tissue [92]. Downregulation of prxA3a in hybrid aspen (*Populus sieboldii x Populus grandidentata*) reduced lignin content 10-20% [93]. *Arabidopsis* mutations in peroxidases AtPrx53 [39], AtPrx2, AtPrx25, AtPrx71 and AtPrx72 [67, 68] affect lignin content and structure. However, contradictory results have often been obtained from transgenic plants, making the role of some lignin peroxidases inconclusive. For example, downregulation of the TP02 in tobacco to 40-80% of wildtype had no significant change in lignin levels [94]. Overexpression of *P.*

trichocarpa PXP3-4 to 800-fold has no effect on lignin quantity, degree of condensation or monolignol composition [95]. Suppression of Pox 25, Pox 29 and Pox 36 in hybrid aspen (*Populus sieboldii X P. gradidentata*) showed no significant reduction of lignin content [96]. CWPO-C from poplar callus (*Populus alba L.*) has been proposed to be involved in lignification; however, transgenics with perturbation of CWPO-C have not yet been produced and its role remains to be determined.

Wood possesses high economic value and the study of lignification can help to produce better plant biomass for commercial applications. The woody angiosperm *P. trichocarpa* has been used as a model for studying wood formation because its fast growth and because its genome sequence is known [97]. All the monolignol biosynthetic enzymes have been identified in *P. trichocarpa* based on the xylem-specific expression [98]. Most of the enzymes have been characterized [99]. However, because of the lack of the identification of specific peroxidases involved in lignification, the knowledge of the polymerization step in *P. trichocarpa* for lignin biosynthesis is incomplete. Identification of the lignin peroxidases in *P. trichocarpa* may help us to reduce lignin deposition more effectively for biomass utilization. So far, the only peroxidase that has been identified in *P. trichocarpa* is the PXP3-4, which showed no novel phenotype when overexpressed 800-fold [95]. In this study, we aimed to identify a class III peroxidase in *P. trichocarpa* involved in lignin polymerization.

Table 5.1 – Summary of the lignin peroxidases transgenics and mutants in plants.

	Gene	Species	Approach	Outcome	References
1	TobAnPOD (anionic)	Tomato	Overexpression	1. Lignin increased by 20% in leaf, 49% in fruit, and 106% in fruit outer epidermal tissue. 2. Lignin content in wounded transformed fruit increased by more than 20-fold	Hortscience 28: 218–221. (1993)
2	TP02 (anionic)	Tobacco	Downregulation	1. Significant suppression of peroxidase expression in the range of 40-80% 2. No significant difference in lignin levels was observed	Transgenic Res. 5: 263–270. (1996)
3	TP02 (anionic)	Tobacco	Downregulation	1. Lignin content in leaf, stem, and root was unchanged 2. Reduction in wound-induced deposition of lignin-like polymers	Plant Physiol. 114: 1187–1196. (1997)
4	TPX1 (cationic)	Tomato	Overexpression	1. 40–220% increment of lignin content of the leaf was found in transgenic plants 2. Shoot phenotype of transgenic plants was similar to wildtype	Physiol. Plantarum 106: 355–362. (1999)
5	ATP-A2 /AtPrx53 (anionic)	Arabidopsis	Mutant	1. The promoter of AtPrx53 directs GUS reporter expressed in lignified tissues 2. Mutant with increased lignin levels also shows increased levels of ATP A2 mRNA	Plant Mol Biol. 44: 231–243. (2000)
6	Pox 25 Pox 29 Pox 36	Hybrid Aspen	Downregulation	1. No significant suppression of lignin content	Holzforschung 55: 335–339. (2001)
7	TP60 (cationic)	Tobacco	Downregulation	1. Lignin reductions of up to 40–50% 2. Both guaiacyl and syringyl levels decreased 3. No observable differences in overall growth and development	Phytochemistry 64: 163–176. (2003)
8	prxA3a (anionic)	Hybrid Aspen	Downregulation	1. Lower lignin content and modified lignin composition 2. Highest lignin reduction line displays a higher syringyl/vanillin (S/V) ratio	J. Plant Res. 116: 175–182. (2003)
9	TP60 (cationic)	Tobacco	Downregulation	1. 20% reduction in lignin 2. No significant gross changes in sugar content and composition	Phytochemistry 71: 531–542. (2010)
10	AtPrx72 (cationic)	Arabidopsis	Mutant	1. Homologue of ZePrx 2. Low content in syringyl units 3. Decrease in the amount of lignin	Planta 237: 1599–1612. (2013)
11	AtPrx2, AtPrx25, AtPrx71 (all cationic)	Arabidopsis	Mutant	1. Homologue of CWPO-C 2. Significant decrease in thelignin content of AtPrx2 and AtPrx25 deficient mutants 3. Altered lignin structures in AtPrx2, AtPrx25 and AtPrx71 deficient mutants	J. Agric. Food Chem. 61, 3781–3788. (2013)

Tomato: *Lycopersicon esculentum* Mill; Tobacco: *Nicotiana tabacum;*
Hybrid Aspen: *Populus sieboldii x Populus gradidentata;* Arabidopsis*: Arabidopsis thaliana*

Based on transcriptome analysis of different tissues of *P. trichocarpa*, PtrPO2, a unique anionic peroxidase, was identified as peroxidase that is both xylem-abundant and xylem-specific. PtrPO2 shares low amino acid identity with lignin peroxidases in other plants. PtrPO2 was downregulated in xylem using an RNAi construct under the control of a 4-coumaric acid:coenzyme A (CoA) ligase (Ptr4CL) promoter. The PtrPO2 downregulated transgenics have reduced growth, reddish internodes and a 20% reduction in lignin content. The content of xylan and mannan is also affected. The discovery and characterization of this lignin peroxidase will help us to better understand the entire lignification process and provide new insights for the future modification of lignin.

5.2 Materials and Methods

5.2.1 Plant Materials

Clonal propagules of *Populus trichocarpa* (Nisqually-1) wildtype and transgenic PtrPO2 were grown in a greenhouse in soil containing a 1:1 ratio of peat moss to potting-mix, using 16 h light and 8 h dark photoperiod for six months. Stem differentiating xylem (SDX) tissues were harvested following Shi et al. (2010).

5.2.2 RNA Extractions

50 to 100 mg of xylem, phloem, leaf and shoot frozen powder were used to purify total RNA using the RNeasy Plant RNA Isolation kit (Qiagen, Limburg, Netherlands) following the manufacturer's protocol with a DNase on-column digestion. A260/A280 ratios of the RNA ranged from 1.9 to 2.1 and RNA integrity was estimated using an Agilent 2100 Bioanalyzer RIN (RNA integrity number) values ranged from 8.6 to 10.0.

5.2.3 Transcriptome (RNA-seq) and Differentially Expressed Gene (DEG) Analysis

For tissue specific *P. trichocarpa* peroxidase analysis, 1 μg RNA from different tissues of three wildtype plants were used. For transcriptome analysis of PtrPO transgenics, 1 μg RNA from 2 trees from each transgenic line or wildtype *P. trichocarpa* was used, except for PtrPO2-8 where only one plant was available. Following the RNA-seq library preparation (Illumina, San Diego, CA), mRNA was purified using poly-T oligo-attached magnetic beads. The mRNA was then fragmented, reverse transcribed into double-strand cDNA, followed by end repair and 3 ′end adenylation. The cDNA was ligated with multiplex adapters and PCR amplified to produce the RNA-seq libraries. The RNA-seq libraries were adjusted to 1 nM and pooled for multiplex sequencing on a Hiseq (Illumina, San Diego, CA). The DEG analysis also followed Li et al (2011). The resulting sequences were mapped to the *P. trichocarpa* genome v2.0, gene annotation v2.2 (www.phytozome.org) using TOPHAT [100]. The frequency of raw counts was determined by BEDtools and normalized using the

Trimmed mean of M value (TMM) [101, 102]. The genes with counts lower than 15 per million per library were filtered out, and DEGs were obtained by pairwise comparisons of transgenic and WT libraries using edgeR/Bioconductor [103]. The significance of DEGs is based on a false discovery rate (FDR) of 0.05.

5.2.4 Identification of Class III Peroxidases in *P. trichocarpa* and Phylogenetic Analysis

The class III peroxidases of *A. thaliana* and *P. trichocarpa* were retrieved from The PeroxiBase (http://peroxibase.toulouse.inra.fr/). Class III peroxidases of *P. trichocarpa* from the latest publication were also used for comparison [38]. Amino acid alignment was performed using Vector NTI software (Invitrogen, Grand Island, NY) [104]. Phylogenetic analysis was carried out using MEGA 5.1 [105] with a bootstrap resampling of 1,000 replicates and probabilities >50%.

5.2.5 RNA-Interference (RNAi) Plasmid Constructions and Plant Transformation

An RNA-silencing construct with an inverted repeat was prepared as in our previous study [106]. A 680 bp GUS linker (GL) was amplified with a pair of primers, 5′-TGACCTCGAGGTCGACGATATCGTCGTCATGAAGATGCGGAC-3′ and 5′-CTAGACTAGTCCCGGGGGTACCATCCACGCCGTATTCGGTG-3′, and cloned into the pCR2.1 vector, resulting in pCR2.1-GL. The inverted repeat consists of chimeric sequences from PtrPO2 obtained using specific primer sets (**Table 5.2**). The sense and antisense

fragments were inserted into pCR2.1-GL to produce pCR2.1-sense-GL-antisense. The sense-GL-antisense fragment was further cloned into pBI121-Ptr4CLp behind the *P. trichocarpa* 4-coumaric acid:coenzyme A ligase (4CL) promoter (Ptr4CLp) replacing the GUS gene. The construct was introduced into *Agrobacterium tumefaciens* (C58) by the freeze thaw method [107] and transferred into *P. trichocarpa* following our established method [108].

Table 5.2 – Primer list for PtrPO2 for RNAi construction.

Primer name	Sequence
PtrPO2-SF	GACTACTAGTGTTGCTCTTTTAGGAAGTCACTCTG
PtrPO2-SR	TGCAGAGCTCGACAACAACACCACAGCCCTTGA
PtrPO2 AS-F	CTCGAGGTTGCTCTTTTAGGAAGTCACTCTG
PtrPO2 AS-R	GGATCCGACAACAACACCACAGCCCTTGA

5.2.6 Real-time PCR (RT-PCR)

Gene-specific primer sets were designed for PtrPO1, PtrPO2, PtrPO3 and PtrPO8 (**Table 5.3**). RT-PCR was performed following Li et al., [109]. 150 ng total RNA was reverse-transcribed using TaqMan reverse transcription reagents (Life Technologies, Grand Island, NY). Each Real-time PCR reaction was carried out in a 25 µL mixture of first strand cDNA (equivalent to 5 ng of total RNA), 5 pmol specific primer sets and 12.5 µL of 2X SYBR green PCR master mix (Roche, Basel, Switzerland). The products of the RT-PCR were detected using the 7900 HT Sequence Detection System (Life Technologies, Grand Island,

NY). The program of RT-PCR is: 95 °C for 10 min, then 45 cycles of 95 °C for 15 sec and 60 °C for 1 min, after which a thermal denaturing cycle was added, to determine the dissociation curve of the PCR products to check the amplification specificity.

Table 5.3 – Primer list for RT-PCR.

Primer name	Sequence
PtrPO1-RT-F	TCTGATATTCTTGCGCTTGCAGCC
PtrPO1-RT-R	TCTCGCCTTCCCAAGGGAACATTA
PtrPO2-RT-F	AAGTCACTCTGTTGGCCGAGTTCA
PtrPO2-RT-R	ACCGGCCTTTAAGGTACTCAGCAT
PtrPO3-RT-F	ATCCATGCATCCATCGTTTGCAGC
PtrPO3-RT-R	TGGTTGTTCCTGCATTCTTTGCCC
PtrPO8-RT-F	AGCTCACAGTGTTGGGAGAACTCA
PtrPO8-RT-R	TCAGGGTTTAGTGCTGGGTCAACT
18S-RT-F	CGAAGACGATCAGATACCGTCCTA
18S-RT-R	TTTCTCATAAGGTGCTGGCGGAGT

5.2.7 Lignin Content and Carbohydrate Determination

The procedure followed our lab protocol [110]. Debarked stems were placed in 100% acetone, and held for 2 days at room temperature. The acetone was replaced three times by 90% acetone at 48-h intervals. After drying, wood was ground in a Wiley mill with a 40-mesh screen and the wood powder was further screened between 40-mesh and 60-mesh. The resulting wood meal (40-60 mesh) was used for lignin content determination to estimate acid-soluble lignin (ASL) and acid-insoluble lignin (Klason) lignin [111]. 100 mg of oven-

dried wood powder was mixed with 1.5 mL of 72% sulfuric acid for 90 min and then diluted to 57.5 mL with distilled water. The solution was heated at 121 ˚C for 150 min. The solution was then filtered through a crucible. The supernatant of the solution was collected for ASL and carbohydrate analysis. The residual lignin on the crucible was used to measure the acid-insoluble lignin by weight. For ASL, the solution was 10-fold diluted with distilled water and absorbance measured at 205 nm. The extinction coefficient for ASL is 110 $g^{-1} \cdot cm^{-1}$ at 205 nm [112]. For carbohydrate analysis, the solution was neutralized by calcium carbonate overnight at room temperature. The supernatant was filtered and analyzed using analytical HPLC (Shodex SUGAR SPO 810, 8 × 30 mm, Pb2+ cation exchange column, Showa Denko America, Inc., NY) with distilled water as eluent, at a flow rate of 0.5 mL/min, at 80°C and sugars were identified by refractive index.

5.2.8 Nitrobenzene Oxidation for Lignin Composition

Followed Chen's protocol [113], 200 mg of oven-dried extractive free wood powder was used to determine the lignin composition by nitrobenzene oxidation. Following oxidation, the sample was analyzed by HPLC using a Zorbax SB-C3 5 μm, 4.6 x 150-mm column (Agilent, Santa Clara, CA). Analysis of reactions was carried out using an HPLC gradient (solvent A, 10 mM formic acid in water; solvent B, 10 mM formic acid in acetonitrile; 10% B for 3 min, 10 to 20% B for 5 min, 20 to 30% B for 6 min, 30% B to 100% for 2 min, 100% B for 2 min; flow rate: 1.5 mL/min, at 40°C). A standard curve was quantified in a Diode-Array Detector

SL (Agilent, Santa Clara, CA) based on authentic compounds, 4-hydroxybenzoic acid, 4-hydroxybenzaldehyde, vanillic acid, syringic acid, vanillin and syringaldehyde [114].

5.2.9 Mechanical Properties of Wood

About 20 cm long stem sections were cut from the bottom of the stem of the transgenic tree. The stems are kept from drying in plastic bags. One segment with a length-to-width ratio of 22 was cut from each stem section and debarked before measuring the mechanical properties. A three-point bending test was conducted to measure the modulus of elasticity (MOE) by an MTS Alliance RF/300 universal mechanical tester as previously described [109].

5.3 Results

5.3.1 PtrPO2 is a Xylem-Abundant and Xylem-Specific Class III Peroxidase in *Populus trichocarpa*

A total of 101 *P. trichocarpa* class III peroxidases (PtrPOs) were retrieved from The PeroxiBase (http://peroxibase.toulouse.inra.fr/) for identification of putative lignin peroxidases. Of the 101 *P. trichocarpa* class III peroxidases, 12 entries were removed because seven are pseudogenes (PtPrx[P]14, PtPrx[p]17, PtPrx[p]54, PtPrx[p]62, PtPrx[p]66,

PtPrx[p]81, PtPrx[p]103), which cannot be expressed as functional proteins due to a frame shift in the coding region, and five in the database are redundant gene records, which are PtPrx11_Trichobel (Pxp11) and PtPrx03_trichobel (Pxp3-4) for PtPrx03, PtPrx[P]12 for PtPrx87, PtPrx[P]32 for PtPrx25 and PtPrx[P]83 for PtPrx83. Compared to the 93 *P. trichocarpa* class III PtrPOs studied by Ren et al. (2014) [38], only 6 of the class III peroxidases are not in The PeroxiBase. 5 of 6 are pseudogenes (*), which are the PRX5*, PRX8*, PRX32*, PRX47*, PRX69*, and an extra PRX81 was included in the analysis. After manual editing, a total 90 *P. trichocarpa* class III peroxidases were analyzed in this study.

To identify peroxidases functionally associated with lignin polymerization, we carried out transcriptome analysis to determine the transcript abundance of these 90 peroxidases in the stem differentiating xylem (SDX) of *P. trichocarpa*. From the SDX transcriptome (RNA-seq) data, 48 peroxidases had no detectable transcripts and these were excluded from further study. Of the remaining 42 peroxidases, seven peroxidases are abundant in *P. trichocarpa* SDX, which are PtrPO1 (POPTR_0005s21740) for 47.2% of the total reads of the class III peroxidase transcripts, PtrPO8 (POPTR_0004s01510) for 35.0%, PtrPO3 (POPTR_0005s11070) for 3.7%, PtrPO2 (POPTR_0006s13190) for 3.1%, PtPrx01 (POPTR_0003s21640) for 2.4%, PtPrx26 (POPTR_0017s06550) for 2.2%, PtPrx18 (POPTR_0001s34660) for 2.0%, and the rest of the 4.4 % are transcript reads for 35 low-expressed class III peroxidases (**Figure 5.1**).

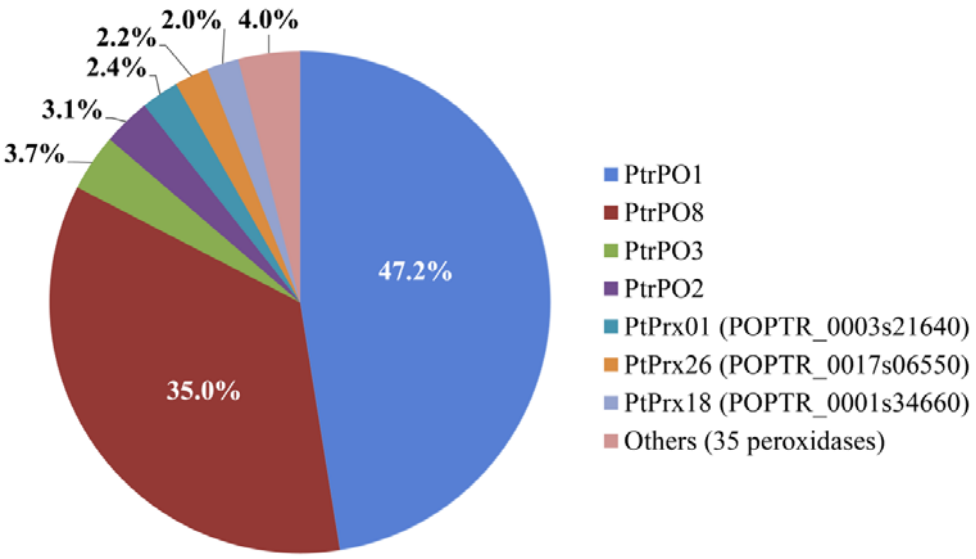

Figure 5.1 – The quantification of transcript abundance of the 42 detectable class III peroxidases in the stem wood of *P. trichocarpa*. PtrPO1: POPTR_0005s21740, PtrPO2: POPTR_0006s13190, PtrPO3: POPTR_0005s11070, PtrPO8: POPTR_0004s01510, PtPrx01: POPTR_0003s21640, PtPrx26: POPTR_0017s06550 and PtPrx18: POPTR_0001s34660.

The number of putative lignin peroxidases was narrowed down further by tissue specificity. Transcriptome analysis for all 42 class III peroxidases was carried out using four different tissues, which are SDX (X), phloem (P), leaf (L) and shoot tip (S) (**Figure 5.2**). Compared to the expression pattern of some well-known xylem-specific monolignol biosynthetic genes 4-coumaric acid:coenzyme A (CoA) ligases (Ptr4CL3 and Ptr4CL5) and hydroxycinnamoyl-CoA:shikimic acid hydroxycinnamoyl transferases (PtrHCT1 and PtrHCT6) (**Figure 5.2, bottom**), five class III PtrPOs were identified as SDX-specific class III peroxidases, which are PtrPO2, PtPrx37(POPTR_0007s01580), PtPrx19 (POPTR_0001s18270), PtPrx82 (POPTR_0017s09640) and PtPrx15 (POPTR_0010s04550). Among the 5 xylem-specific PtrPOs, the transcript abundance of PtrPO2 is highest and the

transcript level is up to 254.7-fold more than the other SDX-specific PtrPOs.

Overall, 42 out of 90 class III peroxidases gene transcripts are detectable in the SDX of *P. trichocarpa* and PtrPO2 is identified as the best candidate of the most xylem-abundant and xylem-specific peroxidases in *P. trichocarpa* (**Figures 5.1 and 5.2**). Moreover, downregulation of the other three xylem-abundant peroxidases, the PtrPO1, PtrPO3 or PtrPO8, had no significant lignin reduction (**Unpublished data**). Therefore, PtrPO2 was selected to be analyzed in detail to verify its role in lignin polymerization.

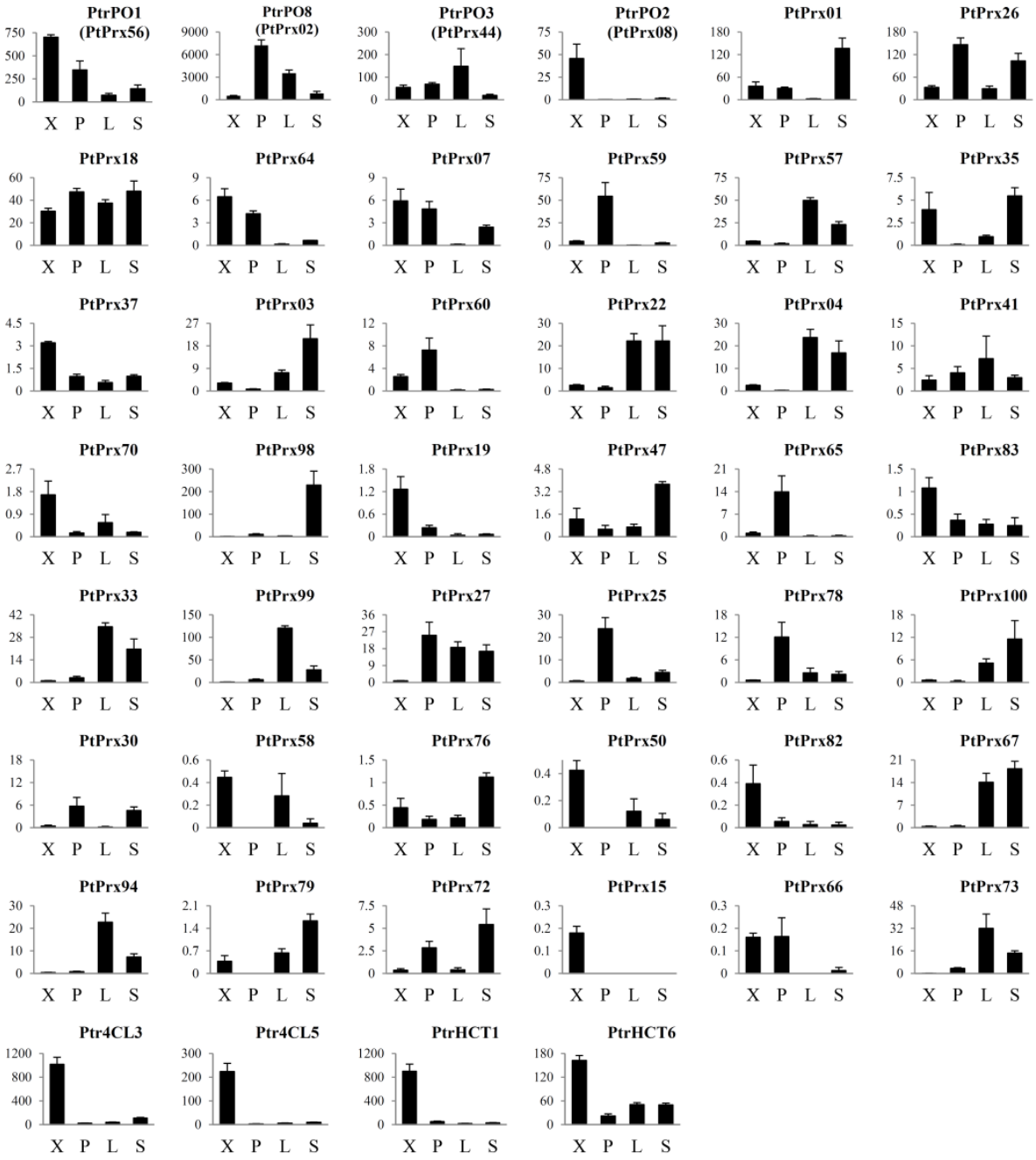

Figure 5.2 – Transcript abundance of the 42 detectable class III peroxidases in different tissues in *P. trichocarpa* and SDX-specific expressed monolignol biosynthetic genes (Ptr4CL3, Ptr4CL5, Pt4HCT1 and PtrHCT6). Transcript levels were counted from RNA-seq and RPM (reads per million). X, SDX. P, phloem. L, leaf. S. shoot. Error bars represent SE of three replicates.

5.3.2 PtrPO2 Shares Conserved Motifs with Coniferyl Alcohol-Specific Peroxidase from *Arabidopsis thaliana* and Sinapyl Alcohol-Specific Peroxidase from *Zinnia elegans*

The amino acid sequence of PtrPO2 (POPTR_0006s13190) was used to identify conserved structural motifs by comparing classic lignin peroxidases, the coniferyl alcohol (G)-specific peroxidase (ATP-A2) from *Arabidopsis thaliana* and the sinapyl alcohol (S)-specific peroxidase (ZePrx) from *Zinnia elegans*. Although the amino acid identity of PtrPO2 and ATP-A2 (32.4%) or ZePrx (33.2%) is low, the alignment still showed several conserved amino acid in the structural motifs (**Figure 5.3**), such as active sites (black box), substrate-binding sites (red box) and a signature structural motif for G- or S-specific peroxidase (green box). Similar to the known cell wall peroxidases (ATP-A2 and ZePrx), PtrPO2 lacks a C-terminal extension peptide.

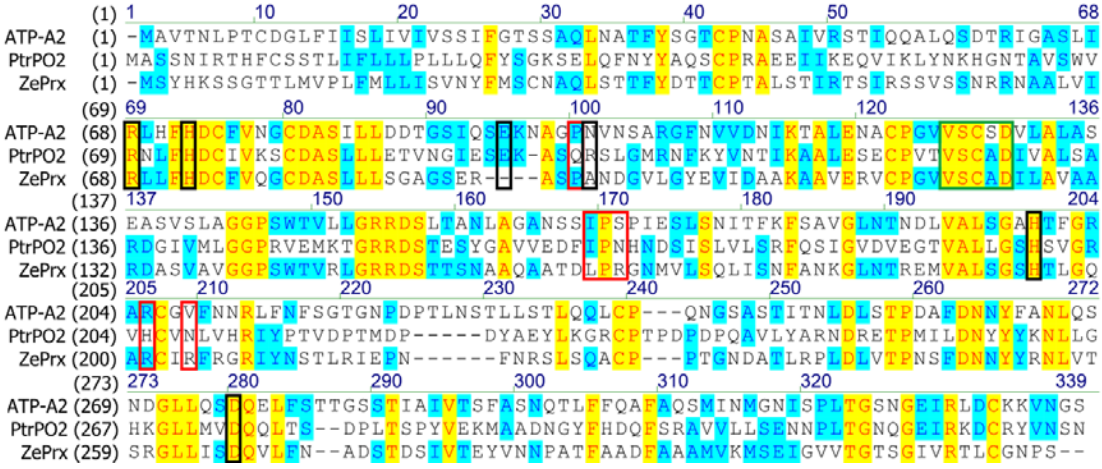

Figure 5.3 – Amino acid alignment of PtrPO2, classic G peroxidase (ATP-A2) and classic S peroxidase (ZePrx). The identical amino acids are in yellow, and conserved substitutions are in blue. The active site (black box), substrate-binding site (red box) and S or G peroxidase structure motif (green box) are indicated. [39, 115, 116].

5.3.3 PtrPO2 is an Unusual Peroxidase in the SDX of *P. trichocarpa*

We first examined the amino acid identity of PtrPO2 in *P. trichocarpa* compared to several lignin peroxidases from tomato, French bean, *Z. elegans*, tobacco, *Arabidopsis*, hybrid aspen (*P. sieboldii x P. grandidentata*), *Populus alba* L. and *P. trichocarpa*. PtrPO2 showed about 30% identity to most of the lignin peroxidases, except for higher identity of 53.9% with TP60 in tobacco (**Table 5.4**). PtrPO2 is an anionic peroxidase with a pI of 5.87 and TP60 is a cationic peroxidase with a pI of 8.89 (**Table 5.5**), indicating PtrPO2 and TP60 are distinct. Two poplar peroxidases (prxA3a and PXP3-4) show high sequence identity (50-60%) to FBP1 and ATP-A2 from *Arabidopsis*, but none of the known poplar lignin peroxidases (prxA3a from hybrid aspen, PXP3-4 from *P. trichocarpa* and CWPO-C from *Populus alba* L.) is similar to PtrPO2.

Table 5.4 – Amino acid sequence identity (%) of PtrPO2 and lignin peroxidases among plant species.

	TPX1	FBP1	ZPO-C	ZePrx	TP60	ATP-A2	prxA3a	PXP3-4	CWPO-C	PtrPO2
TPX1	100.0									
FBP1	37.3	100.0								
ZPO-C	40.6	36.5	100.0							
ZePrx	35.4	38.2	34.8	100.0						
TP60	32.2	31.4	34.7	32.3	100.0					
ATP-A2	38.3	53.7	35.8	41.2	32.7	100.0				
prxA3a	38.0	58.7	35.4	38.5	30.4	60.6	100.0			
PXP3-4	35.8	54.3	34.1	38.1	29.7	54.2	66.1	100.0		
CWPO-C	41.6	35.9	36.9	37.3	32.4	41.7	39.4	37.9	100.0	
PtrPO2	33.5	29.4	32.0	33.2	53.9	32.4	30.7	31.4	28.7	100.0

Gene accession numbers : TPX1 (L13654), FBP1 (AF149277), ZPO-C (AB023959), ZePrx (AJ880392), TP60 (AF149251), ATP-A2 (X99952), prxA3a (Q43049),PXP3-4 (X97350), CPWPO-C (AB210901).

Table 5.5 – Summary of protein properties of PtrPOs and lignin peroxidases among plants.

Peroxidases	Species	Protein length	M.W. (kDa)	pI	Type	Reference
PtrPO2	*P. trichocarpa*	331	37	5.87	anionic	this article
prxA3a	*P. sieboldii x P. gradidentata*	347	37.1	4.44	anionic	Osakabe et al., 1994
FBP1	*Phaseolus vulgaris* L.	340	36.5	5.75	anionic	Zimmerlin et al., 1994
PXP3-4	*P. trichocarpa*	343	36.7	4.47	anionic	Christensen et al., 1998
TPX1	*Lycopersicon esculentum*	328	35.9	7.66	cationic	El Mansouri et al., 1999
ATP-A2	*Arabidopsis thaliana*	335	35	4.72	anionic	Østergaard et al., 2000
CWPO-C	*P. alba* L.	324	34.6	8.66	cationic	Aoyama et al., 2002
TP60	*Nicotiana tabacum*	326	37.2	8.89	cationic	Blee et al., 2003
Zeprx	*Zinnia elegans*	321	34.2	8.61	cationic	Gabaldón et al., 2005
ZPO-C	*Zinnia elegans*	316	34.8	8.80	cationic	Sasaki et al., 2006

A phylogenetic analysis was performed with PtrPO2 and the 73 class III peroxidases *in Arabidopsis* (AtPrxs) (**Figure 5.4**). Among the 73 class III peroxidases in *Arabidopsis*, all lignin peroxidases previously identified in *Arabidopsis* (AtPrx53, AtPrx2, AtPrx25, AtPrx71 and AtPrx72) show low amino acid identity to PtrPO2 (29.5-37.2%). Of 73 AtPrxs, PtrPO2 shows highest identity to AtPrx21 (69.3%), which is a peroxidase expressed in roots, leaves and stems. AtPrx21 had been identified in a study of abiotic or biotic stresses in *Arabidopsis*, but its role in lignification is still not defined [57, 58].

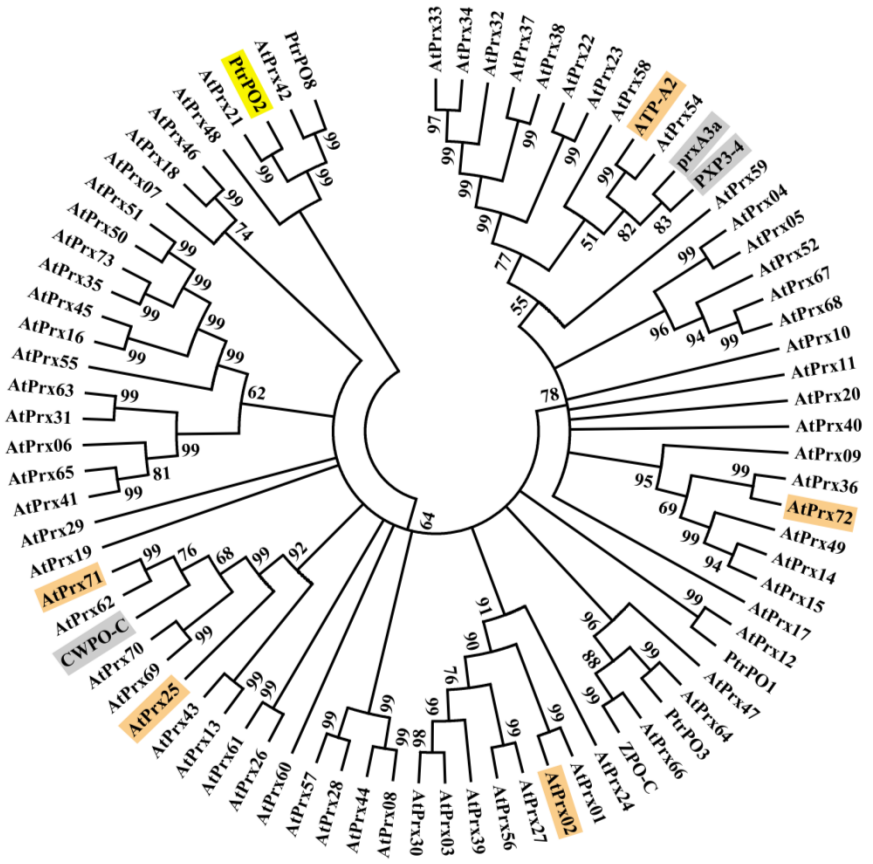

Figure 5.4 – Phylogenetic analysis between the PtrPOs, poplar lignin peroxidases (CWPO-C, prxA3a and PXP3-4), *Arabidopsis* lignin peroxidase (ATP-A2, AtPrx2, AtPrx 25, AtPrx71 and AtPrx72) and all class III peroxidases in *Arabidopsis*.

Therefore, PtrPO2 is the xylem-abundant and xylem-specific peroxidase (**Figures 5.1 and 5.2**) in *P. trichocarpa*. The amino acid sequence of PtrPO2 shows conserved structural motifs to the classic G- and S-specific lignin peroxidase (**Figure 5.3**) indicting a possible catalytic activity for both G and S subunits. PtrPO2 seems to be a unique anionic peroxidase, although it shows a relationship (53.9% identity) to a cationic lignin peroxidase TP60 in tobacco (**Tables 5.4 and 5.5**). Moreover, of 73 class III peroxidases in *Arabidopsis*, PtrPO2

shows an identity of 69.3% to the AtPrx21 (**Figure 5.4**), which is a peroxidase related to pathogen resistance. Therefore, PtrPO2 may be considered as a putative lignin peroxidase in *P. trichocarpa* and the role of PtrPO2 in lignification was studied by RNAi downregulation.

5.3.4 Downregulation of PtrPO2 in *P. trichocarpa*

A pBI121-based construct was made to overexpress the PtrPO2-RNAi under the control of a 4-coumaric acid:coenzyme A ligase (4CL) promoter (4CLp) (**Figure 5.5**). The PtrPO2 RNAi *P. trichocarpa* transgenics were generated following our protocol [107] (see Materials and Methods).

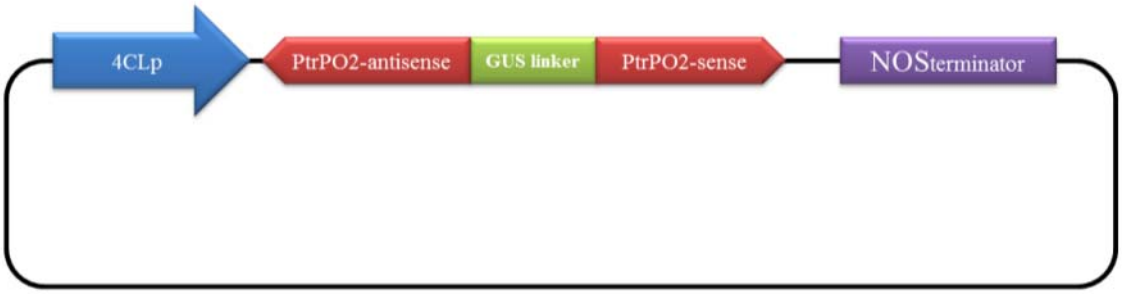

Figure 5.5 – The illustration of pBI121-based RNAi construct for downregulation of PtrPO2 in *P. trichocarpa*.

Six transgenic lines were obtained with downregulation of PtrPO2 (**Figure 5.6**). Three individual lines (PtrPO2-8, PtrPO2-9 and PtrPO2-10) were selected for further analysis.

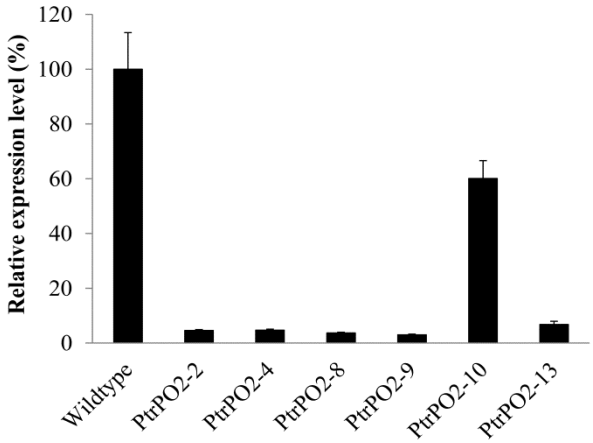

Figure 5.6 – Transcript abundance of PtrPO2 in PtrPO2 downregulated *P. trichocarpa* transgenics. Error bars represent SE of three replicates.

The specificity of the RNAi downregulation was tested using Real-time PCR. For the four most xylem-abundant class III peroxidases (PtrPO1, PtrPO2, PtrPO3 and PtrPO8) in SDX, only the transcript level of PtrPO2 was severely downregulated (**Figure 5.7**).

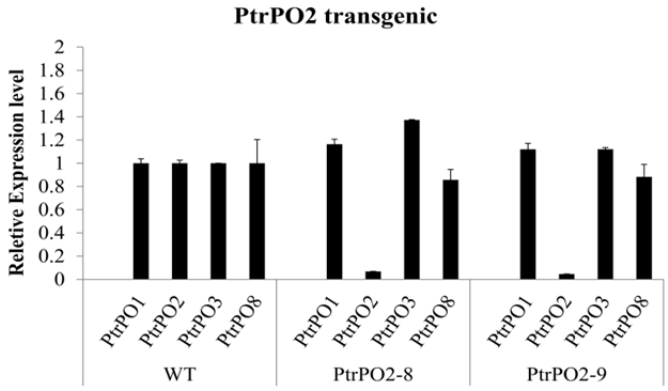

Figure 5.7 – The RNAi specificity for PtrPO2 downregulation *P. trichocarpa* transgenics. Error bars represent SE of two replicates.

5.3.5 PtrPO2 Downregulated Transgenics in *P. trichocarpa* have Reduced Growth and Reddish Internodes in the Stem Wood

Compared to the height of wildtype trees, the six-month-old PtrPO2 downregulated transgenic shows significant height reduction in the PtrPO2-8 and PtrPO2-9 transgenic lines, which have ~95% PtrPO2 transcript reduction (**Figure 5.8A**).

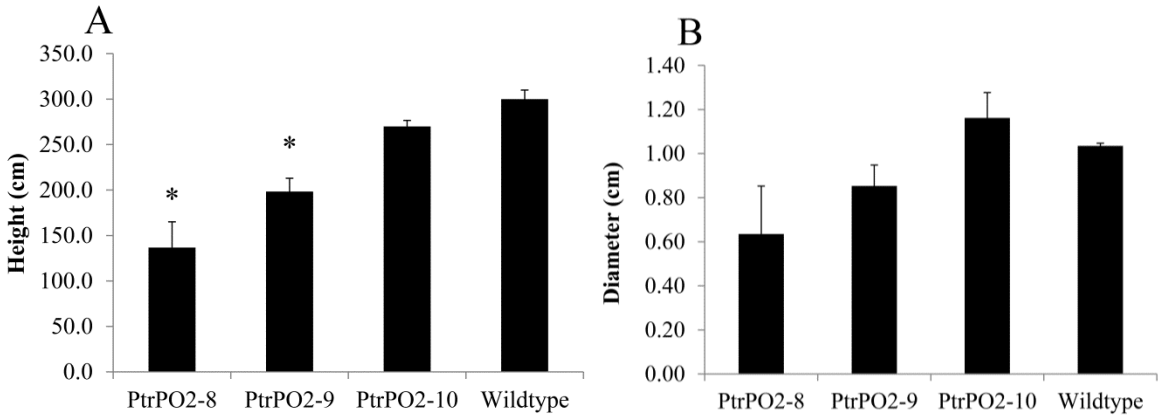

Figure 5.8 – Reduced growth phenotype in PtrPO2 downregulated *P. trichocarpa* transgenics. (**A**) Height. (**B**) Diameter. Error bars represent SE of three replicates. *, $p < 0.05$.

In addition, a pink or red internode of stem wood was observed when PtrPO2 is downregulated compared to the pale yellow color of the wildtype tree stem (**Figure 5.9D**). The PtrPO2-10 line with ~40% downregulation of PtrPO2 showed pinkish color in the stem wood (**Figure 5.9C**) and both PtrPO2-8 and PtrPO2-9 with ~95% downregulation of PtrPO2 showed reddish color (**Figures 5.9A and 5.9B**). Moreover, PtrPO2-8 and PtrPO2-9 have shorter internodes. The extractive free wood powder of the PtrPO2 downregulated

transgenics also showed brownish color compared to the pale yellow color of wildtype (**Figure 5.10**).

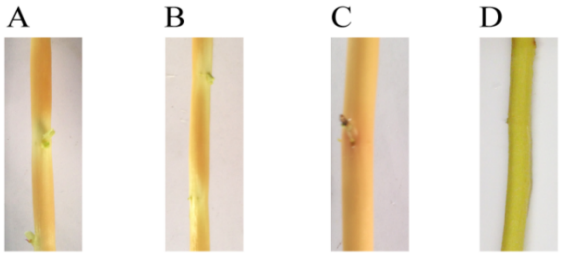

Figure 5.9 – Red internodes of stem wood in the PtrPO2 downregulated *P. trichocarpa* transgenics. (**A**) PtrPO2-8 transgenic. (**B**) PtrPO2-9 transgenic. (**C**) PtrPO2-10 transgenic. (**D**) Wildtype.

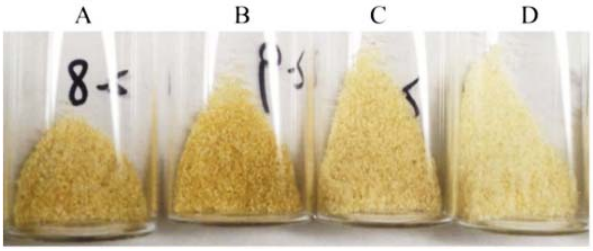

Figure 5.10 – Reddish wood powder of the PtrPO2 downregulated *P. trichocarpa* transgenics. (A) PtrPO2-8 transgenic. (B) PtrPO2-9 transgenic. (C) PtrPO2-10 transgenic. (D) Wildtype.

5.3.6 Cell Wall Component Analysis of PtrPO2 Downregulated Transgenics

To further investigate whether downregulation of PtrPO2 affects lignification and wood composition in *P. trichocarpa*, the stems of the transgenic and wildtype trees were analyzed

for lignin and carbohydrate content. Compared to the wildtype, the lignin content of the three lines, PtrPO2-8, PtrPO2-9 and PtrPO2-10, showed reduction in Klason lignin ranging from 17.8% to 23.2 % ($p < 0.001$; **Table 5.6**) and total lignin contents were also significant reduced ($p < 0.001$; **Table 5.6**) in all PtrPO2 downregulated transgenics. This result suggests PtrPO2 is important for lignification and indicates that PtrPO2 is a lignin peroxidase in *P. trichocarpa* and, in addition, xylan content was significant increased ($p < 0.005$; **Table 5.6**), where the content of mannan was significant decreased ($p < 0.05$; **Table 5.6**). Cellulose, arabinan and galactan content had no significant changes.

Table 5.6 – Cell wall composition of PtrPO2 transgenics and wildtype *P. trichocarpa*.

	Wildtype	PtrPO2-8	PtrPO2-9	PtrPO2-10	Prob > |t|
Lignin*					
Klason	16.8 ± 0.2	13.2 ± 0.1	12.9 ± 0.2	13.8 ± 0.1	**<0.001**
Acid-Soluble	3.7 ± 0.0	4.0 ± 0.2	4.0 ± 0.2	3.6 ± 0.2	0.242
Total	20.5 ± 0.2	17.2 ± 0.3	16.9 ± 0.0	17.4 ± 0.2	**<0.001**
Polysaccharide*					
Arabinan	0.8 ± 0.1	0.7 ± 0.0	0.7± 0.0	0.7 ± 0.3	0.559
Xylan	16.1 ± 0.1	17.5 ± 0.3	16.9 ± 0.1	18.0 ± 0.1	**0.003**
Mannan	2.4 ± 0.1	1.7 ± 0.0	1.7 ± 0.1	2.1 ± 0.4	**0.023**
Galactan	1.9 ± 0.3	1.4 ± 0.3	1.7 ± 0.1	2.2 ± 0.3	0.482
Glucan	46.0 ± 0.1	45.0 ± 0.1	44.9 ± 0.6	45.5 ± 0.4	0.884

*Values are means ± SE (n = 2 for lignin and polysaccharide analysis).
Prob >|t| value in bold indicates significant changes using JMP analysis ($p < 0.05$).
*Values are percentage of vacuum-dried and extractive-free wood weight

5.3.7 Mechanical Properties of the Wood of PtrPO2 Downregulated Transgenics

To examine the effect of PtrPO2 downregulation on mechanical properties, we determined the modulus of elasticity (MOE) by three point bending. MOE reveals the resistance of the stem to the pressure of bending, which estimates the elasticity of the stem. All stem wood samples from PtrPO2 downregulated transgenics showed significantly lower MOE (37-60%) than the wildtype (**Figure 5.11**), which means that the mechanical properties of PtrPO2 downregulated transgenics has significantly changed and decreased in elasticity and bending strength.

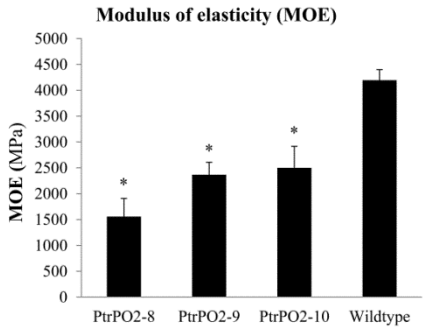

Figure 5.11 – Modulus of elasticity (MOE) of PtrPO2 downregulated transgenic stem wood. Error bars represent SE of three replicates. *, $p < 0.05$.

5.3.8 Lignin Composition Analysis of PtrPO2 Downregulated Transgenics

To determine whether the decrease in MOE results from altered lignin composition in the PtrPO2 downregulated transgenics, the lignin composition of wildtype and PtrPO2

downregulated transgenics was examined by nitrobenzene oxidation. In wildtype, the ratio of syringyl (S) to guaiacyl (G) subunits is 2.1, and with trace amounts (0.5%) of 4-hydroxyphenyl (H) subunits (**Table 5.7**). The S subunits are represented by the sum of syringaldehyde and syringic acid, and where the sum of vanillin and vanillic acid represents the G subunits. In line 10 with ~40% downregulation of PtrPO2, the S subunits were reduced by 10.1%, while the G subunit content was similar to wildtype. In the severe PtrPO2 downregulated transgenic lines (PtrPO2-8 and PtrPO2-9), S subunits were reduced by 20% and G subunits were decreased around 10 % (**Table 5.7**). Moreover, H subunits increased ~3-fold in PtrPO2 downregulated transgenics (**Table 5.7**).

Table 5.7 – Lignin composition of PtrPO2 transgenics and wildtype *P. trichocarpa*.

Molar ratio %*	Wildtype	PtrPO2-8	PtrPO2-9	PtrPO2-10
4-Hydroxybenzaldehyde	0.5 ± 0.0	1.4 ± 0.0	1.6 ± 0.0	1.7 ± 0.0
4-Hydroxybenzoic acid	—	—	—	—
Vanillin	14.9 ± 0.7	12.5 ± 0.2	12.4 ± 0.2	14.5 ± 0.7
Vanillic acid	1.8 ± 0.1	2.4 ± 0.2	2.7 ± 0.2	2.0 ± 0.1
Syringaldehyde	29.5 ± 1.6	23.4 ± 0.4	24.5 ± 0.0	27.3 ± 1.2
Syringic acid	5.1 ± 0.0	3.7 ± 0.1	4.0 ± 0.0	3.8 ± 0.0
H†	0.5 ± 0.0	1.4 ± 0.0	1.6 ± 0.0	1.7 ± 0.0
V‡	16.7 ± 0.0	14.9 ± 0.5	15.1 ± 0.5	16.5 ± 1.0
S§	34.5 ±1.6	27.2 ± 0.4	28.5 ± 0.0	31.1 ± 1.2
S/V ratio	2.1 ± 0.0	1.8 ± 0.0	1.9 ± 0.0	1.9 ± 0.0
H/V ratio	0.04 ± 0.00	0.13 ± 0.00	0.14 ± 0.00	0.14 ± 0.00

—, below detection limits.
*Results are means ± SE (n = 2), assuming that lignin's C9 molecular mass is 210 g/mole.
†Sum of 4-hydroxybenzaldehyde and 4-hydroxybenzoic acid.
‡Sum of vanillin and vanillic acid
§Sum of syringaldehyde and syringic acid.

5.3.9 Differentially Expressed Gene (DEG) Analysis of the PtrPO2 Downregulated Transgenics

Because functional redundancy is expected among the class III peroxidase and laccase families in *P. trichocarpa*, we performed transcriptome analysis to identify any differentially expressed oxidases (peroxidases or laccases) in PtrPO2 downregulated transgenics, which may compensate for the reduction of PtrPO2. Besides the significant downregulation of PtrPO2, only one of the 42 xylem-abundant class III peroxidases, PtPrx35, was found with significant overexpression (**Table 5.8**). None of the laccases had significant expression changes in all PtrPO2 downregulated transgenics (**Table 5.9**). For monolignol biosynthesis, of the 21 monolignol biosynthetic enzymes, PtrPAL3 shows higher expression in all PtrPO2 downregulated transgenic lines (**Table 5.10**).

Table 5.8 – Expression of the xylem-abundant *P. trichocarpa* peroxidases in PtrPO2 downregulated transgenics

Gene	Accession number	Log_2FC (PtrPO2-8)	FDR (PtrPO2-8)	Log_2FC (PtrPO2-9)	FDR (PtrPO2-9)	Log_2FC (PtrPO2-10)	FDR (PtrPO2-10)
PtrPO1	POPTR_0005s21740	-0.4	0.99	-0.2	1.00	-0.3	1.00
PtrPO2	POPTR_0006s13190	-5.1	**<0.01**	-5.6	**<0.01**	-1.7	**<0.01**
PtrPO3	POPTR_0005s11070	0.0	1.00	0.3	0.91	-0.1	1.00
PtrPO8	POPTR_0004s01510	0.3	1.00	0.6	0.33	0.3	1.00
PtPrx01	POPTR_0003s21640	-0.3	1.00	-0.2	1.00	-0.1	1.00
PtPrx03	POPTR_0001s05050	0.2	1.00	0.4	1.00	-2.2	**0.02**
PtPrx04	POPTR_0004s14240	0.3	0.98	0.9	**0.01**	0.7	0.11
PtPrx07	POPTR_0004s05140	-0.8	0.93	-0.4	1.00	-0.4	1.00
PtPrx15	POPTR_0010s04550	0.9	1.00	-1.5	1.00	0.7	1.00
PtPrx18	POPTR_0001s34660	-1.1	0.21	-0.6	0.56	-1.2	**0.02**
PtPrx19	POPTR_0001s18270	-1.8	0.30	-1.5	0.18	-2.1	**0.04**
PtPrx22	POPTR_0001s04850	-2.9	0.37	-0.7	1.00	-1.8	0.44
PtPrx25	POPTR_0017s06570	1.5	0.26	1.9	**0.03**	0.5	1.00
PtPrx26	POPTR_0017s06550	0.0	1.00	-0.1	1.00	-0.3	1.00
PtPrx27	POPTR_0007s02580	0.1	1.00	0.7	0.95	-0.4	1.00
PtPrx30	POPTR_0007s13420	2.4	**<0.01**	0.6	0.97	-0.6	1.00
PtPrx33	POPTR_0001s04820	-0.1	1.00	0.6	1.00	-1.9	0.69
PtPrx35	POPTR_0007s05100	1.4	**<0.01**	1.3	**<0.01**	2.4	**<0.01**
PtPrx37	POPTR_0007s01580	-0.2	1.00	-0.2	1.00	0.0	1.00
PtPrx41	POPTR_0013s15250	-0.6	1.00	0.6	0.94	-0.2	1.00
PtPrx47	POPTR_0010s24340	-0.1	1.00	-1.6	1.00	1.4	1.00
PtPrx50	POPTR_0018s13150	-0.8	1.00	-0.7	1.00	-1.6	0.87
PtPrx57	POPTR_0005s21750	0.1	1.00	0.1	1.00	-1.3	0.33
PtPrx58	POPTR_0005s14190	-4.7	0.97	0.4	1.00	-0.5	1.00
PtPrx59	POPTR_0005s07390	-0.5	0.80	-0.1	1.00	-0.1	1.00
PtPrx60	POPTR_0019s00340	-0.7	0.51	-0.5	0.50	-0.2	1.00
PtPrx64	POPTR_0011s06080	-0.3	1.00	-0.2	1.00	0.1	1.00
PtPrx65	POPTR_0002s01960	-0.7	1.00	-0.1	1.00	-2.1	**0.02**
PtPrx66	POPTR_0002s03260	0.1	1.00	-2.7	0.69	-2.5	0.78
PtPrx67	POPTR_0002s06590	0.4	1.00	0.6	1.00	-1.8	0.28
PtPrx70	POPTR_0004s15200	-0.3	1.00	0.1	1.00	-0.2	1.00
PtPrx72	POPTR_0149s00200	-3.2	1.00	1.8	0.93	0.9	1.00
PtPrx73	POPTR_0016s14030	-0.8	1.00	0.7	1.00	-1.1	1.00
PtPrx76	POPTR_0466s00210	0.3	1.00	-1.5	1.00	0.7	1.00
PtPrx78	POPTR_0006s06890	0.1	1.00	1.9	0.32	1.0	1.00
PtPrx79	POPTR_0006s28320	-0.7	1.00	-1.1	0.95	-0.9	1.00
PtPrx82	POPTR_0017s09640	-3.2	1.00	-3.2	1.00	-3.2	1.00
PtPrx83	POPTR_0001s02870	0.0	1.00	0.3	1.00	0.8	0.59
PtPrx94	POPTR_0007s10040	0.4	1.00	-0.2	1.00	0.0	1.00
PtPrx98	POPTR_0003s21620	0.2	1.00	0.5	1.00	-0.4	1.00
PtPrx99	POPTR_0001s04840	0.1	1.00	0.4	1.00	-1.1	1.00
PtPrx100	POPTR_0001s04870	-2.8	0.84	-1.1	1.00	-5.9	0.11
PtPrx[P]26	POPTR_0017s06560	-0.5	1.00	-0.1	1.00	-0.4	1.00
PtPrx[P]54	POPTR_0014s13100	-1.1	1.00	-1.0	0.85	-0.1	1.00

FC, fold change. False discovery rate (FDR) <0.05 are in bold.

Table 5.9 – Expression of the *P. trichocarpa* laccases in PtrPO2 downregulated transgenics

Gene	Accession number	Log_2FC (PtrPO2-8)	FDR (PtrPO2-8)	Log_2FC (PtrPO2-9)	FDR (PtrPO2-9)	Log_2FC (PtrPO2-10)	FDR (PtrPO2-10)
PtrLAC01	POPTR_0001s14010	-1.2	0.498	-0.8	0.621	-0.6	0.947
PtrLAC02	POPTR_0001s18500	-0.5	1.000	-0.7	0.629	-0.4	1.000
PtrLAC03	POPTR_0001s21380	0.0	1.000	0.0	1.000	0.0	1.000
PtrLAC04	POPTR_0001s25580	0.6	0.925	0.5	0.881	0.9	0.335
PtrLAC05	POPTR_0001s35740	1.1	0.374	0.3	1.000	1.5	**<0.05**
PtrLAC06	POPTR_0001s41160	1.3	0.263	0.7	0.812	-0.1	1.000
PtrLAC07	POPTR_0001s41170	0.2	1.000	0.1	1.000	0.1	1.000
PtrLAC08	POPTR_0004s16370	0.4	1.000	1.1	0.638	0.5	1.000
PtrLAC09	POPTR_0005s22240	3.1	1.000	0.0	1.000	0.0	1.000
PtrLAC10	POPTR_0005s22250	0.0	1.000	0.0	1.000	2.3	1.000
PtrLAC11	POPTR_0006s08740	-0.3	1.000	-0.5	0.589	-0.3	1.000
PtrLAC12	POPTR_0006s08780	0.4	1.000	-0.1	1.000	0.1	1.000
PtrLAC13	POPTR_0006s09520	0.0	1.000	0.0	1.000	0.0	1.000
PtrLAC14	POPTR_0006s09830	0.4	0.918	0.1	1.000	0.2	1.000
PtrLAC15	POPTR_0006s09840	0.3	1.000	0.1	1.000	0.2	1.000
PtrLAC16	POPTR_0007s13050	0.7	0.286	1.0	**<0.05**	0.5	0.617
PtrLAC17	POPTR_0008s06430	0.5	0.774	0.1	1.000	0.3	1.000
PtrLAC18	POPTR_0008s07370	-0.3	1.000	-0.5	0.767	-0.2	1.000
PtrLAC19	POPTR_0008s07380	-0.2	1.000	-0.2	1.000	-0.3	1.000
PtrLAC20	POPTR_0009s03940	0.7	0.312	0.2	1.000	0.1	1.000
PtrLAC21	POPTR_0009s04720	-0.2	1.000	-0.6	0.617	-1.3	**<0.05**
PtrLAC22	POPTR_0009s10550	-0.1	1.000	0.2	1.000	0.0	1.000
PtrLAC23	POPTR_0009s15840	-0.5	1.000	-0.8	0.364	-0.5	0.888
PtrLAC24	POPTR_0009s15860	-0.6	0.940	-0.9	0.298	-0.6	0.809
PtrLAC25	POPTR_0010s19080	-1.1	0.086	-0.8	0.111	-1.2	**<0.05**
PtrLAC26	POPTR_0010s19090	0.0	1.000	-0.1	1.000	0.1	1.000
PtrLAC27	POPTR_0010s20050	-0.1	1.000	-0.3	1.000	-0.1	1.000
PtrLAC28	POPTR_0011s06880	-2.3	1.000	-0.1	1.000	0.0	1.000
PtrLAC29	POPTR_0011s12090	-0.5	0.785	-0.5	0.363	-0.4	0.643
PtrLAC30	POPTR_0011s12100	-0.4	0.829	-0.2	1.000	-0.2	1.000
PtrLAC31	POPTR_0012s04620	-2.3	1.000	-2.4	1.000	-2.3	1.000
PtrLAC32	POPTR_0013s14890	-0.4	1.000	1.2	0.977	-0.7	1.000
PtrLAC33	POPTR_0014s09610	-0.3	1.000	0.0	1.000	-0.8	0.536
PtrLAC34	POPTR_0015s04340	0.0	1.000	0.0	1.000	0.0	1.000
PtrLAC35	POPTR_0015s04350	0.0	1.000	0.0	1.000	0.0	1.000
PtrLAC36	POPTR_0015s04370	-0.1	1.000	-0.1	1.000	0.0	1.000
PtrLAC37	POPTR_0016s11500	0.0	1.000	2.2	1.000	0.0	1.000
PtrLAC38	POPTR_0016s11520	0.0	1.000	0.0	1.000	0.0	1.000
PtrLAC39	POPTR_0016s11540	0.0	1.000	0.0	1.000	0.0	1.000
PtrLAC40	POPTR_0016s11950	-0.4	0.965	-0.8	0.095	-0.7	0.161
PtrLAC41	POPTR_0016s11960	0.6	0.699	-0.1	1.000	-0.1	1.000
PtrLAC42	POPTR_0019s11810	-1.8	0.561	0.4	1.000	-1.4	0.477
PtrLAC43	POPTR_0019s11820	-2.5	0.301	0.5	1.000	-1.8	0.278
PtrLAC44	POPTR_0019s11830	-1.0	1.000	0.7	0.945	-1.1	0.769
PtrLAC45	POPTR_0019s11850	-0.4	1.000	0.3	1.000	-2.0	0.224
PtrLAC46	POPTR_0019s11860	-0.6	1.000	0.4	1.000	-0.7	1.000
PtrLAC47	POPTR_0019s14530	0.4	1.000	0.6	0.427	0.6	0.523
PtrLAC48	POPTR_0091s00270	0.0	1.000	0.0	1.000	0.0	1.000
PtrLAC49	POPTR_0958s00200	0.4	0.933	0.1	1.000	0.2	1.000

FC, fold change. False discovery rate (FDR) < 0.05 are in bold.

Table 5.10 – Expression of the *P. trichocarpa* monolignol biosynthetic genes in PtrPO2 downregulated transgenics

Gene	Accession number	Log_2FC (PtrPO2-8)	FDR (PtrPO2-8)	Log_2FC (PtrPO2-9)	FDR (PtrPO2-9)	Log_2FC (PtrPO2-10)	FDR (PtrPO2-10)
PtrPAL1	POPTR_0006s12870	1.2	**<0.01**	0.8	0.06	1.5	**<0.01**
PtrPAL2	POPTR_0008s03810	0.8	0.19	0.4	0.64	0.9	0.05
PtrPAL3	POPTR_0016s09230	1.2	**<0.01**	0.9	**<0.01**	1.4	**<0.01**
PtrPAL4	POPTR_0010s23100	0.7	0.33	0.3	0.93	0.8	0.09
PtrPAL5	POPTR_0010s23110	0.6	0.57	0.3	1.00	0.8	0.11
PtrC3H3	POPTR_0006s03180	0.5	0.62	0.3	0.93	0.7	0.18
PtrC4H1	POPTR_0013s15380	0.6	0.62	0.1	1.00	0.8	0.28
PtrC4H2	POPTR_0019s15110	0.4	0.98	0.2	1.00	0.8	0.12
Ptr4CL3	POPTR_0001s07400	-0.3	1.00	-0.6	0.40	-6.8	**<0.01**
Ptr4CL5	POPTR_0003s18720	-0.3	1.00	-1.0	**0.01**	0.7	0.16
PtrHCT1	POPTR_0003s18210	0.3	0.97	0.0	1.00	0.5	0.57
PtrHCT6	POPTR_0001s03440	0.9	0.08	0.5	0.59	1.0	**0.01**
PtrCCoAOMT1	POPTR_0009s10270	0.4	0.97	0.0	1.00	0.5	0.76
PtrCCoAOMT2	POPTR_0001s31220	0.5	0.79	0.4	0.83	0.8	0.19
PtrCCoAOMT3	POPTR_0008s13600	0.3	1.00	0.0	1.00	0.4	0.84
PtrCOMT2	POPTR_0012s00670	0.3	1.00	-0.1	1.00	0.3	1.00
PtrCAld5H1	POPTR_0005s11950	0.3	1.00	-0.5	0.85	0.2	1.00
PtrCAld5H2	POPTR_0007s13720	0.4	1.00	0.1	1.00	0.6	0.51
PtrCCR2	POPTR_0003s17980	0.7	0.26	0.4	0.77	0.7	0.12
PtrCAD1	POPTR_0009s09870	0.4	0.84	-0.1	1.00	0.5	0.51
PtrCAD2	POPTR_0016s07910	0.2	1.00	0.1	1.00	-0.5	0.83

FC, fold change. False discovery rate (FDR) < 0.05 are in bold.

5.4 Discussion

Class III peroxidases have been considered to play important roles in lignification. Because of the large gene family of the class III peroxidases in higher plants, it is difficult to identify the peroxidases involved in lignification due to functional redundancy. Nevertheless, isolation of cationic (basic) or anionic (acidic) peroxidases from plant cell walls or plant

suspension cells had identified some lignin peroxidases [40, 64, 70, 71, 74, 81, 89]. Recently, using computational and structural simulation, several *Arabidopsis* class III peroxidases, had also been identified and validated using *Arabidopsis* mutants [56, 66-68, 117, 118]. However, in woody plants such as poplar, the identity of lignin peroxidases was still not conclusive [93, 95, 96]. Identification of lignin peroxidases in *P. trichocarpa* is important to understand the whole monolignol biosynthetic pathway in a woody plant and to design better strategies to reduce recalcitrance of biomass.

Here, we identified PtrPO2 as a unique lignin peroxidase in *P. trichocarpa*. Using transcriptome analysis, PtrPO2 is the most xylem-abundant and the xylem-specific peroxidase among 42 detectable class III peroxidases in the secondary differentiating xylem (SDX) tissue of *P. trichocarpa* (**Figure 5.2**). Downregulation of the PtrPO2 showed reduced growth (**Figure 5.8**) and red internode of stem phenotype (**Figure 5.9**). Moreover, lignin content was significant decreased by ~20% and xylan and mannan content were significant increased (**Table 5.6**). The change in wood composition in PtrPO2 downregulated transgenics is similar to Ptr-mir397 transgenic with downregulation of laccases [110]. Also, the decreased MOE values of the PtrPO2 downregulated transgenic lines indicate the reduced stiffness and bending strength of stem (**Figure 5.11**), which may result from the lignin reduction. In addition, one peroxidase, the PtPrx35, showed significant overexpression in all PtrPO2 downregulated transgenic lines, which suggests a role in lignification and functional redundancy among class III peroxidase family, but further experiments are require to validate

this hypothesis.

5.4.1 PtrPO2 is an Unusual Peroxidase Involved in Lignification

Identification of peroxidases with high amino acid identity to other lignin peroxidase among plant species recently had led to the discovery of the new lignin peroxidases [67, 117, 118]. For example: lignin peroxidases in *Arabidopsis,* the AtPrx2, AtPrx25 and AtPrx71 are homologues of CWPO-C, AtPrx66, AtPrx47 and AtPrx64 are homologues of ZPO-C and AtPrx72 is the homologue of ZePrx. However, PtrPO2 is a unique peroxidase because the low amino acid identity between PtrPO2 and other lignin peroxidases in several plants (**Tables 5.4 and 5.5**).

PtrPO2 showed 30% amino acid identity to most plant lignin peroxidases, except a higher identity with TP60 in tobacco (**Table 5.4**). Although PtrPO2 shows 53.9% of amino acid identity with TP60, PtrPO2 is anionic peroxidase, which is different from TP60, the cationic peroxidase (**Table 5.5**). In an early study of peroxidases, anionic peroxidases were considered the main contribution to the cell wall peroxidase activity and to lignification because their high affinity to the lignin precursors, where cationic peroxidases were implicated in auxin catabolism [36, 80, 119, 120]. Recent studies on recombinant peroxidases reveal both cationic and anionic peroxidases are capable to oxidize coniferyl alcohol or sinapyl alcohol but with different preferences. For example, the anionic peroxidase, ATP-A2, prefers coniferyl alcohol [39, 66] and cationic peroxidases, the ZePrx and CWPO-C, prefer

sinapyl alcohol [40, 76-80]. In addition, ZPO-C, a cationic peroxidase, shows activity for sinapyl alcohol as well as coniferyl alcohol [70] and the anionic peroxidases, PXP3-4 and TPX1, show syringaldazine-oxidizing activity [61, 74, 75]. In fact, the closest homolog of TP60 in *P. trichocarpa* is PtrPO8 (POPTR_0004s01510), which has 80.7% amino acid identity and is also a cationic peroxidase with pI value of 7.73. However, the PtrPO8 downregulated *P. trichocarpa* did not observe reduction in lignin content.

PtrPO2 is distinct from previously identified poplar peroxidases, the PXP3-4, prxA3a and CWPO-C (**Table 5.4**). Among the 90 class III peroxidases, PXP3-4 shows highest identity to PtPrx03 (POPTR_0001s05050), prxA3a has highest identity to PtPrx98 (POPTR_0003s21620) and PtPrx75 (POPTR_0016s13280) is the closest homolog to CWPO-C. However, PtPrx03, PtPrx98 and PtPrx75 were excluded in this study because they are not xylem-abundant or xylem-specific in *P. trichocarpa*.

5.4.2 PtrPO2 Possesses Similar Structural motifs to G- and S-Specific Peroxidases

Anionic peroxidase ATP-A2 is a well-studied G-specific peroxidase. The amino acids P69, I138, P139, S140, and R175 were identified as key determinants of the conformation and hydrophobicity of the ATP-A2 substrate-binding site [39]. The oxidation of sinapyl alcohol is thought to be sterically hindered owing to unfavorable hydrophobic interactions between the sinapyl alcohol methoxy atoms and the conserved I138 and P139 residues at the substrate binding site [39]. PtrPO2 has conserved the I138 and P139 residues, which indicate

that PtrPO2 may prefer coniferyl alcohol, as a G-specific peroxidase (2nd red box in **Figure 5.3**). However, PtrPO2 has the motif of VSCAD, which is considered characteristic of an S peroxidase, where G peroxidases have a motif of VSCSD (green box in **Figure 5.3**) [116, 121]. Therefore, PtrPO2 has characteristics of both G and S peroxidases, which may explain why both G and S subunit content are decreased in PtrPO2 downregulated transgenics (**Table 5.7**).

5.4.3 Reddish Internode of Stem in PtrPO2 Downregulated Transgenics

A reddish stem wood has been identified in mutant or transgenic plants when the monolignol biosynthetic pathway is disturbed. The most prominent reddish stem phenotype is observed when cinnamyl alcohol dehydrogenase (CAD) is downregulated or silenced in maize (*bm*) and sorghum (*bmr*) mutant [122-125], tobacco [126, 127], poplar [128] pine [129-132] and *Arabidopsis* [133]. In addition to CAD, the reddish color of stems are also observed in mutant or transgenics with reduced activity of 4CL [134, 135], caffeic acid *O*-methyltransferase (COMT) [136], cinnamoyl-CoA reductase (CCR) [137] or caffeoyl-coenzyme A-*O*-methyltransferase (CCOAOMT) [138]. The reddish coloration had been studied and considered as the result from the polymerization of the hydroxycinnamaldehydes in the transgenics to synthesize the wine-red dehydrogenation polymer in lignin [126, 139], or incorporation of novel monolignol monomers [140].

In this study, the reddish color of the stem internode is observed when PtrPO2 is downregulated (**Figure 5.9**). This reddish phenotype in the PtrPO2 downregulated transgenics has not been reported for a lignin peroxidase in downregulated plants. The reddish coloration of stem may also be a consequence of the involvement of lignin polymerization in *P. trichocarpa* [134].

5.4.4 The Role of Peroxidases and Laccases in Lignin Polymerization

In the early studies, the role of peroxidase was considered to be more likely than laccase in the lignification because of the lack of detection of laccase activity in some plants [18, 59], lignification requires the presence of hydrogen peroxide [141] and downregulation of laccase in *P. trichocarpa* transgenics showed no change in lignin content [142]. Moreover, peroxidase has far higher specific activities towards phenolic compounds examined compared to laccase [143].

However, laccase in lignification was re-emphasized in 1983 because the improved procedures for identification of laccase in *Acer pseudoplatanus* [21, 144], but laccase was still suggested to involved only in the early stages of lignification. Later on, laccase activity was detected and correlated with lignification in plants [22, 23, 31, 145-149]. In *Arabidopsis*, a triple mutant of LAC4, LAC11 and LAC17 have completely abolished lignin deposition and arrested plant growth [150].

In *P. trichocarpa*, overexpression of the microRNA (Ptr-mirRNA397) can downregulate 17 PtrLACs and reduced Klason lignin content up to 22% [110]. In this study, we provided additional evidence that a peroxidase PtrPO2 can affect lignin content in *P. trichocarpa*. Therefore, both peroxidases and laccases should be considered important for lignification in *P. trichocarpa*.

5.4.5 Transcriptome Analysis of PtrPO2 Downregulated Transgenics

Because of the large number of number of the class III transgenic, in this study, we performed the transcriptome analysis to reveal the putative oxidase that may also involve in lignification. We successfully identify the PtrPO2 as the xylem-abundant and xylem-specific class III peroxidase among 101 class III peroxidase in *P. trichocarpa*. Manipulation of the PtrPO2 expression in *P. trichocarpa* can affect lignin content, which suggests PtrPO2 is a lignin peroxidase. Moreover, because functional redundancy is believed to exist among class III peroxidase, we also performed transcriptome analysis to identify the differential expressed peroxidase when PtrPO2 is downregulated. In PtrPO2 downregulated transgenics, an overexpression of PtPrx35 was observed (**Table 5.8**). So far, the function of PtPrx35 is still unknown in *P. trichocarpa*. None of the laccases have significant expression change when PtrPO2 was downregulated (**Table 5.9**), which indicates the specific role of PtrPO2 in lignification. Although PtrPAL3 shows a higher expression in all PtrPO2 downregulated transgenic lines (**Table 5.10**), the role of PtrPAL3 in stem wood forming tissue is less

important than subgroup A of the five PAL genes (PtrPAL2, 4 and 5) [151], which has no significant changed in the PtrPO2 downregulated transgenics.

5.5 References

1. Lockhart, J., *Breaking down the complex regulatory web underlying lignin biosynthesis.* The Plant cell, 2013. **25**(11): p. 4282.

2. Fry, W. and J. White, *Big trees. Palo Alto*, 1938, CA: Stanford Univ. Press.

3. Sarkanen, K.V.L.C.H., *Lignins: occurrence, formation, structure and reactions*1971, New York: Wiley-Interscience. p. 95-163.

4. Vance, C., T. Kirk, and R. Sherwood, *Lignification as a mechanism of disease resistance.* Annual review of phytopathology, 1980. **18**(1): p. 259-288.

5. Carder, A., *Forest giants of the world, past and present.* 1994.

6. Koch, G.W., et al., *The limits to tree height.* Nature, 2004. **428**(6985): p. 851-4.

7. Novaes, E., et al., *Lignin and biomass: a negative correlation for wood formation and lignin content in trees.* Plant Physiol, 2010. **154**(2): p. 555-61.

8. Hu, W.J., et al., *Repression of lignin biosynthesis promotes cellulose accumulation and growth in transgenic trees.* Nat Biotechnol, 1999. **17**(8): p. 808-12.

9. Eckardt, N.A., *Probing the mysteries of lignin biosynthesis: the crystal structure of caffeic acid/5-hydroxyferulic acid 3/5-O-methyltransferase provides new insights.* Plant Cell, 2002. **14**(6): p. 1185-9.

10. Chen, F. and R.A. Dixon, *Lignin modification improves fermentable sugar yields for biofuel production.* Nat Biotechnol, 2007. **25**(7): p. 759-61.

11. Studer, M.H., et al., *Lignin content in natural Populus variants affects sugar release.* Proceedings of the National Academy of Sciences of the United States of America, 2011. **108**(15): p. 6300-5.

12. Li, L., et al., *Combinatorial modification of multiple lignin traits in trees through multigene cotransformation.* Proceedings of the National Academy of Sciences of the United States of America, 2003. **100**(8): p. 4939-44.

13. Chen, F. and R.A. Dixon, *Lignin modification improves fermentable sugar yields for biofuel production.* Nat Biotech, 2007. **25**(7): p. 759-761.

14. Higuchi, T., *Biochemistry and molecular biology of wood*1997, Berlin; New York: Springer.

15. Erdtman, H., *Dehydrierungen in der Coniferylreihe. II. Dehydrodi-isoeugenol.* Justus Liebigs Annalen der Chemie, 1933. **503**(1): p. 283-294.

16. Freudenberg, K., *Biosynthesis and constitution of lignin.* Nature, 1959. **183**(4669): p. 1152-5.

17. Freudenberg, K., *Lignin: Its Constitution and Formation from p-Hydroxycinnamyl Alcohols: Lignin is duplicated by dehydrogenation of these alcohols; intermediates explain formation and structure.* Science, 1965. **148**(3670): p. 595-600.

18. Harkin, J.M. and J.R. Obst, *Lignification in Trees: Indication of Exclusive Peroxidase Participation.* Science, 1973. **180**(4083): p. 296-298.

19. Adler, E., *Lignin chemistry—past, present and future.* Wood Science and Technology, 1977. **11**(3): p. 169-218.

20. Higuchi, T., *Biosynthesis of lignin.* Biosynthesis and biodegradation of wood components, 1985: p. 141-160.

21. Sterjiades, R., J.F. Dean, and K.E. Eriksson, *Laccase from Sycamore Maple (Acer pseudoplatanus) Polymerizes Monolignols.* Plant physiology, 1992. **99**(3): p. 1162-8.

22. O'Malley, D.M., et al., *The role of of laccase in lignification.* The Plant Journal, 1993. **4**(5): p. 751-757.

23. Bao, W., et al., *A laccase associated with lignification in loblolly pine xylem.* Science, 1993. **260**(5108): p. 672-4.

24. Takahama, U., *Oxidation of hydroxycinnamic acid and hydroxycinnamyl alcohol derivatives by laccase and peroxidase. Interactions among p-hydroxyphenyl, guaiacyl and syringyl groups during the oxidation reactions.* Physiologia plantarum, 1995. **93**(1): p. 61-68.

25. Richardson, A., D. Stewart, and G.J. McDougall, *Identification and partial characterization of a coniferyl alcohol oxidase from lignifying xylem of Sitka spruce (Picea sitchensis).* Planta, 1997. **203**(1): p. 35-43.

26. Ros Barcelo, A., *Lignification in plant cell walls.* International review of cytology, 1997. **176**: p. 87-132.

27. Hatfield, R. and W. Vermerris, *Lignin formation in plants. The dilemma of linkage specificity.* Plant physiology, 2001. **126**(4): p. 1351-7.

28. Ralph, J., et al., *Lignins: natural polymers from oxidative coupling of 4-hydroxyphenyl-propanoids.* Phytochemistry Reviews, 2004. **3**(1-2): p. 29-60.

29. Davin, L.B., et al., *Dissection of lignin macromolecular configuration and assembly: comparison to related biochemical processes in allyl/propenyl phenol and lignan biosynthesis.* Natural product reports, 2008. **25**(6): p. 1015-90.

30. Weng, J.-K., et al., *Emerging strategies of lignin engineering and degradation for cellulosic biofuel production.* Current opinion in biotechnology, 2008. **19**(2): p. 166-172.

31. Dean, J.F.D. and E.K.L. Eriksson, *Laccase and the Deposition of Lignin in Vascular Plants*, in *Holzforschung - International Journal of the Biology, Chemistry, Physics and Technology of Wood*1994. p. 21.

32. Koua, D., et al., *PeroxiBase: a database with new tools for peroxidase family classification.* Nucleic Acids Res, 2009. **37**(Database issue): p. D261-6.

33. Sharma, P. and R.S. Dubey, *Ascorbate peroxidase from rice seedlings: properties of enzyme isoforms, effects of stresses and protective roles of osmolytes.* Plant Science, 2004. **167**(3): p. 541-550.

34. Passardi, F., et al., *The class III peroxidase multigenic family in rice and its evolution in land plants.* Phytochemistry, 2004. **65**(13): p. 1879-93.

35. Barceló, A.R., et al., *Basic peroxidases: The gateway for lignin evolution?* Phytochemistry Reviews, 2004. **3**(1-2): p. 61-78.

36. Campa, A., *Biological roles of plant peroxidases: known and potential function.* Peroxidases in chemistry and biology, 1991. **2**: p. 25-50.

37. Matsui, T., et al., *Activity of the C-terminal-dependent vacuolar sorting signal of horseradish peroxidase C1a is enhanced by its secondary structure.* Plant & cell physiology, 2011. **52**(2): p. 413-20.

38. Ren, L.-L., et al., *Subcellular Relocalization and Positive Selection Play Key Roles in the Retention of Duplicate Genes of Populus Class III Peroxidase Family.* The Plant Cell Online, 2014.

39. Ostergaard, L., et al., *Arabidopsis ATP A2 peroxidase. Expression and high-resolution structure of a plant peroxidase with implications for lignification.* Plant Molecular Biology, 2000. **44**(2): p. 231-43.

40. Gabaldon, C., et al., *Cloning and molecular characterization of the basic peroxidase isoenzyme from Zinnia elegans, an enzyme involved in lignin biosynthesis.* Plant Physiol, 2005. **139**(3): p. 1138-54.

41. Bindschedler, L.V., et al., *Peroxidase-dependent apoplastic oxidative burst in Arabidopsis required for pathogen resistance.* The Plant journal : for cell and molecular biology, 2006. **47**(6): p. 851-63.

42. Lovrekovich, L., H. Lovrekovich, and M.A. Stahmann, *Tobacco mosaic virus-induced resistance to Pseudomonas tabaci in tobacco.* Phytopathology, 1968. **58**(7): p. 1034-5.

43. Fry, S.C., *Cross-Linking of Matrix Polymers in the Growing Cell-Walls of Angiosperms.* Annual Review of Plant Physiology and Plant Molecular Biology, 1986. **37**: p. 165-186.

44. Espelie, K.E. and P.E. Kolattukudy, *Purification and characterization of an abscisic acid-inducible anionic peroxidase associated with suberization in potato (Solanum tuberosum).* Arch Biochem Biophys, 1985. **240**(2): p. 539-45.

45. Abeles, F.B., et al., *Induction of 33-kD and 60-kD Peroxidases during Ethylene-Induced Senescence of Cucumber Cotyledons.* Plant Physiology, 1988. **87**(3): p. 609-15.

46. Lagrimini, L.M., et al., *The consequence of peroxidase overexpression in transgenic plants on root growth and development.* Plant Molecular Biology, 1997. **33**(5): p. 887-895.

47. Whetten, R.W., J.J. MacKay, and R.R. Sederoff, *Recent Advances in Understanding Lignin Biosynthesis.* Annu Rev Plant Physiol Plant Mol Biol, 1998. **49**: p. 585-609.

48. Amaya, I., et al., *Improved germination under osmotic stress of tobacco plants overexpressing a cell wall peroxidase.* FEBS Lett, 1999. **457**(1): p. 80-4.

49. Llorente, F., et al., *A novel cold-inducible gene from Arabidopsis, RCI3, encodes a peroxidase that constitutes a component for stress tolerance.* Plant J, 2002. **32**(1): p. 13-24.

50. Bernards, M.S.D.R.F., *Oxidases, peroxidases and hydrogen peroxide: The suberin connection.* Phytochemistry Reviews, 2004. **3**(1-2): p. 1-2.

51. Gazaryan, I.G., et al., *Mechanism of indole-3-acetic acid oxidation by plant peroxidases: anaerobic stopped-flow spectrophotometric studies on horseradish and tobacco peroxidases.* The Biochemical journal, 1996. **313 (Pt 3)**: p. 841-7.

52. Bernards, M.A., et al., *Biochemical characterization of the suberization-associated anionic peroxidase of potato.* Plant Physiology, 1999. **121**(1): p. 135-46.

53. Allison, S.D. and J.C. Schultz, *Differential activity of peroxidase isozymes in response to wounding, gypsy moth, and plant hormones in northern red oak (Quercus rubra L.).* Journal of chemical ecology, 2004. **30**(7): p. 1363-79.

54. Hiraga, S., et al., *A large family of class III plant peroxidases.* Plant Cell Physiol, 2001. **42**(5): p. 462-8.

55. Duroux, L. and K.G. Welinder, *The peroxidase gene family in plants: a phylogenetic overview.* Journal of molecular evolution, 2003. **57**(4): p. 397-407.

56. Ostergaard, L., et al., *Computational analyses and annotations of the Arabidopsis peroxidase gene family.* FEBS Letters, 1998. **433**(1-2): p. 98-102.

57. Tognolli, M., et al., *Analysis and expression of the class III peroxidase large gene family in Arabidopsis thaliana.* Gene, 2002. **288**(1-2): p. 129-38.

58. Cosio, C. and C. Dunand, *Specific functions of individual class III peroxidase genes.* J Exp Bot, 2009. **60**(2): p. 391-408.

59. Nakamura, W., *Studies on the biosynthesis of lignin. I. Disproof against the catalytic activity of laccase in the oxidation of coniferyl alcohol.* J Biochem, 1967. **62**(1): p. 54-61.

60. Botella, M.A., et al., *Induction of a tomato peroxidase gene in vascular tissue.* FEBS Lett, 1994. **347**(2-3): p. 195-8.

61. Quiroga, M., et al., *A tomato peroxidase involved in the synthesis of lignin and suberin.* Plant Physiol, 2000. **122**(4): p. 1119-27.

62. Smith, C.G., et al., *Tissue and subcellular immunolocalisation of enzymes of lignin synthesis in differentiating and wounded hypocotyl tissue of French bean (Phaseolus vulgaris L.).* Planta, 1994. **192**(2): p. 155-164.

63. Zimmerlin, A., P. Wojtaszek, and G.P. Bolwell, *Synthesis of dehydrogenation polymers of ferulic acid with high specificity by a purified cell-wall peroxidase from French bean (Phaseolus vulgaris L.).* Biochem J, 1994. **299 (Pt 3)**: p. 747-53.

64. Lagrimini, L.M., et al., *Molecular cloning of complementary DNA encoding the lignin-forming peroxidase from tobacco: Molecular analysis and tissue-specific expression.* Proc Natl Acad Sci U S A, 1987. **84**(21): p. 7542-6.

65. Blee, K.A., et al., *A lignin-specific peroxidase in tobacco whose antisense suppression leads to vascular tissue modification.* Phytochemistry, 2003. **64**(1): p. 163-176.

66. Nielsen, K.L., et al., *Differential activity and structure of highly similar peroxidases. Spectroscopic, crystallographic, and enzymatic analyses of lignifying Arabidopsis*

thaliana peroxidase A2 and horseradish peroxidase A2. Biochemistry, 2001. **40**(37): p. 11013-21.

67. Shigeto, J., et al., *Putative Cationic Cell-Wall-Bound Peroxidase Homologues in Arabidopsis, AtPrx2, AtPrx25, and AtPrx71, Are Involved in Lignification.* Journal of Agricultural and Food Chemistry, 2013. **61**(16): p. 3781-3788.

68. Herrero, J., et al., *Bioinformatic and functional characterization of the basic peroxidase 72 from Arabidopsis thaliana involved in lignin biosynthesis.* Planta, 2013. **237**(6): p. 1599-612.

69. Masuda, H., H. Fukuda, and A. Komamine, *Changes in Peroxidase Isoenzyme Patterns during Tracheary Element Differentiation in a Culture of Single Cells Isolated from the Mesophyll of Zinnia elegans.* Zeitschrift für Pflanzenphysiologie, 1983. **112**(5): p. 417-426.

70. Sato, Y., et al., *Isolation and characterization of a novel peroxidase gene ZPO-C whose expression and function are closely associated with lignification during tracheary element differentiation.* Plant Cell Physiol, 2006. **47**(4): p. 493-503.

71. Sato, Y., et al., *Separation and characterization of the isoenzymes of wall-bound peroxidase from cultured Zinnia cells during tracheary element differentiation.* Planta, 1995. **196**(1): p. 141-147.

72. Gabaldón, C., et al., *Characterization of the last step of lignin biosynthesis in Zinnia elegans suspension cell cultures.* FEBS Letters, 2006. **580**(18): p. 4311-4316.

73. Osakabe, K., et al., *Molecular cloning of two tandemly arranged peroxidase genes from Populus kitakamiensis and their differential regulation in the stem.* Plant Molecular Biology, 1995. **28**(4): p. 677-89.

74. Christensen, J.H., et al., *Purification and characterization of peroxidases correlated with lignification in poplar xylem.* Plant Physiol, 1998. **118**(1): p. 125-35.

75. Christensen, J.H., et al., *The syringaldazine-oxidizing peroxidase PXP 3-4 from poplar xylem: cDNA isolation, characterization and expression.* Plant Molecular Biology, 2001. **47**(5): p. 581-93.

76. Tsutsumi, Y., K. Matsui, and K. Sakai, *Substrate-Specific Peroxidases in Woody Angiosperms and Gymnosperms Participate in Regulating the Dehydrogenative Polymerization of Syringyl and Guaiacyl Type Lignins*, in *Holzforschung - International Journal of the Biology, Chemistry, Physics and Technology of Wood*1998. p. 275.

77. Sasaki, S., et al., *Role of Tyr residues on the protein surface of cationic cell-wall-peroxidase (CWPO-C) from poplar: potential oxidation sites for oxidative polymerization of lignin.* Phytochemistry, 2008. **69**(2): p. 348-55.

78. Sasaki, S., et al., *Lignin dehydrogenative polymerization mechanism: a poplar cell wall peroxidase directly oxidizes polymer lignin and produces in vitro dehydrogenative polymer rich in beta-O-4 linkage.* FEBS Lett, 2004. **562**(1-3): p. 197-201.

79. Sasaki, S., et al., *The cationic cell-wall-peroxidase having oxidation ability for polymeric substrate participates in the late stage of lignification of Populus alba L.* Plant Molecular Biology, 2006. **62**(6): p. 797-807.

80. Aoyama, W., et al., *Sinapyl alcohol-specific peroxidase isoenzyme catalyzes the formation of the dehydrogenative polymer from sinapyl alcohol.* Journal of Wood Science, 2002. **48**(6): p. 497-504.

81. Polle, A., T. Otter, and F. Seifert, *Apoplastic Peroxidases and Lignification in Needles of Norway Spruce (Picea abies L.).* Plant Physiol, 1994. **106**(1): p. 53-60.

82. Fagerstedt, K., P. Saranpää, and R. Piispanen, *Peroxidase activity, isoenzymes and histological localisation in sapwood and heartwood of Scots pine (Pinus sylvestris L.).* Journal of Forest Research, 1998. **3**(1): p. 43-47.

83. Karkonen, A., et al., *Lignification related enzymes in Picea abies suspension cultures.* Physiol Plant, 2002. **114**(3): p. 343-353.

84. Marjamaa K, K.E.L.T.K.P.S.P.F.K.V., *Monolignol oxidation by xylem peroxidase isoforms of Norway spruce (Picea abies) and silver birch (Betula pendula).* Tree physiology, 2006. **26**(5): p. 605-11.

85. Koutaniemi, S., et al., *Characterization of basic p-coumaryl and coniferyl alcohol oxidizing peroxidases from a lignin-forming Picea abies suspension culture.* Plant Molecular Biology, 2005. **58**(2): p. 141-57.

86. Fagerstedt, K.V., et al., *Cell wall lignin is polymerised by class III secretable plant peroxidases in Norway spruce.* Journal of Integrative Plant Biology, 2010. **52**(2): p. 186-194.

87. Koutaniemi, S., et al., *Expression profiling of the lignin biosynthetic pathway in Norway spruce using EST sequencing and real-time RT-PCR.* Plant Molecular Biology, 2007. **65**(3): p. 311-28.

88. McDougall, G.J., *Cell-wall-associated peroxidases from the lignifying xylem of angiosperms and gymnosperms: monolignol oxidation.* Holzforschung, 2001. **55**(3): p. 246-249.

89. Imberty, A., R. Goldberg, and A.-M. Catesson, *Isolation and characterization of Populus isoperoxidases involved in the last step of lignin formation.* Planta, 1985. **164**(2): p. 221-226.

90. Marjamaa, K., et al., *Monolignol oxidation by xylem peroxidase isoforms of Norway spruce (Picea abies) and silver birch (Betula pendula).* Tree physiology, 2006. **26**(5): p. 605-11.

91. El Mansouri, I., et al., *Biochemical and phenotypical characterization of transgenic tomato plants overexpressing a basic peroxidase.* Physiologia plantarum, 1999. **106**(4): p. 355-362.

92. Kavousi, B., et al., *Consequences of antisense down-regulation of a lignification-specific peroxidase on leaf and vascular tissue in tobacco lines demonstrating enhanced enzymic saccharification.* Phytochemistry, 2010. **71**(5-6): p. 531-42.

93. Li, Y., et al., *Down-regulation of an anionic peroxidase in transgenic aspen and its effect on lignin characteristics.* J Plant Res, 2003. **116**(3): p. 175-82.

94. McIntyre, C.L., H.M. Bettenay, and J.M. Manners, *Strategies for the suppression of peroxidase gene expression in tobacco. II. In vivo suppression of peroxidase activity in transgenic tobacco using ribozyme and antisense constructs.* Transgenic research, 1996. **5**(4): p. 263-70.

95. Christensen, J.H., et al., *Xylem peroxidases: purification and altered expression.* Progress in Biotechnology, 2001. **18**: p. 171-176.

96. Tamura, T., N. Morohoshi, and S. Yasuda, *Suitability of Peroxidase-Suppressed Transgenic Hybrid Aspen (Populus sieboldii X Populus gradidentata) for Pulping*, in *Holzforschung*2001. p. 335.

97. Tuskan, G.A., et al., *The genome of black cottonwood, Populus trichocarpa (Torr. & Gray).* Science, 2006. **313**(5793): p. 1596-604.

98. Shi, R., et al., *Towards a systems approach for lignin biosynthesis in Populus trichocarpa: transcript abundance and specificity of the monolignol biosynthetic genes.* Plant & cell physiology, 2010. **51**(1): p. 144-63.

99. Wang, J.P., et al., *Complete Proteomic-Based Enzyme Reaction and Inhibition Kinetics Reveal How Monolignol Biosynthetic Enzyme Families Affect Metabolic Flux and Lignin in Populus trichocarpa.* The Plant Cell Online, 2014. **26**(3): p. 894-914.

100. Trapnell, C., L. Pachter, and S.L. Salzberg, *TopHat: discovering splice junctions with RNA-Seq.* Bioinformatics, 2009. **25**(9): p. 1105-11.

101. Quinlan, A.R. and I.M. Hall, *BEDTools: a flexible suite of utilities for comparing genomic features.* Bioinformatics, 2010. **26**(6): p. 841-2.

102. Robinson, M.D. and A. Oshlack, *A scaling normalization method for differential expression analysis of RNA-seq data.* Genome biology, 2010. **11**(3): p. R25.

103. Robinson, M.D., D.J. McCarthy, and G.K. Smyth, *edgeR: a Bioconductor package for differential expression analysis of digital gene expression data.* Bioinformatics, 2010. **26**(1): p. 139-40.

104. Lu, G. and E.N. Moriyama, *Vector NTI, a balanced all-in-one sequence analysis suite.* Briefings in Bioinformatics, 2004. **5**(4): p. 378-388.

105. Tamura, K., et al., *MEGA5: Molecular Evolutionary Genetics Analysis Using Maximum Likelihood, Evolutionary Distance, and Maximum Parsimony Methods.* Molecular biology and evolution, 2011. **28**(10): p. 2731-2739.

106. Miki, D., R. Itoh, and K. Shimamoto, *RNA silencing of single and multiple members in a gene family of rice.* Plant Physiol, 2005. **138**(4): p. 1903-13.

107. Holsters, M., et al., *Transfection and transformation of Agrobacterium tumefaciens.* Mol Gen Genet, 1978. **163**(2): p. 181-7.

108. Song, J., et al., *Genetic transformation of Populus trichocarpa genotype Nisqually-1: a functional genomic tool for woody plants.* Plant Cell Physiol, 2006. **47**(11): p. 1582-9.

109. Li, Q., et al., *Down-regulation of glycosyltransferase 8D genes in Populus trichocarpa caused reduced mechanical strength and xylan content in wood.* Tree Physiology, 2011. **31**(2): p. 226-236.

110. Lu, S., et al., *Ptr-miR397a is a negative regulator of laccase genes affecting lignin content in Populus trichocarpa.* Proceedings of the National Academy of Sciences, 2013. **110**(26): p. 10848-10853.

111. Yeh, T.F., et al., *Rapid screening of wood chemical component variations using transmittance near-infrared spectroscopy.* Journal of Agricultural and Food Chemistry, 2005. **53**(9): p. 3328-32.

112. Dence, C.W., *The Determination of Lignin*, in *Methods in Lignin Chemistry*, S. Lin and C. Dence, Editors. 1992, Springer Berlin Heidelberg. p. 33-61.

113. Chen, C.L., *Nitrobenzene and Cupric Oxide Oxidations*, in *Methods in Lignin Chemistry*, S. Lin and C. Dence, Editors. 1992, Springer Berlin Heidelberg. p. 301-321.

114. Liu, J., et al., *A standard reaction condition and a single HPLC separation system are sufficient for estimation of monolignol biosynthetic pathway enzyme activities.* Planta, 2012. **236**(3): p. 879-85.

115. Kjærsgård, I.H., et al., *Sequence and RT-PCR expression analysis of two peroxidases from Arabidopsis thaliana belonging to a novel evolutionary branch of plant peroxidases.* Plant Molecular Biology, 1997. **33**(4): p. 699-708.

116. Gomez Ros, L.V., et al., *Structural motifs of syringyl peroxidases are conserved during angiosperm evolution.* Journal of Agricultural and Food Chemistry, 2007. **55**(10): p. 4131-8.

117. Herrero, J., A. Esteban-Carrasco, and J.M. Zapata, *Looking for Arabidopsis thaliana peroxidases involved in lignin biosynthesis.* Plant Physiology and Biochemistry, 2013. **67**(0): p. 77-86.

118. Tokunaga, N., et al., *Analysis of expression profiles of three peroxidase genes associated with lignification in Arabidopsis thaliana.* Physiol Plant, 2009. **136**(2): p. 237-49.

119. Mader, M., *Origin of the Heterogeneity of Peroxidase Isoenzyme Group Gr from Nicotiana tabacum. I. Conformation.* Zeitschrift für Pflanzenphysiologie, 1980. **96**(4): p. 283-296.

120. Lagrimini, L.M., et al., *Peroxidase Overproduction in Tomato: Wound-induced Polyphenol Deposition and Disease Resistance.* HortScience, 1993. **28**(3): p. 218-221.

121. Barcelo, A.R., L.V. Ros, and A.E. Carrasco, *Looking for syringyl peroxidases.* Trends in Plant Science, 2007. **12**(11): p. 486-91.

122. Grand, C., et al., *Comparison of lignins and of enzymes involved in lignification in normal and brown midrib (bm3) mutant corn seedlings.* Physiologie vegetale, 1985. **23**: p. 905-911.

123. Pillonel, C., et al., *Involvement of cinnamyl-alcohol dehydrogenase in the control of lignin formation in Sorghum bicolor L. Moench.* Planta, 1991. **185**(4): p. 538-544.

124. Zhang, K., et al., *GOLD HULL AND INTERNODE2 encodes a primarily multifunctional cinnamyl-alcohol dehydrogenase in rice.* Plant Physiology, 2006. **140**(3): p. 972-83.

125. Halpin, C., et al., *Brown-midrib maize (bm1)--a mutation affecting the cinnamyl alcohol dehydrogenase gene.* The Plant journal : for cell and molecular biology, 1998. **14**(5): p. 545-53.

126. Higuchi, T., et al., *Red-brown color of lignified tissues of transgenic plants with antisense CAD gene: Wine-red lignin from coniferyl aldehyde.* Journal of Biotechnology, 1994. **37**(2): p. 151-158.

127. Ralph, J., et al., *NMR characterization of altered lignins extracted from tobacco plants down-regulated for lignification enzymes cinnamylalcohol dehydrogenase and cinnamoyl-CoA reductase.* Proceedings of the National Academy of Sciences of the United States of America, 1998. **95**(22): p. 12803-8.

128. Baucher, M., et al., *Red Xylem and Higher Lignin Extractability by Down-Regulating a Cinnamyl Alcohol Dehydrogenase in Poplar.* Plant Physiology, 1996. **112**(4): p. 1479-1490.

129. Lapierre, C., et al., *Lignin Structure in a Mutant Pine Deficient in Cinnamyl Alcohol Dehydrogenase.* Journal of Agricultural and Food Chemistry, 2000. **48**(6): p. 2326-2331.

130. MacKay, J., et al., *Modified Lignin and Delignification with a CAD-Deficient Loblolly Pine*, in *Holzforschung*1999. p. 403.

131. MacKay, J.J., et al., *Inheritance, gene expression, and lignin characterization in a mutant pine deficient in cinnamyl alcohol dehydrogenase.* Proceedings of the National Academy of Sciences of the United States of America, 1997. **94**(15): p. 8255-60.

132. Ralph, J., et al., *Abnormal lignin in a loblolly pine mutant.* Science, 1997. **277**(5323): p. 235-9.

133. Sibout, R., et al., *CINNAMYL ALCOHOL DEHYDROGENASE-C and -D are the primary genes involved in lignin biosynthesis in the floral stem of Arabidopsis.* The Plant cell, 2005. **17**(7): p. 2059-76.

134. Voelker, S.L., et al., *Antisense Down-Regulation of 4CL Expression Alters Lignification, Tree Growth, and Saccharification Potential of Field-Grown Poplar.* Plant Physiology, 2010. **154**(2): p. 874-886.

135. Xu, B., et al., *Silencing of 4-coumarate:coenzyme A ligase in switchgrass leads to reduced lignin content and improved fermentable sugar yields for biofuel production.* New Phytologist, 2011. **192**(3): p. 611-625.

136. Vignols, F., et al., *The brown midrib3 (bm3) mutation in maize occurs in the gene encoding caffeic acid O-methyltransferase.* The Plant Cell Online, 1995. **7**(4): p. 407-16.

137. Van Acker, R., et al., *Improved saccharification and ethanol yield from field-grown transgenic poplar deficient in cinnamoyl-CoA reductase.* Proceedings of the National Academy of Sciences, 2014. **111**(2): p. 845-850.

138. Meyermans, H., et al., *Modifications in Lignin and Accumulation of Phenolic Glucosides in Poplar Xylem upon Down-regulation of Caffeoyl-Coenzyme A O-Methyltransferase, an Enzyme Involved in Lignin Biosynthesis.* Journal of Biological Chemistry, 2000. **275**(47): p. 36899-36909.

139. Kaur, H., et al., *Environmental Stresses of Field Growth Allow Cinnamyl Alcohol Dehydrogenase-Deficient Nicotiana attenuata Plants to Compensate for their Structural Deficiencies.* Plant Physiology, 2012. **159**(4): p. 1545-1570.

140. Saathoff, A.J., et al., *Downregulation of Cinnamyl-Alcohol Dehydrogenase in Switchgrass by RNA Silencing Results in Enhanced Glucose Release after Cellulase Treatment.* PLoS ONE, 2011. **6**(1): p. e16416.

141. Kärkönen, A., et al., *Lignification related enzymes in Picea abies suspension cultures.* Physiologia plantarum, 2002. **114**(3): p. 343-353.

142. Ranocha, P., et al., *Laccase down-regulation causes alterations in phenolic metabolism and cell wall structure in poplar.* Plant physiology, 2002. **129**(1): p. 145-55.

143. Wallace, G. and S.C. Fry, *Action of diverse peroxidases and laccases on six cell wall-related phenolic compounds.* Phytochemistry, 1999. **52**(5): p. 769-773.

144. Bligny, R. and R. Douce, *Excretion of laccase by sycamore (Acer pseudoplatanus L.) cells. Purification and properties of the enzyme.* The Biochemical journal, 1983. **209**(2): p. 489-96.

145. Driouich, A., et al., *Characterization and localization of laccase forms in stem and cell cultures of sycamore.* The Plant Journal, 1992. **2**(1): p. 13-24.

146. Sato, Y., et al., *Molecular Cloning and Expression of Eight Laccase cDNAs in Loblolly Pine (Pinus taeda)*.* Journal of Plant Research, 2001. **114**(2): p. 147-155.

147. Liu, L., et al., *A laccase-like phenoloxidase is correlated with lignin biosynthesis in Zinnia elegans stem tissues.* The Plant Journal, 1994. **6**(2): p. 213-224.

148. Richardson, A. and G.J. McDougall, *A laccase-type polyphenol oxidase from lignifying xylem of tobacco.* Phytochemistry, 1997. **44**(2): p. 229-235.

149. Richardson, A., J. Duncan, and G.J. McDougall, *Oxidase activity in lignifying xylem of a taxonomically diverse range of trees: identification of a conifer laccase.* Tree physiology, 2000. **20**(15): p. 1039-1047.

150. Zhao, Q., et al., *LACCASE Is Necessary and Nonredundant with PEROXIDASE for Lignin Polymerization during Vascular Development in Arabidopsis.* The Plant Cell Online, 2013. **25**(10): p. 3976-3987.

151. Shi, R., et al., *Regulation of phenylalanine ammonia-lyase (PAL) gene family in wood forming tissue of Populus trichocarpa.* Planta, 2013. **238**(3): p. 487-497.